BOWEN VOLUME
PART ONE

American Journal of Science

Established in 1818 by Benjamin Silliman

EDITORS
CHESTER R. LONGWELL - JOHN RODGERS

ASSOCIATE EDITORS

REGINALD A. DALY — A. F. BUDDINGTON
CAMBRIDGE, MASS. — PRINCETON, N. J.

CARL O. DUNBAR — RICHARD F. FLINT
HENRY MARGENAU — HAROLD G. CASSIDY
HORACE WINCHELL — G. EVELYN HUTCHINSON
NEW HAVEN, CONN.

LEASON H. ADAMS — WILMOT H. BRADLEY
WASHINGTON, D. C.

WILLIAM H. TWENHOFEL — HOWEL WILLIAMS
ORLANDO, FLORIDA — BERKELEY, CALIF.

FREDERICK J. ALCOCK — CECIL E. TILLEY
OTTAWA, CANADA — CAMBRIDGE, ENGLAND

GEORGE GAYLORD SIMPSON — ADOLPH KNOPF
NEW YORK, N. Y. — STANFORD, CALIF.

STERLING TOWER
NEW HAVEN, CONNECTICUT
1952

PAYNE & LANE, *Printers*, New Haven, Conn.

Printed in the United States of America

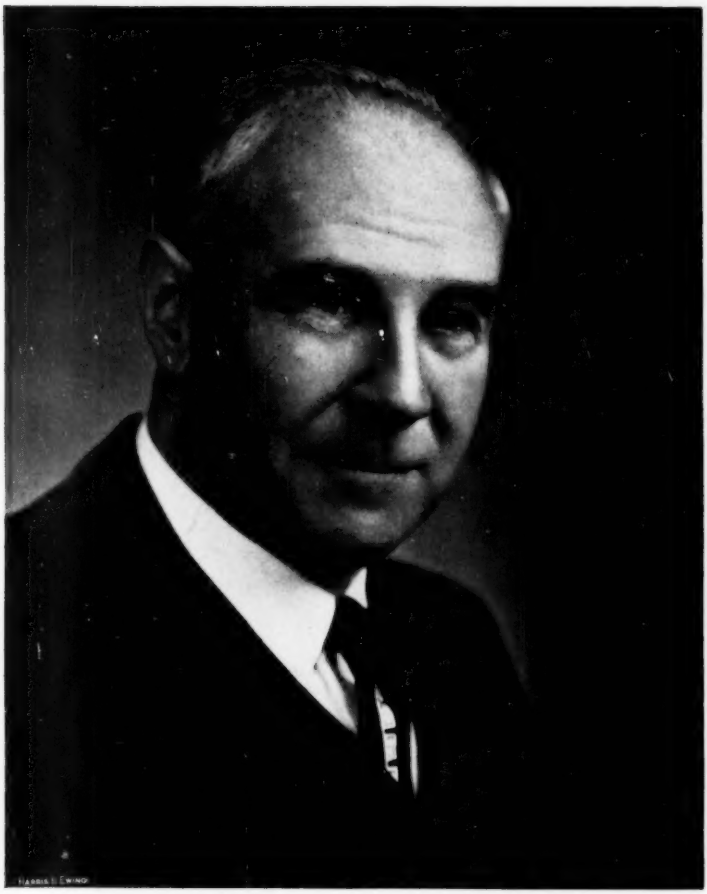

Norman L. Bowen

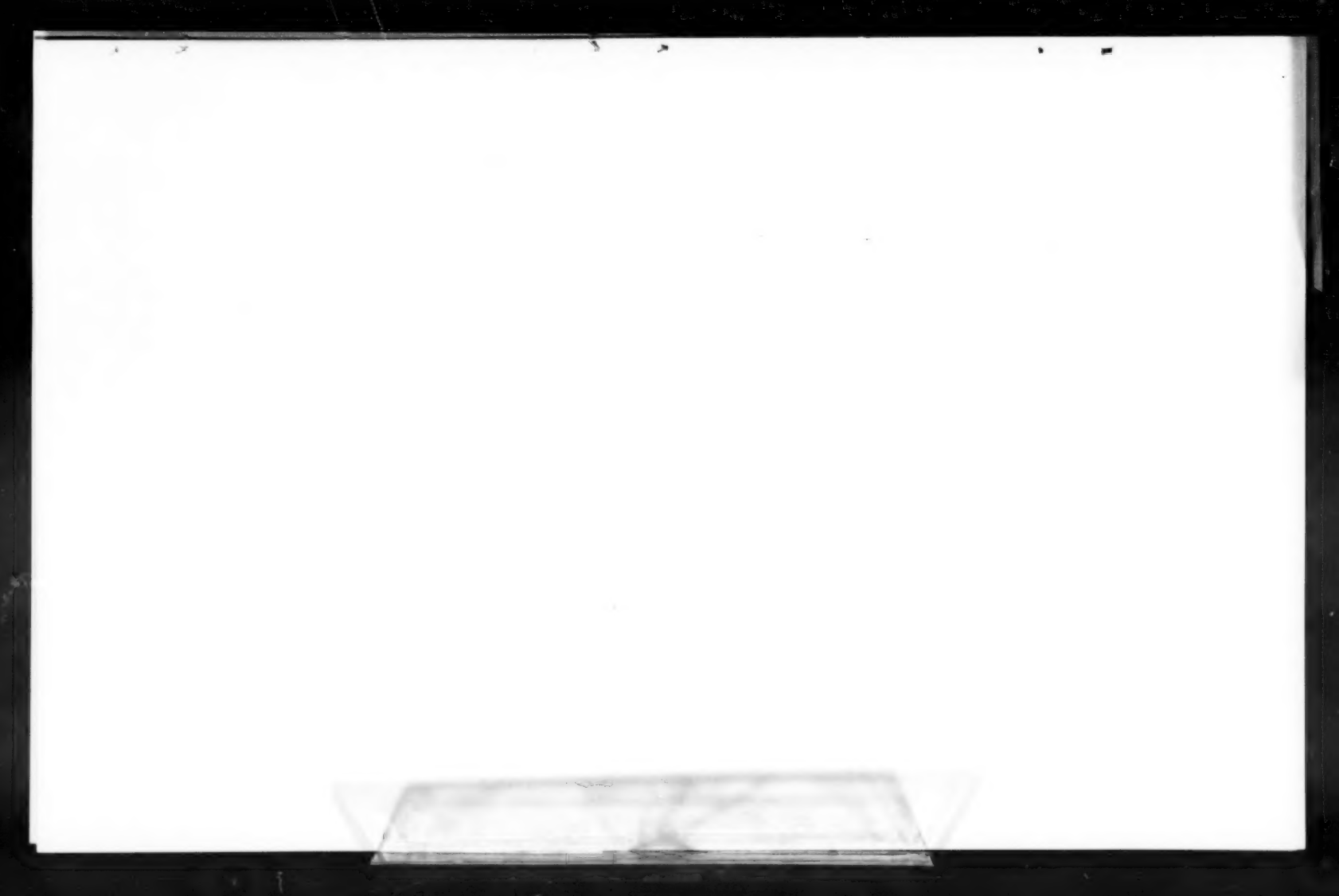

American Journal of Science

Established in 1818 by Benjamin Silliman

EDITORS

CHESTER R. LONGWELL - JOHN RODGERS

ASSOCIATE EDITORS

REGINALD A. DALY, CAMBRIDGE, MASS. — A. F. BUDDINGTON, PRINCETON, N. J.

CARL O. DUNBAR — RICHARD F. FLINT

HENRY MARGENAU — HAROLD G. CASSIDY

HORACE WINCHELL — G. EVELYN HUTCHINSON

NEW HAVEN, CONN.

LEASON H. ADAMS — WILMOT H. BRADLEY

WASHINGTON, D. C.

WILLIAM H. TWENHOFEL, ORLANDO, FLORIDA — HOWEL WILLIAMS, BERKELEY, CALIF.

FREDERICK J. ALCOCK, OTTAWA, CANADA — CECIL E. TILLEY, CAMBRIDGE, ENGLAND

GEORGE GAYLORD SIMPSON, NEW YORK, N. Y. — ADOLPH KNOPF, STANFORD, CALIF.

BOWEN VOLUME

PART ONE

NEW HAVEN, CONNECTICUT

1952

GEOPHYSICAL LABORATORY
Carnegie Institution of Washington
Publication No. 1200

DEDICATED TO

NORMAN L. BOWEN

IN GRATEFUL APPRECIATION

BY THE AUTHORS

Geological science is not concerned solely with the nature of the materials of the earth. Geology is even more concerned with processes, with the changes to which earth materials have been subjected. It seeks to know not only what earth substances are, but how they have come to be what they are, what factors have led to the observed arrangements and associations.

* * * * *

To observe and to attempt to reach conclusions based on the observations is not enough; we must also, insofar as may be possible, devise experiments which will test the conclusions. . . . For . . . geology, experiment has come to be quite as important as field and laboratory observation in evaluating conditions of genesis. . . . Experiment is a necessary check upon inference from observation, whenever experiment is possible, and it is an activity that should be more generally pursued.

* * * * *

I urge the desirability of studies of phase equilibrium. Such studies have direct applicability to the solution of problems arising from an enormous range of geologic phenomena. The separation of gases from lavas and all the volcanic phenomena that attend it are concerned with phase equilibrium. The separation of crystals from a molten magma, its corollary the solution of crystalline material in magmas, and all the phenomena of rock diversity that may be connected with these processes are likewise questions of phase equilibrium. The formation of hydrothermal solutions from magmas, the introduction of various substances, including valuable minerals, into surrounding rock through their agency, and the many phase changes that accompany these phenomena fall in the same category. The chemical attack of atmospheric agencies upon crystalline rocks, the resultant formation of solid decomposition products, on the one hand, and of aqueous solutions, upon the other, the later deposition of various substances from these solutions, the recrystallization of these products when they are subjected to high temperatures and pressures upon deep burial—all these present problems in which questions of phase equilibrium are paramount.

In many of the processes mentioned, equilibrium is not attained, but this fact should not lead one to doubt the importance of laboratory studies of phase equilibrium. The only practical method of studying these changes is to determine equilibrium relations first and then to determine what factors lead to failure of equilibrium together with the magnitude and direction of their effects.

Mente et malleo atque catino.

EXCERPTS FROM THE WRITINGS OF N. L. BOWEN

FOREWORD

In the year 1910 a young student, Norman L. Bowen, came to the Geophysical Laboratory of the Carnegie Institution of Washington. He made a phase-equilibrium study of a silicate system and was permitted to use these results for a thesis for the degree of Doctor of Philosophy at Massachusetts Institute of Technology. After obtaining his degree Dr. Bowen joined the staff of the Geophysical Laboratory and eagerly, vigorously, and ably pursued his laboratory studies of the phase-equilibrium relations of the rock-forming minerals. Ability, energy, and opportunity had met. By 1915, when he published *The Later Stage of the Evolution of Igneous Rocks*, his reputation among petrologists was established. By 1928, when his book *The Evolution of Igneous Rocks* appeared, his fame was worldwide, and his work was recognized as the most fundamental and far-reaching of any produced in recent years.

A skilled and resourceful experimenter in a difficult chemical field, Bowen has continued his studies and is still developing new techniques and skillfully applying the facts of experiment to the origin of igneous and metamorphic rocks. He has been an inspiration to his colleagues. He did not stop with experiment but carried his results to the field and checked them with the rocks he was attempting to explain. He has thus done much to bridge the gap between the views of the chemist and those of the geologist.

Now at the age of sixty-five years he is retiring from the staff of the Geophysical Laboratory which he has served so long and so well. He has been on the staff since college days with only a short break, during which he returned to Queen's University as Professor of Mineralogy, and the longer break from 1937 to 1945 when he was Distinguished Service Professor of Petrology at the University of Chicago. His colleagues and those who have been visitors at Geophysical Laboratory in past years salute him, and to their friend and counselor affectionately dedicate this volume.

TABLE OF CONTENTS

PART ONE

List of Systems Investigated at Geophysical Laboratory
Leason H. Adams 1

The Differentiation of a Composite Aplite from the Priblof Islands, Alaska ..... *Tom. F. W. Barth* 27

Chemical Petrology of Some Metamorphosed Adirondack Gabbroic, Syenitic and Quartz Syenitic Rocks
A. F. Buddington 37

Relations between Composition and Indices of Refraction in Natural Plagioclase ..... *F. Chayes* 85

Two New Crystalline Phases of the Anorthite Composition, $CaO \cdot Al_2O_3 \cdot 2SiO_2$ ..... *G. L. Davis and O. F. Tuttle* 107

The Symmetry Change in the High-Temperature Alkali-Feldspar Series .. *Gabrielle Donnay* and *J. D. H. Donnay* 115

On the Granulites of Lapland ..... *Pentti Eskola* 133

Orthopyroxenes of the Bushveld Type, Ion Substitutions, and Changes in Unit Cell Dimensions ..... *H. H. Hess* 173

Twinning Frequency in Feldspar Phenocrysts from a Quartz Latite Sill at Sierra Blanca, Texas ..... *Earl Ingerson* 189

Significance of Variation in the High-Low Inversion of Quartz
M. L. Keith and *O. F. Tuttle* 203

Japanese Twins of Quartz ..... *S. Kozu* 281

Thermochemistry of Plagioclase and Alkali Feldspars
F. C. Kracek and *K. J. Neuvonen* 293

PART TWO

The Effect of Temperature on the Symmetry of High Temperature Soda-Rich Feldspars *Wm. S. MacKenzie* 319

The System H_2O—Na_2O—SiO_2 at 400° C.
G. W. Morey and *J. M. Hesselgesser* 343

Heat of Formation of Merwinite and Monticellite
K. J. Neuvonen 373

The Chemistry of the Keweenawan Lavas ..... *Paul Niggli* 381

The System Diopside—Forsterite—Anorthite
E. F. Osborn and *D. B. Tait* 413

A Reconnaissance of Liquidus Relations in the System $K_2O \cdot 2SiO_2$—FeO—SiO_2 ..... *Edwin Roedder* 435

Leucite, Potash Nepheline, and Clinopyroxene from Volcanic Lavas from Southwestern Uganda and Adjoining Belgian Congo ..... *Th. G. Sahama* 457

The System FeO—Al_2O_3—SiO_2
J. F. Schairer and *Kenzo Yagi* 471

Single-Crystal Measurements on Paracelsian .... *J. V. Smith* 513

Temperature Scales and Silicate Research .... *R. B. Sosman* 517

Some Trends of Basaltic Magma in Limestone Syntexis
C. E. Tilley 529

The Angle between the *a*-Axis and the Trace of the Rhombic Section on the {010}-Pinacoid in the Plagioclases
George Tunell 547

Optical Studies on Alkali Feldspars ..... *O. F. Tuttle* 553

The MgO—Al_2O_3—SiO_2—H_2O System and the Related Metamorphic Facies ..... *H. S. Yoder, Jr.* 569

American Journal of Science

Bowen Volume

PART ONE

LIST OF SYSTEMS INVESTIGATED AT GEOPHYSICAL LABORATORY

L. H. ADAMS

THE Geophysical Laboratory started as a group working at the U.S. Geological Survey and receiving financial support from the Carnegie Institution of Washington. Owing largely to the success of the new approach to petrology, there was created a separate department of the Institution, which since 1907 has occupied the present building and site. This organization had as its original objective the investigation of mineral solution and fusion under high temperatures and pressures. Later the scope of the Laboratory's interest was enlarged to include other subjects in Earth science, but the core of the work has continued to be the determination of melting relations of combinations—commonly called "systems"—of rock-forming compounds.

The first comprehensive investigation of silicate mixtures at the Laboratory or elsewhere was the now historic one involving the two compounds albite and anorthite of the plagioclase feldspar series. These pioneering studies by Day, Allen, and Iddings demonstrated the practicability of studying rock formation by laboratory experimentation, and they laid the foundation for what has come to be a half-century of intensive investigation of silicate systems involving the major rock-forming oxides. Of these oxides, the most important are nine—namely, silica, alumina, ferric oxide, ferrous oxide, lime, magnesia, soda, potash, and water—which together make up nearly 99 per cent of the material of the Earth's crust. The time and effort required for the investigation of a silicate system increase rapidly with the number of components. To work out a two-component

system may take the time of one investigator for a part of a year or more than a year; a three-component system may require several years, the work being carried on at the maximum possible speed; and to work out *completely* a four-component system might require decades of active experimentation. By extrapolation to systems of more components it would appear at first sight that only in the far distant future could it be expected that the ultimate goal—namely, a reasonable knowledge of the nine-component system involving the major oxides—could be attained. Fortunately, however, by "short cuts" suggested by the accumulated experience and by a proper selection of the particular areas for investigation, gratifying progress has been made, so that already we are in a position to provide a useful (even though not complete) quantitative basis for petrology and to lay down some broad principles of petrogenesis.

The following list of the systems investigated at the Geophysical Laboratory has been assembled in the belief that such a list will be found convenient by students in the field of experimental petrology and that it will serve as an encouragement to present and prospective investigators. In preparing the list a primary subdivision has been made in accordance with the number of components so that there are listed, in order, systems with two components, those with three components, and so on. It should be noted that in conformity with common usage a mixture of two ingredients is called a binary system only when all phases occurring in the system can be produced (stoichiometrically) from the two specified ingredients. Thus albite—water is truly binary, but orthoclase—water is not binary at all temperatures because of the appearance of leucite and of a liquid more siliceous than orthoclase which cannot be made (stoichiometrically) from orthoclase and water. When the end members form phases that cannot be represented in terms of the end members, they are said to constitute a "join." Alternatively two such end members may be said to form a pseudo-binary system; thus, phase relations for mixtures of orthoclase and water at temperatures above the incongruent melting point of orthoclase belong to the orthoclase—water "join" in the four-component system potash—alumina—silica—water. In the tabulation presented here such a system will be called the *two-end-member* join orthoclase—water. Similarly, we may have

ternary systems and three-end-member joins, and so on. A member of the latter class might be called a pseudo-ternary system or a ternary section.

In this connection it may be noted that in the classification of systems a *component* does not need to be an actual compound. Thus, although $2K_2O \cdot 3SiO_2$ is not known to exist, we may deal with the *binary* system $2K_2O \cdot 3SiO_2$—SiO_2 because all phases in the range of composition from $2K_2O \cdot 3SiO_2$ to SiO_2 may be represented in terms of the two specified end members. Furthermore, in accordance with the generally accepted definition of a component, binary systems may include compositions for which the amount of one component is negative—provided only that all phases occurring in the systems may be produced stoichiometrically from the specified amounts (positive or negative) of the chosen components.

It should be noted that the amount of information available for the systems here listed varies greatly. In some instances there is a complete coverage of compositions, and in others only fragmentary data have been obtained.

Chemical formulas of minerals may usually be written in several ways. Thus, jadeite may be written as $Na_2O \cdot Al_2O_3 \cdot 4SiO_2$ or $NaAlSi_2O_6$, which, obviously, is $\frac{1}{2}Na_2O \cdot Al_2O_3 \cdot 4SiO_2$. There are two kinds of choices represented here. The first is the choice as to writing the formula as a succession of oxides or writing the elements consecutively. This is, of course, a matter of personal preference, but the former alternative is believed by the author to be the one most easily remembered and is the one adopted here. On the other hand, it appears to have been considered by some in the past that the "half formula" $NaAlSi_2O_6$ is preferable because it corresponds to the molecular weight of the compound; but it must be remembered that no one knows what the molecular weights of such compounds are. To be sure, in the system albite—anorthite the correspondence of the liquidus and solidus temperatures with certain simple physical chemical principles lends support to the notion that the molecular weight of albite is represented by its "half formula." The difficulty is that such considerations may be said to prove too much. Certainly they leave us without a physical picture of a particular molecule or of a unique molecular grouping in a lattice consisting of an array of sodium, calcium, aluminum, silicon and oxygen atoms scattered throughout space.

In this catalogue of various systems the arrangement follows to a certain extent that used by Hall and Insley (ref. 62). Specifically, the arrangement here is as follows:

1. The formulas of the compounds, following the usual practice, are written by oxides (whenever this is possible) and in an order determined first by the valence of the cation and then alphabetically—except for the volatile oxides CO_2 and H_2O which are written last.

2. In the grouping of the components for *system designation* the components are written in an order determined first by the valence of the cation in the first oxide, and then alphabetically —except for H_2O and CO_2 (and also O) which are placed last, as in writing the formulas of the components.

3. The systems are listed alphabetically, with grouping successively by oxides and compounds.

In many instances there are included "subsystems" within systems, e.g., binary systems within binary systems, binary and ternary systems within ternary systems, and so on; but it has not been deemed necessary to be completely consistent by listing all possible permutations. The successive categories in the present list are: binary systems; two-end-member joins; ternary systems; three-end-member joins; and so on. It should be noted that FeO, as a component under equilibrium conditions, is accompanied by a certain amount of Fe and Fe_2O_3. Thus, the iron-bearing silicate liquids always contain a finite amount of Fe_2O_3; and a system derived from two ingredients (for example), of which one is FeO, will usually not be strictly binary.

It should be noted that the temperatures given in the various papers listed are in terms of what is sometimes called the "Geophysical Laboratory Scale," of which representative fixed points (thermodynamic scale) are the melting points of zinc, 419.4°; silver, 960.2°; gold, 1062.6°; diopside, 1391.5°; palladium, 1549.5°; and platinum, 1755°. For other details and for a comparison with other temperature scales, the paper by R. B. Sosman in this volume should be consulted.

Binary Systems

Components	References	Remarks
Ag—S	81	
Ag_2S—Sb_2S_3	67	
Al_2O_3—SiO_2	24, 26, 58, 125 (n. 57, p. 274), 135, 136	
B_2O_3—H_2O	84	
B_2O_3—SiO_2	58, 92, 100	
BaF_2—ZnF_2	65	
BaO—SiO_2	46, 58	
$BaO \cdot SO_3$—H_2O	99	
$BaO \cdot SiO_2$—$CaO \cdot SiO_2$	46	
BeO—SiO_2	58	Miscibility data.
CaF_2—ZnF_2	65	
CaO—Al_2O_3	115, 116, 135, 136	
CaO—CO_2	68, 139, 141	
CaO—Fe_2O_3	143	
CaO—SiO_2	8, 9, 35, 44, 45, 58	
$CaO \cdot Al_2O_3$—$2CaO \cdot Al_2O_3 \cdot SiO_2$	115, 116	
$CaO \cdot Al_2O_3$—$CaO \cdot SiO_2$	115, 116	
$3CaO \cdot 5Al_2O_3$—$2CaO \cdot Al_2O_3 \cdot SiO_2$	115, 116	
$5CaO \cdot 3Al_2O_3$—$2CaO \cdot SiO_2$	115, 116	
$CaO \cdot Al_2O_3 \cdot 2SiO_2$—$Al_2O_3$	115, 116	
$CaO \cdot Al_2O_3 \cdot 2SiO_2$—$2CaO \cdot Al_2O_3 \cdot SiO_2$	115, 116	
$CaO \cdot Al_2O_3 \cdot 2SiO_2$—$CaO \cdot MgO \cdot 2SiO_2$	107	Not quite binary.
$CaO \cdot Al_2O_3 \cdot 2SiO_2$—$CaO \cdot SiO_2$	108, 115, 116	
$CaO \cdot Al_2O_3 \cdot 2SiO_2$—$SiO_2$	115, 116	

BINARY SYSTEMS (*Cont.*)

Components	References	Remarks
$2CaO \cdot Al_2O_3 \cdot SiO_2$—$2CaO \cdot MgO \cdot 2SiO_2$	47, 109	
$2CaO \cdot Al_2O_3 \cdot SiO_2$—$CaO \cdot SiO_2$	109, 115, 116	
$2CaO \cdot Al_2O_3 \cdot SiO_2$—$2CaO \cdot SiO_2$	115, 116	
$CaO \cdot MgO \cdot 2SiO_2$—$2CaO \cdot MgO \cdot 2SiO_2$	48, 49	
$CaO \cdot MgO \cdot 2SiO_2$—$CaO \cdot SiO_2$	48, 49, 130	
$CaO \cdot MgO \cdot 2SiO_2$—$H_2O$	H. S. Yoder (unpub.), see 156	
$CaO \cdot MgO \cdot 2SiO_2$—$2MgO \cdot SiO_2$	18, 19	
$CaO \cdot MgO \cdot 2SiO_2$—$SiO_2$	18, 19, 48, 49	
$2CaO \cdot MgO \cdot 2SiO_2$—$CaO \cdot SiO_2$	48, 49, 130	
$2CaO \cdot MgO \cdot 2SiO_2$—$2CaO \cdot SiO_2$	48, 49	
$CaO \cdot SO_3$—H_2O	99, 110	
$CaO \cdot SiO_2$—$S_2O \cdot SiO_2$	46	
$2CaO \cdot SiO_2$—$2FeO \cdot SiO_2$	34	
$2CaO \cdot SiO_2$—SiO_2	35, 58, 115, 116	
CoO—SiO_2	58	Miscibility data.
Cs_2O—SiO_2	72	
FeO—Al_2O_3	134	
FeO—MgO	30	
FeO—SiO_2	29, 58, 59	
Fe_2O_3—H_2O	99, 111, 145	
Fe_2O_3—SiO_2	36, 58, 59	
Fe_2O_3—Fe_2O	61, 142	
$2FeO \cdot SiO_2$—$2MgO \cdot SiO_2$	30, 32, 124	
FeS—S	120	

Binary Systems (*Cont.*)

Components	References	Remarks
$I—H_2O$	75	
$KCNS—H_2O$	78	
$KI—H_2O$	76	
$K_2O—SiO_2$	57, 58, 72, 82, 83, 88	
$K_2O \cdot Al_2O_3—SiO_2$	131	No data at $K_2O \cdot Al_2O_3$ end.
$K_2O \cdot Al_2O_3 \cdot 2SiO_2—Al_2O_3$	131	
$K_2O \cdot Al_2O_3 \cdot 2SiO_2—K_2O \cdot Al_2O_3 \cdot 4SiO_2$	131	
$K_2O \cdot Al_2O_3 \cdot 2SiO_2—K_2O \cdot 2SiO_2$	131	
$K_2O \cdot Al_2O_3 \cdot 2SiO_2—Na_2O \cdot Al_2O_3 \cdot 2SiO_2$	21, 25, 126, 128	
$K_2O \cdot Al_2O_3 \cdot 2SiO_2—SiO_2$	131	
$K_2O \cdot Al_2O_3 \cdot 4SiO_2—Al_2O_3$	131	
$K_2O \cdot Al_2O_3 \cdot 4SiO_2—CaO \cdot Al_2O_3 \cdot 2SiO_2$	132	
$K_2O \cdot Al_2O_3 \cdot 4SiO_2—CaO \cdot MgO \cdot 2SiO_2$	22, 27, 129	
$K_2O \cdot Al_2O_3 \cdot 4SiO_2—K_2O \cdot 2SiO_2$	131	
$K_2O \cdot Al_2O_3 \cdot 4SiO_2—2MgO \cdot SiO_2$	J. F. Schairer (in press)	
$K_2O \cdot Al_2O_3 \cdot 4SiO_2—SiO_2$	93, 131	
$K_2O \cdot Al_2O_3 \cdot 6SiO_2—H_2O$	55, 56, 99	Not binary at high temperatures.
$K_2O \cdot CaO \cdot SiO_2—K_2O \cdot 2SiO_2$	103	
$2K_2O \cdot CaO \cdot 6SiO_2—K_2O \cdot 2SiO_2$	103	
$K_2O \cdot MgO \cdot SiO_2—K_2O \cdot MgO \cdot 3SiO_2$	123	
$K_2O \cdot MgO \cdot SiO_2—K_2O \cdot SiO_2$	123	
$K_2O \cdot MgO \cdot SiO_2—K_2O \cdot 2SiO_2$	123	
$K_2O \cdot MgO \cdot SiO_2—MgO$	123	

BINARY SYSTEMS (*Cont.*)

Components	References	Remarks
$K_2O \cdot MgO \cdot SiO_2$—$SiO_2$	123	
$K_2O \cdot MgO \cdot 3SiO_2$—$K_2O \cdot MgO \cdot 5SiO_2$	123	
$K_2O \cdot MgO \cdot 3SiO_2$—$K_2O \cdot 2SiO_2$	123	
$K_2O \cdot MgO \cdot 3SiO_2$—$2MgO \cdot SiO_2$	123	
$K_2O \cdot MgO \cdot 5SiO_2$—$K_2O \cdot 4SiO_2$	123	
$K_2O \cdot MgO \cdot 5SiO_2$—$2MgO \cdot SiO_2$	123	
$K_2O \cdot MgO \cdot 5SiO_2$—$SiO_2$	123	
$K_2O \cdot P_2O_5$—$Na_2O \cdot P_2O_5$	G. W. Morey (unpub.)	
$2K_2O \cdot P_2O_5$—H_2O	G. W. Morey (unpub.)	
$2K_2O \cdot P_2O_5$—$2Na_2O \cdot P_2O_5$	G. W. Morey (unpub.)	
$K_2O \cdot SO_3$—H_2O	3, G. W. Morey (unpub.), see 156	
$K_2O \cdot SiO_2$—$CaO \cdot SiO_2$	103	
$K_2O \cdot SiO_2$—$K_2O \cdot 2SiO_2$	82, 83	
$K_2O \cdot SiO_2$—$Na_2O \cdot SiO_2$	77	
$K_2O \cdot SiO_2$—SiO_2	58, 82, 83	
$K_2O \cdot 2SiO_2$—Al_2O_3	131	
$K_2O \cdot 2SiO_2$—$K_2O \cdot 4SiO_2$	82, 83	
$K_2O \cdot 2SiO_2$—$Na_2O \cdot SiO_2$	77	
$K_2O \cdot 2SiO_2$—$Na_2O \cdot 2SiO_2$	77	
$K_2O \cdot 4SiO_2$—SiO_2	58, 82, 83	
Li_2O—SiO_2	72, 74	
$Li_2O \cdot CO_2$—SiO_2	105, 106	
$Li_2O \cdot SO_3$—H_2O	G. W. Morey (unpub.), see 156	
$Li_2O \cdot SiO_2$—$Na_2O \cdot SiO_2$	79	

BINARY SYSTEMS (*Cont.*)

Components	References	Remarks
$Li_2O \cdot SiO_2$—$Na_2O \cdot 2SiO_2$	79, 80	
MgF_2—ZnF_2	65	
MgO—Al_2O_3	135, 136	
MgO—$2MgO \cdot SiO_2$	23	
MgO—SiO_2	10, 13, 23, 58	
$MgO \cdot Al_2O_3$—$2MgO \cdot SiO_2$	119	
$2MgO \cdot SiO_2$—SiO_2	13, 23, 58	
MnF_2—ZnF_2	65	
MnO—SiO_2	58	Miscibility data.
$3MnO \cdot Al_2O_3 \cdot 3SiO_2$—$3Y_2O_3 \cdot 5Al_2O_3$	149	
NH_3—H_2O	71	
NH_4F—ZnF_2	65	
NH_4NO_3—H_2O	6	
NaCl—H_2O	2, 5, 7	Aqueous solutions under high pressure.
Na_2O—B_2O_3	104	
Na_2O—SiO_2	58, 72, 73, 80, 88	
$Na_2O \cdot Al_2O_3$—$Na_2O \cdot Al_2O_3 \cdot 2SiO_2$	131	
$Na_2O \cdot Al_2O_3$—SiO_2	131	
$Na_2O \cdot Al_2O_3 \cdot 2SiO_2$—$Al_2O_3$	131	
$Na_2O \cdot Al_2O_3 \cdot 2SiO_2$—$CaO \cdot Al_2O_3 \cdot 2SiO_2$	14	
$Na_2O \cdot Al_2O_3 \cdot 2SiO_2$—$Na_2O \cdot Al_2O_3 \cdot 6SiO_2$	60, 131, 150	
$Na_2O \cdot Al_2O_3 \cdot 2SiO_2$—$Na_2O \cdot 2SiO_2$	131	
$Na_2O \cdot Al_2O_3 \cdot 6SiO_2$—$Al_2O_3$	131	

BINARY SYSTEMS (*Cont.*)

Components	References	Remarks
$Na_2O \cdot Al_2O_3 \cdot 6SiO_2$—$CaO \cdot Al_2O_3 \cdot 2SiO_2$	15, 16, 41, 42, 43	
$Na_2O \cdot Al_2O_3 \cdot 6SiO_2$—$2FeO \cdot SiO_2$	31, 33	
$Na_2O \cdot Al_2O_3 \cdot 6SiO_2$—$H_2O$	54, 55, 56, 99, H. S. Yoder (unpub.), see 156	Not strictly binary.
$Na_2O \cdot Al_2O_3 \cdot 6SiO_2$—$Na_2O \cdot 2SiO_2$	131	
$Na_2O \cdot Al_2O_3 \cdot 6SiO_2$—$SiO_2$	131	
$Na_2O \cdot B_2O_3$—$Na_2O \cdot SiO_2$	92	
$Na_2O \cdot B_2O_3$—SiO_2	92	
$Na_2O \cdot 2B_2O_3$—H_2O	G. W. Morey (unpub.), see 156	
$Na_2O \cdot 3B_2O_3$—H_2O	G. W. Morey (unpub.), see 156	
$Na_2O \cdot 4B_2O_3$—H_2O	G. W. Morey (unpub.), see 156	
$Na_2O \cdot 4B_2O_3$—SiO_2	92	
$Na_2O \cdot 2CaO \cdot 3SiO_2$—$Na_2O \cdot 2SiO_2$	95	
$5Na_2O \cdot Fe_2O_3 \cdot 8SiO_2$—$Fe_2O_3$	36	
$5Na_2O \cdot Fe_2O_3 \cdot 8SiO_2$—$Na_2O \cdot SiO_2$	36	
$5Na_2O \cdot Fe_2O_3 \cdot 8SiO_2$—$Na_2O \cdot 2SiO_2$	36	
$Na_2O \cdot P_2O_5$—H_2O	G. W. Morey (unpub.)	
$2Na_2O \cdot P_2O_5$—H_2O	G. W. Morey (unpub.), see 156	
$3Na_2O \cdot 2P_2O_5$—H_2O	G. W. Morey (unpub.)	
$Na_2O \cdot SO_3$—H_2O	4, 53, 99	
$Na_2O \cdot P_2O_5$—$2Na_2O \cdot P_2O_5$	102	
$Na_2O \cdot SiO_2$—$CaO \cdot SiO_2$	95	
$Na_2O \cdot SiO_2$—$Na_2O \cdot 2SiO_2$	94	
$Na_2O \cdot SiO_2$—SiO_2	58, 94, 95	

Binary Systems (*Cont.*)

Components	References	Remarks
$Na_2O \cdot 2SiO_2$—Al_2O_3	131	
$Na_2O \cdot 2SiO_2$—SiO_2	58, 94	
NiO—SiO_2	58	Miscibility data.
PbO—SiO_2	58	Miscibility data.
$PbO \cdot SO_3$—H_2O	99	
Rb_2O—H_2O	72	
SiO_2—H_2O	98, 99	
SnO_2—SiO_2	58, 99	
SrF_2—ZnF_2	65	
Sr_2O—SiO_2	46, 58	
$Tl_2O \cdot SO_3$—H_2O	G. W. Morey (unpub.), see 156	
$ZnCl_2$—ZnF_2	65	
ZnO—SiO_2	58	Miscibility data.
$2ZnO \cdot GeO_2$—$2ZnO \cdot SiO_2$	66	
ZnS—H_2O	99	

Two-End-Member Joins

Components	References	Remarks
$CaO \cdot Al_2O_3 \cdot 2SiO_2$—$2MgO \cdot SiO_2$	11, 12	
$3CaO \cdot Al_2O_3 \cdot 3SiO_2$—$H_2O$	147	
$2CaO \cdot MgO \cdot 2SiO_2$—$2CaO \cdot SiO_2$	48, 49, 108	
$CaO \cdot SiO_2$—$MgO \cdot SiO_2$	9, 23	

TWO-END-MEMBER JOINS (*Cont.*)

Components	References	Remarks
$FeO \cdot SiO_2$—$MgO \cdot SiO_2$	30, 124	
$K_2O \cdot Al_2O_3 \cdot 4SiO_2$—$K_2O \cdot MgO \cdot 5SiO_2$	J. F. Schairer (in press), see 155	
$K_2O \cdot Al_2O_3 \cdot 6SiO_2$—$CaO \cdot Al_2O_3 \cdot 2SiO_2$	52, 132	Largely binary.
$K_2O \cdot Al_2O_3 \cdot 6SiO_2$—$K_2O \cdot 4SiO_2$	131	Partially binary.
$K_2O \cdot Al_2O_3 \cdot 6SiO_2$—$Na_2O \cdot Al_2O_3 \cdot 6SiO_2$	52, 126	Largely binary.
$Li_2O \cdot SiO_2$—$Na_2O \cdot SiO_2$	79, 80	
$MgO \cdot SiO_2$—H_2O	99	
$Na_2O \cdot Al_2O_3 \cdot 2SiO_2$—$CaO \cdot MgO \cdot 2SiO_2$	J. F. Schairer, H. S. Yoder, K. Yagi (unpub.) see 156	
$Na_2O \cdot Al_2O_3 \cdot 4SiO_2$—$CaO \cdot MgO \cdot 2SiO_2$	J. F. Schairer, H. S. Yoder, K. Yagi (unpub.) see 156	
$Na_2O \cdot Al_2O_3 \cdot 4SiO_2$—$H_2O$	146	
$Na_2O \cdot Al_2O_3 \cdot 4SiO_2$—$Na_2O \cdot FeO_3 \cdot 4SiO_2$	J. F. Schairer (unpub.)	
$Na_2O \cdot Fe_2O_3 \cdot 4SiO_2$—$Fe_2O_3$	36	
$Na_2O \cdot Fe_2O_3 \cdot 4SiO_2$—$5Na_2O \cdot Fe_2O_3 \cdot 8SiO_2$	36	Largely binary.
$Na_2O \cdot Fe_2O_3 \cdot 4SiO_2$—$Na_2O \cdot 2SiO_2$	36	
$Na_2O \cdot SiO_2$—Fe_2O_3	36	Largely binary.
$Na_2O \cdot 2SiO_2$—FeO	J. F. Schairer, R. D. Thwaite (unpub.), see 156	
$Na_2O \cdot 2SiO_2$—H_2O	94, 101	
$Na_2O \cdot 4SiO_2$—FeO	J. F. Schairer, R. D. Thwaite (unpub.), see 156	
$Na_2O \cdot 6SiO_2$—FeO	J. F. Schairer, R. D. Thwaite (unpub.), see 156	

Components	References	Remarks
$CaO—Al_2O_3—SiO_2$	40, 58, 114, 115, 116, 137, 138, 147	
$CaO—B_2O_3—SiO_2$	100	
$CaO—CO_2—H_2O$	69	
$CaO—FeO—SiO_2$	35	
$CaO—FeO—MgO$	133	
$CaO—MgO—Al_2O_3$	117, 118	
$CaO—MgO—SiO_2$	48, 49, 50, 58, 108, 130	
$CaO·Al_2O_3·2SiO_2—CaO·MgO·2SiO_2—CaO·SiO_2$	107	
$CaO·MgO·2SiO_2—2MgO·SiO_2—SiO_2$	17, 18	
$2CaO·Al_2O_3·SiO_2—2CaO·MgO·2SiO_2—CaO·SiO_2$	109	
Cu—Fe—S	86, 87	
$CuO—SO_3—H_2O$	113, 145	
$FeO—Al_2O_3—SiO_2$	58, 59, 134	
$FeO—Fe_2O_3—SiO_2$	29, 59	
$FeO—MgO—Fe_2O_3$	121	
$FeO—MgO—SiO_2$	30, 58	
$Fe_2O_3—SO_3—H_2O$	112, 145	
$K_2O—Al_2O_3—SiO_2$	131	
$K_2O—CaO—SiO_2$	103	
$K_2O—MgO—SiO_2$	123	
$K_2O—Na_2O—SiO_2$	77	
$K_2O—SiO_2—H_2O$	Burlew, Burke (unpub.), see 156	
$K_2O—ZnO—SiO_2$	66	
$K_2O·Al_2O_3·2SiO_2—Na_2O·Al_2O_3·2SiO_2—SiO_2$	126, 128	

TERNARY SYSTEMS (*Cont.*)

Components	References	Remarks
$K_2O \cdot Al_2O_3 \cdot 4SiO_2$—$CaO \cdot Al_2O_3 \cdot 2SiO_2$—$SiO_2$	132	
$K_2O \cdot Al_2O_3 \cdot 4SiO_2$—$CaO \cdot MgO \cdot 2SiO_2$—$SiO_2$	129	
$K_2O \cdot Al_2O_3 \cdot 4SiO_2$—$2MgO \cdot SiO_2$—$SiO_2$	J. F. Schairer (unpub.)	
$K_2O \cdot Al_2O_3 \cdot 6SiO_2$—$Na_2O \cdot Al_2O_3 \cdot 6SiO_2$—$CaO \cdot Al_2O_3 \cdot 2SiO_2$	52	Not completely ternary.
$K_2O \cdot Al_2O_3 \cdot 6SiO_2$—$Na_2O \cdot Al_2O_3 \cdot 6SiO_2$—$H_2O$	38	Not ternary at high temperatures.
$K_2O \cdot CO_2$—$K_2O \cdot SiO_2$—$K_2O \cdot 2SiO_2$	105, 106	
$K_2O \cdot MgO \cdot SiO_2$—$K_2O \cdot MgO \cdot 3SiO_2$—$K_2O \cdot 2SiO_2$	123	
$K_2O \cdot MgO \cdot SiO_2$—$K_2O \cdot MgO \cdot 3SiO_2$—$2MgO \cdot SiO_2$	123	
$K_2O \cdot MgO \cdot SiO_2$—$K_2O \cdot SiO_2$—$K_2O \cdot 2SiO_2$	123	
$K_2O \cdot MgO \cdot 3SiO_2$—$K_2O \cdot MgO \cdot 5SiO_2$—$2MgO \cdot SiO_2$	123	
$K_2O \cdot MgO \cdot 5SiO_2$—$K_2O \cdot 4SiO_2$—$SiO_2$	123	
$K_2O \cdot MgO \cdot 5SiO_2$—$2MgO \cdot SiO_2$—$SiO_2$	123	
$K_2O \cdot SiO_2$—$K_2O \cdot 2SiO_2$—$Na_2O \cdot SiO_2$	77	
$K_2O \cdot SiO_2$—$Na_2O \cdot SiO_2$—SiO_2	77	
$K_2O \cdot SiO_2$—SiO_2—H_2O	89	
$K_2O \cdot 2SiO_2$—$Na_2O \cdot SiO_2$—$Na_2O \cdot 2SiO_2$	77	
$K_2O \cdot 2SiO_2$—$Na_2O \cdot 2SiO_2$—SiO_2	77	
$Li_2O \cdot SiO_2$—$Na_2O \cdot SiO_2$—SiO_2	80	
$Li_2O \cdot SiO_2$—$Na_2O \cdot 2SiO_2$—SiO_2	80	
MgO—Al_2O_3—SiO_2	58, 70, 119, J. F. Schairer (in press)	
MgO—SiO_2—H_2O	37	
Na_2O—Al_2O_3—SiO_2	131	

TERNARY SYSTEMS (*Cont.*)

Components	References	Remarks
Na_2O—B_2O_3—H_2O	G. W. Morey (unpub.)	
Na_2O—B_2O_3—SiO_2	92	
Na_2O—CaO—SiO_2	58, 95	
Na_2O—FeO—SiO_2	J. F. Schairer, R. D. Thwaite (unpub.), see 156	
Na_2O—Fe_2O_3—SiO_2	28, 35	
Na_2O—MgO—SiO_2	58, G. W. Morey (unpub.)	Miscibility data.
Na_2O—P_2O_5—H_2O	64	
Na_2O—SiO_2—H_2O	Morey, Hesselgesser (unpub.), see 155, 156	
$Na_2O \cdot Al_2O_3 \cdot 6SiO_2$—$CaO \cdot Al_2O_3 \cdot 2SiO_2$—$CaO \cdot MgO \cdot 2SiO_2$	19, 20	
$Na_2O \cdot Al_2O_3 \cdot 6SiO_2$—$CaO \cdot Al_2O_3 \cdot 2SiO_2$—$SiO_2$	J. F. Schairer (unpub.)	
$Na_2O \cdot CO_2$—$NaOH$—H_2O	96	
$Na_2O \cdot SiO_2$—$CaO \cdot SiO_2$—SiO_2	95	
$Na_2O \cdot SiO_2$—Fe_2O_3—SiO_2	36	
O—Cu—CuO	122	
O—Cu_2O—CuO	140	
O—Fe_3O_4—Fe_2O_3	61, 63	
ZnO—B_2O_3—SiO_2	66	

THREE-END-MEMBER JOINS

Composition	References	Remarks
$CaO \cdot Al_2O_3 \cdot 2SiO_2$—$2CaO \cdot Al_2O_3 \cdot SiO_2$—FeO	125	
$CaO \cdot Al_2O_3 \cdot 2SiO_2$—$CaO \cdot SiO_2$—FeO	125	
$CaO \cdot Al_2O_3 \cdot 2SiO_2$—FeO—$Al_2O_3$	125	
$CaO \cdot Al_2O_3 \cdot 2SiO_2$—FeO—$SiO_2$	125	
$CaO \cdot Al_2O_3 \cdot 2SiO_2$—$2MgO \cdot SiO_2$—$SiO_2$	11, 12	Almost completely ternary.
$2CaO \cdot Al_2O_3 \cdot SiO_2$—$CaO \cdot SiO_2$—FeO	125	
$2CaO \cdot MgO \cdot 2SiO_2$—$CaO \cdot SiO_2$—FeO	133	
$CaO \cdot SiO_2$—FeO—MgO	133	
FeO—$2FeO \cdot 2Al_2O_3 \cdot 5SiO_2$—$2MgO \cdot 2Al_2O_3 \cdot 5SiO_2$	M. L. Keith (unpub.), see 155	
FeO—MgO—$2Al_2O_3 \cdot 5SiO_2$	M. L. Keith (unpub.), see 155	
FeO—$2MgO \cdot 2Al_2O_3 \cdot 5SiO_2$—$MgO \cdot SiO_2$	M. L. Keith (unpub.), see 155	
$K_2O \cdot Al_2O_3 \cdot 4SiO_2$—$K_2O \cdot MgO \cdot 3SiO_2$—$K_2O \cdot MgO \cdot 5SiO_2$	J. F. Schairer (in press), see 155	
$K_2O \cdot Al_2O_3 \cdot 4SiO_2$—$K_2O \cdot MgO \cdot 3SiO_2$—$2MgO \cdot SiO_2$	J. F. Schairer (in press), see 155	
$K_2O \cdot Al_2O_3 \cdot 4SiO_2$—$K_2O \cdot MgO \cdot 3SiO_2$—$SiO_2$	J. F. Schairer (in press), see 155	
$K_2O \cdot Al_2O_3 \cdot 4SiO_2$—$K_2O \cdot MgO \cdot 5SiO_2$—$SiO_2$	J. F. Schairer (in press), see 155	
$K_2O \cdot Al_2O_3 \cdot 4SiO_2$—$2MgO \cdot 2Al_2O_3 \cdot 5SiO_2$—$MgO \cdot SiO_2$	J. F. Schairer (in press)	
$K_2O \cdot Al_2O_3 \cdot 4SiO_2$—$2MgO \cdot 2Al_2O_3 \cdot 5SiO_2$—$2MgO \cdot SiO_2$	J. F. Schairer (in press)	
$K_2O \cdot Al_2O_3 \cdot 4SiO_2$—$2MgO \cdot 2Al_2O_3 \cdot 5SiO_2$—$SiO_2$	J. F. Schairer (in press)	
$K_2O \cdot Al_2O_3 \cdot 6SiO_2$—$2MgO \cdot 2Al_2O_3 \cdot 5SiO_2$—$3Al_2O_3 \cdot 2SiO_2$	J. F. Schairer (in press), see 155	
$K_2O \cdot MgO \cdot 5SiO_2$—$K_2O \cdot 5MgO \cdot 12SiO_2$—$2MgO \cdot SiO_2$	123	
$K_2O \cdot MgO \cdot 5SiO_2$—$K_2O \cdot 5MgO \cdot 12SiO_2$—$SiO_2$	123	
$K_2O \cdot MgO \cdot SiO_2$—$K_2O \cdot 2SiO_2$—$K_2O \cdot 4SiO_2$	123	
$Na_2O \cdot Al_2O_3 \cdot 2SiO_2$—$Na_2O \cdot Al_2O_3 \cdot 6SiO_2$ —$CaO \cdot Al_2O_3 \cdot 2SiO_2$	J. F. Schairer (unpub.)	β—Al_2O_3 is found.

THREE-END-MEMBER JOINS (*Cont.*)

Composition	References	Remarks
$Na_2O \cdot Al_2O_3 \cdot 2SiO_2$—$CaO \cdot MgO \cdot 2SiO_2$—$SiO_2$	J. F. Schairer (unpub.), see 156	
$Na_2O \cdot Al_2O_3 \cdot 2SiO_2$—FeO—$SiO_2$	33	
$Na_2O \cdot Al_2O_3 \cdot 2SiO_2$—$Na_2O \cdot Fe_2O_3 \cdot 4SiO_2$—$5Na_2O \cdot Fe_2O_3 \cdot 8SiO_2$	J. F. Schairer, R. D. Thwaite (unpub.), see 155, 156	
$Na_2O \cdot Al_2O_3 \cdot 2SiO_2$—$Na_2O \cdot Fe_2O_3 \cdot 4SiO_2$—$Na_2O \cdot 2SiO_2$	J. F. Schairer, R. D. Thwaite unpub.), see 155, 156	
$Na_2O \cdot Al_2O_3 \cdot 2SiO_2$—$Na_2O \cdot Fe_2O_3 \cdot 4SiO_2$—$SiO_2$	J. F. Schairer, R. D. Thwaite (unpub.), see 156	
$Na_2O \cdot Al_2O_3 \cdot 2SiO_2$—$Na_2O \cdot SiO_2$—$Na_2O \cdot 2SiO_2$	144	
$Na_2O \cdot Al_2O_3 \cdot 6SiO_2$—$Na_2O \cdot Fe_2O_3 \cdot 4SiO_2$—$Na_2O \cdot 2SiO_2$	J. F. Schairer, R. D. Thwaite (unpub.), see 156	
$Na_2O \cdot 4SiO_2$—Al_2O_3—Fe_2O_3	J. F. Schairer, R. D. Thwaite (unpub.), see 155, 156	

QUATERNARY SYSTEMS

Components	References	Remarks
CaO—FeO—Al_2O_3—SiO_2	125	
CaO—FeO—MgO—SiO_2	133	
CaO—MgO—Al_2O_3—SiO_2	11, 39, 47, 107, 109	
CuO—Fe_2O_3—SO_3—H_2O	145	
FeO—Al_2O_3—Fe_2O_3—SiO_2	59	Miscibility data.
FeO—MgO—Al_2O_3—SiO_2	M. L. Keith (unpub.), see 155	
K_2O—Al_2O_3—SiO_2—H_2O	O. F. Tuttle (unpub.)	
K_2O—CaO—Al_2O_3—SiO_2	132	

Quaternary Systems (*Cont.*)

Components	References	Remarks
K_2O—MgO—Al_2O_3—SiO_2	J. F. Schairer (in press)	
K_2O—Na_2O—Al_2O_3—SiO_2	126, 128	
K_2O—SiO_2—CO_2—H_2O	97	
$K_2O \cdot Al_2O_3 \cdot 6SiO_2$—$Na_2O \cdot Al_2O_3 \cdot 6SiO_2$—$SiO_2$—$H_2O$	N. L. Bowen, O. F. Tuttle (unpub.)	Not entirely quaternary.
MgO—Al_2O_3—SiO_2—H_2O	148	
$NaCl$—NaF—Na_2SO_4—H_2O	51	
Na_2O—Al_2O_3—Fe_2O_3—SiO_2	136, J. F. Schairer (unpub.), see 156	
Na_2O—Al_2O_3—SiO_2—H_2O	G. W. Morey (unpub.)	
Na_2O—CaO—Al_2O_3—SiO_2	14, 15, H. S. Yoder (in press)	
Na_2O—CaO—B_2O_3—SiO_2	90	
Na_2O—FeO—Al_2O_3—SiO_2	31, 33	
Na_2O—MgO—SiO_2—H_2O	G. W. Morey (unpub.)	
$Na_2O \cdot Al_2O_3 \cdot 2SiO_2$—$CaO \cdot Al_2O_3 \cdot 2SiO_2$—$2CaO \cdot Al_2O_3 \cdot SiO_2$—$CaO \cdot SiO_2$	H. S. Yoder (in press)	

Four-End-Member Join

Components	References	Remarks
$K_2O \cdot Al_2O_3 \cdot 4SiO_2$—$2MgO \cdot SiO_2$—$2MgO \cdot 2Al_2O_3 \cdot 5SiO_2$—$SiO_2$	J. F. Schairer (in press)	

Quinary Systems

Components	References	Remarks
K_2O—CaO—MgO—Al_2O_3—SiO_2	129	
Na_2O—CaO—MgO—Al_2O_3—SiO_2	19, 20, 156, J. F. Schairer (unpub.)	
K_2O—Na_2O—Al_2O_3—SiO_2—H_2O	N. L. Bowen, O. F. Tuttle (unpub.)	

REFERENCES

1. Adams, L. H., 1914. Calibration tables for copper-constantan and platinum-platinrhodium thermoelements: Am. Chemical Soc. Jour., vol. 36, pp. 65-72.
2. Adams, L. H., 1931. Equilibrium in binary systems under pressure. I. An experimental and thermodynamic investigation of the system, NaCl—H_2O, at 25°: Am. Chemical Soc. Jour., vol. 53, pp. 3769-3813.
3. Adams, L. H., 1932. Equilibrium in binary systems under pressure. II. The system, K_2SO_4—H_2O at 25°: Am. Chemical Soc Jour., vol. 54, pp. 2229-2243.
4. Adams, L. H., 1938. The freezing point—solubility curves of hydrates and other compounds under pressure: AM. JOUR. SCI., 5th ser., vol. 35-A, pp. 1-18.
5. Adams, L. H., and Gibson, R. E., 1930. The melting curve of sodium chloride dihydrate. An experimental study of an incongruent melting at pressures up to twelve thousand atmospheres: Am. Chemical Soc. Jour., vol. 52, pp. 4252-4264.
6. Adams, L. H., and Gibson, R. E., 1932. Equilibrium in binary systems under pressure. III. The influence of pressure on the solubility of ammonium nitrate in water at 25°: Am. Chemical Soc. Jour., vol. 54, pp. 4520-4537.
7. Adams, L. H., and Hall, R. E., 1931. The influence of pressure on the solubility of sodium chloride in water. A new method for the measurement of the solubilities of electrolytes under pressure: Washington Acad. Sci. Jour., vol. 21, pp. 183-194.
8. Allen, E. T., White, W. P., and Wright, F. E., 1906. On wallastonite and pseudo-wallastonite—polymorphic forms of calcium metasilicate: AM. JOUR. SCI., 4th ser., vol. 21, pp. 89-108.
9. Allen, E. T., and White, W. P., 1909. Diopside and its relations to calcium and magnesium metasilicates (with optical study by F. E. Wright and Esper S. Larsen): AM. JOUR. SCI., 4th ser., vol. 27, pp. 1-47.
10. Allen, E. T., Wright, F. E., and Clement, J. K., 1906. Minerals of the composition $MgSiO_3$; a case of tetramorphism: AM. JOUR. SCI., 4th ser., vol. 22, pp. 385-438.
11. Andersen, Olaf, 1915. The system anorthite—forsterite—silica: AM. JOUR. SCI., 4th ser., vol. 39, pp. 407-454.
12. Andersen, Olaf, 1916. Das System: Anorthit—Forsterit—Kieselsäure: Neues Jahrb., Beilage—Band 40, pp. 701-758.
13. Andersen, Olaf, and Bowen, N. L., 1914. Das binäre System Magnesiumoxyd-Silicium-2-oxyd: Zeitschr. anorg. Chemie, vol. 87, pp. 283-299.
14. Bowen, N. L., 1912. The binary system: $Na_2Al_2Si_2O_8$ (nephelite, carnegieite)—$CaAl_2Si_2O_8$ (anorthite): AM. JOUR. SCI., 4th ser., vol. 33, pp. 551-573.
15. Bowen, N. L., 1913. The melting phenomena of the plagioclase feldspars: AM. JOUR. SCI., 4th ser., vol. 35, pp. 577-599.
16. Bowen, N. L., 1913. Die Schmelzerscheinungen bei den Plagioklas-Feldspaten: Zeitschr. anorg. Chemie, vol. 82, pp. 283-307.
17. Bowen, N. L., 1914. The ternary system: diopside—forsterite—silica: AM JOUR. SCI., 4th ser., vol. 38, pp. 207-264.
18. Bowen, N. L., 1914. Das ternäre System: Diopsid-Forsterit-Silicium-2-oxyd: Zeitschr. anorg. Chemie, vol. 90, pp. 1-66.

19. Bowen, N L., 1915. The crystallization of haplobasaltic, haplodioritic, and related magmas: Am. Jour. Sci., 4th ser., vol. 40, pp. 161-185.
20. Bowen, N. L., 1916. Das Ternäre System: Diopsid-Anorthit-Albit: Zeitschr. anorg. allg. Chem., vol. 94, pp. 23-50.
21. Bowen, N. L., 1917. The sodium-potassium nephelites: Am. Jour. Sci., 4th ser., vol. 43, pp. 115-132.
22. Bowen, N. L., 1922. Genetic features of alnoitic rocks from Isle Cadieux, Quebec: Am. Jour. Sci., 5th ser., vol. 3, pp. 1-34.
23. Bowen, N. L., and Andersen, Olaf, 1914. The binary system MgO—SiO_2: Am. Jour. Sci., 4th ser. vol. 37, pp. 487-500.
24. Bowen, N. L., and Greig, J. W., 1924. The system; Al_2O_3—SiO_2: Am. Ceramic Soc. Jour., vol. 7, pp. 238-254.
25. Bowen, N. L., and Greig, J. W., 1925. The crystalline modifications of $NaAlSiO_4$: Am. Jour. Sci., 5th ser., vol. 10, pp. 204-212.
26. Bowen, N. L., Greig, J. W., and Zies, E. G., 1924. Mullite, a silicate of alumina: Washington Acad. Sci. Jour., vol. 14, pp. 183-191.
27. Bowen, N. L., and Schairer, J. F., 1929. The system: leucite—diopside: Am. Jour. Sci., 5th ser., vol. 18, pp. 301-312.
28. Bowen, N. L., and Schairer, J. F., 1929. The fusion relations of acmite: Am. Jour. Sci., 5th ser., vol. 18, pp. 365-374.
29. Bowen, N. L., and Schairer, J. F., 1932. The system FeO—SiO_2: Am. Jour. Sci., 5th ser., vol. 24, pp. 177-213.
30. Bowen, N. L., and Schairer, J. F., 1935. The system MgO—FeO—SiO_2: Am. Jour. Sci., 5th ser., vol. 29, pp. 151-217.
31. Bowen, N. L., and Schairer, J. F., 1936. The system, albite-fayalite: Nat. Acad. Sci. Proc., vol. 22, pp. 345-350.
32. Bowen, N. L., and Schairer, J. F., 1936. The problem of the intrusion of dunite in the light of the olivine diagram. 16th Internat. Geol. Cong. Rept., pp. 391-396.
33. Bowen, N. L., and Schairer, J. F., 1938. Crystallization equilibrium in nepheline-albite-silica mixtures with fayalite: Jour. Geology, vol. 46, pp. 397-411.
34. Bowen, N. L., Schairer, J. F., and Posnjak, E., 1933. The system, Ca_2SiO_4—Fe_2SiO_4: Am. Jour. Sci., 5th ser., vol. 25, pp. 273-297.
35. Bowen, N. L., Schairer, J. F., and Posnjak, E., 1933. The system, CaO—FeO—SiO_2: Am. Jour. Sci., 5th ser., vol. 26, pp. 193-284.
36. Bowen, N. L., Schairer, J. F., and Willems, H. W. V., 1930. The ternary system: Na_2SiO_3—Fe_2O_3—SiO_2: Am. Jour. Sci., 5th ser., vol. 20, pp. 405-455.
37. Bowen, N. L., and Tuttle, O. F., 1949. The system MgO—SiO_2—H_2O: Geol. Soc. America Bull., vol. 60, pp. 439-460.
38. Bowen, N. L., and Tuttle, O. F., 1950. The system $NaAlSi_3O_8$—$KAlSi_3O_8$—H_2O: Jour. Geology, vol. 58, pp. 489-511.
39. Buddington, A. F., 1922. On some natural and synthetic melilites: Am. Jour. Sci., 5th ser., vol. 3, pp. 35-87.
40. Davis, G. L., and Tuttle, O. F., 1952. Two new crystalline phases of the anorthite composition, $CaO \cdot Al_2O_3 \cdot 2SiO_2$: Am. Jour. Sci., present vol.
41. Day, A. L., and Allen, E. T., 1905. The isomorphism and thermal properties of the feldspars. Part I. Thermal study; Iddings, J. P., Part II, Optical study: Carnegie Inst. Washington Pub. 31.
42. Day, A. L., and Allen, E. T., 1905. The isomorphism and thermal properties of the feldspars: Am. Jour. Sci., 4th ser., vol. 19, pp. 93-142.

43. Day, A. L., and Allen, E. T., 1905. Der Isomorphismus und die thermischen Eigenschaften der Feldspate: Zeitschr. physikal. Chemie, vol. 54, pp. 1-54.

44. Day, A. L., and Shepherd, E. S., 1906. The lime-silica series of minerals (with optical study by F. E. Wright): Am. Jour. Sci., 4th ser., vol. 22, pp. 265-302.

45. Day, A. L., and Shepherd, E. S., 1906. The lime-silica series of minerals: Am. Chemical Soc. Jour., vol. 28, pp. 1089-1114.

46. Eskola, Pentti, 1922. The silicates of strontium and barium: Am. Jour. Sci., 5th ser., vol. 4, pp. 331-375.

47. Ferguson, J. B., and Buddington, A. F., 1920. The binary system akermanite-gehlenite: Am. Jour. Sci., 4th ser., vol. 50, pp. 131-140.

48. Ferguson, J. B., and Merwin, H. E., 1919. The ternary system CaO—MgO—SiO_2: Nat. Acad. Sci. Proc., vol. 5, pp. 16-18.

49. Ferguson, J. B., and Merwin, H. E., 1919. The ternary system CaO—MgO—SiO_2: Am. Jour. Sci., 4th ser., vol. 48, pp. 81-123.

50. Ferguson, J. B., and Merwin, H. E., 1919. Wollastonite and related solid solutions in the ternary system lime—magnesia—silica: Am. Jour. Sci., 4th ser., vol. 48, pp. 165-189.

51. Foote, H. W., and Schairer, J. F., 1930. The system Na_2SO_4—NaF—NaCl—H_2O. I. The ternary systems with water and two salts. II. The quaternary system at 25° and 35°: Am. Chemical Soc. Jour., vol. 52, pp. 4202-4217.

52. Franco, R. R., and Schairer, J. F., 1951. Liquidus temperatures in mixtures of the feldspars of soda, potash, and lime: Jour. Geology, vol. 59, pp. 259-267.

53. Gibson, R. E., 1927. The system sodium sulphate-water: I. The densities and specific volumes of aqueous solutions of sodium suphate between 25° and 40°, and the fictive volumes of sodium sulphate in solution: Jour. Physical Chem., vol. 31, pp. 496-510.

54. Goranson, R. W., 1936. Silicate—water systems: the solubility of water in albite-melt: Am. Geophys. Union Trans., 17th Ann. Meeting, pp. 257-259. (Nat. Res. Council, Washington, D. C.)

55. Goranson, R. W., 1938. High temperature and pressure phase equilibria in the albite—water and orthoclase—water systems: Am. Geophys. Union Trans., 19th Ann. Meeting, pp. 271-273. (Nat. Res. Council, Washington, D. C.)

56. Goranson, R. W., 1938. Silicate—water systems: Phase equilibria in the $NaAlSi_3O_8$—H_2O and $KAlSi_3O_8$—H_2O systems at high temperatures and pressures: Am. Jour. Sci., 5th ser., vol. 35-A, pp. 71-91.

57. Goranson, R. W., and Kracek, F. C., 1932. An experimental investigation of the phase relations of $K_2Si_4O_9$ under pressure: Jour. Physical Chem., vol. 36, pp. 913-926.

58. Greig, J. W., 1927. Immiscibility in silicate melts: Am. Jour. Sci., 5th ser., vol. 13, pp. 1-44, 133-154.

59. Greig, J .W., 1927. On liquid immiscibility in the system FeO—Fe_2O_3—Al_2O_3—SiO_2: Am. Jour. Sci., 5th ser., vol. 14, pp. 473-484.

60. Greig, J. W., and Barth, Tom. F. W., 1938. The system, $Na_2O \cdot Al_2O_3 \cdot 2SiO_2$ (nephelite, carnegieite)—$Na_2O \cdot Al_2O_3 \cdot 6SiO_2$ (albite): Am. Jour. Sci., 5th ser., vol. 35-A, pp. 93-112.

61. Greig, J. W., Posnjak, E., Merwin, H. E., and Sosman, R. B., 1935. Equilibrium relationships of Fe_3O_4, Fe_2O_3, and oxygen: Am. Jour. Sci., 5th ser., vol. 30, pp. 239-316.

62. Hall, F. P., and Insley, H. Phase diagrams for ceramists. Issued as Part II of the November 1947 issue of The Journal of the American Ceramic Society.

63. Hostetter, J. C., and Sosman, R. B., 1916. The dissociation of ferric oxide in air: Am. Chemical Soc. Jour., vol. 38, pp. 1188-1198.

64. Ingerson, E., and Morey, G. W., 1943. Preparation and properties of some compounds in the system H_2O—Na_2O—P_2O_5: Am. Mineralogist vol. 28, pp. 448-455.

65. Ingerson, E., and Morey, G. W., 1951. Double flourides of zinc: Am. Mineralogist, vol. 36, pp. 778-780.

66. Ingerson, E., Morey, G. W., and Tuttle, O. F., 1948. The systems K_2O—ZnO—SiO_2, ZnO—B_2O_3—SiO_2, and Zn_2SiO_4—Zn_2GeO_4: Am. Jour. Sci., vol. 246, pp. 31-40.

67. Jensen, E., 1947. The system silver sulfide—antimony trisulfide: Norske vidensk.-akad. Oslo, Mat.-naturv. Kl., no. 2.

68. Johnston, J., 1910. The thermal dissociation of calcium carbonate: Am. Chemical Soc. Jour., vol. 32, pp. 938-946.

69. Johnston, J., and Williamson, E. D., 1916. The complete solubility curve of calcium carbonate: Am. Chemical Soc. Jour., vol. 38, pp. 975-983.

70. Keith, M. L., and Schairer, J. F., 1952. The stability field of saphirine in the system MgO—Al_2O_3—SiO_2: Jour. Geology, vol. 60, pp. 181-186.

71. Kracek, F. C., 1930. Vapor pressures of solutions and the Ramsay-Young rule. Application to the complete system water—ammonia: Jour. Physical Chem., vol. 34, pp. 499-521.

72. Kracek, F. C., 1930. The cristobalite liquidius in the alkali oxide-silica systems and the heat of fusion of cristobalite: Am. Chemical Soc. Jour., vol. 52, pp. 1436-1442.

73. Kracek, F. C., 1930. The system sodium oxide—silica: Jour. Physical Chem., vol. 34, pp. 1583-1598.

74. Kracek, F. C., 1930. The binary system Li_2O—SiO_2: Jour. Physical Chem., vol. 34, pp. 2641-2650.

75. Kracek, F. C., 1931: Solubilities in the system water—iodine to 200°: Jour. Physical Chem., vol 35, pp. 417-422.

76. Kracek, F. C., 1931. The solubility of potassium iodide in water to 240°: Jour. Physical Chem., vol. 35, pp. 947-949.

77. Kracek, F. C., 1932. The ternary system, K_2SiO_3—Na_2SiO_3—SiO_2: Jour. Physical Chem., vol. 36, pp. 2529-2542.

78. Kracek, F. C., 1936. Solubility in the system, KCNS—H_2O: Washington Acad. Sci. Jour., vol. 26, pp. 307-313.

79. Kracek, F. C., 1939. Phase equilibrium relations in the system, Na_2SiO_3—Li_2SiO_3: Am. Chemical Soc. Jour., vol. 61, pp. 2157-2161.

80. Kracek, F. C., 1939. Phase equilibrium relations in the system, Na_2SiO_3—Li_2SiO_3—SiO_2: Am. Chemical Soc. Jour., vol. 61, pp. 2863-2877.

81. Kracek, F. C., 1946. Phase relations in the system sulfur—silver and the transitions in silver sulfide: Am. Geophys. Union Trans., vol. 27, pp. 364-374.

82. Kracek, F. C., Bowen, N. L., and Morey, G. W., 1929. The system potassium metasilicate—silica: Jour. Physical Chem., vol. 33, pp. 1857-1879.

83. Kracek, F. C., Bowen, N. L., and Morey, G. W., 1937. Equilibrium relations and factors influencing their determination in the system K_2SiO_3—SiO_2: Jour. Physical Chem., vol. 41, pp. 1183-1193.

84. Kracek, F. C., Morey, G. W., and Merwin, H. E., 1938. The system, water-boron oxide: Am. Jour. Sci., 5th ser., vol. 35-A, pp. 143-171.

85. Kracek, F. C., 1951. Phase transformations in one-component silicate systems. *In* Smoluchowski, Mayer, and Weyl, Phase transformations in solids, John Wiley & Sons, Inc., New York. pp. 257-277.

86. Merwin, H. E., Lombard, R. H., and Allen, E. T., 1923. Cubanite: identity with chalmersite; magnetic properties: Am. Mineralogist, vol. 8, pp. 135-137.

87. Merwin, H. E., and Lombard, R. H., 1937. The system, Cu—Fe—S: Econ. Geology, vol. 32, pp. 203-284.

88. Morey, G. W., 1914. New crystalline silicates of potassium and sodium, their preparation and general properties: Am. Chemical Soc. Jour., vol. 36, pp. 215-230.

89. Morey, G. W., 1917. The ternary system H_2O—K_2SiO_3—SiO_2 (microscopic study by C. N. Fenner): Am. Chemical Soc. Jour., vol. 39, pp. 1173-1229.

90. Morey, G. W., 1932. The effect of boric oxide on the devitrification of the soda-lime-silica glasses. The quarternary system, Na_2O—CaO—B_2O_3—SiO_2: Am. Ceramic Soc. Jour., vol. 15, pp. 457-475.

91. Morey, G. W., 1942. Solubility of solids in water vapor: Am. Soc. Testing Materials Proc., vol. 42, pp. 980-988.

92. Morey, G. W., 1951. The ternary system Na_2O—B_2O_3—SiO_2: Soc. Glass Technology Jour., vol. 35, pp. 270-283.

93. Morey, G. W., and Bowen, N. L., 1922. The melting of potash feldspar. Am. Jour. Sci., 5th ser., vol. 4, pp. 1-21.

94. Morey, G. W., and Bowen, N. L., 1924. The binary system sodium metasilicate-silica: Jour. Physical Chem., vol. 28, pp. 1167-1179.

95. Morey, G. W., and Bowen, N. L., 1925. The ternary system sodium metasilicate-calcium metasilicate-silica: Soc. Glass Technology Jour., vol. 9, pp. 226-264.

96. Morey, G. W., and Burlew, J. S., 1938. Studies of solubility in systems containing alkali and water: I. General Introduction. II. A filter autoclave for solubility measurements at elevated temperatures and atmospheric pressure. III. Solubility of NaOH in a saturated Na_2CO_3 solution between 60 and 70° C.: Am. Jour. Sci., 5th ser., vol. 35-A, pp. 185-215.

97. Morey, G. W., and Fleischer, M., 1940. Equilibrium between vapor and liquid phases in the system CO_2—H_2O—K_2O—SiO_2: Geol. Soc. America Bull. 51, pp. 1035-1057.

98. Morey, G. W., and Hesselgesser, J. M., 1951. The solubility of quartz and some other substances in superheated steam at high pressures: Am. Soc. Mechanical Engineers Trans., October 1951, pp. 865-875.

99. Morey, G. W., and Hesselgesser, J. M., 1951. The solubility of some minerals in superheated steam at high pressures: Econ. Geology, vol. 46, pp. 821-835.

100. Morey, G. W., and Ingerson, E., 1937. The melting of danburite: A study of liquid immiscibility in the system, CaO—B_2O_3—SiO_2: Am. Mineralogist, vol. 22, pp. 37-47.

101. Morey, G. W., and Ingerson, E., 1938. The system, water-sodium disilicate: Am. Jour. Sci., 5th ser., vol. 35-A, pp. 217-225.

102. Morey, G. W., and Ingerson, E., 1944. The binary system $NaPO_3$—$Na_4P_2O_7$: Am. Jour. Sci., vol. 242, pp. 1-6.

103. Morey, G. W., Kracek, F. C., and Bowen, N. L., 1930. The ternary system K_2O—CaO—SiO_2 (with correction): Soc. Glass Technology Jour., vol. 14, pp. 149-187.

104. Morey, G. W., and Merwin, H. E., 1936. Phase equilibrium relationships in the binary system, sodium oxide-boric oxide, with some measurements of the optical properties of the glasses: Am. Chemical Soc. Jour., vol. 58, pp. 2248-2254.

105. Niggli, Paul, 1913. The phenomena of equilibria between silica and the alkali carbonates: Am. Chemical Soc. Jour., vol. 35, pp. 1693-1727.

106. Niggli, Paul, 1913. Gleichgewichtserscheinungen zwischen Alkalicarbonaten und Kieselsäure: Zeitschr. anorg. Chemie, vol. 84, pp. 229-272.

107. Osborn, E. F., 1942. The system $CaSiO_3$—diopside—anorthite: Am. Jour. Sci., vol. 240, pp. 751-788.

108. Osborn, E. F., 1943. The compound merwinite ($3CaO.MgO.2SiO_2$) and its stability relations within the system CaO—MgO—SiO_2. (Preliminary report.): Am. Ceramic Soc. Jour., vol. 26, pp. 321-332.

109. Osborn, E. F., and Schairer, J. F., 1941. The ternary system pseudowollastonite—akermanite—gehlenite: Am. Jour. Sci., vol. 239, pp. 715-763.

110. Posnjak, E., 1938. The system, $CaSO_4$—H_2O: Am. Jour. Sci., 5th ser., vol. 35-A, pp. 247-272.

111. Posnjak, E., and Merwin, H. E., 1919. The hydrated ferric oxides: Am. Jour. Sci., 4th ser., vol. 47, pp. 311-348.

112. Posnjak, E., and Merwin, H. E., 1922. The system Fe_2O_3—SO_3—H_2O: Am. Chemical Soc. Jour., vol. 44, pp. 1965-1994.

113. Posnjak, E., and Tunell, G., 1929. The system, cupric oxide-sulphur trioxide-water: Am. Jour. Sci., 5th ser., vol. 18, pp. 1-34.

114. Rankin, G. A., 1912. Beitrag Zur Untersuchung der Portlandzementklinker. Ueber die hypothetische Verbindung $8CaO \cdot Al_2O_3 \cdot 2SiO_2$: (Nebst optischen Untersuchungen, by F. E. Wright). Zeitschr. anorg. Chemie, vol. 75, pp. 63-66.

115. Rankin, G. A., 1915. Das ternäre System: CaO—Al_2O_3—SiO_2 (Nebst optischen Studien, by F. E. Wright): Zeitschr. anorg. allg. Chemie, vol. 92, pp. 213-296.

116. Rankin, G. A., 1915. The ternary system CaO—Al_2O_3—SiO_2 (with optical study by F. E. Wright): Am. Jour. Sci., 4th ser., vol. 39, pp. 1-79.

117. Rankin, G. A., and Merwin, H. E., 1916. The ternary system CaO—Al_2O_3—MgO: Am. Chemical Soc. Jour., vol. 38, pp. 568-588.

118. Rankin, G. A. and Merwin, H. E., 1916. Das ternäre System: Calciumoxyd—Alminumoxyd—Magnesiumoxyd.; Zeitschr. anorg. allg. Chemie, vol. 96, pp. 291-316.

119. Rankin, G. A., and Merwin, H. E., 1918. The ternary system MgO—Al_2O_3—SiO_2: Am. Jour. Sci., 4th ser., vol. 45, pp. 301-325.

120. Roberts, H. S., 1935. Polymorphism in the FeS—S solid solutions: I. Thermal study: Am. Chemical Soc. Jour., vol. 57, pp. 1034-1038.

121. Roberts, H. S., and Merwin, H. E., 1931. The system MgO—FeO—Fe_2O_3 in air at one atmosphere: Am. Jour. Sci., 5th ser., vol. 21, pp. 145-157.

122. Roberts, H. S., and Smyth, F. H., 1921. The system copper: cupric oxide: oxgyen: Am. Chemical Soc. Jour., vol. 43, pp. 1061-1079.

123. Roedder, E. W., 1951. The system K_2O—MgO—SiO_2: Am. Jour. Sci., vol. 249, pp. 81-130, 224-248.

124. Sahama, Th. G., and Torgeson, D. R., 1949. Some examples of the application of thermochemistry to petrology: Jour. Geology, vol. 57, No. 3, pp. 255-262.

125. Schairer, J. F., 1942. The system CaO—FeO—Al_2O_3—SiO_2: I. Results of quenching experiments on five joins: Am. Ceramic Soc. Jour., vol. 25, pp. 241-274.

126. Schairer, J. F., 1950. The alkali—feldspar join in the system $NaAlSiO_4$—$KAlSiO_4$—SiO_2: Jour. Geology, vol. 58, pp. 512-517.

127. Schairer, J. F., 1951. Phase transformations in polycomponent silicate systems. *In* Smoluchowski, Mayer, and Weyl, Phase transformations in solids, John Wiley & Sons, Inc., New York, pp. 278-295.

128. Schairer, J. F., and Bowen, N. L., 1935. Preliminary report on equilibrium-relations between feldspathoids, alkali-feldspars, and silica: Am. Geophys. Union Trans., 16th Ann. Meeting, pp. 325-328. (Nat. Res. Council, Washington, D. C.)

129. Schairer, J. F., and Bowen, N. L., 1938. The system, leucite—diopside—silica: Am. Jour. Sci., 5th ser., vol. 35-A, pp. 289-309.

130. Schairer, J. F., and Bowen, N. L., 1942. The binary system $CaSiO_3$—diopside and the relations between $CaSiO_3$ and akermanite: Am. Jour. Sci., vol. 240, pp. 725-742.

131. Schairer, J. F., and Bowen, N. L., 1947. Melting relations in the system Na_2O—Al_2O_3—SiO_2 and K_2O—Al_2O_3—SiO_2: Am. Jour. Sci., vol. 245, pp. 193-204.

132. Schairer, J. F., and Bowen, N. L., 1947. The system anorthite—leucite—silica: Soc. géol. Finlande Bull., vol. 20, pp. 67-87.

133. Schairer, J. F., and Osborn, E. F., 1950. The system CaO—MgO—FeO—SiO_2: I. Preliminary data on the join $CaSiO_3$—MgO—FeO: Am. Ceramic Soc. Jour., vol. 33, pp. 160-167.

134. Schairer, J. F., and Yagi, K., 1952. The system FeO—Al_2O_3—SiO_2: Am. Jour. Sci., present vol.

135. Shepherd, E. S., and Rankin, G. A., 1909. The binary systems of alumina with silica, lime and magnesia (with optical study by F. E. Wright): Am. Jour. Sci., 4th ser., vol. 28, pp. 293-333.

136. Shepherd, E. S., and Rankin, G. A., 1910. Die binären systeme, von Tonerde mit Kieselsäure, Kalk und Magnesia. (Nebst optischen Untersuchungen, by F. E. Wright.) Zeitschr. anorg. Chemie, vol. 68, pp. 370-420.

137. Shepherd, E. S., and Rankin, G. A., 1911. Preliminary report on the ternary system CaO—Al_2O_3—SiO_2: a study of the constitution of portland cement (with optical report by F. E. Wright): Ind. and Eng. Chemistry, vol. 3, pp. 211-227.

138. Shepherd, E. S., and Rankin, G. A., 1911. Vorläfiger Bericht über das ternäre System CaO—Al_2O_3—SiO_2. Eine Untersuchung über die Konstitution der Portlandzement Klinker. (Nebst optischen Untersuchungen, by F. E. Wright): Zeitschr. anorg. Chemie, vol. 71, pp. 19-64.

139. Smyth, F. H., and Adams, L. H., 1923. The system, calcium oxide-carbon dioxide: Am. Chemical Soc. Jour., vol. 45, pp. 1167-1184.

140. Smyth, F. H., and Roberts, J. S., 1920. The system cupric oxide, cuprous oxide, oxygen. Am. Chemical Soc. Jour., vol. 42, pp. 2582-2607.

141. Sosman, R. B., Hostetter, J. C., and Merwin, H. E., 1915. The dissociation of calcium carbonate below 500° C.: Washington Acad. Sci. Jour., vol. 5, pp. 563-569.

142. Sosman, R. B., and Hostetter, J. C., 1916. The oxides of iron: I. Solid solution in the system Fe_2O_3—Fe_3O_4: Am. Chemical Soc. Jour., vol. 38, pp. 807-833.

143. Sosman, R. B., and Merwin, H. E., 1916. Preliminary report on the system lime: ferric oxide: Washington Acad. Sci. Jour., vol. 6, pp. 532-537.

144. Tilley, C. E., 1933. The ternary system, Na_2SiO_3—$Na_2Si_2O_5$—$NaAlSiO_4$: Min. pet. Mitt., Zeitschr. Kristallographie, vol. 43, pp. 406-421.

145. Tunell, G., and Posnjak, E., 1931. A portion of the system, ferric oxide—cupric oxide—sulphur trioxide—water: Jour. Physical Chem., vol. 35, pp. 929-946.

146. Yoder, H. S., Jr., 1950. The jadeite problem: Am. Jour. Sci., vol. 248, pp. 225-248, 312-334.

147. Yoder, H. S., Jr., 1950. Stability relations of grossularite: Jour. Geology, vol. 58, No. 3, pp. 221-253.

148. Yoder, H. S., Jr., 1952. The MgO—Al_2O_3—SiO_2—H_2O System and the related metamorphic facies: Am. Jour. Sci., present vol.

149. Yoder, H. S., Jr., and Keith, M. L., 1951. Complete substitution of aluminum for silicon: the system $3MnO \cdot Al_2O_3 \cdot 3SiO_2$—$3Y_2O_3 \cdot 5Al_2O_3$: Am. Mineralogist, vol. 36, pp. 519-533.

150. Yoder, H. S. Jr., and Weir, C. E., 1951. Change of free energy with pressure of the reaction nepheline + albite = 2 jadeite: Am. Jour. Sci., vol. 249, pp. 683-694.

151. Adams, L. H., 1946. Annual report of the Director of the Geophysical Laboratory, 1945-1946: Carnegie Inst. Washington Year Book 45, pp. 23-35.

152. Adams, L. H., 1947. Annual report of the Director of the Geophysical Laboratory, 1946-1947: Carnegie Inst. Washington Year Book 46, pp. 27-51.

153. Adams, L. H., 1948. Annual report of the Director of the Geophysical Laboratory, 1947-1948: Carnegie Inst. Washington Year Book 47, pp. 27-51.

154. Adams, L. H., Annual report of the Director of the Geophysical Laboratory, 1948-1949: Carnegie Inst. Washington Year Book 48, pp. 29-55.

155. Adams, L. H., 1950. Annual report of the Director of the Geophysical Laboratory, 1949-1950: Carnegie Inst. Washington Year Book 49, pp. 27-59.

156 Adams, L. H., 1950. Annual report of the Director of the Geophysical Laboratory, 1950-1951: Carnegie Inst. Washington Year Book 50, pp. 33-63.

Geophysical Laboratory
Carnegie Institution of Washington
Washington, D. C.

THE DIFFERENTIATION OF A COMPOSITE APLITE FROM THE PRIBILOF ISLANDS, ALASKA

TOM. F. W. BARTH

ABSTRACT. The mode of occurrence and the field relations of an aplite intrusion are displayed by figure 1. The chilled margins show a higher content of alkalies and silica, but a lower content of Al, Fe, Mg, Ca, than does the coarse grained, granular central portion. This arrangement may be explained on the theory of thermodiffusion as described by W. Wahl, whereas crystallization differentiations would have resulted in the opposite arrangement.

INTRODUCTION

IN 1948 the author, working as a consultant to the Geological Survey, had an opportunity to visit the Pribilof Islands in the Bering Sea. It is hoped that a description of the geology and petrology of these islands soon will be published elsewhere. The subject of the present paper is simply the petrology of a composite aplite dike occurring on the southeastern shore of the island of St. George but showing no further relation to other rock types in the island.

I

The aplite is intrusive into massive peridotite and is overlaid by various glacial sediments which, in turn, are overlaid by recent lava flows of basaltic habit. The aplite is composite in character, exhibiting very fine grained chilled margins and a medium grained granular central portion. See map and profile in figure 1.

There is an appreciable difference in composition between the chilled-margin rock and the central-portion rock. The transition is gradual but seems to take place over a small distance (less than one meter); the width of the fine grained margins is about 10 m., the width of the total intrusion about 400 m.

In table 1 are listed the chemical composition, norm, and mode of the two portions of the dike.

The central portion is holocrystalline, granular, essentially consisting of plagioclase (strongly zoned oligoclase, $n \backsim 1.543$) in tabular subhedral crystals forming a sort of blocky mesh, with clear quartz filling the interstices between feldspars.

Fresh red garnet is present in very small amounts (n = 1790). Sericite has replaced a good deal of the plagioclase, in many cases beginning with the inner zone and leaving the rim relatively fresh. Chlorite occurs in elongated, unoriented shreds and in scaly masses between feldspars.

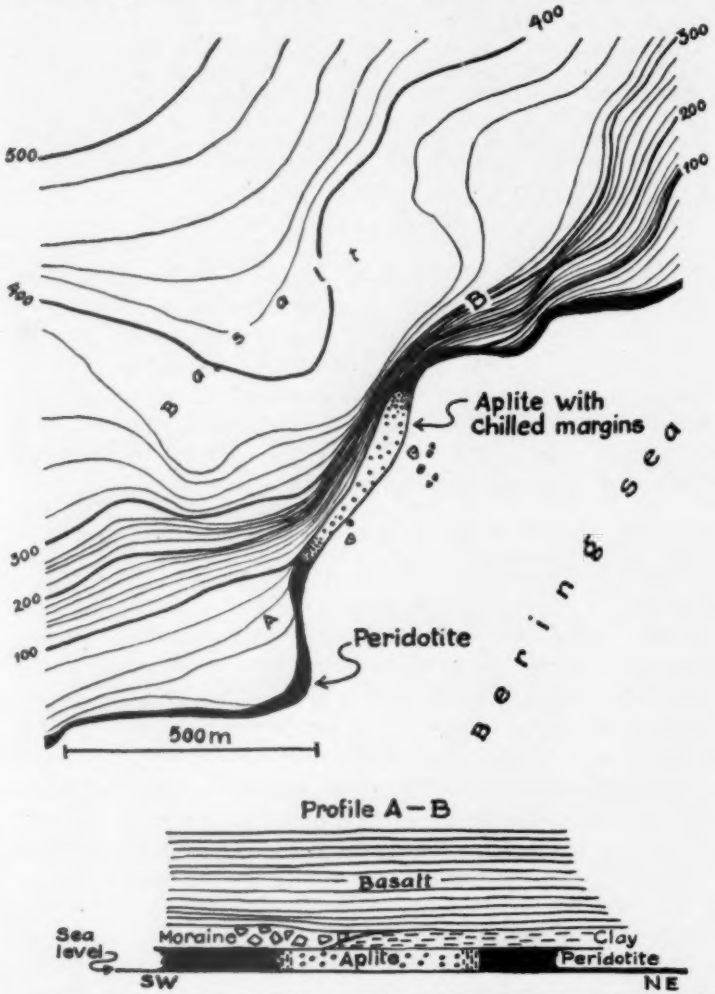

Fig.1. Map of aplite intrusion on the southeastern shore of St. George Island, Pribilof Group, Alaska. Curves of equal elevation are given for every 20 feet. Position 56° 34½' North, 169° 29½' East.

The marginal portions are made up of a very finely grained, almost dense rock with small, poorly defined phenocrysts of an albite-rich, non-perthitic alkali feldspar partly altered to sericite and quartz. The groundmass consists essentially of countless small, needlelike laths of albite-rich feldspar displaying a very definite subparallel orientation; they are altered and intergrown with quartz, sericite, chlorite, and a nameless yellowish powdery product, probably iron staining. A very small amount of garnet is present.

Nobody will doubt that the central and the marginal rock portions are genetically related. If formed according to the laws of crystallization differentiation, the marginal rock portion must correspond to a late fraction derived from the central-portion rock magma, for chemically the marginal rocks are higher in alkalies and silica, lower in lime and magnesia, and mineralogically the reaction series of the feldspars are more advanced in the marginal rocks than in the central rocks.

However, the mode of occurrence makes this genetical sequence impossible. Obviously the chilled margins congealed *before* the coarser-grained central portions. It seems hard to explain this fact by any of the following theories of magmatic differentiation: fractional crystallization, liquid immiscibility, gaseous transfer, or assimilation. Thus by a process of elimination, thermodiffusion, as described by Wahl (1946), presents itself as a possible cause.

II

The Soret effect and similar phenomena have been declared by competent petrologists (Becker, 1897*a*, *b*; Harker, 1893, 1894; Bowen, 1915, 1921, 1928) to be of no practical importance in the differentiation of magmas because no adequate force was known to them which could make mineral molecules migrate toward the chilled margins of a magma body. And crystallization fractionation was proposed as the most plausible cause of the inhomogeneities observed in composite dikes. This conclusion remained unchallenged by observational facts so long as attention was focused on just one group of composite dikes: dark margins of basic composition (corresponding to an early stage of crystallization), and light central portions of silicic composition (corresponding to a later period of crystallization).

Some of the first composite dikes described were of the type characterized by a central portion of granite or granite porphyry, and marginal zones of diabase or diorite porphyry (see review by Harker in his Skye memoir, 1904, pp. 198-200).

Alkaline composite dikes were described by Brögger (1890*a b*; 1894) from the Oslo district. They too exhibit basic margins, thus indicating that a migration of the dark mineral constituents took place toward the chilled borders; but Vogt (1893) demonstrated that iron is strongly concentrated in the marginal parts, which again is contrary to the Bowen series.

Composite dikes of gabbroic core and granitic margins were later described (Lausitz, Germany; Scottish Islands). And in the ultrabasic dikes of the Skye and Mull areas the marginal zones commonly contain pyroxene and plagioclase which are less calcic than those of the central portions of the dikes; furthermore the central portions carry olivine, the marginal zones do not. In these bodies, as is the case in the Pribilof dike, the marginal zones represent a mineral assemblage belonging to a later period of crystallization than does that of the central portions.

Analogously, the composite stock of Mount Johnson, Monteregian Hills, Canada (Adams, 1903, p. 239), shows the following relations: The marginal phases are made up of a coarse-grained, highly feldspathic syenite passing inward rather abruptly into a dark-colored rock with large porphyritic white feldspars, which in turn loses its porphyritic character and passes into an essexite which toward the very core becomes richer in pyroxene and often holds some olivine.

The formation of the "contact facies" of such dikes cannot be explained satisfactorily on the theory of the simple Soret effect, or on the theory of "composite intrusions," or on the theory of simple crystal-fractionation.

Wahl has pointed out that such vertical stocks are, indeed, enlargements on a huge scale of a separation tube successfully used by Clusius and Dickel (1938, p. 546; 1939*a*, pp. 148-149; 1939*b*, pp. 397, 451) in an experiment designed to separate gaseous isotopes. The effect is here a combination of (*a*) thermal diffusion along a horizontal thermal gradient between the central, strongly heated part of the tube and the chilled walls, and (*b*) vertical convections upward in the central, heated portion, and downward along the walls. By this

arrangement great differences of concentration were achieved at the upper and lower ends of the tube. Wahl therefore concluded that a differentiation of the magma in the Mount Johnson neck was effected by thermodiffusion. The alkaline aluminosilicates migrated toward the chilled walls of the stock, forming a feldspathic syenite, entailing an enrichment of anorthite and ferromagnesian silicates in the central portions (corresponding to an olivine-essexite).

It would seem reasonable that the same mechanism applied to the differentiation in the Pribilof dike. Obviously the magmatic melt was here intruded into a cold environment, and a considerable horizontal temperature gradient must have existed between the hot magma at the center of the vertical dike and its walls. Just as in the Clusius separation tube the gradient would create a Soret effect which, augmented by vertical convection currents, would separate the magma into two portions, viz., an outer shell rich in alkali silicates (which would quickly congeal and form the chilled margins), and a central portion relatively enriched in Ca, Al, Fe, Mg.

III

The dominant role of oxygen in rock melts is well known. In the present rocks, oxygen makes up about 94 per cent by volume, and can be regarded as a "solvent" in which the cations (silicon and metals) distribute themselves. Under equilibrium conditions they will be statistically distributed throughout this solvent, but if a thermal gradient is introduced the homogenous distribution is disturbed, the cations will move, and compositional gradients will ensue. A fractionation of the oxygen isotopes may likewise take place, but the total amount of oxygen will remain rather constant in any part of the melt, due to the large total bulk of oxygen.

The subject to investigate is therefore the migration of the cations in relation to a "stationary" framework of oxygen of constant volume. As reference volume we choose the so-called standard rock cell (Barth, 1948, pp. 50-60), i.e., a cell containing 160 oxygen ions. The direction of the migration of the several cations depends not only on the molecular weights but also on the interatomic forces, on the temperature, the pressure, the relative concentrations, etc., and can not readily be predicted.

Table 2 shows the composition of the two standard cells expressed in numbers of cations (including protons). Let us assume that the dike fissure first was filled by the homogeneous undifferentiated magma of composition as given in column 3. Through diffusion this magma split up into two portions: one marginal portion (column 1) representing 1/10 of the original magma, and one central portion (column 2) representing 9/10 of the original magma. The actual separation was not complete, for transitional facies exist. But for the sake of simplicity, let us assume that the original homogeneous magma space was partitioned off by an imaginary membrane into two compartments, corresponding to 1/10 and 9/10 of the original space. By diffusion through this "membrane" the two different magma portions developed. By simple inspection of table 2 it will be seen that, referred to a unit of 1600 oxygens (i.e., a unit of 10 standard cells), the cations listed below had to pass through the "membrane."

Migration into the marginal compartment:

5	Si
1	Na
1	K
7	cations

Migration into the central compartment:

2	Al
2	Fe
1	Mg
2	Ca
4	H
7	cations + 4 protons

In addition, small fractions of a Ti-ion and of a P-ion had to migrate into the central compartment.

These figures demonstrate that the necessary migration is, indeed, on a modest scale. More than 2600 atoms are present in the reference volume (1600 oxygens and 1034 cations), but a net diffusion of only 7 atoms each way through the imaginary membrane suffices to explain the observed compositional differences between the chilled-margin rock and the central rock.

Another thing is that the actual mechanism of diffusion requires a livelier transport. Thermodynamic equilibrium at a phase boundary does not mean a state of no motion; it means that an equal number of identical atoms or molecules migrate both ways, the net result of the transport being zero.

Molten silicates possess an ionic constitution in analogy with solid silicates. The extent of ionic dissociation is comparable to that of aqueous solutions of strong electrolytes.

Typical cations are Na^+, K^+, Ca^{2+}, Mg^{2+}, Fe^{2+} which occupy no fixed positions in the melt but exhibit a high degree of mobility. They will move freely back and forth through the "membrane" and, as seen from table 2, for all these ions a small difference in concentration exists between the central and the marginal portions.

The anions in the melt are predominantly polymerized silicon-oxygen tetrahedra linked together by oxygen bridges to one-, two-, or three-dimensional networks. The network is similar to that found in crystalline silicates but more irregular.

The silicon ions are strongly bound in the center of the oxygen tetrahedra and will probably have to migrate as (SiO_4)-ions, or even as larger, polymerized Si-O-chains. The net movement of 5 silicon ions (out of a total of 571 silicon ions, or less than 1 per cent, see table 2), through the membrane probably involved the simultaneous transmission of many more oxygen ions (which must be balanced by an oxygen transport in the opposite direction). It has not been possible to carry out any determination of the oxygen isotopes in the present material, but in view of the interesting results of Silverman (1951, pp. 26-42) and others on the isotopic composition of oxygen in natural rocks and minerals, there is not much doubt that isotopic differences would be found between the chilled-margin rocks and the central rocks.

As distinct from mathematics and theoretical physics, natural phenomena cannot be treated with schematic accuracy; all schematic classifications are to be regarded as idealized cases that approximately correspond to the physical facts.

Bowen has proved that fractional crystallization is the main factor controlling igneous rock differentiation. Bowen has contributed more than anybody else to the advancement of igneous geology of the present century. But this does not mean that nature behaves so schematically that all igneous theory

must conform to the tenets of crystal fractionation. The Pribilof composite aplite furnishes one example of a differentiation mechanism which cannot be explained by fractional crystallization. Nor can it be satisfactorily explained by any other generally accepted process of differentiation. And it remains to be seen whether the thermodiffusion hypothesis here presented will withstand the test of time. It is, indeed, worth remembering that for most of the igneous bodies actually studied no complete or satisfactory explanation has been proposed.

In spite of the important strides forward in theoretical petrology in the last few decades, there is still very much that is not known. This should be recognized by every student of rocks and should remind us that it is our duty to be constantly on the outlook for new evidence and for new principles in the interpretation of petrogenic problems.

TABLE 1

Chemical Analyses of (1) Chilled Margin and (2) Central Portion of the Composite Aplite Dike

	(1)	(2)
SiO_2	71.89	64.35
TiO_2	trace	.23
Al_2O_3	15.64	17.76
Fe_2O_3	.78	.56
FeO	1.13	3.91
MnO	.03	.15
MgO	.24	.96
CaO	.62	2.79
Na_2O	5.16	4.18
K_2O	3.18	2.39
P_2O_5	.08	.50
H_2O+	1.26	1.86
H_2O-	.39	.41
CO_2	nil	trace
Sum	100.40	100.05

	(1)	(2)
Q	25.3	19.8
Or	18.0	13.5
Ab	45.0	36.5
An	2.0	10.0
C	3.2	4.8
En	0.6	2.6
Fs	1.0	5.2
Ap	0.3	1.1
Il	...	0.4
Mt	0.8	0.6

Mode of (1)	
Quartz	25.5
Feldspar	58.0
Sericite	11.2
Chlorite	2.8
Limonite	1.2
Apatite	0.3

Mode of (2)	
Quartz	21.3
Feldspar	51.5
Sericite	13.6
Chlorite	10.4
Garnet	0.5
Apatite	1.1
Ore	1.0

Analyst: Brynjolf Bruun.

TABLE 2

Comparison of Standard Cells: (1) Chilled-margin Rock (2) Central-portion Rock, (3) Calculated Composition of the Standard Cell of the Magma before Differentiation

	(1)	(2)	(3)
Si	62.0	56.6	57.1
Ti	...	6.1	0.1
Al	15.8	18.4	18.2
Fe*	1.3	3.2	3.0
Mg	0.3	1.3	1.2
Ca	0.6	2.6	2.5
Na	8.6	7.1	7.3
K	3.5	2.7	2.8
P	0.1	.4	.4
H	7.2	11.2	10.8
O	160.0	160.0	160.0

*Ferrous iron, ferric iron, and manganese are added together.

Columns (1) and (2) are recalculated from the corresponding columns of table 1. The average composition as given in column 3 corresponds to 1 part of the chilled-margin phase and 10 parts of the central-portion phase. It is not possible to determine the average composition with certainty. The intrusion is about 400 m. wide, the marginal parts are about 10 m. wide. If the intrusion is circular the proportion margin: core is 1:10; but less if the intrusion has the shape of a plate. However, the accurate figure is of no consequence for the following discussion, and is, therefore, somewhat arbitrarily taken as 1:10.

REFERENCES

Adams, F. D., 1903. The Monteregian Hills—a Canadian petrographical province: Jour. Geology, vol. 11, pp. 239-282.

Barth, T. F. W., 1948. Oxygen in rocks: a basis for petrographic calculations: Jour. Geology, vol. 56, pp. 50-60.

Becker, G. F., 1897*a*. Some queries on rock differentiation: AM. JOUR. SCI., 4th ser., vol. 3, pp. 21-40.

———, 1897*b*. Fractional crystallization of rocks: AM. JOUR. SCI., 4th ser., vol. 4, pp. 257-261.

Bowen, N. L., 1915. The later stages of the evolution of the igneous rocks: Jour. Geology, vol. 23, supplement to No. 8, pp. 1-91.

———, 1921. Diffusion in silicate melts: Jour. Geology, vol. 29, pp. 295-317.

———, 1928. The evolution of the igneous rocks, Princeton University Press, Princeton, New Jersey.

Brögger, W. C., 1890*a*. Die Mineralien der nephelin-syenitischen Pegmatitgänge der südnorwegischen Nephelinsyenite: Zeitscher. Kristallographie, vol. 16, p. 85.

———, 1890*b*. Die silurischen Etagen 2 und 3. Kristiania.

———, 1894. Die Eruptivesteine des Kristianiagebietes, vol. 2, Kristiania.

Clusius, K., and Dickel, G., 1938. New process for separation of gas mixtures and isotopes: Naturwissenschaften, vol. 26, p. 546.

———, and ———, 1939*a*. The separating-tube process for liquids: Naturwissenschaften, vol. 27, pp. 148-149.

———, and ———, 1939*b*. Isolation of the light chlorine isotop of atomic weight 34.979 in a separating tube: Naturwissenschaften, vol. 27, p. 486.

———, and ———, 1939*c*. Das Trennrohr: Zeitschr. physikal. Chemie, Abt. B, vol. 44, pp. 397-473.

Harker, A., 1893. Berthelot's principle applied to magmatic concentration: Geol. Mag., vol. 10, pp. 546-547.

———, 1894. Carrock Fell: a study in the variations of igneous rock-masses. Part I. The gabbro: Geol. Soc. London Quart. Jour., vol. 50, pp. 311-337.

———, 1904. The tertiary igneous rocks of Skye, Mem. Geol. Survey United Kingdom, Glasgow.

Silverman, S. R., 1951. The isotope geology of oxygen: Geochim. et Cosmochim. Acta, vol. 2, pp. 26-42.

Vogt, J. H. L., 1893. Bildung von Erzlagerstätten durch Differentiationsprocesse in basischen Eruptivmagmata: Zeitschr. prakt. Geol., p. 4.

Wahl, W., 1946. Thermal diffusion-convection as a cause of magmatic differentiation. I.: Am. Jour. Sci., vol. 244, pp. 417-441.

Mineralogisk Geologisk Museum
Oslo, Norway

CHEMICAL PETROLOGY OF SOME METAMORPHOSED ADIRONDACK GABBROIC, SYENITIC AND QUARTZ SYENITIC ROCKS

A. F. BUDDINGTON

ABSTRACT. The chemical petrology of 16 metamorphosed Adirondack gabbroic rocks is discussed in the light of 15 new chemical analyses of their minerals comprising 9 of hornblende, 5 of garnet and one of augite. Four of the rock analyses are new. There is a direct sensitive correlation between the composition of the rocks and the composition of their minerals consistent with an origin through mineral reconstitution with little change in bulk chemical composition. The nature and composition of the minerals also depend on whether the rock was reconstituted under relatively dry conditions or in the presence of hydrous fluids carrying F or Cl or F and Cl.

Chemical aspects of the metamorphism of some charnockitic syenitic and quartz syenitic rocks are also discussed in the light of new chemical analyses of 6 specimens of the major rocks, of 4 related small pegmatite seams and 2 garnets. The pegmatite seams are in large part garnetiferous and the product of local metamorphic recrystallization with some metamorphic differentiation.

The metamorphism of the gabbroic, syenitic and quartz syenitic rocks occurred in connection with regional high grade dynamothermal metamorphism in a large part in the presence of intergranular films of fluid related to a subjacent rising granitic magma. The granite magma later intruded the metamorphosed rocks and locally developed a superimposed reconstitution on the early facies. The rocks were in part metamorphosed under conditions of the upper temperature range for the amphibolite facies and in part in the granulite facies. A geologic map showing the regional variation in the nature and intensity of metamorphism is given. The problem of the garnets at the Barton Mine is discussed and reasons given for preferring an origin as an aspect of regional metamorphism rather than through local recrystallization directly consequent on syenite intrusion as advocated by some other students.

INTRODUCTION AND ACKNOWLEDGMENTS

THE cost of the field and laboratory expenses and of the chemical analyses was covered in part by grants from the A. H. Phillips Fund administered by the Department of Geology, Princeton University, and in part by funds of the Eugene Higgins Trust allocated to Princeton University. Dr. H. L. James and J. R. Smith prepared the mineral concentrates for chemical analysis. All chemical analyses were made in the Laboratory for Rock Analysis at the University of Minnesota. The optical data for the hornblendes and hypersthenes were determined by J. R. Smith. The writer is indebted to Professors

H. H. Hess and Arie Poldervaart for several suggestions leading to improvement of the report.

The specimens from which the rock analyses were made and those from which the minerals were concentrated have come from portions of the same outcrop but may have been as much as several feet apart. There may therefore be a slight variation in composition between them, but the similarity is adequate for all but the most detailed correlation.

The minerals were concentrated for analysis both by use of the Frantz magnetic separator and by heavy liquids. All concentrates were checked with the microscope and were at least 99.5 per cent pure.

PREVIOUS WORK

The metamorphism of the Adirondack gabbroic, syenitic and quartz syenitic rocks has been discussed in more or less detail by most previous workers in this region. A general survey of the literature and references may be found in a memoir by Buddington (1939). Recently a most excellent study of the chemical mineralogy of a reconstituted gabbroic rock at the Barton garnet mine has been published by Levin (1950). Many significant features of the gabbroic and quartz syenitic rocks will not be referred to in this paper as they have previously been adequately treated in the literature.

SUCCESSION OF INTRUSIONS AND DEFORMATIONS

The nature and time sequence of intrusions and deformations in the Adirondack area is pertinent to an understanding of the metamorphism of the gabbroic and quartz syenitic rocks, and as inferred by the writer is given in the accompanying table 1.

CHEMICAL PETROLOGY OF RECONSTITUTED GABBROIC ROCKS

Chemical Analyses of Rocks and Minerals

The chemical analyses of the gabbroic rocks and of certain minerals of which they are composed are given in the accompanying tables (2, 3, 4 and 5).

The numbers of the hornblende analyses are the same as those of the analyzed rocks from which the hornblende was separated. The analyst for nos. 1, 7, and 9 was Eileen K. Oslund, for nos.

2, 3, 4, 5, 6 and 8, Lee C. Peck and for no. 10, S. B. Levin (1950), p. 548).

The numbers of the garnet analyses are the same as those of the analyzed rocks from which the garnet was separated. The analyst for analyses nos. 7, 8, 12, 13, 14, 15, 16 and 17 was Lee C. Peck, for no. 9, Eileen K. Oslund, for no. 10, S. B. Levin (1950, p. 534) and for no. 11, S. J. Shand (1945, p. 257).

TABLE 1

Succession of Intrusions and Deformations

Basalt, as unmetamorphosed dikes.

Intrusive contact

(C) *Period of orogenic deformation and metamorphism*

Hornblende granite and subordinate alaskite, microcline granite and local soda-granite; occurring in phacolithic and thick sheet-like masses; now gneisses in part.

Intrusive contact

(B) *Period of orogenic deformation and metamorphism* (main regional development of garnet)

Hypersthene diabase; occurs as dikes in the quartz syenitic and charnockitic series, probably as sheets in metasediments; now largely gneisses.

Intrusive contact

(A) *Period of orogenic folding*

Quartz syenitic and charnockitic series; mafic syenite, pyroxene syenite, pyroxene quartz syenite, hornblende granite; and fayalite-hedenbergite granite; occurring as differentiated facies of thick extensive sheets; now largely gneisses.

Intrusive contact

Olivine diabase or gabbro; occurs as extensive sheets and small lenses, locally as dikes; largely metamorphosed.

Intrusive contact

Anorthosite series; anorthosite and gabbroic anorthosite with subordinate pyroxene gabbro, mafic gabbro and ultramafic pyroxenitic gneiss (with ilmenite magnetite) as differentiates; some diorite sheets; border facies of larger masses are metamorphosed to gneisses.

Intrusive contact

Grenville series, metasediments; biotitic, hornblendic, garnetiferous and pyroxenic quartz-feldspar gneisses, feldspar-quartz granulite, quartzite, amphibolite, marble, skarn and migmatitic facies of many of the foregoing.

TABLE 2

Chemical and Modal Analyses of Reconstituted Gabbros and Some Other Rocks

	1	2	3	4	5	6	7	8	9	10	11	12	13	14	15	16	17
SiO_2	49.75	46.50	51.66	50.35	49.41	49.34	44.78	46.25	45.85	46.3	47.56	47.88	47.16	53.35	55.10	53.11	38.91
Al_2O_3	17.87	16.86	16.85	22.10	16.61	16.93	17.64	17.51	18.44	16.2	16.33	18.90	14.45	14.97	22.10	19.65	6.98
Fe_2O_3	1.73	1.96	2.48	1.25	1.73	2.25	2.80	1.81	2.69	2.2	0.54	1.39	1.61	3.31	.66	1.10	5.58
FeO	8.76	8.93	6.48	3.41	7.82	5.39	9.63	10.20	9.81	9.4	11.13	10.45	13.81	10.61	4.17	7.62	29.07
MgO	5.40	8.16	5.94	4.19	9.84	7.60	7.11	9.34	6.57	11.8	11.03	7.10	5.24	1.72	1.67	1.39	3.85
CaO	9.81	10.78	8.70	11.69	9.14	11.13	10.13	8.69	8.80	9.2	8.01	8.36	8.13	6.43	8.69	8.18	6.55
Na_2O	3.41	2.69	2.91	3.71	2.79	3.11	2.87	2.48	3.24	2.7	2.52	2.75	3.09	3.50	4.06	4.17	1.00
K_2O	.67	.49	1.64	.92	.63	1.13	.64	.55	.90	0.6	.48	.81	1.20	3.74	1.31	1.91	.42
H_2O+	.37	1.30	1.12	.55	.40	.91	1.28	.67	.81	0.8	1.01	.43	.48	.14	.50	.24	.34
H_2O-	.04	.05	.05	.01	.05	.09	.13	.10	.06	....	.11	.18	.12	.10	.04	.04	.07
CO_2	.14	.35	.59	.58	.13	.09	....	.09	....	....	....	.12	.35	....	.24	.18	....
TiO_2	1.56	1.27	.97	.48	.91	1.28	2.38	1.83	2.03	0.7	.65	1.20	3.37	1.38	.92	1.62	4.70
P_2O_5	.14	.18	.25	.08	.12	.27	.42	.28	.33	....	.28	.20	.57	.71	.27	.67	1.61
MnO	.17	.15	.13	.04	.16	.12	.35	.18	.27	0.1	.16	.16	.24	....	.08	.12	.52
BaO	....	....	.05	....	....	....	....	....	....	....	....	....	....	....	....	....	....
Cl	.01	....	.04	.49	....	....	....	....	.35	....	....	....	....	....	.04	....	....
S	....	....	....	....	....	.08	.03	....	....	....	....	.07	.14	....	....	....	.52
Total	99.83	99.67	99.86	99.85	99.74	99.72	100.19	99.98	100.15	100.00	99.81	100.00	99.96	99.96	99.85	100.00	100.12
Less 0 for Cl & S	....	....	....	99.74	....	....	100.18	....	100.07	....	....	....	....	....	99.84	....	99.93

TABLE 2 (Cont.)

Chemical and Modal Analyses of Reconstituted Gabbros and Some Other Rocks

	1	2	3	4	5	6	7	8	9	10	11	12	13	14	15	16	17
APPROXIMATE MODE																	
Quartz	....	....	6.8	....	....	....	....	....	....	....	....	....	0.8	3.4	3.	0.5	....
Orthoclase	....	....	....	....	....	....	....	....	....	....	....	....	1.8	....	2.	4.9	0.5
Plagioclase	An_{45} 49.	An_{54} 29.6	An_{30} 36.5	An_{55} 48.9	An_{54} 41.9	An_{45} 49.	An_{47} 30.0	An_{54} 31.9	An_{44} 46.5	An_{30} 20.	An_{42-46} 30.9	An_{26} 33.	An_{24} 40.9	61.9	An_{40} 73.	An_{44} 60.3	11.
Olivine	....	....	....	....	....	....	....	....	....	....	7.7	3.	....	....	....	....	....
Hypersthene	En44 Fs56 5.5	....	....	....	En65 Fs35 18.9	....	1.0	En62 Fs38 16.4	En56 Fs44 21.8	En71 Fs29 6.9	....	8.	24.1	12.6	7.	7.9	53.7
Augite	2.2	....	....	0.1	1.9	16.	....	....	....	Tr	27.7	7.	....	2.8	....	....	
Hornblende	42.0	68.9	38.7	27.5	36.8	32.	60.5	41.9	24.2	61.2	7.4	27.	0.2	0.4	4.	3.1	0.3
Biotite	....	0.4	11.2	....	....	1.	0.8	0.6	0.2	0.9	1.8	....	....	....	1.5	....	....
Magnetite	....	....	....	....	....	1.5	....	....	2.8	...	0.6	2.	9.4	8.2	2.	3.7	15.
Ilmenite	1.0	0.2	....	....	0.2		1.7	1.8		...							
Sphene	....	....	0.7	0.6	0.1	....	....	....	....	0.1	....	....	....	....	Tr	0.3	....
Apatite	0.3	0.5	0.8	0.2	0.2	0.5	1.0	0.7	0.5	Tr	....	0.3	2.1	2.1	0.5	1.5	3.5
Scapolite	....	....	4.7	22.7	....	....	....	....	....	....	....	....	....	....	....	....	....
Garnet	....	....	....	....	....	....	5.0	6.7	4.0	11.	23.8	20.	20.7	8.0	7.	17.6	16.
Zircon	....	....	....	....	....	....	....	....	....	....	....	....	....	0.4	....	....	....
Ratio Mol Per Cent CaO, MgO, FeO + MnO																	
CaO	40.4	42.4	39.	58.	31.4	42.6	36.	29.	34.	27.7	25.	31.5	31.	37.	60.5	51.	18.8
MgO	31.1	30.	37.5	30.	47.4	41.	36.	44.	35.6	50.	48.	37.5	28.	14.	16.5	12.	15.4
FeO + MnO	28.5	27.6	23.5	12.	21.2	16.4	28.	27.	30.4	22.3	27.	31.	41.	49.	23.	37.	65.8

TABLE 3

Chemical Analyses and Optical Properties of Hornblendes

	1	2	3	4	5	6	7	8	9	10
SiO_2	42.66	43.13	42.03	42.91	42.66	43.60	41.25	41.06	40.54	43.50
Al_2O_3	11.21	13.09	12.59	12.45	12.50	11.33	13.26	15.47	14.43	13.15
Fe_2O_3	3.57	2.56	4.48	4.34	3.62	4.02	3.56	2.47	3.48	3.39
FeO	14.18	12.49	11.80	10.89	8.82	9.88	13.50	13.20	13.08	9.38
MgO	10.19	11.39	10.81	11.34	13.15	12.41	10.27	10.85	10.05	14.25
CaO	11.42	11.01	11.43	12.04	11.51	12.03	10.22	10.00	10.77	10.58
Na_2O	1.62	1.66	1.24	1.20	1.85	1.38	1.82	2.27	2.16	2.53
K_2O	1.34	.70	1.39	1.49	1.46	1.34	.83	.61	1.05	.68
H_2O+	.94	1.85	1.93	1.67	.88	1.63	1.48	1.75	1.17	1.15
H_2O-	.04	.01	.03	.08	.06	.05	.06	.01	.03	.12
TiO_2	2.02	1.71	1.47	.93	2.00	2.09	2.96	1.85	2.42	1.12
MnO	.19	.20	.26	.15	.14	.19	.47	.18	.23	.09
F	.91	.05	.12	.11	1.07	.16	.11	.04	.08	.30
Cl	.03	.....	.....	.....	.....	.....	.04	....	.63	.....
Total	100.32	99.85	99.58	99.60	99.72	100.11	99.83	99.76	100.12	100.24
Less 0 for F + Cl	99.93	99.83	99.53	99.55	99.27	100.04	99.78	99.74	99.95	100.12
Sp. G.	3.273	3.218	.....	.....	.....	.....	3.259	3.236	3.270	3.172
	Ratio Mol Per Cent CaO, MgO, FeO + MnO									
CaO	31.	30.	32.	33.	31.	32.	29.	28.	30.5	28.
MgO	39.	43.	42.	43.5	50.	47.	40.5	43.	40.	52.5
FeO + MnO	30.	27.	25.	23.5	19.	21.	30.5	29.	29.5	19.5

TABLE 3 (Cont.)

Chemical Analyses and Optical Properties of Hornblendes

	1	2	3	4	5	6	7	8	9	10
Optical Properties										
n^X	1.665	1.659	1.665	1.663	1.657	1.662	1.666	1.666	1.670	1.658
n^Z	1.691	1.684	1.687	1.684	1.680	1.684	1.689	1.693	1.696	1.676
$n^X - n^Z$	.026	.025	.022	.021	.023	.022	.023	.027	.026	.018
2 V	75.3°	80.6°	68.6°	73°	84°	72.4°	81°	81.4°	78.5°	95°
$Z \wedge C$	15°	15°	15°	19°	16°	16°	17°	16°	14°	16°
X	light yellowish olive green	pale greenish straw	pale straw	light straw	pale greenish straw	pale olive green	light straw yellow	light straw yellow	pale yellowish olive green	olive green
Y	brownish yellow	greenish brown	brownish green	green	greenish brown	greenish brown	brownish yellow	brownish yellow	brownish yellow	light brown
Z	dark olive green	olive green	green	bluish green	olive green	olive green	dark olive green	dark olive green	dark olive green	brown
Ratio Mol Per Cent CaO to CaO + MgO + FeO (+ MnO)										
Rock	40.4	42.4	39.	58.	31.4	42.6	36.	29.	34.	27.7
Hornblende ..	31.	30.	32.	33.	31.	32.	29.	28.	30.5	28.
Ratio Mol Per Cent MgO to FeO (+ MnO)										
Rock	1.09	1.62	1.61	2.23	2.24	2.47	1.29	1.62	1.17	2.22
Hornblende ..	1.28	1.61	1.65	1.85	2.65	2.20	1.33	1.46	1.36	2.70
Garnet	.....	.....	.....	.....	.....	.....	.46	.55	.57	1.03
Hypersthene .	0.78	.....	.....	.....	1.86	.....	....	1.63	1.27	2.45

TABLE 4

Chemical Analyses of Garnet

	7	8	9	10	11	12	13	14	15	16	17
SiO_2	38.24	38.54	38.85	39.29	41.30	38.90	37.19	37.53	37.48	37.23	36.86
Al_2O_3	21.80	22.13	21.98	22.12	19.78	22.39	21.02	20.29	21.01	20.91	20.46
Fe_2O_3	.82	.39	.62	.78	1.80	.65	1.28	2.14	1.12	1.40	1.63
FeO	25.37	25.71	24.38	19.63	17.80	22.42	28.61	29.54	27.25	28.37	30.90
MgO	6.96	8.29	8.18	11.48	10.60	9.02	3.08	1.37	3.48	2.13	1.56
CaO	4.69	3.68	4.64	6.16	6.98	6.11	7.41	7.40	8.45	9.01	7.26
Na_2O	....	.01	....	....	....	.10	.02	.12	.07	.04	.09
K_2O	....	.05	....	....	....	.05	.09	.04	.03	.02	.10
H_2O+	.17	.13	.08	....	.54	.09	.16	.07	.11	.12	.06
H_2O-	.06	.04	.00	.03	....	.00	.00	.00	.05	.04	.04
TiO_2	.25	.04	.09	.05	.15	.14	.38	.25	.66	.13	.16
MnO	1.72	1.10	1.47	.38	.49	.48	.93	1.77	.82	.92	1.13
Total	100.08	100.11	100.29	99.87	99.44	100.35	100.17	100.52	100.53	100.32	100.25

* Density = 3.968

TABLE 4 (Cont.)

Chemical Analyses of Garnet

	7	8	9	10	11	12	13	14	15	16	17
Mol Per Cent Garnet Molecules											
Almandite	59.2	57.5	49.	40.	43.6	52.4	67.0	70.	60.3	63.4	70.0
Pyrope	23.7	29.0	31.	43.	35.6	30.2	10.5	4.6	13.9	8.6	6.4
Grossularite	10.5	9.6	13.8	14.	14.	14.4	16.4	14.2	20.7	21.6	16.3
Andradite	2.6	1.3	2.3	2.	5.6	2.	4.1	7.0	3.3	4.3	4.9
Spessartite	4.0	2.6	3.9	1.	1.2	1.	2.0	4.2	1.8	2.1	2.4
Ratio Mol Per Cent CaO, MgO, FeO (+ MnO) in Garnet											
CaO	13.1	10.3	12.8	16.3	19.	16.6	21.3	21.9	23.7	26.	19.5
MgO	27.5	31.8	31.6	42.5	40.3	34.4	12.4	5.6	13.7	8.5	6.5
FeO +MnO	59.4	57.9	55.6	41.2	40.7	49.0	66.3	72.5	62.6	65.5	74.0
Ratio Mol Per Cent CaO to CaO + MgO + FeO (+MnO)											
Rock	36.	29.	34.	27.7	25.	31.5	31.	37.	60.5	51.	18.8
Garnet	13.1	10.3	12.8	16.3	19.	16.6	21.3	21.9	23.7	26.	19.5
Ratio Mol Per Cent FeO (+ MnO) to MgO											
Rock	.78	.61	.85	.45	.56	.83	1.46	3.50	1.40	3.08	4.3
Garnet	2.16	1.82	1.76	.97	1.01	1.48	5.35	13.0	4.57	7.7	11.4

TABLE 5

Chemical Analyses of Pyroxenes

	13	14
SiO_2	50.54	50.33
Al_2O_3	2.74	2.32
Fe_2O_3	2.42	1.88
FeO	12.80	18.23
MgO	9.65	6.92
CaO	20.16	18.39
Na_2O	.75	.61
K_2O	.07	.07
H_2O+	.17	.16
H_2O-	.04	.09
TiO_2	.25	.28
MnO	.15	.83
	99.74	100.11
Mol. per cent CaO, MgO, FeO+MnO		
CaO	46.	43.
MgO	31.	22.6
FeO+MnO	23.	34.4

(13) Augite, from garnet-augite-oligoclase granulite, dike one mile W of Elizabethtown, N. Y. Analyst, Lee C. Peck. From rock of analysis 13.

(14) Ferroaugite, from ferroaugite syenite gneiss; quarry NE of Moody Lake, Saranac Quad. Analyst, Lee C. Peck. From rock of analysis 14.

Reconstituted Gabbroic and Other Rocks and Some Associated Minerals.

(1) Amphibolite gneiss, 25-foot thick layer enclosed in hornblende granite, 0.9 mile W of Strifts School, Lowville Quad. Analyst, J. J. Engel.

(2) Amphibolite gneiss, from contact zone between alaskite and marble; 4 miles N of Dekalb Junction (Ogdensburg Quad.). Analyst, S. S. Goldich, Geol. Soc. America Mem. 7, no. 157.

(3) Biotitic amphibolite gneiss, slightly granitized facies of gabbro which is intersected by a network of granite pegmatite veinlets. Hill at Stellaville (Russell Quad.) just S of old pyrite mine shaft. Analyst, A. Willman, Geol. Soc. America Mem. 7. no. 167.

(4) Hornblende-labradorite-scapolite granoblastic anorthositic gabbro gneiss. Bed of Bullock Brook, 1.8 miles W of South Russell (Russell Quad.). Analyst, R. B. Ellestad, Geol. Soc. America Mem. 7, no. 177.

(5) Hornblende-hypersthene amphibolite gneiss, from included angular fragment in hornblende granite, 1.5 miles S of Brandon (Malone Quad.). Analyst, A. Willman, Geol. Soc. America Mem. 7, no. 57.

(6) Augitic amphibolite gneiss, 0.25 mile E of Geers Corners (Lake Bonaparte Quad.). Analyst, R. B. Ellestad, Geol. Soc. America Mem. 7, no. 51.

(7) Almanditic amphibolite gneiss with porphyroblastic garnet, one mile S of junction of Cook Pond Outlet and Grass River (Stark Quad.). Analyst, Eileen K. Oslund.

(8) Almanditic amphibolite gneiss with porphyroblastic garnet, 2.5 miles ESE of St. Regis Falls (Nicholville Quad.). Analyst, Lee C. Peck, Geol. Soc. America Mem. 7, no. 55.

(9) Almanditic amphibolite gneiss with porphyroblastic garnet, 1.6 miles a little N of due E of Rainbow (Saranac Quad.), north end of hill. Analyst, J. J. Engel. Garnet crystals up to 1 inch in diameter with thin sheath of recrystallized plagioclase. Locally a rudimentary sheath of hornblende outside of plagioclase around garnet, granoblastic matrix. Sp. G. garnet = 3.968.

(10) Pyralmandite amphibolite, porphyroblastic garnet, Barton Mine, Gore Mtn. (Thirteenth Lake Quad.). Computed by S. B. Levin (1950, p. 546).

(11) Pyralmanditic olivine pyroxene metagabbro gneiss, corona garnet, Barton Mine, Gore Mtn. Analyst, S. J. Shand (1945, p. 257). Mode is based on average of 3 given by Levin (1950, p. 544).

(12) Almandite-pyroxene-hornblende-oligoclase granoblastic gneiss, wall rock of titaniferous magnetite deposit, Split Rock Mine, Westport (Port Henry Quad.). Analyst, W. F. Hillebrand (Kemp, 1899, pp. 399-400).

(13) Almandite-augite-oligoclase granulite, one mile W of Elizabethtown (Elizabethtown Quad.). Analyst, W. F. Hillebrand (Kemp and Ruedemann, 1910, p. 55.).

(14) Almanditic ferroaugite syenite gneiss, quarry NE of Moody Lake (Saranac Quad.). Analyst, Lee C. Peck, Geol. Soc. America Mem. 7, no. 109.

(15) Gabbroic anorthosite gneiss, average of grab sample for 2.5 miles across strike SE of Long Pond outlet to 1.5 miles NW of Willsboro (Willsboro Quad.), Geol. Soc. America Mem. 7, no. 20. Disseminated poikiloblasts of almandite, and some corona almandite.

(16) Almanditic augite—andesine gneiss, 2.5 miles NE of Cross (Ausable Quad.). Analyst, R. B. Ellestad. A reconstituted migmatite of gabbroic anorthosite veins and pyroxene skarn in contact zone between anorthosite and marble. Geol. Soc. America Mem. 7, no. 40.

(17) Almanditic ultramafic pyroxenite gneiss, road cut about 2 miles NW of Willsboro, Willsboro Quad. Segregation layer several feet thick in gabbroic anorthosite gneiss. Analyst, J. A. Maxwell. Sp. G. of rock = 3.654. Orthopyroxene is eulite [En_{23} Fs_{77}, (–) $2V = 73.7°$].

VARIATION IN COMPOSITION OF PLAGIOCLASE

The plagioclase, where least affected by the reconstitutive chemical reactions, uniformly varies between Ab_{55} An_{45} and Ab_{38} An_{62}, generally a sodic labradorite.

Some data pertinent to the problem of what happens to the plagioclase during reconstitution are given in tables 6 and 7.

The normative per cent of plagioclase does not, of course, directly correspond to the modal plagioclase of the unaltered rock since the alumina which is actually in pyroxene is calculated as forming anorthite in the norm and similarly the slight amount of soda in the pyroxene is calculated as albite in the norm. This may result in the composition of the normative

TABLE 6

Data Pertinent to Variation of Plagioclase with Reconstitution

	Non-garnetiferous Amphibolitic Gneisses						Garnetiferous Amphibolitic Rocks				Coronite Metagabbro	Granoblastic garnet, pyroxene, hornblende, gneiss	Garnet, pyroxene, granulite	Metapyroxene syenite
	1	2	3	4	5	6	7	8	9	10	11	12	13	14
Per Cent CaO in Rock Compared with CaO in Hornblende, Garnet and Pyroxene														
Rock	9.81	10.78	8.70	11.69	9.14	11.13	10.13	8.69	8.80	9.2	8.01	8.36	8.13	6.43
Hornblende	11.42	11.01	11.43	12.04	11.51	12.03	10.22	10.00	10.77	10.58	....	....	....	....
Garnet	....	....	....	....	....	....	4.69	3.68	4.64	6.16	6.98	6.11	7.41	7.40
Pyroxene	....	....	....	....	....	....	....	....	....	....	....	....	20.16	18.39
Per Cent An in Normative and Modal Composition of Plagioclase Compared														
Norm	50.	57.	52.	60.	55.	51.	59.	61.	56.	60.	60.	60.	45.	32.
Mode	45.	54.	30.	55.	54.	45.	47.	54.	44.	50.	42. to 46.	26.	24.	25.
Per Cent of Total Normative and Modal Plagioclase Compared														
Norm	64.12	58.23	57.	76.03	58.25	61.26	58.65	59.33	62.46	52.30	55.71	64.28	53.59	....
Mode	49.	29.6	36.5*	48.9†	41.9	49.	30.0	31.9	46.5	20.	30.9	33.	40.9	....

* Also 4.7 per cent scapolite present

† Also 22.7 per cent scapolite present

feldspar having up to a maximum of 3 per cent more anorthite in the norm than in the mode and a maximum of 4 per cent more total feldspar in the norm than in the mode. The normative feldspar, nevertheless, forms a good basis for comparison with the modes of the reconstituted rocks.

The amphibolitic gneisses (table 2, nos. 1, 2, 4, 6) in which hornblende is practically the only ferromagnesian mineral have a plagioclase which is very slightly more sodic than might be expected in the primary rock but in general the changes in the nature of the plagioclase have been largely physical, a granulation and recrystallization. In no. 5 the rock carries considerable hypersthene in addition to hornblende and the mode and the norm are practically the same. The Stellaville biotitic amphibolite (no. 3) differs from the dominantly hornblende amphibolite in that the modal plagioclase (An_{30}) is very much more sodic than the norm (An_{52}).

The total amount of modal plagioclase, however, is commonly 20-30 per cent less than that of the norm, mostly as a result of reaction of the primary ferromagnesian minerals with plagioclase to yield hornblende. In rocks with 30 to 40 per cent hornblende about 15 to 25 per cent of the original modal plagioclase has entered into the hornblende reaction.

In the granoblastic garnetiferous amphibolites 20-60 per cent of the original plagioclase has been used up in the reactions to yield hornblende and garnet, and the composition of the new modal plagioclase is a little more albitic than the original and also slightly more so than in the case of the non-garnetiferous amphibolites.

Similarly, in the garnetiferous gneiss and granulite (table 2, nos. 12 and 13) there has been a loss of 47-57 per cent of the normative plagioclase to yield garnet, hornblende and pyroxene. These two rocks also contain the most sodic plagioclases of all the reconstituted garnetiferous rocks. The lime of the plagioclase has in part gone to form additional augite from the primary olivine and hypersthene.

Number 11 (table 2) is representative of one type of reconstituted metagabbros which have relicts of the original ophitic texture preserved, and relicts and *apparent* relicts of the original primary minerals.

In table 7 is given the average composition of two types of garnetiferous olivine-augite metagabbro gneiss with relicts of

TABLE 7

Variation of Composition of Plagioclase with Modal Composition of Reconstituted Rocks

	Granoblastic hornblende hypersthene amphibolite	Granoblastic Garnet hornblende hypersthene amphibolite	Ophitic Garnet corona olivine augite gneiss	Ophitic garnet olivine augite gneiss	Granoblastic garnet augite granulite	Granoblastic garnet hornblende amphibolite
	An_{50+}	An_{50+}	An_{40-50}	An_{30-40}	An_{25-30}	An_{47}
Plagioclase	46.8	36.6	40.9	43.7	40.9	30.
Olivine	...	2.0	4.0	7.4	...	...
Hypersthene	15.4	15.8	4.7	6.5	...	1.
Augite	5.2	4.2	18.1	16.7	24.1	...
Hornblende	26.7	31.9	8.2	1.1	0.2	60.5
Biotite	0.9	0.3	1.4	6.8	...	0.8
Magnetite and Ilmenite	4.5	1.6	0.7	1.2	9.4	1.7
Apatite	0.5	0.6	0.3	0.5	2.1	1.0
Garnet	...	6.2	21.6	15.8	20.7	5.0
Spinel	...	0.8	0.1	0.3	...	...
Potash feldspar	...	...	...	...	0.8	1.0
Number averaged ..	9.	3.	3.	3.	1.	1.

primary ophitic structure. The two types are based on the composition of the plagioclase which in one case varies between An_{40-50} and in the other between An_{30-40}. In both cases relicts of primary olivine, augite, and hypersthene are also preserved. The *apparent* relicts of primary plagioclase, however, have similar composition to the granoblastic plagioclase of the matrix and are much more sodic (as low as An_{34}) than would be expected if they were really inherited unmodified relicts of the original feldspar. This has been previously noted (Buddington 1939, pp. 271-272) and the conclusion drawn that such *apparent* primary plagioclase must have undergone a change in composition without any fundamental change in form. Levin (1950, p. 538) states that in the Gore Mountain gabbro uncrushed plagioclase of ophitic texture is between An_{40} and An_{46} with An_{45} most common. Since the norm of the gabbro gives the plagioclase as An_{60}, it would appear that this is another example where the primary plagioclase has in part become more sodic without granulation and recrystalliatzion. The granoblastic material (p. 544) is here too reported to have the same composition as the *apparent* primary plagioclase. The total amount of feldspar is much less than in the primary rock.

Variation in Composition of Hornblende

The hornblendes have a variation which in general correlates directly with the bulk chemical composition of the rock (fig. 1). They uniformly carry a higher percentage of lime than the rock in which they occur while the ratio of MgO to FeO in the hornblende may be the same, greater or less than that in the related rock depending on the mineralogy which in turn depends in part on the chemical composition of the rock.

The hornblendes (table 3, nos. 4 and 6) with the highest percentage of lime occur in the rocks with the highest percentage of the same constituent.

Where hornblende is almost the only mafic mineral, the ratio of MgO to FeO might be expected to be similar in both the hornblende and the rock of which it is a part. This is true in the case of nos. 2, 3 and 7. In no. 4 the hornblende has a lower ratio of MgO/FeO than the rock. This may be due to a lack of correspondence between the analyzed hornblende and that of the analyzed rock—the rock is of somewhat variable compo-

sition—or it may be due in part to differential fractionation of hornblendes by the magnetic separator.

Bowen and Schairer (1935, p. 551) have expressed the opinion that in a rock formed by recrystallization during metamorphism and containing olivine, pyroxene and amphibole, the amphibole would be more magnesian than the pyroxene and the pyroxene in turn more magnesian than the olivine. Ramberg (1949, pp. 38-43) on the other hand postulates that the coexisting garnet and hornblende of metamorphic quartz-bearing enderbitic rocks and of basic rocks should be less magnesian than the rhombic pyroxene. In the rocks under consideration the hornblende in three cases (1, 5, and 10) is more magnesian than the hypersthene and the rock of which they are a part, and in two examples (8 and 9) is slightly less magnesian than the associated hypersthene. The hornblende of the Geers gabbro (no. 6) is less magnesian than the rock and the augite from which it is derived. The secondary augite of the Gore Mountain metagabbro has an Mg/Fe ratio of 61/39 whereas the primary olivine is Mg/Fe = 73-83/17-27 (Levin, 1950, p. 539). In this case also the secondary pyroxene is less magnesian than the olivine. Much more data will be necessary to elucidate this problem. The development of garnet as an additional mineral to amphibole must of course be a modifying factor. In a recent paper Ramberg and DeVore (1951, pp. 193-211) give data which indicate that for exceptionally magnesia-rich silicates the olivine is richer in magnesia than the associated hypersthene but that otherwise the orthopyroxene is more magnesia-rich than the paired olivine.

Where garnet is the major mafic mineral accompanying the hornblende (7 and 10) the ratio of MgO to FeO in the hornblende is about the same where the rock (7) and garnet have a low ratio of MgO to FeO and is higher (10) in the hornblende than in the rock where the ratio of MgO to FeO is high in both rock and garnet.

The garnetiferous amphibolitic gneisses (tables 2 and 3, nos. 8 and 9) contain hornblende, hypersthene and garnet. The amount and the composition of the normative plagioclase in the two rocks is similar but in no. 8 there has been a much greater loss of the plagioclase to yield a larger amount of hornblende than in no. 9. The rock of no. 8 however has much more MgO than that of no. 9 so that the chemical composition of the two

is different. The relationships of the ratio of MgO to FeO in the minerals of the two rocks are also different.

The hornblendes (1-6) of the non-garnetiferous rocks are commonly a green variety as distinguished from the hornblendes associated with garnets where the hornblende is dark olive green to brown in one position of extinction. The green hornblendes of the non-garnetiferous facies (1-6) uniformly carry a slightly higher to considerably higher percentage of potash (average 1.29 K_2O) than do the hornblendes (7-10) of the garnetiferous facies (average 0.79 K_2O). The hornblendes of the non-garnetiferous facies also have a higher ratio of K_2O to Na_2O (0.87) than do the hornblendes (ratio of K_2O to $Na_2O = 0.36$) of the garnetiferous facies. The *total* alkalies in the hornblendes of each facies are about the same. The development of hornblende in the non-garnetiferous rocks thus tends to result in an associated more sodic plagioclase than does the hornblende of the garnetiferous facies.

The hornblendes of the garnetiferous facies are uniformly higher in alumina than those of the non-garnetiferous facies. The Dekalb hornblende (no. 2) is the highest in alumina of the hornblendes from the non-garnetiferous facies, and the rock in which it occurs is actually locally very slightly garnetiferous.

Two of the hornblendes (table 3, nos. 1 and 5) have higher amounts than normal of F and one (no. 9) carries an abnormal per cent of Cl. In all three cases the per cent of H_2O+ is correspondingly less as called for by the principle of substitution of F or Cl for OH. These three rocks also carry the highest content of total alkalies. The hornblende no. 5 came from a small contact metamorphosed angular inclusion of gabbro in granite. No. 1 came from a 25-foot layer of amphibolite included in granite and the amphibolite from which the hornblende no. 9 was taken is also near intrusive granite. The hornblende of the intrusive granite is a variety in the border zone between femaghastingsite and ferrohastingsite with about 1 per cent, more or less, of fluorine. The geologic environment is such that the high halogens and alkalies of these hornblendes of the reconstituted gabbros can reasonably be inferred as derived from solutions related to the granitic magmas.

Variation in Composition of Garnet

The variation in the composition of the CaO, MgO and FeO

(+ MnO) ratios of the rock and corresponding garnet is shown in figure 1. There is in general a systematic relationship. The Elizabethtown garnet (no. 13) is exceptionally high in CaO for the composition of the rock. The rock is a granulite without hornblende representing a different type of metamorphism from the others.

The two major molecules of the garnets are almandite and pyrope. The ratio of FeO/MgO is uniformly much greater in the garnet than in the host rock. In general the ratio of FeO/MgO in the garnet increases with an increase in the ratio of FeO/MgO in the gabbroic rocks though there is considerable

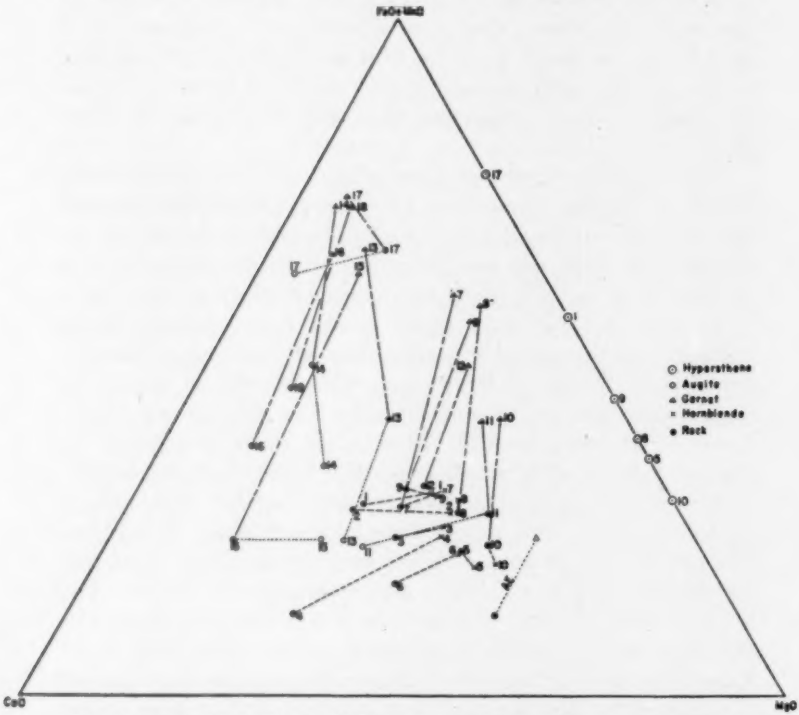

Fig. 1. CaO, FeO+MnO, MgO; mol per cent ratios for Adirondack rocks and corresponding minerals. Data for orthopyroxenes (1, 5, 8, 9, 10 and 17) are based on indices of refraction using Poldervaart's curves. They of course must carry a little CaO so that they should actually lie a little off the MgO-FeO line toward CaO. The line AE is that for a magnesia-rich eclogite and its garnet from the Jagerfontein mine, South Africa. (Williams, 1932) for comparison.

range in variation of the garnets for similar FeO/MgO ratios in the rock. Numbers 8 and 11, for example, have a similar ratio of FeO/MgO in the rock but the garnet of no. 8 has a ratio of 1.82 FeO/MgO whereas that of no. 11 is only 1.01 FeO/MgO. The metagabbro (Buddington, 1939, p. 60, analysis no. 56) has about the same FeO/MgO ratio as the Gore Mountain metagabbro and its garnet ($n = 1.767$) is similar.

There is very little variation in the per cent of CaO in the garnet-bearing gabbroic rocks. There is considerable variation in the ratio of CaO to CaO+MgO+FeO in the rocks but there is no significant correlation between this variation and the amount of CaO in the garnet. This is well exemplified in rocks nos. 13 and 15, table 2, where the garnets have a similar ratio of CaO to CaO+MgO+FeO but the rocks have ratios of CaO to CaO + MgO + FeO of 31 and 60.5, respectively. However, the garnets (nos. 7, 8, 9, 10, 11, 12) with FeO/MgO ratio between 0.97 and 2.16 (< 60 per cent almandite) all have a CaO/CaO + MgO + FeO ratio of less than 19 per cent (less than 20 per cent grossularite + andradite) whereas garnets (13, 14, 15, 16, 17) with a higher FeO/MgO ratio than 2.16 (> 60 per cent almandite) all have a CaO/CaO+MgO+FeO ratio of greater than 4 (more than 20 per cent grossularite plus andradite).

As might be expected, the garnets with a high FeO/MgO ratio (7, 8, 9) in general have a slightly higher spessartite content than the magnesia-rich garnets (nos. 10, 11, 12).

The variation in composition of the garnets with variation in the nature of the enclosing rock is shown in figure 2. As might be expected, the garnets in the CaO-rich anorthositic series of rocks are richer in CaO than those of the gabbro and amphibolite group.

Types of Reconstituted Gabbros

Two major types of reconstituted gabbros are represented by the chemical analyses: garnet-free amphibolite gneisses and garnetiferous gneisses.

The amphibolite gneisses may be largely hornblende and plagioclase (table 2, nos. 1, 2, 3), hypersthenic amphibolite gneiss (5), augitic amphibolite gneiss (6) or hornblende-scapolite-plagioclase gneiss (4). Some of these amphibolite gneisses (4 and 6) represent little change in chemical com-

position from the original rock whereas others (1 and 3) have been somewhat modified. In the case of the latter two there has been a marked removal of both magnesia and ferrous iron from the primary rock to yield the secondary amphibolite. The scapolite type (4) is known from only one locality. The Dekalb amphibolite (2) comes from a zone between an alaskite granite mass and marble. Its origin is somewhat uncertain. The Stellaville (3) and Geers (6) amphibolitic gneisses are parts

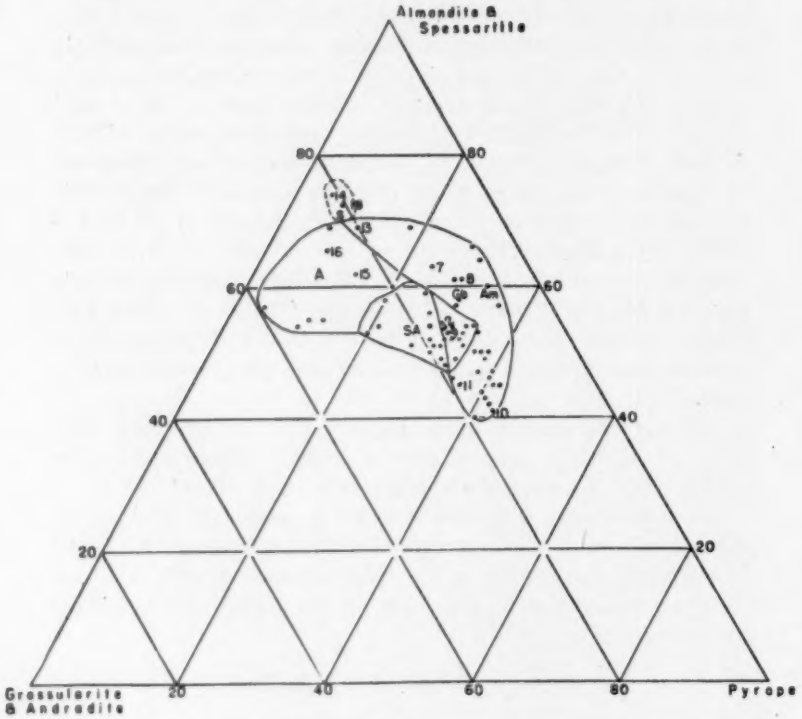

Fig. 2. Composition of garnet in mol per cent as related to different kinds of Adirondack rocks.

A—anorthosite, gabbroic anorthosite gneiss and metamorphosed hybrid anorthosite-skarn gneiss;

SA—gabbroic anorthosite gneiss (called syenite-anorthosite hybrid by Levin), Gb Am—metagabbro, gabbro gneiss. amphibolite gneiss and amphibolite;

S—syenite gneiss. Based on data by Levin (1950, pp. 531-532) and that of present report.

Numbers refer to chemically analyzed garnets.

of sills occurring within metasediments but are cut by granitic sheets and pegmatite veinlets. The Strifts School (1) and Bullock Brook (4) amphibolitic gneisses are wholly enclosed within granite. There is at present no garnet in any of the gabbro from which these amphibolitic gneisses were derived and there is no evidence of any ever having been present.

The garnetiferous gneisses (7-13) include several types. There is a coronite type (11) in which relics of the primary ophitic structure of the gabbro together with relics of primary mafic minerals such as olivine, augite and hypersthene are preserved. The coronite metagabbro type may occur as cores grading outward into sheaths of pyroxene gabbro gneiss or amphibolite gneiss which may or may not be garnetiferous.

Another type is a granoblastic amphibolitic gneiss with euhedral to poikiloblastic garnets. These rocks may be hornblende-garnet-plagioclase amphibolite gneiss (7) or hornblende-hypersthene-garnet-plagioclase amphibolite gneiss (8 and 9). A more advanced modification and recrystallization of this type results in a garnet amphibolite (10) with euhedral garnets enveloped in a shell of hornblende and with gneissic structure indistinct or effectively absent. All of the foregoing types occur for the most part enclosed in granite or in pyroxene quartz syenite gneiss or locally in belts of metasediments. The abundance of hornblende clearly indicates that they have been formed in the presence of hydrous fluids.

There is another type which consists essentially of augite and garnet with considerable iron oxides, and in part a little hypersthene. This type occurs exclusively as dikes either in the pyroxene syenite, pyroxene quartz syenite and older hornblende granite gneiss, or within anorthosite and gabbroic anorthosite gneiss. The rocks are wholly granoblastic and without minerals carrying volatiles. The Elizabethtown (13) granulite dike consists largely of augite (table 5, no. 13), almandite (table 4, no. 13) and oligoclase (An_{24}) with subordinate ilmenite (and magnetite) whereas the normative composition calculates as 13 olivine, 8.2 hypersthene, 12.1 diopside, 48 labradorite (An_{45}) and 8.7 magnetite and ilmenite.

It so happens that all of the plotted non-garnetiferous metamorphosed gabbros for which the hornblendes or garnets have been analyzed can be separated into one area of the triangle (fig. 1) and all the garnetiferous metamorphosed

gabbros into another area without overlap. This is not significant, however, for the position of several analyzed Adirondack non-garnetiferous metagabbros overlap on the area of composition of the garnetiferous facies and the composition of several garnetiferous metagabbro gneisses overlap on the area of the non-garnetiferous facies.

CHEMICAL PETROLOGY OF SOME METAMORPHIC GARNETIFEROUS QUARTZ SYENITIC AND SYENITIC ROCKS

Pyroxene syenitic and quartz syenitic rocks are extensively developed in the Adirondacks. They comprise two different series which occur as separate sheet-like masses: the Diana-Stark complex and the Tupper-Saranac complex, respectively. The rocks of the Diana-Stark complex vary from ferroaugite syenite gneiss with feldspathic ultramafic layers rich in ilmenite and magnetite to ferrohastingsite granite gneiss, all with hypersthene minor in amount and confined to the more mafic facies. The rocks of the Tupper-Saranac complex vary from mafic ferroaugite-hypersthene syenite gneiss (25-30 per cent mafics) through ferrohypersthene and eulite quartz syenite gneiss to fayalite-hedenbergite granite. Orthopyroxene is a common to major mineral throughout most of the facies of the Tupper-Saranac complex. The rocks of the Tupper-Saranac complex (with the possible exception of the fayalite-hedenbergite granite) have been intensely metamorphosed and all have a xenomorphic granular texture. The feldspars are green to green-gray on fresh surface. In part the rocks are garnetiferous. All of these features are those which characterize the charnockitic suite of rocks and this term seems appropriately applicable to at least part of the members of the Tupper-Saranac complex. The garnetiferous facies, however, pass along the strike into similar pyroxenic but non-garnetiferous rocks which may or may not be called charnockitic, depending on the definition of charnockitic. The quartz syenitic rocks of the southeastern part of the map area (fig. 3) also belong to the charnockitic series.

A number of geologists in recent years have interpreted the characteristic features of the charnockitic series at many locaities in other lands as due to plutonic metamorphism of *common* hornblendic rocks. An excellent recent summary has been given by Quensel (1951). One part of this interpretation is that pyroxenes and garnet have formed in lieu of or at the expense

of hornblende. Another interpretation has been that some charnockitic kindreds are the product of plutonic metamorphism and modification of sediments. Neither of these explana-

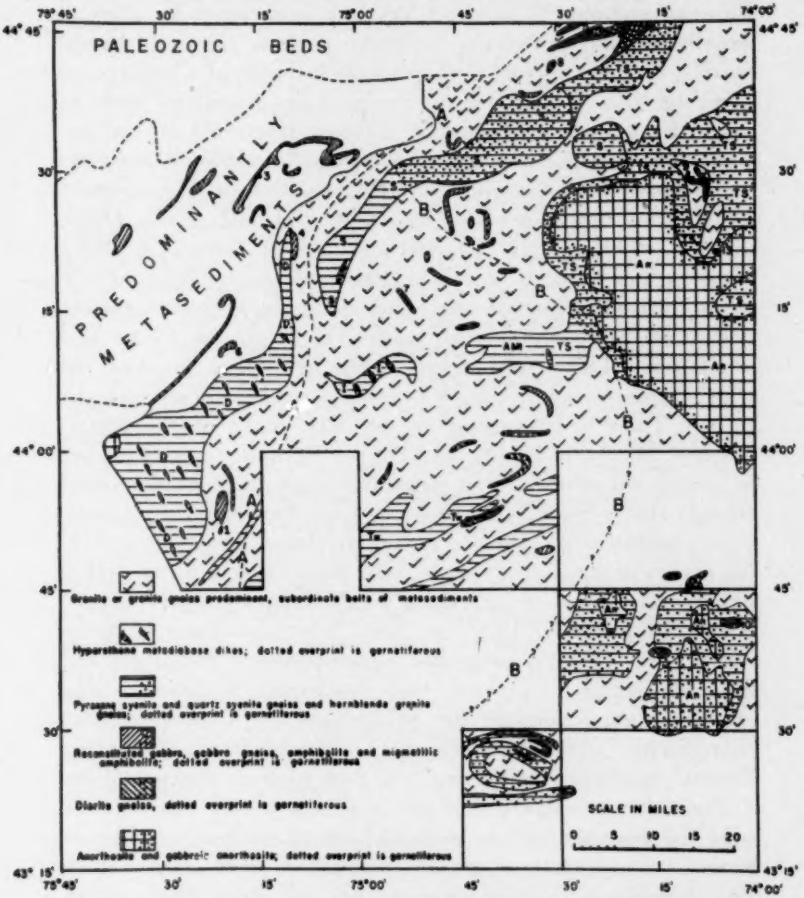

Fig. 3. Generalized map showing distribution of garnetiferous facies of rocks; northwest of line AA, anorthositic, gabbroic, dioritic and quartz syenitic series of rocks are non-garnetiferous; between lines A-A and B-B, gabbro, diabase, and diorite may be garnetiferous whereas quartz syenitic gneisses are non-garnetiferous; northeast, east and southeast of the line B-B, gabbroic anorthositic, gabbroic, dioritic and quartz syenitic gneisses are throughout at least locally garnetiferous. Numbers 1, 2, etc., show location of analyzed rocks. D = Diana complex, S = Stark complex, TS = Tupper-Saranac complex (I = Inlet portion, A Mt. = Arab Mtn. portion), TW = Twitchell Mtn. complex.

tions is applicable to the charnockitic suites of the Tupper-Saranac complex.

The original magmatic origin of the rocks of the Tupper-Saranac complex is attested by their occurrence as dikes in anorthosite and as massive pyroxene perthite sills in Grenville marble, by the occurrence, where in thick sheets, of a superposed layering with a variation in composition consistent with an origin by gravity stratification through fractional crystallization, and especially by their enclosing *far traveled xenoliths* and *xenocrysts* of the older country rock. Details in support of their initial magmatic origin have been previously given. (Buddington, 1939, pp. 116-134; 1948, pp. 28-30. Note: A drafting error occurs in plate 2 of the 1948 reference. There should be no horizontal lines in the small crescents of quartz syenite gneiss at Newman, several miles NE of Santa Clara and at Tupper Lake. The rocks there are felsic members of the Tupper-Saranac complex whose syenitic facies underlie them.) There is also good reason why rocks of the *mineralogical composition* of the Tupper-Saranac complex may be considered as initially of magmatic origin. The Alaska Coast Range, Diana-Stark, Bergen-Jotun and Tupper-Saranac complexes represent a series of "suites" or "tribes" in which pyroxene occurs in successively more felsic facies and in which orthopyroxene becomes of increasingly greater quantitative importance (Buddington, 1939, p. 228). The first three of these suites are commonly recognized as igneous rock complexes and it is reasonable to suppose that the fourth is likewise. The chemical compositions of the members of the Tupper-Saranac charnockitic suite are sufficiently different from the other "suites" mentioned to be consistent with such an interpretation.

There is no evidence that the pyroxene of the charnockitic suite has been derived from hornblende. Locally, the Tupper-Saranac charnockitic rocks are associated in the same region with hornblende granite gneisses of the older Diana-Stark complex. Though both series of rocks have been subjected to the same metamorphism with the development of garnet in each, the hornblende has persisted in each and is in part porphyroblastic. The rocks of the charnockitic series can be traced continuously from an area in which they have been metamorphosed under conditions of the granulite facies to one in which they have been metamorphosed under conditions of the amphibo-

lite facies. There is but little change in the quantity or composition of hornblende in similar rocks in the two areas and the chemical composition of the members of the series remains similar. The hornblende is, in part, of secondary origin from the pyroxene in the charnockitic rocks.

The magma of the Tupper-Saranac complex would have yielded a pyroxenic suite independent of plutonic crystallization or subsequent metamorphism.

Reconstituted Mafic Syenite Gneiss

The composition of a mafic quartz-bearing syenite gneiss (table 8, 14) together with its pyroxene (table 5, 14) and garnet (table 8, 14-G) have been studied. This rock is typical of the basal part of the Tupper charnockitic sheet. There is little or no hornblende in the mafic facies (over 25 per cent total dark minerals) though it is common in the upper felsic facies. The analyzed rock is a mortar gneiss. The mortar is a recrystallized granoblastic aggregate with considerable myrmekite. The garnet occurs both as coronas around the iron oxides and pyroxenes but largely as grains and elongate aggregates in the mortar where it is especially associated with quartz and recrystallized feldspar. Primary microperthite forms the major mineral of the rock. As might be expected, the garnet is richer in the almandite molecule and poorer in pyrope than any of the garnets from the gabbroic rocks. The rock contains inclusions of garnetiferous anorthosite and hornfelsed mafic gneiss and xenocrysts of labradorite. There is no evidence whatever, however, that the garnet could be of xenocrystic origin. The garnet of the syenite gneiss is different in composition from the garnets of the anorthositic rocks and is appropriate for the composition of the rock in which it occurs.

Pegmatitic Recrystallization and Segregation Veins in Felsic Charnockitic Rocks

General

All of the felsic facies of the charnockitic quartz syenitic gneisses in the map area (fig. 3) northeast, east, and southeast of line B-B carry, at least locally, small irregular recrystallization veinlets and seams of green pegmatite-like material. Similar pegmatitic material occurs in the quartz syenite gneisses of the Twitchell Mountain part of the Tupper-Saranac complexes but

not in the Arab Mountain or Inlet parts of the complex and not at all in the Diana-Stark complex. The pegmatite occurs as relatively short thin seams and veinlets parallel to the foliation of the host, as a flattened network of narrow veinlets the mesh of which is elongated parallel to the foliation, as small knots with fingers extending outwards like splashes from a blot, as pegmatitic facies developing at sharp bends in intense small plications of the foliation of the host rock and as veinlets sharply crosscutting the foliation. They are commonly less than an inch in width but rarely are up to several inches thick and are usually less than several feet, often less than several inches in length.

They are in large part massive and are almost uniformly less intensely deformed (if at all) than the country rock. Locally, however, the veinlets, though crosscutting the foliation, have themselves a foliation conformable with that of the country rock (granoblastic). In the massive type a little mortar structure may be present locally.

The chemical analyses of host rock and pegmatite seam are given for several examples in table 8. The host rock is too heterogeneous and the pegmatite is too coarse to determine an accurate mode without extensive research. The modes given are estimates based on a number of thin sections of each analyzed rock and its norm. The pegmatitic facies is too intimately involved with the country gneiss to obtain specimens of either which are certainly purely one or the other. Each of the rocks of the Vermontville and Eagle Bay localities is therefore to a slight extent a mixed facies.

Garnet and Pegmatitic Recrystallization Veins in Pyroxene Syenite Gneiss at Barton Mine

A mass of syenite gneiss occurs on the south side of the Barton Mine. For the most part it is fairly uniform and without any pegmatitic segregations or garnet, but in a local zone a little fine grained garnet is developed together with some coarse garnet associated with coarse pegmatitic syenitic veinlets. No pegmatitic development was noted with the fine garnets. The pegmatite seams are usually only a few inches long and less than an inch wide.

Chemical analyses of the syenitic host rock, and of the garnet are given in table 8.

The host gneiss is a pyroxene syenite gneiss with a granular

texture (±0.5 mm.) and interlocking grains interpreted as due to metamorphic crushing and recrystallization. There are all gradations between such gneiss with a few larger porphyroblastic crystals of microperthite and plagioclase, locally with enclosed relic aggregates or granules of the groundmass, and a vein of uniform pegmatitic recrystallization. The potash feldspar of the host gneiss is more perthitic and with a finer intergrowth than is that of the isolated porphyroblasts and pegmatitic veins. The pegmatitic recrystallizations consist of slightly perthitic potash feldspar, oligoclase, subordinate quartz and accessory ferroaugite, ferrohypersthene, magnetite, ilmenite, apatite and zircon. A little myrmekite is present. Locally, the potash feldspar shows a faint microcline structure. The potash feldspars are 3 to 10 mm. or more in diameter.

In part the pegmatitic recrystallizations carry garnets which are 0.5 cm. to 1.0 cm. in diameter and locally much larger (fig. 4). The larger garnets are euhedral. In thin section the garnets are seen to be quite uniformly surrounded by a narrow shell of plagioclase and in part are associated with pyroxene. The garnets may occur as isolated crystals (with the associated pegmatitic development in the form of pressure shadows along the foliation) or they may occur as a string of garnets in the central zone of a pegmatitic veinlet. Rarely, a large garnet with hornblende and alkali feldspar developed successively in vein matter at the ends of the garnet is found. The foliation is obliterated by the development of the larger garnets and associated pegmatite as though by recrystallization and replacement.

The garnets in the syenite gneiss have been interpreted by Krieger (1937, p. 110) as the product of incorporation by syenitic magma from an older rock. The garnets, however, appear to be definitely coordinate in development with the other minerals of the pegmatitic seams and have an appropriately consistent composition. The garnets in the syenite gneiss do not correspond to those in the metagabbro.

Pegmatitic Veins in Syenite Gneiss at Balfour Pond Quarry

The syenite gneiss at the Balfour Pond road metal quarry is strongly foliated and locally crumpled and plicated. Where the bends in the foliation are sharp there is a tendency for pegmatitic recrystallization to develop as though along poten-

tial shears (cf. Balk, 1932, figs. 2 and 3). The gneiss contains numerous large labradorite xenocrysts. Porphyroblastic hornblende occurs in the gneiss. In addition to the knots of pegmatitic recrystallization there is an occasional crosscutting veinlet of pegmatite. The analyzed pegmatite came from such a vein. The vein is about 3 inches wide, massive, with irregular walls and with its minerals intergrown with those of the host gneiss. The chemical composition of this vein is quite different from that of the host gneiss, being much higher in SiO_2 and K_2O and lower in CaO and FeO. The microperthite has a little very fine exsolution intergrowth of plagioclase and is in part microcline. There is a little garnet as replacement of plagioclase and as coronas around magnetite. Corona garnet also occurs around ferrohastingsite, ferrohypersthene and magnetite in the host gneiss. There is a little recrystallized mortar in the pegmatite. Schorl occurs in one pegmatite vein.

Pegmatitic Recrystallization Veins at Vermontville and Eagle Bay

The pegmatite seams at the Vermontville and Eagle Bay localities occur mostly as narrow seams at slight angles to the foliation of the country rock. No garnet has been observed in the country rock at either locality whereas the pegmatite veins carry sporadic small garnets up to 1.0 cm. in diameter. The garnet is commonly surrounded by a thin shell of granular oligoclase. The potash feldspar in both host gneiss and in the pegmatite seams is strongly microperthitic carrying about 20-25 per cent plagioclase as exsolution intergrowths. In part it has the distinct grid structure of microcline, in part no such structure is observable. The microperthite grains of the pegmatite are commonly about 1.0 cm. in diameter and may be up to 2 centimeters. The microperthite of the host rock is about 0.4 to 1.0 mm. in grain. The orthopyroxene of the Vermontville rocks is a ferrohypersthene-eulite and that of the Eagle Bay rocks is a eulite. There are exsolution spindles of ferroaugite in the orthopyroxene of the pegmatite indicative of the possibility that the original mineral was an iron-rich pigeonite. There is an occasional grain of myrmekite in all the rocks. The texture of the gneiss is xenomorphic granular and that of the pegmatite is hypidiomorphic. The hornblende is in part porphyroblastic in the gneiss and in part xenomorphic granular.

Fayalite Granite Pegmatite, Ausable Forks

The specimen of analyzed pegmatite from the Ausable Forks quarry is from a 6-inch vein which breaks clean from the host rock. It is too coarse grained for a microscopic modal analysis. Individual quartz grains are up to an inch in diameter. The only ferromagnesian mineral present is fayalite slightly altered to iddingsite. The feldspar is exclusively microperthite with the "plume" structure such as also characterizes the feldspar of the host rock.

General Comparison of Pegmatite Seam and Host Rock

In all cases the pegmatite seams carry less CaO and more SiO_2 than the host rock. The decrease in lime is reflected in the mineralogy of several of the pegmatitic facies where augite and/or hornblende is slight and the ferromagnesian mineral is almost wholly ferrohypersthene, eulite or fayalite. The higher silica content is reflected in the higher percentage of quartz in all the pegmatitic facies. Almandite occurs sporadically in all the pegmatitic seams except those in the fayalite granite, even where, as in the Vermontville and Eagle Bay localities, it has not been found in the host rock. Hornblende may occur as an occasional grain in the pegmatitic facies but is the major mineral only in the Balfour Pond quarry pegmatite.

The pegmatite veins approximately parallel to the foliation are in general very similar in composition to the host rock (20 and 20-A and 21 and 21-A) whereas the distinct crosscutting veinlet such as 19-A is strongly differentiated, very much higher in quartz and with a much higher ratio of potash feldspar to oligoclase.

Origin of Pegmatitic Facies

The pegmatitic veinlets have been interpreted by Balk (1932, pp. 29-32) as late magmatic in origin and by Cannon (1937, p. 60) as a product of metamorphic differentiation.

A mode of origin as late residual liquid from magmatic crystallization is favored by the following phenomena. On the Arab Mountain anticline the pegmatitic veinlets occur exclusively in the eastern part, in the most siliceous and latest differentiated facies, near the roof around the plunging nose of an anticline. At Ausable Forks the pegmatite veinlets cannot be of simple

TABLE 8

Chemical Analyses of Syenitic, Quartz Syenitic and Granitic Gneiss, Pegmatitic Facies and Related Garnets

	Barton Mine		Balfour Pond		Vermontville		Eagle Bay		Ausable Forks		Moody Pond	
	18	18-G	19	19-A	20	20-A	21	21-A	22	22-A	14	14-G
SiO_2	57.88	37.21	58.45	69.87	60.51	62.50	70.89	72.24	69.98	75.46	53.35	37.53
Al_2O_3	18.70	20.49	15.71	14.58	14.16	13.91	13.18	13.09	12.37	8.26	14.97	20.29
Fe_2O_3	1.84	1.14	1.61	.56	1.60	1.60	.96	.91	1.11	1.27	3.31	2.14
FeO	5.00	30.88	6.76	1.80	8.02	6.62	3.04	2.09	5.13	6.69	10.61	29.54
MgO	.80	1.79	1.34	.57	1.17	.98	.33	.30	.08	.07	1.72	1.37
CaO	3.60	7.05	4.97	1.69	4.14	3.63	1.63	1.29	1.25	1.08	6.43	7.40
Na_2O	4.64	....	4.08	2.52	3.47	3.44	3.16	3.14	3.99	2.58	3.50	.12
K_2O	5.30	....	3.98	7.42	4.38	4.02	5.29	5.43	4.91	3.34	3.74	.04
H_2O+	.21	.09	.31	.11	.10	.38	.25	.40	.16	.22	.14	.07
H_2O-	.12	.03	.08	.09	.09	.12	.13	.15	.05	.11	.10	.00
TiO_2	1.07	.10	1.46	.24	1.52	1.40	.56	.33	.46	.38	1.38	.25
P_2O_5	.33	....	.61	.09	.58	.46	.11	.09	.04	.01	.71	....
MnO	.08	1.41	.14	.04	.17	.13	.09	.06	.14	.17	....	1.77
CO_2	.15	....	.23	....	....	.51	.19	.30	.07	.05	....	....
S	.01	....	.07	....	....	.06	.03	.02	....	.01	....	....
BaO	.11	....	.14	....	....	.10	.07	.07	....	.01	....	....
Total	99.84	100.19	99.91*	99.58	99.91	99.84*	99.90*	99.90*	99.74	99.71	99.96	100.52
Sp. G	2.751	4.105	2.819	....	....	2.796	2.683	2.653	2.712	2.748	....	....

*Less O for S

TABLE 8 (Cont.)

Chemical Analyses of Syenitic, Quartz Syenitic and Granitic Gneiss, Pegmatitic Facies and Related Garnets

	Barton Mine		Balfour Pond		Vermontville		Eagle Bay		Ausable Forks		Moody Pond	
					NORMS							
Quartz	0.45	....	5.85	21.93	11.07	16.38	27.21	29.67	22.62	39.87	0.48	....
Orthoclase	31.14	....	24.46	43.92	26.13	24.46	31.41	32.25	28.91	19.74	21.68	....
Albite	39.30	....	34.58	20.96	28.82	29.08	26.72	26.75	34.06	24.10	29.34	....
Anorthite	14.46	....	12.23	6.67	10.15	10.15	5.98	3.89	1.39	....	14.46	....
Hypersthene	7.58	....	8.79	3.44	10.96	10.12	4.76	3.39	5.89	8.47	13.80	....
Diopside	0.71	....	6.66	.93	6.12	2.02	.25	....	3.96	4.95	11.21	....
Magnetite	2.55	....	2.32	.81	2.32	2.32	1.39	1.32	1.62	1.86	4.87	....
Ilmenite	2.13	....	2.82	.46	2.89	2.74	1.06	.61	.91	.76	2.74	....
Apatite	.67	....	1.34	.20	1.34	1.01	.27	.20	.10	.02	1.68	....
Corundum	....	....	....	....	....	....	....	....	.51	....	....	....
Calcite	0.30	....	0.50	....	....	1.10	.40	.70	....	....	....	....
					ESTIMATED MODE							
Microperthite and Feldspar	....	....	40.	53.	38.2	34.	45.	49.	63.	....	39.2	....
Plagioclase	....	....	30.	16.	24.9	30.	19.5	15.	4.5	....	22.7	....
Quartz	....	....	10.	23.	11.1	18.	27.	28.7	21.5	....	3.4	....
Orthopyroxene	....	....	4.	....	6.4	12.	2.	4.	....	....	2.8	....
Clinopyroxene	....	....	....	....	7.9	....	0.5	0.5	6.†	....	12.6	....
Hornblende	....	....	12.	5.	6.2	1.	4.5	0.3	Tr.	....	0.4	....
Ilmenite and Magnetite	....	....	2.6	1.2	3.6	2.30	1.0	1.2	1.	....	8.2	....
Apatite	....	....	1.0	0.3	1.3	1.00	0.3	0.2	0.2	....	2.1	....
Zircon	....	....	0.2	0.1	0.4	0.20	0.2	0.1	0.4	....	0.4	....
Garnet	....	....	0.3	0.3	....	0.40	....	1.	....	....	8.0	....
Pyrite	....	....	....	....	....	....	....	....	0.2	....	0.2	....
Fayalite	....	....	....	....	....	....	....	....	3.	....	....	....
Calcite	....	....	....	....	....	1.00	....	....	....	....	....	....

† Hedenbergite

TABLE 8-A

Per Cent Molecules in Garnet of Syenitic Gneiss

	14-G	18-G
Almandite	70.	69.1
Pyrope	4.6	7.2
Grossularite	14.2	16.7
Andradite	7.0	3.6
Spessartite	4.2	3.4

(18) Syenite gneiss, non-garnetiferous, Barton Mine, Gore Mtn., Thirteenth Lake Quad. Analyst, H. Baadsgaard.

(18-G) Almandite from pegmatitic seams in syenite gneiss (18), Barton Mine, Gore Mtn., 13th Lake Quad. Analyst, J. A. Maxwell.

(19) Quartz syenite gneiss. Quarry 0.7 mile S of Balfour Pond, Newcomb Quad. Analyst, H. Baadsgaard. Primary perthite is completely reconstituted to clear potash feldspar (faint microcline structure) and clear plagioclase and mafic minerals to ferrohastingsite and ferrohypersthene with a little almandite as coronas around magnetite.

(19-A) Hornblende granite pegmatite. 3-inch vein across foliation of host rock (19). Quarry 0.7 mile S of Balfour Pond, Newcomb Quad. Analysts, G. Kahan and R. B. Ellestad.

(20) Hornblende-pyroxene syenite gneiss, quarry one mile ENE of Vermontville, Saranac quadrangle. The analyzed rock contained a little pegmatitic veining. Analysts, G. Kahan and R. B. Ellestad.

(20-A) Ferrohypersthene quartz syenite pegmatite with sporadic garnet. From syenite gneiss of (20), quarry one mile ENE of Vermontville, Saranac Quad. Analyst, Eileen H. Oslund.

(21) Ferrohastingsite-eulite granite gneiss, road cut 0.8 mile NW of Eagle Bay, Big Moose Quad. Analyst, Eileen H. Oslund.

(21-A) Eulite granite pegmatite seam in ferrohastingsite-eulite granite gneiss (21), road cut 0.8 mile NW of Eagle Bay, Big Moose Quad. Analyst, Eileen H. Oslund.

(22) Fayalite-hedenbergite granite, quarry seven-eighths of a mile NE of Ausable Forks, Ausable Quad. Analyst, R. W. Perlich.

(22-A) Fayalite granite pegmatite vein 6 inches wide in quartz syenite (22) host. Analyst, H. Baadsgaard.

(14) Garnet-pyroxene syenite gneiss or granulite, Moody Pond Quarry, Saranac Quad. Analyst, A. H. Phillips.

(14-A) Almandite from syenite of (14).

metamorphic differentiation for they occur exclusively in undeformed fayalite hedenbergite granite which forms the uppermost portion of a syenitic sheet. Pegmatitic veinlets occur largely in the quartz syenitic rocks with 10 per cent or more of quartz and rarely in syenite or mafic syenite gneiss. Pegmatite veinlets occur in substantial development in amphibolite layers included within quartz syenite gneiss. The pegmatite veinlets are uniformly less deformed than the host rock. No pegmatitic veinlets

have been found within the sheet of phacoidal quartz syenite and granite gneiss of the Diana-Stark complex which occurs in the same area though it is thought to have undergone metamorphism at a similar time.

An origin by metamorphic differentiation on the other hand is favored by the following phenomena. The evidence that the foliation of most of the quartz syenitic rocks was developed after their complete consolidation is very strong. The primary pegmatites in these rocks, if present, should therefore be deformed to a similar degree as the host rock and this is not the case. The pegmatite veinlets often carry sporadic corona garnet or disseminated garnets with an oligoclase shell. This would be consistent with an interpretation that they developed under similar conditions as the country rock most of which also carries corona garnet. Most of the pegmatite veinlets do not have a visible foliation. Some, however, do have a foliation which crosses them and is parallel to that of the host rock. This too would be consistent with the idea that they originated in the last stages of metamorphism. Locally, as at Gore Mountain, there are all gradations between isolated porphyroblasts of potash feldspar and pegmatitic recrystallizations locally occurring as pressure shadows to garnet which seem clearly of an origin by metamorphic recrystallization. The individual garnets in this rock are part of a concretionary structure and are surrounded by a shell of oligoclase. The pegmatite veins which are more or less parallel to the foliation have a similar mineralogy and composition to that of the host rock. All the pegmatite veins with the exception of those in the fayalite-hedenbergite granite have irregular borders and their minerals are intergrown with those of the host rock.

The evidence is consistent with an hypothesis that the pegmatite seams (except for those in the fayalite-hedenbergite granite) are the result of recrystallization along fractures or foliation planes with some metamorphic differentiation. The metamorphic differentiation is at a minimum in the case of the seams along the foliation and at a maximum in the distinctly crosscutting veins. The metamorphism proceeded under conditions which resulted in the sporadic formation of garnet as porphyroblasts and coronas in the pegmatite seams even whether there is or is not garnet in the host rock. The metamorphic recrystallization and differentiation must have occurred at a high temperature

(somewhere around 625°C.) to account for the degree of original solid solution indicated by the now unmixed microperthitic feldspars using the solvus as determined by Bowen and Tuttle (1950) as a guide.

If the pegmatitic development in the gneisses occurred when the quartz syenitic and granitic facies of the Tupper-Saranac complex was still wet or damp from their own original primary fluids, whereas in general the syenitic facies of the charnockites and the rocks of the Diana-Stark complex were solid and dry, it would explain why pegmatite developed in the former rocks and not in the latter. The fayalite-hedenbergite granite is massive and the pegmatite veins in it are of late residual fluid origin. More work must be done before the significance of the massive character of the fayalite-hedenbergite granite can be evaluated.

The writer has no satisfactory explanation which is consistent with all the phenomena, but the balance of evidence is definitely accordant with an origin of the pegmatitic seams as a product of regional metamorphism.

ORIGIN OF GARNETIFEROUS FACIES OF GABBROIC ROCKS

Previous Hypotheses

The author (Buddington, 1939, pp. 258-282) has stated it as his conclusion that the first major metamorphism and reconstitution of the diabasic or gabbroic rocks was effected in a period of orogenic deformation (B, table 1) under conditions of regional dynamo-thermal metamorphism with but little introduction or elimination of material. The development of the garnetiferous facies of the rocks was in large part effected in the presence of a slight but variable amount of permeating fluids assumed to be related to rising subjacent granite magmas in their early stages of emplacement at levels well below that of present exposure. The fluids were probably present in large parts as intergranular films. The presence of such fluids is indicated directly by the hydroxyl and fluorine of the secondary hornblende and by chlorine and carbon dioxide in local secondary scapolite. Later, the granite magmas were emplaced at the level of their present exposure and effected a superimposition of local or large scale reconstitution on the already metamorphosed rocks to yield amphibolite and migmatitic amphibolite gneiss. Any pre-existing garnet was destroyed in immediate direct con-

tact zones with the granite but was preserved or recrystallized away from the contact (Buddington, 1939, pp. 183-188).

The origin of the reconstituted gabbro at the Barton garnet mine (table 2, no. 10) in the southeastern Adirondacks has been studied by Shand (1945), Shaub (1949) and Levin (1950) and the origin of a garnetiferous reconstituted gabbro dike has been discussed by Jaffe (1946).

Shand (1945, p. 262) interpreted the corona garnet at the Barton mine as due to thermal metamorphism, whereas Levin (1950, p. 561) explained the corona garnet as of deuteric origin and the porphyroblastic garnet as a local recrystallization of corona garnet through contact metamorphism produced by adjoining intrusive quartz syenite. Shaub (1949) concluded that the large garnets and associated hornblende rims and related minerals developed from retained isolated pegmatitic or deuteric solutions having more or less spherical outlines enclosed within hornblende diorite. Jaffe (1946) ascribed the origin of the garnets in a post-anorthosite reconstituted gabbro dike within the anorthosite as due to thermal metamorphism.

Regional Variation in Intensity of Metamorphism and Significance

General.—Levin has thoroughly studied a number of reconstituted garnetiferous gabbros in the southeastern Adirondacks and on the basis of this work has raised many objections to the hypothesis that they are due to regional dynamo-thermal metamorphism.

It is the writer's belief that the origin of the garnets at any one locality, or in the southeast Adirondacks in general, cannot be treated as an isolated problem and solved exclusively in the light of such phenomena as are found there. Regional studies have led to the interpretation that the problem of the reconstituted gabbros in the southeastern Adirondacks is part of one and the same problem as that of the reconstituted gabbros in the Adirondacks as a whole. It is also very probably only one aspect of the more general problem of the origin of the garnet in *both* the reconstituted gabbros and in the quartz syenitic gneisses. If the implications of regional studies conflict with the implications of local studies, neither can be ignored but some solution must be found which will satisfy both.

The regional relationships of the garnetiferous rocks are shown in figure 3. This map is generalized. The gabbro and quartz syenitic rocks within the areas marked garnetiferous are not uniformly garnetiferous. Garnet is apparently not common but does occur locally in the syenitic and quartz syenitic rocks of the Thirteenth Lake and Indian Lake quadrangles. The exact positions of lines A-A and B-B have not been defined. Nevertheless, the map is believed to show the kinds of relationships which are present. There is a systematic variation in the nature of the metamorphism from west and northwest to east and southeast which appears to demonstrate that a regional factor is a fundamental element in the development of the garnetiferous facies. A discussion of certain significant points follows.

Garnet and gabbroic rocks.—There is no garnet in the gabbroic masses north and west of the Diana complex or of the line A-A (fig. 3). Garnet does not occur, however, in all gabbro masses distributed throughout the eastern part of the map area east of line A-A. The development of garnet, where it does occur in the gabbro masses, also is not uniform but may be confined to certain portions or layers. Relics of unmetamorphosed gabbro may occur with an ophitic structure in cores surrounded by sheaths or envelopes with a strongly gneissic foliation or a zone reconstituted to amphibolite gneiss. The garnet may occur in the core and not in either the pyroxene gneiss or the amphibolite gneiss, or it may occur in both the core and the amphibolite sheath or in local zones within the gneissic facies.

It is stated (Levin, 1950, p. 524) that the garnet occurs in portions of some gabbroic rocks in which recrystallization of the primary minerals had not occurred or had reached only an incipient stage, and (p. 527) that foliation is absent in the least modified facies of the gabbro and is not generally evident in the metagabbro facies, including the Barton ore. It is true that corona garnet occurs locally in reconstituted gabbro with primary ophitic structure. Associated with such patches and lenses, however, there is also a foliated facies even on a microscopic scale in which there is granular recrystallization of primary augite to secondary augite, hornblende and biotite with concomitant development of corona garnet. The interchange of materials to permit the development of these secondary minrals would be adequate to permit rotation of the primary plagio-

clases to yield the foliated structure. Foliation is present in part of the garnet ore and some of the garnets have the fabric of porphyroblasts with a greater development of hornblende (locally with associated secondary plagioclase) in pressure shadows (see plate 1, fig. 2 and plate 2, fig. 1 of Levin's paper). The garnets to a subordinate extent tend to occur in lenses and strings oriented parallel to the foliation and connected by coalescing hornblende with minor feldspar. These lenses are greatly extended parallel to a line and have no great continuity down dip. Where recrystallization has progressed furthest the foliation is lost.

Members of the anorthositic series of rocks varying from anorthosite through gabbro and melanocratic gabbro to ultramafic pyroxenitic gneiss occur in the northwest, central, and eastern Adirondacks. No garnet whatever has been found in the northwestern rocks, whereas it is common as coronas and porphyroblasts in all the members of the deformed facies in the central and eastern Adirondacks. Secondary porphyroblastic almandite is also common in the deformed gabbroic anorthosite-pyroxene skarn mixed rocks of the eastern Adirondacks (Buddington, 1950). Analyses 15, 16 and 17 (tables 2 and 4) are of the rock and almandite from gabbroic anorthosite gneiss, gabbroic anorthosite gneiss mafic from incorporation of pyroxene skarn, and an ultramafic pyroxenitic gneiss; all are members of the anorthositic series in the eastern Adirondacks and all have been regionally metamorphosed.

Garnet and pyroxene quartz syenitic series.—There is no garnet in the pyroxene syenite and quartz syenite, and hornblende granite gneisses west of line B-B (fig. 3). This includes the Diana complex, south part of the Stark complex, and the Inlet, Arab Mountain and Twitchell Mountain masses except in pegmatite seams. To the east of line B-B, on the contrary, corona garnet is common in the similar and continuous belt of pyroxene syenite and quartz syenite gneisses and hornblende granite gneiss of the Stark complex and in the Tupper-Saranac complex.

It has been stated that the syenite in the southeastern region is garnet-free and that there is no evidence of post-syenite garnet (Levin, 1950, p. 556). This statement appears to be based on the assumption that wherever garnet crystals and corona garnet

occur in the quartz syenitic gneisses it is a product of inheritance by incorporation of material from disintegration of garnetiferous anorthosite or reconstituted garnetiferous gabbro. This hypothesis is incompatible with the fact that we find corona garnet in coarse pegmatite-like recrystallizations of the quartz syenite gneiss in the southeastern Adirondacks and also in the syenite and quartz syenite gneisses in the same fashion as in the northern Adirondacks though perhaps more sporadically. There are inadequate data in the literature on the details of occurrence and distribution of accessory garnet in the southeastern Adirondacks but what there is is consistent with reconnaissance studies made by the author in this area. Garnet occurs as coronas around grains of magnetite or ilmenite strongly elongated in the foliation planes of a mafic syenite gneiss, 5.2 miles northwest of Gore Mountain or 0.6 mile northwest of the outlet of Thirteenth Lake. Cannon (1937, p. 25) writes of the porphyritic quartz syenite in the Piseco Lake quadrangle, "In addition, garnet is present in nearly all specimens as grains embedded in plagioclase. In a few specimens garnet occurs also as reaction rims on magnetite pyroxene or hornblende, especially at contacts with plagioclase" and (p. 22) of the equigranular quartz syenite "garnet occurs sporadically." Krieger (1937, p. 59) writes of the syenite in the Thirteenth Lake quadrangle, "garnet is not a common mineral in the syenite of the Thirteenth Lake quadrangle. Wherever garnet does occur in the syenite, it is usually confined to the contact with some other rock or near the garnet deposits. Garnet, mainly as small crystals and irregular masses is common in the granite and more acid phases of the syenite." Miller (1917, p. 23) describes the quartz syenite of the Blue Mountain quadrangle as carrying garnet sporadically in small amounts, and (1916, p. 14) the syenite of the Lake Pleasant quadrangle as carrying garnet occasionally. All of the foregoing quadrangles are in the southeastern Adirondacks.

Whereas the recrystallized microperthite grains of the quartz syenite gneiss of the belts southeast of line A-A (fig. 3) carry a strong perthitic intergrowth, the potash feldspar of granoblastic gneiss of similar composition northwest of line A-A carries only a little intergrowth of plagioclase. This indicates metamorphism at a lower temperature, that of the amphibolite facies, for the northwest area.

Are the Garnets in Syenitic Rocks at Barton Mine Xenocrysts or Porphyroblasts?

A "light garnet ore" at the west end of the Barton mine is described by Levin (1950, pp. 549-551) as consisting of syenite and syenitic hybrid facies. He interprets the rocks as resulting from partial and selective assimilation of metagabbro by quartz syenitic magma whereby a coarse-grained garnetiferous hornblende-plagioclase rock of light dioritic or soda gabbroic character is formed. The garnets are described as xenocrysts embedded in the hybrid matrix but as almost entirely rimless due to the syenite having largely "shelled" the original garnets from their hornblende shell during incorporation. Data for three examples of the hybrids in which these supposed "shelled garnets" occur are given. Two are composed of 75 and 80 per cent plagioclase (An_{40} and An_{52}, respectively) without any potash feldspar and a third contains 45 per cent plagioclase (An_{45}) and 5 per cent potash feldspar. The composition of the first two

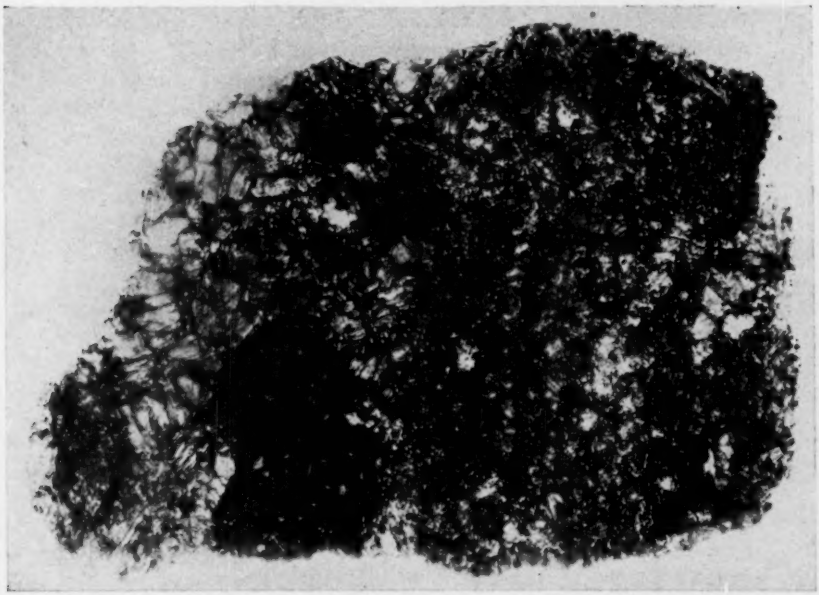

Fig. 4. Syenite gneiss with a few thin pegmatitic seams on right. Coarse pegmatitic syenite gneiss with almandite (black in pegmatite) at left. Barton Mine.

rocks is that of normal gabbroic anorthosite only very slightly modified and the basis for assuming that enough syenitic magma entered the gabbroic anorthosite to shell the garnets is not given and is apparently quite inconsistent with the data. In the same discussion the garnets are referred to as of essentially the same composition as these of the main garnet deposit. Again, this statement appears to be inconsistent with the data given. The data on the composition of the garnets are quoted below.

Composition of Garnets in Contaminated Syenite and in Assumed Syenite-Anorthosite Hybrid at Barton Mine (after Levin)

No.	Rock	ALM	PYR	GROSS	AND	SPESS
B-14	Contaminated syenite gneiss	64	8	21	4	3
B-25	Syenite-anorthosite hybrid*	51	31	11	6	1
Range of 11 garnets, metagabbro ore		40-49	37-43	10-14	2-3	1

* Stated to contain 80 per cent plagioclase (An_{40}) and no potash feldspar. This would make it a very slightly modified gabbroic anorthosite.

It will be noted that there is a *distinct* difference in the composition of the garnet in the syenite and that in the metagabbro and so-called syenite-anorthosite hybrid (actually gabbroic anorthosite). It will also be noted that in figure 2 the garnets from rock inferred by Levin to be of syenite-anorthosite hybrid nature do not lie in the field for garnets from rocks intermediate between anorthosite and syenite but in the field for rock intermediate between anorthosite and gabbro. The rock from the Hooper Thirteenth Lake Deposit (Levin, 1950, pp. 563-564) from which several of the SA garnets came is also described as consisting of 70-85 per cent plagioclase (An_{50-54}), mafic minerals and no orthoclase. This is a typical gabbroic anorthosite gneiss.

Evidence that the garnets in the pyroxene syenite gneiss at the Barton Mine are in part metamorphic porphyroblasts *in situ* has previously been given.

The following hypothesis is presented here as an alternative. Gabbroic anorthosite and gabbroic anorthosite with mafic schlieren were intruded by a lens of gabbro. These were in turn intruded by pyroxene quartz syenite. The syenite was locally contaminated with material from the gabbroic and anorthositic rocks. The latter were locally slightly modified by solutions from the syenite magma. The whole complex was then deformed and recrystallized locally to yield a coarse garnetiferous facies in

each type of rock. The composition of the garnets varies consistently with that of the host rock.

Garnetiferous Hypersthene Metadiabase Dikes

Hypersthene metadiabase dikes, in part reconstituted, cut the foliation of the pyroxene syenite and quartz syenite gneisses and hornblende granite gneiss of the Diana complex, south part of the Stark complex and the Inlet and Arab Mountain masses. In the Diana complex the material of these dikes is partly granulated but there is little or no reconstitution. To the east, however, in the area between lines A-A and B-B the dikes are characteristically garnetiferous and granoblastic.

As has been noted, the statement has been made (Levin, 1950, p. 556) that garnet does not occur in the normal pyroxene quartz syenite of the southeastern Adirondacks and that the garnet of the reconstituted garnetiferous gabbros can not therefore be of post-syenite age. The actual relationships found in the Inlet, Arab Mountain, and south part of the Stark masses prove that this argument is invalid, since garnetiferous reconstituted metadiabase dikes actually do occur here in garnet-free pyroxene syenite and quartz syenite gneisses.

The garnet is not of deuteric origin for it is found exclusively in the deformed facies, occurs both as corona garnet and as euhedral garnets and does not occur in the numerous dikes of similar age, nature and relationships west of line A-A. The dikes have very fine-grained chill border zones. They must have been emplaced under moderate depth conditions, in an environment where almandite has never been proven to form as a primary or deuteric mineral.

Garnet in Contact Zones of Syenite and Quartz Syenite with Gabbro

There are in the southeastern Adirondacks many examples where the quartz syenite masses are in contact with or include zones of garnetiferous amphibolite. The amphibolites with very coarse garnets especially *appear* to be related to such relationships. Indeed so strikingly is this the case that it was a major factor in leading Levin (1950) to the conclusion that the Barton garnet ore is an extreme metagabbro facies whose large garnets were derived from microscopic corona garnet during the peripheral metamorphism of the gabbro by intrusive syenite magma.

In the northeastern quarter of the map area (fig. 3), however, there are as many or more examples where porphyroblastic (garnet) amphibolites representing reconstituted gabbros are included in the younger granite, miles from any exposed quartz syenite. Neither is the garnet directly related to contact zones of younger granite with amphibolite or gabbro. Many masses of amphibolite without garnet (representing reconstituted gabbro) are included within the younger granite between the Tupper-Saranac and Stark complexes. Again, west of line A-A (fig. 3) there are many miles of contact between granite and amphibolite but never a garnet.

There is unequivocal evidence that both corona and porphyroblastic garnet was developed at least locally in the pyroxene quartz syenitic rocks throughout the area east of line B-B (fig. 3). This is proof that since the syenite is younger than the gabbro there was a period of metamorphism in which garnet developed on a regional scale in appropriate rocks in post-syenite time. Gabbro is certainly an appropriate rock for the development of garnet and one must assume that at least some garnet formed in the gabbros during this period of metamorphism. The garnetiferous hypersthene metadiabase dikes which are themselves younger than the quartz syenite may be cited as confirmatory evidence insofar as the northwest Adirondacks are concerned.

However, if the hypothesis is adopted that all the garnet as we now find it was developed during a period of regional metamorphism post-syenite and post-hypersthene diabase in age, there remains to be explained the fact that the coarsest development of garnet in amphibolite by reconstitution of gabbro occurs in part in contact zones with quartz syenite. On one hypothesis, a possible factor in the metamorphic recrystallization and differentiation of the pegmatitic seams in part of the quartz syenite gneisses has been interpreted to be a residual film of primary fluid at the time of deformation. Such a fluid would presumably migrate through border zones of rock such as metagabbro gneiss or gabbroic anorthosite gneiss during deformation and accentuate the growth of garnet crystals. This hypothesis of regional metamorphism for the garnets in contact zones of gabbro with quartz syenite thus has something in common with that of contact metamorphism in that the fluid accentuating the exceptionally coarse recrystallization came from

the quartz syenite. It is very probable, however, that the fluid present during the regional metamorphism of these rocks came in large part from the rising younger granite magma. This is indicated by the occasional presence of schorl as at Balfour Pond quarry. Schorl has never been attributed to a genetic relationship with the quartz syenitic rocks.

GENERAL CONCLUSIONS

In summary we interpret the development of garnet in the metamorphosed igneous rocks in terms of regional dynamothermal metamorphism, before the emplacement of the younger granites at their present level of exposure and later than the hypersthene diabase and all older formations such as the syenitic and quartz syenitic series, olivine gabbro, and anorthositic series of rocks. The intensity of metamorphism varied in such a way that in the northwest (northwest of line A-A), the rocks were metamorphosed under the conditions of the amphibolite facies, and garnet did not develop in any of the rocks of the anorthositic series, gabbro sheets, pyroxene syenite and quartz syenitic series, metadiabase or hybrids of pyroxene quartz syenite with the older rocks. Within an intermediate belt to the southeast (area between lines A-A and B-B), garnet did develop locally in reconstituted gabbro and diabase masses but not in the pyroxene syenite and quartz syenite gneisses. Southeast, east and northeast of the intermediate belt (northeast, east and southeast of the line B-B) garnet further developed in the border facies of the anorthositic rocks and and their melanocratic segregates, in parts of the olivine gabbro and in the pyroxene syenite and quartz syenite gneisses and the hornblende granite gneiss of the Diana-Stark complex. The interpretation is that the intensity of metamorphic conditions in the northwest was not sufficient to permit the development of garnet in any of the rocks. To the east, in similar or the same rocks, the intensity increased so that garnet first developed in some of the gabbro and diabase and then farther east and northeast under the most intense conditions the garnet developed in the pyroxene quartz syenitic and related hornblende granite gneisses in addition to the other rocks. Contemporaneously pegmatitic recrystallization seams with some associated metamorphic differentiation and development of sporadic garnet

formed in the felsic quartz syenite gneisses of the eastern belt and also in part of the intermediate belt of metamorphism.

The development of garnet is interpreted to occur in the last stage of an epoch of regional dynamothermal metamorphism, in large part in the presence of fluids emanating from a rising granite magma mass. These were the *geologic* conditions. They do not necessarily lead to the inference that stress was an essential factor at the time of formation of the garnet or that it was an essential factor in the *physicochemical* as distinguished from the *geologic* conditions. The actual development of the garnet may have been largely a reconstitution phenomenon with some metamorphic differentiation in strained rocks similar to an annealing process under hydrostatic conditions. The point has been made (Levin, 1950) that garnet has developed in undeformed gabbro and therefore in such a case at least is not related to dynamic metamorphism. This seems reasonable in strictly physicochemical terms. From the geologic standpoint, however, we suspect that stress actually did loosen the intergrain boundaries of the ophitic gabbro so that they could be lubricated by a film of fluid or that the plagioclase in the boundary zone was strained so as to facilitate the development of the garnet reaction. It may also be noted that the garnets have a set of fractures oriented about at right angles to the foliation and interpreted as formed consequent on stress. A few of these fractures have plagioclase along them indicative that stress was present at some time during the development of the porphyroblastic garnets. In the core of the anorthosite mass where there is little or no deformation there is no garnet but in the granoblastic border facies garnet is common. The complete recrystallization of the gabbro with the development of much hornblende and of coarse garnet crystals in both the gabbro and the syenite gneiss at the Barton Mine would suggest some actual movement of fluids as well as favorable diffusion.

The hypothesis of regional dynamo-thermal metamorphism for the geologic conditions accompanying the development of the garnetiferous facies admittedly meets many apparent inconsistencies for which we do not have any explanation at this time but it is favored as satisfying more requirements than any other.

In contrast to the type of reconstitution where hornblende

has formed consequent on the introduction of some fluid, there is also the type where reconstitution has proceeded in such fashion as to yield essentially anhydrous minerals only, as in the case of some coronite metagabbro and granoblastic garnet-augite-iron oxide granulites (tables 2, 13 and 14). The coronite type occurs both in the cores of metagabbro dikes with anhydrous granoblastic granulite border zones, and also in cores of ophitic metagabbro which are surrounded by sheaths of amphibolitic gneiss. Anhydrous granulite has been found exclusively in metagabbroic dikes within the syenite, pyroxene quartz syenitic and related hornblende granite gneisses and within the anorthosite and gabbroic anorthosite gneisses. A possible interpretation is that in the case of the coronite metagabbro within amphibolitic shells there was not sufficient stress to deform the core so as to permit its penetration by adequate fluid to yield hornblende though this occurred in the more strongly deformed envelope. In the case of the coronitic and granoblastic anhydrous granulite dikes, the country rock was such as to afford no adequate access to the hornblende forming fluids. The hypothesis then would be that the garnetiferous amphibolitic gneisses were reconstituted under relatively "wet" conditions and the anhydrous non-hornblendic coronites and granulites under relatively "dry" conditions. The syenite gneisses also have in part yielded garnet-augite-iron ore granulites as exemplified by the Moody Pond rock (table 2, no. 14).

The rocks in the east and southeast are thought to have been reconstituted at higher temperatures than those in the northwest. The factor of temperature may therefore be an element in controlling the distribution of constituents between the various minerals of the different rocks. Unfortunately, however, no two gabbros from different temperature zones proved to be sufficiently similar in chemical composition to yield trustworthy evidence on this factor.

An hypothesis has been suggested by Ramberg (1948, pp. 567-568) that the major and minor features of the rocks here discussed are the product of very large scale intermigration of non-volatile material during metamorphism of solid rock. The evidence is clear that volatiles have had a widespread entry into much of the rock though usually not necessarily more than as a mere intergranular film. The evi-

dence is equally clear, however, that the movement of non-volatile materials has been on a small scale, usually a matter of not more than a few feet. The development of garnet by diffusion in anorthosite gneiss bordering diabase dikes wholly reconstituted under "anhydrous" conditions has nowhere been observed for more than a centimeter. Large garnets, indicative of maximum intermigration, occur exclusively in rocks where H_2O, Cl, F, etc., have pervaded the rock so as to permit development of hornblende.

The substantial excess of temperature of the rocks in the east and southeast as compared with those in the northwest during the period of metamorphism may be explained by the rocks in the east and southeast having been downfolded into the earth's crust to a depth of several miles or so more than in the northwest with a consequent rise of temperature. A minimum of about 625° C. would appear to be necessary to explain the perthitic character (Bowen and Tuttle, 1950) of the feldspar of the metamorphic veins. The eastern arc of rocks of the deep granulite environment has subsequently risen so as to now be exposed at the same topographic levels as the rocks of the amphibolite facies or in part at higher altitudes.

The tie-lines connecting respectively the garnet and the rock of which they are a part have a different orientation for the anhydrous pyroxenic granulite facies (nos. 11, 13, 14 and 17) from those of the hornblende-garnet granulite facies (nos. 10, 8, 12, 9 and 7). The garnet of the augite garnet granulite (nos. 13 and 14) tends to be more calcic than the garnet of the hornblende-garnet granulites of equivalent composition.

The problem arises as to why there are no eclogites in the Adirondack area. A tie line (AE) for a magnesia-rich eclogite and its garnet from the Jagerfontein mine in South Africa is shown for comparison. The writer has found in the literature no description of an eclogite (together with adequate description of its garnet) corresponding to any of the Adirondack garnet gabbros here discussed. The Adirondack rocks have a different ratio of iron, lime and magnesia. The geologic occurrence of some eclogites is such as to preclude an origin as a high pressure facies formed under exceptionally high pressure conditions, though an origin as a high pressure facies formed as an unstable assemblage under moderate pres-

sure and moderate temperature conditions below its normal thermodynamically stable field is a possibility (Dengo, 1950). It may be that the temperature of metamorphism of the Adirondack granulites was too high for the pressure and composition concerned to permit the development of eclogite.

After a major period of metamorphism, younger granite magmas invaded the complex of metamorphosed rocks and formed by far the major rock southeast of the Diana and Stark complexes. In the northwest the development of amphibolite was much accentuated and extended at this time. Amphibolite layers are also widespread within the main granite bodies throughout the Adirondacks. Garnet in the immediate contact zone of garnetiferous amphibolite with granite has been destroyed, though there may be some recrystallization of garnet a short distance away from the contact. No evidence has been found that garnet developed directly in connection with migmatitization of amphibolite by the granites.

The secondary mineral associations of the Adirondack garnetiferous rocks, both the hornblendic garnetiferous assemblage and the pyroxenic garnetiferous association seem appropriately classified as belonging to the "granulite facies" whereas the non-garnetiferous amphibolites, especially those of the northwest, are equally appropriately classified as the "amphibolite facies."

References

Balk, Robert, 1932. Geology of the Newcomb quadrangle. New York State Mus. Bull. 290.

Bowen, N. L., and Schairer, J. F., 1935. Grünerite from Rockport, Massachusetts and a series of synthetic fluoramphiboles: Am. Mineralogist, vol. 20, pp. 543-551.

———, and Tuttle, O. F., 1950. The system $NaAlSi_2O_6$—$KAlSi_2O_6$—H_2O Jour. Geology, vol. 58, pp. 489-511.

Buddington, A. F., 1939. Adirondack igneous rocks and their metamorphism: Geol. Soc. America Mem. 7.

———, 1948. Origin of granitic rocks of the northwest Adirondacks: Geol. Soc. America Mem. 28, pp. 21-43.

———, 1950. Composition and genesis of pyroxene and garnet related to Adirondack anorthosite and anorthosite-marble contact zones: Am. Mineralogist, vol. 35, pp. 659-670.

Cannon, R. S., 1937. Geology of the Piseco Lake quadrangle: New York State Mus. Bull. 312.

Dengo, Gabriel, 1950. Eclogitic and glaucophane amphibolites in Venezuela: Am. Geophys. Union Trans., pp. 873-878.

Eskola, Pentti, 1921. On the eclogites of Norway: Vidensk. Skr. I, Mat.-Naturv. Kl., no. 8.

Hess, H. H., 1949. Chemical composition and optical properties of common clinopyroxenes: Am. Mineralogist, vol. 34, pp. 621-666.

Jaffe, Howard W., 1946. Postanorthosite gabbro near Avalanche Lake in Essex County, N. Y.: Jour. Geology, vol. 54, pp. 105-116.

Kemp, J F., 1899. The titaniferous iron ores of the Adirondacks: U. S. Geol. Survey, Ann. Rept. 19, part 3, pp. 377-422.

———, and Ruedemann, Rudolf, 1910. Geology of the Elizabethtown and Port Henry Quadrangles, N. Y.: New York State Mus. Bull. 138.

Krieger, M. H., 1937. Geology of the Thirteenth Lake quadrangle: New York State Mus. Bull. 308.

Levin, S. Benedict, 1950. Genesis of some Adirondack garnet deposits: Geol. Soc. America Bull., vol. 61, pp. 519-565.

Miller, W. J., 1916. Geology of the Lake Pleasant quadrangle: New York State Mus. Bull. 182.

———, 1917. Geology of the Blue Mountain quadrangle: New York State Mus. Bull. 192.

Poldervaart, A., 1950. Correlation of physical properties and chemical composition in plagioclase, olivine and orthopyroxene series: Am. Mineralogist, vol. 35, pp. 1067-1079.

Quensel. Percy, 1951. The charnockite series of the Varberg district on the southwestern coast of Sweden: K. svenska vetensk. akad., Arkiv for Mineralogi och Geologi, Band 1, no. 10.

Ramberg, Hans, 1948. Titanic iron ore formed by dissociation of silicates in granulite facies: Econ. Geology, vol. 43, pp. 553-570.

———, 1949. The facies classification of rocks: Jour. Geology, vol. 57, pp. 18-54.

———, and DeVore, G., 1951. The distribution of Fe and Mg in coexisting olivines and pyroxenes: Jour. Geology, vol. 59, pp. 193-211.

Shand, S. J., 1945. Coronas and coronites: Geol. Soc. America Bull., vol. 56, pp. 247-266.

Shaub, B. M., 1949. Paragenesis of the garnet and associated minerals of the Barton Mine near North Creek, New York: Am. Mineralogist, vol. 34, pp. 573-582.

Williams, A. F., 1932. The genesis of the diamond: E. Benn, London.

Princeton University
Princeton, New Jersey

RELATIONS BETWEEN COMPOSITION AND INDICES OF REFRACTION IN NATURAL PLAGIOCLASE

F. CHAYES

ABSTRACT. New determinative charts for the refractive index-composition relation are presented. Possible discontinuities in the relation are discussed. While complete optical continuity is not disproved by the data, sample descriptions based on one or two breaks in the series suggest simple relations between the commonly measured natural plagioclases and the albite and anorthite polymorphs produced by laboratory synthesis.

ORGANIZATION, DISTRIBUTION, AND REJECTION OF DATA

THE work reported here began as an attempt to improve existing determinative charts for sodic plagioclase and has been gradually extended to cover the full range of composition. A preliminary discussion of the gamma index has already been published (Chayes, 1950), but since that time the collection of data has been materially enlarged and subjected to more extensive numerical analysis. Although the principal objective of the work is descriptive, the results may interest readers not particularly concerned with petrography because of the questions they raise—and the answers they suggest—with regard to the relations between optical properties and the proposed temperature modifications in the plagioclase series.

The measurements used have been culled from the technical literature of more than half a century. After a little reading, one finds that the same localities are cited over and over again; as there are far more optical measurements than chemical analyses, one is tempted to expand the sample by assuming that all plagioclase from a single site is of one composition. The temptation is particularly strong because the practice is so common, but the wisdom of resisting it is amply demonstrated by the careful work of Ernst and Nieland (1934) on the famous Linosa andesine, the composition of which apparently varies all the way from An_{38} to An_{54}.

In terms of reported chemical composition the distribution of data is as shown in table 1. There are probably hundreds of partial and full optical determinations in the literature but the group tallied in table 1 is a very large proportion of those

TABLE 1

Frequency of Data

An content	Values used	Values rejected	Total
≤ 10	18	1	19
11 - 20	8	1	9
21 - 30	8	0	8
31 - 40	5	0	5
41 - 50	0	3	3
51 - 60	8	2	10
61 - 70	5	0	5
71 - 80	4	0	4
81 - 90	3	1	4
91 - 100	7	0	7
Totals	66	8	74

for which chemical analyses are available. I am indebted to Professor Harry Hess for permission to include some unpublished results in the labradorite-bytownite range and to colleagues at the Geophysical Laboratory for a group of 9 new analyses extending over the entire composition range. All previously unpublished measurements are given in Appendix A, which also contains a list of sources.

I have tried to include only optical data obtained from the same specimen—or at least the same collection—as the analytical sample, though a few advertent and no doubt several inadvertent exceptions to this rule have been allowed. Where more than one analysis is reported the results are treated as entirely independent. If an analysis is not regarded as applicable to his material by the author of a particular set of optical measurements, it has not been used with them. If different analyses are cited in different papers on optics of the "same" plagioclase—a very common occurrence in albite and anorthite—each properly paired set of indices and compositions is regarded as a separate determination and the calculations are carried through without regard to the fact that the determinations are for material from the same locality. This procedure is surely open to criticism, but the alternatives are even less satisfactory; we must either select some one determination as preferable or average both the compositions and the indices for all the specimens from the same locality. The first alternative discards much valuable information and the second misuses it.

The problem of rejecting suspicious or faulty determinations is troublesome, for if we knew how to distinguish a good result from a bad one we would have no need for an empirically determined curve. In order of increasing anorthite content, the final rejections are as follows:

1. *Baveno* (Pagliano, 1937) An_3. All three indices are much too low even for pure albite.

2. *Cala Francesca* (Riva, 1902) An_{13}. All three indices far too low for An_{13} but fit $An_{7.5}$ nicely.

3. *Rochesauve* (Michel-Lévy and Lacroix, 1890; Fouquet, 1894). Apparently both papers describe the same specimen. Optics are identical, but in 1890 it was An_{40} and in 1894, An_{45}.

4. *Santa Lucia*, Azores (Fouquet, 1894). Two specimens are described, both with composition An_{48}. Optics of one seem about normal but the other has partial birefringences .0068 and .0007, so that 2V is far too small for any known plagioclase. Both results were discarded though it is possible that neither is in error.

5. *Quebec* (Duparc and Gysin, 1926) An_{55}. All three indices are far too low for An_{55} but agree quite well with An_{50}.

6. *Carlton Peak* (Winchell, 1900) An_{59}. All three indices far too high but agree well with An_{65}.

7. *Bönskär* (Lundegårdh, 1941) An_{86}. Extreme indices are about those of An_{83} but β indicates An_{78}. Partial birefringences are those of a positive mineral but plagioclase of this composition is always described as negative.

The chief occasion for rejecting results in which all three indices are those of a plagioclase of different composition is not so much that the observed composition is unexpected as that one or more of the indices are unique. Item 5, above, is an excellent example of this; it happens that the collection contains no other specimen with $\gamma = 1.562$. This one determination thus fixes a datum point which has as much weight in the calculations as others based sometimes on as many as ten or more determinations. Duparc and Gysin published this description along with two others (Inschitobel, Spruce Pine) and in

all three An seems suspiciously low. In the other two, however, the indices are not unique, and the compositions are subsequently averaged with others.

The rejections have the unfortunate effect of deleting all the data for calcic andesine. Information on the optics of andesine is sparse and contradictory. Refinement and satisfactory interpretation of the determinative chart require drastic increase in the data for the intermediate plagioclases.

The chart is designed for use on common plagioclase and I believe is now based broadly enough that discrepancies must be attributed either to experimental error or to uncommon plagioclase. In the light of recent studies (cf. U. S. Geol. Survey Bull. 980, 1951) one immediately suspects the chemical analyses, but the possibility that highly precise and internally consistent optical measurements are subject to pronounced interlaboratory bias cannot be excluded. Nor may one exclude the occasional occurrence of anomalous plagioclases. But results suspect for any one of these reasons have no place in calculations designed to yield a chart for use on common plagioclase.

Although treatment of the data involves somewhat more arithmetic than is usual, it differs from conventional procedure in only one fundamental respect. The index of refraction is used throughout as independent variable; indices have been rounded to the third place, and An values (weight per cent) reported for each value of each index have been averaged to yield the datum points listed in tables 2, 3, and 4. In order to facilitate comparison with previous work, however, composition is shown as abscissa in all the graphs.

For the β index (table 3) a single line of best fit calculated over the entire range seems about all the data permit. Differences between observed and expected values are neither large nor systematic, and there appears to be no empirical justification for further curve fitting. Although the existence of departures from linearity in the β- An relation is not disproved in this fashion, it is safe to say that any which may exist must be very small.

To the α and γ indices (tables 2 and 4) three successive approximations are applied. The first is a linear equation calculated over the entire range; it proves to be unsatisfactory in both cases because of small but systematic dis-

TABLE 2

Average An (Weight Per Cent) for Different Values of α

α	Average An	No. of Determinations	α	Average An	No. of Determinations
1.528	1.8	4	1.555	51.7	5
1.529	1.1	10	1.556	53.6	2
1.530	1.6	2	1.560	60.0	2
1.531	8.2	2	1.561	62.0	1
1.532	7.6	1	1.562	64.9	2
1.534	13.1	2	1.565	69.7	1
1.535	15.7	2	1.566	75.5	2
1.537	20.0	2	1.569	78.1	2
1.538	17.4	1			
1.539	22.0	4	1.571	87.9	2
			1.574	93.5	4
1.540	24.0	1	1.575	97.0	1
1.542	25.0	1	1.576	96.0	2
1.543	28.8	1			
1.545	35.7	4			
1.546	38.0	1			
1.548	40.0	1			

TABLE 3

Average An (Weight Per Cent) for Different Values of β

β	Average An	No. of Determinations	β	Average An	No. of Determinations
1.532	0.6	3	1.550	38.0	1
1.533	1.5	10	1.552	40.0	1
1.534	1.5	2	1.558	51.3	2
1.535	3.2	2	1.559	55.3	2
1.536	9.2	2			
1.537	13.0	1	1.564	62.0	1
1.538	13.2	1	1.565	62.8	1
1.539	15.7	2	1.566	63.8	1
			1.568	69.7	1
1.541	20.9	1			
1.542	19.0	1	1.571	76.0	1
1.543	20.9	4	1.573	76.2	1
1.544	21.6	1	1.576	86.0	1
1.546	25.0	1			
1.548	28.8	1	1.581	90.9	1
1.549	35.7	3	1.582	93.9	2
			1.583	97.0	1
			1.584	96.0	2

TABLE 4

Average An (Weight Per Cent) for Different Values of γ

γ	Average An	No. of Determinations	γ	Average An	No. of Determinations
1.538	0.8	1	1.562	50.6	1
1.539	1.3	13	1.563	53.2	2
			1.564	53.9	3
1.540	1.6	2	1.568	56.5	1
1.541	8.2	2	1.569	62.0	1
1.543	11.6	2			
1.544	15.1	2	1.570	62.8	1
1.545	17.4	1	1.571	64.8	2
1.546	20.6	3	1.574	69.7	1
1.547	21.9	3	1.576	75.5	2
1.548	24.0	1	1.578	78.1	1
1.549	25.0	1			
			1.581	85.9	1
1.550	28.8	1	1.584	89.7	1
1.553	36.3	4	1.586	92.9	3
1.556	40.0	1	1.587	95.4	1
			1.588	96.3	3

crepancies over large portions of the composition range. The second approximation is a parabola, again extending over the full range. The third utilizes all the data for separate treatments of the sodic and calcic plagioclases; this is a modification of, and, I believe, an improvement over, the procedure used in the preliminary note, in which all data for intermediate plagioclases were discarded and lines calculated for the extremes of the range were simply extrapolated into the central region.

The systematic discrepancies appearing in the full-range linear calculations for α and γ are eliminated by each of the others and in this respect there is little to choose between the subsequent treatments. But the limited range linear regressions for α and γ permit prediction of the indices of certain anomalous forms of albite and anorthite described elsewhere in this volume, and the procedure which utilizes all the data yields a threefold subdivision of the series with discontinuities very near those proposed recently by Cole, Sörum, and Taylor (1951).

Even after deletion of the highly discrepant or doubtful measurements described above, very few of the individual measurements agree exactly with the expected values. It is con-

ventional in work of this sort to attribute such minor discrepancies to experimental error, but we cannot be sure here that this is their only source. The work of Köhler (1942) and his associates indicates that small changes in the orientation and perhaps also in the shape of the optical indicatrix may be induced by sufficiently prolonged heating of almost any natural plagioclase of the type suitable for high grade optical study. Differences in thermal history may thus be partly responsible for the remaining variation.

FULL RANGE LINEAR CALCULATIONS

Figure 1 shows the data and calculated linear regression lines for each index. With few exceptions the discrepancies between observed and calculated compositions are small, and the correlation in each case is very high; $r_\alpha = 0.9976$, $r_\beta = 0.9761$, $r_\gamma = 0.9975$. Using variance as a measure of variability, the smallest of these coefficients indicates that more than 95 per cent of the total variation of composition is accounted for by a single linear relation between index and composition.

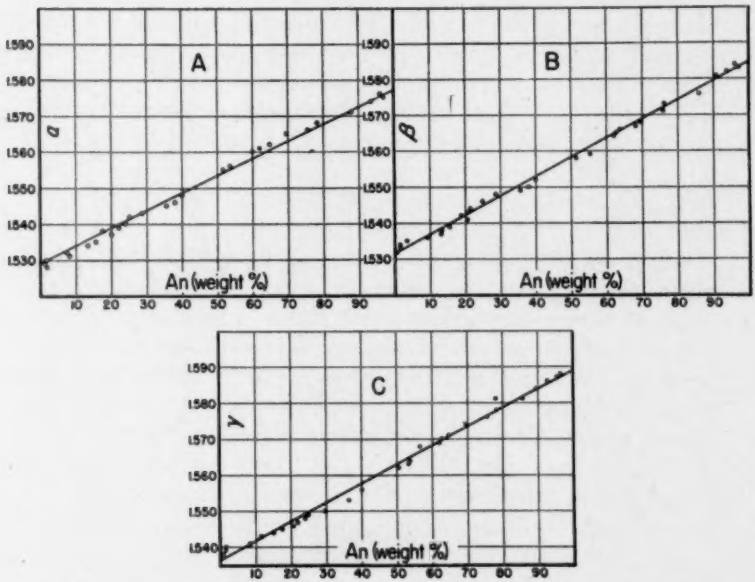

Fig. 1. Full range regression of An content with η. A — α, B — β, C — γ.

With correlation as high as this, there is no justification for more involved fitting unless the discrepancy between observed and expected values appears to be systematic. There seems to be no pronounced tendency toward systematic discrepance in the β relation.

With α and γ, however, the case is quite otherwise. At the calcic end of the series the γ line fits very nicely, but in the range $15 < An < 55$ all 11 datum points indicate an excess of observed over expected anorthite, while in the region $0 < An < 15$ all 5 points indicate a deficiency of observed anorthite. These relations have already been described (Chayes, 1950). For α, systematic deviations from the single straight line extend over an even larger range. Of the 16 datum points in the region $0 < An < 40$, 12 show an excess of observed over expected An and only 2 a deficiency, while in the region $50 < An < 80$, all 8 datum points show less than the expected amount of An. The systematic discrepancies involve fully half the data for γ and nearly three-fourths of the data for α. Despite the unusually high correlation there is thus good reason

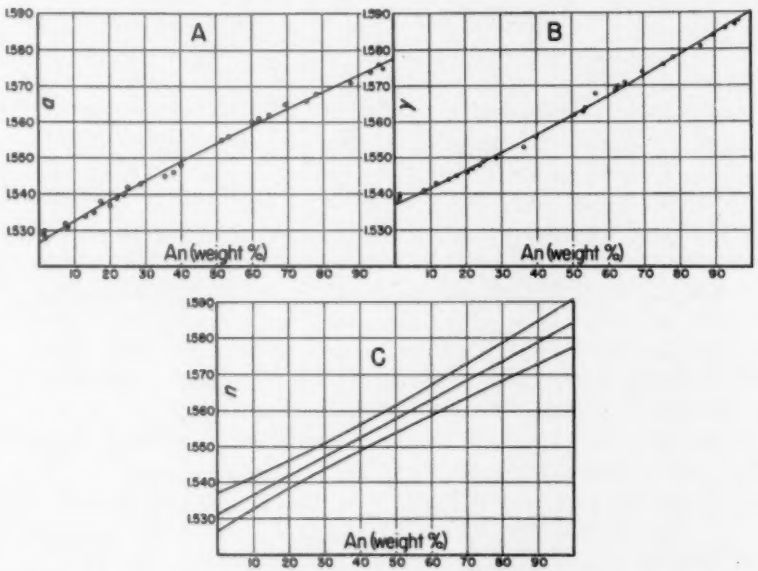

Fig. 2. Second order regression of An content with α and γ. A — α, B — γ, C — a possible determinative chart.

to suppose that a more adequate sample description could be found.

SECOND ORDER REGRESSIONS FOR α AND γ

A slight curvature of the α and γ regression lines tends to reduce or eliminate the systematic residual variance.[1] Figure 2 shows the datum points and second order regression lines for each of these indices. The sequences of signs of the deviations are still patchy, particularly at the calcic end of the range, but the sizes of the deviations are so reduced that it is hard to think of them as invalidating the proposed relation. The pattern of figure 2C is similar to that predicted by both Mallard and Pockels (1906) for a "homogeneous" isomorphous series extending without break from albite to anorthite, but nearly every optical crystallographer who has studied the plagioclase series has concluded that it is not isomorphous (e.g., see Pockels, 1892; Wulff, 1902; Wallerant, 1896).[2] Although the curvatures shown by the new α and γ lines are of the type generated by the Mallard and Pockels hypotheses, the reduction of total birefringence in the intermediate range is apparently less than indicated by either of these formulations. This objection was raised, among others, by Becke (1906), and since he was convinced that the series is completely isomorphous, Becke was obliged to conclude that the Mallard and Pockels definitions of "homogeneous optical isomorphism" were wrong.

While it is true that these hypotheses have not been applied successfully to systems of triclinic symmetry, it is also true that much of the early work was characterized by a cavalier disregard of the fallibility of chemical analysis. Chiefly because of uncertainty on this score we are even now in no position to decide whether the theories are wrong or the observations inadequate. But apparently neither hypothesis gives a satisfactory account of the generally accepted variation of optic angle or extinction position in the central region of the plagioclase series.

If the plagioclase series is not isomorphous according to the criteria of optical crystallography, the elimination of sys-

[1] For an opposite but mistaken opinion, see Chayes, 1950.

[2] Even Michel-Levy (1895, p. 94) suggested the possibility of a break in the vicinity of calcic oligoclase.

tematic deviations from the linear regression of composition on index by insertion of a second or higher order term is open to question; for if the resulting equation is regarded as anything more than a purely descriptive device, it clearly implies that there is no discontinuity in the series. From the very slight curvature of the parabolas in figure 2 and the close fit of the datum points to them it is clear that the discontinuity must be a rather minor affair; its size and location in each extreme index are nevertheless crucial to a rationalization of the optical properties of high temperature albite as well as those of certain anomalous materials of anorthite composition described elsewhere in this volume (see Davis and Tuttle).

LIMITED RANGE LINEAR REGRESSIONS FOR α AND γ

As the nature of the sampling precludes detailed statistical testing, the mere decision to confine the calculations to particular portions of the range in effect prejudges the issue as to whether or not there is a discontinuity. We have to be particularly careful, therefore, to avoid any hidden commitment about the location of the discontinuity. It has been apparent from the early stages of the work that most of the data lie at the extremes of the composition range, and that for intermediate compositions there is little information. Indeed much of what little information there is about the optical properties of andesine and labradorite is highly inconsistent.

As an entry to the problem I therefore simply abandoned data for the intermediate compositions and fitted regression lines for α and γ in the regions where the information was most abundant, and, presumably, most reliable. Extrapolation of these new regression lines into the central region yields a better check with observed values than do the full range regression lines shown in figure 1. The calculations had reached this stake at the time of publication of the earlier note on γ (Chayes, 1950), in which the existence of a discontinuity is regarded as supported by the procedure. Final results of the calculations over the two 30 per cent ranges are shown with data for the central region in figure 3a. Total (calculated) birefringence is identical for both pairs of lines at An_{40}; $\gamma - \alpha$ is here 0.006, and as smaller values are almost never reported, a break in the series at An_{40} would be very convenient.

The objective of the calculations was to establish a new and more reliable determinative chart, and in this connection it

seemed both wasteful and potentially misleading to abandon all data in the region $30 < An < 70$. I therefore cast about for some procedure which would use this information without requiring an arbitrary choice of the range of the new equations, and hence of the location of the discontinuity in each index relation, prior to the calculations.

From inspection of figure 3a it is obvious that the α line calculated for sodic plagioclases may be extrapolated all the way to An_{70} without serious error. Similarly, the γ line calculated for calcic plagioclase picks up the observed values quite well as far down as An_{30}. New calculations were therefore run for α in the regions $0 < An < 70$ and $60 < An < 100$, and for γ in the regions $0 < An < 40$ and $30 < An < 100$, with results shown in figure 3b. The "discontinuities" shown at $An_{30.4}$ for γ and $An_{66.1}$ for α are simply the points of intersection of the two equations for each index. The earlier twofold subdivision of the series now gives way to a threefold

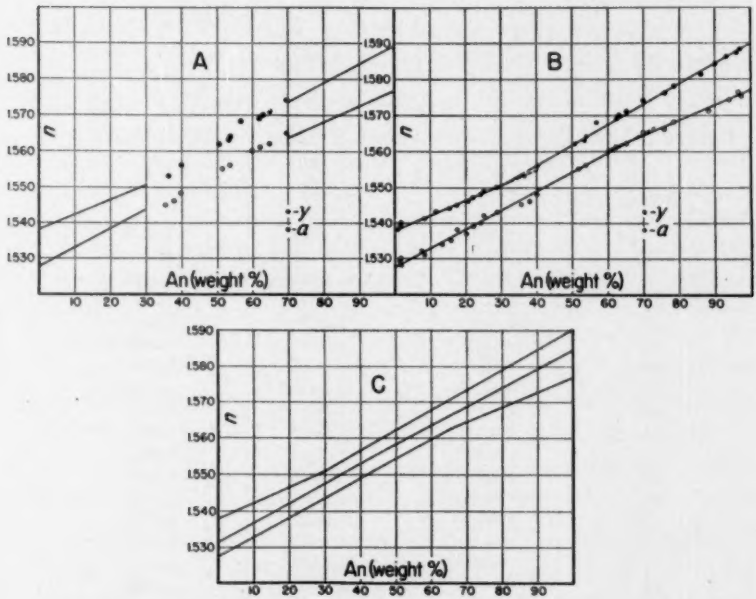

Fig. 3. Limited range linear regression of An content with α and γ.
A — for the regions $0 < An < 30$ and $70 < An < 100$.
B — Graphs of equations 1-3.
C — Determinative chart.

classification but two of the index regressions are common for each pair of adjacent classes. The distinction between sodic and intermediate plagioclase is only in the rate of change of composition with γ; the distinction between intermediate and calcic plagioclase is only in the rate of change of composition with α. At the extremes of the composition range, where the data are abundant, the sample description reached in this fashion is almost indistinguishable from that yielded by the calculations from which measurements in the intermediate composition range are excluded.

A determinative chart (fig. 3c) of any desired size may be prepared by plotting the following sets of equations:

$$\text{An} = 1875.71\,\alpha - 2864.98; \quad 0 < \text{An} < 66.1 \qquad (1a)$$
$$\text{An} = 2393.99\,\alpha - 3674.84; \quad 66.1 < \text{An} < 100 \qquad (1b)$$
$$\text{An} = 1879.72\,\beta - 2878.69; \quad 0 < \text{An} < 100 \qquad (2)$$
$$\text{An} = 2343.59\,\gamma - 3604.31; \quad 0 < \text{An} < 30.4 \qquad (3a)$$
$$\text{An} = 1771.28\,\gamma - 2716.63; \quad 30.4 < \text{An} < 100 \qquad (3b)$$

In table 5 the indices yielded by these equations are listed for the entire series in 5 per cent increments of An.

TABLE 5

Indices of Refraction Calculated from Equations (1-3) for 5 Per Cent (Weight) Increments of An

An	α	β	γ
0	1.5274	1.5314	1.5379
5	1.5301	1.5341	1.5400
10	1.5327	1.5367	1.5422
15	1.5354	1.5394	1.5443
20	1.5381	1.5420	1.5465
25	1.5408	1.5447	1.5486
30	1.5434	1.5474	1.5507
35	1.5461	1.5500	1.5535
40	1.5488	1.5527	1.5563
45	1.5514	1.5553	1.5592
50	1.5541	1.5580	1.5620
55	1.5568	1.5607	1.5648
60	1.5594	1.5633	1.5677
65	1.5621	1.5660	1.5705
70	1.5643	1.5686	1.5733
75	1.5664	1.5713	1.5762
80	1.5684	1.5740	1.5790
85	1.5705	1.5766	1.5818
90	1.5726	1.5793	1.5846
95	1.5747	1.5819	1.5875
100	1.5768	1.5846	1.5903

OPTIC ANGLE

As might be expected, the optic angles calculated from eq. (1-3) do not agree particularly well with the standard Reinhard diagram (1931). The number of sign changes is the same, but they are differently situated; in general they are displaced toward anorthite so that the optically positive region of sodic plagioclase is expanded and the optically negative region of calcic plagioclase is reduced. In the intermediate composition range 2V is always greater than 80°, whereas both the Reinhard curve and the Köhler modification indicate that measured values in this region are often smaller. It is interesting to note, however, that the calculated sign change in andesine lies to the right of the crossing proposed by Köhler, so that the change of sign in the supposed high temperature plagioclases is actually bracketed by those measured directly and calculated from the indices of the so-called low temperature plagioclases.

The combination of very large optic angle and very small total birefringence makes 2V extraordinarily sensitive to small differences in index. At An_{25}, for instance, the Reinhard diagram shows a minimum of 82°(—) while the calculated 2V is 88°(—). Now although a difference of 6° in optic angle is certainly large in relation to the precision with which 2V may be measured directly under optimum circumstances, it is not of much consequence when 2V is calculated from the indices. The expected indices at An_{25} are 1.5407, 1.5447, and 1.5486. If the extreme indices are presumed correct in the fourth place, β need be increased by only 0.0005 to yield the Reinhard value of 88°(—) for the optic angle. But of course some error attaches to each of the predicted index values, and if the increment to β in this calculation were distributed over all three indices, the required shift in each index would amount to no more than 2 or 3 in the fourth place.

INDICES OF SOME ANOMALOUS COMPOUNDS OF PLAGIOCLASE COMPOSITION

Synthetic albite crystals of sufficient size to permit measurement of refractive indices were first prepared hydrothermally by Tuttle and Bowen (1950), and it then became clear that albite produced in the laboratory was not identical with that ordinarily occurring in crystals of the type optical crystal-

lographers like to measure. For reasons described at considerable length elsewhere (Köhler, 1942, 1950; Bowen and Tuttle, 1950; Tuttle and Bowen, 1950; Tuttle, 1952) there is now a fair measure of agreement that natural albite of the type described in standard works on optical crystallography is a low temperature form, while that produced by hydrothermal synthesis, like the phenocrysts of certain lavas, is a high-temperature modification. The high-temperature form is nevertheless metastable at very low temperature under experimental conditions, for it can be formed far below the proposed inversion point, and to date the low temperature modification has not been synthesized at any temperature.

Subsequent to the synthesis of high-temperature albite two anomalous compounds of anorthite composition, formed by slow cooling of an anorthite melt from very high temperatures, were brought to the notice of the Laboratory. A short account of this development, together with a description of further experimental work, appears elsewhere in this volume (Davis and Tuttle). One of these new "anorthites" is hexagonal, the other is orthorhombic, and the refractive indices of both differ considerably from those of natural anorthite.

It happens that the indices of high temperature albite and both new forms of anorthite are readily obtained from the index regressions for natural plagioclase, shown in figure 3c. For convenience, the indices of all three forms, as well as those of natural albite and anorthite, are shown in table 6.

TABLE 6

Indices of Refraction of Natural and Synthetic Plagioclase End-Members

	α	β	γ
*Natural albite (low temp.) ...	1.5274	1.5314	1.5379
Synthetic albite (high temp.)..	1.527	1.532	1.534
*Natural anorthite	1.5768	1.5846	1.5903
Orthorhombic anorthite	1.553	1.580	1.584
Uniaxial anorthite	.....	1.585 (w)	1.590 (e)

* See table 5.

In all three cases an index very close to the β index of natural albite or anorthite appears in the anomalous form. In high temperature albite it is the β index, in orthorhombic anor-

thite it is γ, and in uniaxial anorthite it is ω. The two albites also agree in α, while ϵ of uniaxial anorthite is the same as γ of ordinary anorthite. Uniaxial anorthite may thus be regarded as a normal anorthite which has somehow lost its α, and high albite as normal albite with γ lowered a little. If the γ line for *calcic* plagioclase (fig. 3c) is extended to the left, its n intercept at An_0 is 1.5337, which agrees, within the error of measurement, with the observed γ of high albite. If the α regression line for *sodic* plagioclase is now extended to the right, its n intercept at An_{100} turns out to be 1.5807, compared with a measured value of 1.580 for β in the orthorhombic form. If the α regression line for calcic plagioclase is reflected across this extended sodic-plagioclase α line it intersects the β regression line at An_{100}, the whole operation resulting in a uniaxially positive material with ω equal to β and ϵ equal to γ of natural anorthite, just as observed in uniaxial anorthite.

The γ and β indices of orthohombic anorthite have already been shown to be the β of normal anorthite and the An_{100} intercept of the extended sodic plagioclase α line repectively. The derivation of α for the orthohombic form is not so straightforward, and it may in fact be quite unrelated to the indices of natural plagioclase. It can be obtained, however, by rotating the extended sodic plagioclase α line downward about its intersection with the calcic plagioclase α line (An_{66}) through an angle four times that between the original calcic plagioclase α line and its reflection, which yields ω of uniaxial anorthite.

We like to think of the plagioclase group as a series or group of series and it does not seem impossible that the paths traced out by the transformed index regression lines leading to high albite and uniaxial anorthite represent real series. All that is required in each case is the reorientation of a single index regression line over some 30 per cent of the composition range. It is otherwise with orthorhombic anorthite, however; for in this case the α of natural plagioclase is used twice, first to form β, and then to reach α of the new form, while the γ of natural plagioclase simply disappears without trace. It happens, however, that the γ and α lines for sodic plagioclase converge at An_{100} ($\alpha = 1.5807$, $\gamma = 1.5806$), so that β_{or} may be regarded as an extension of the γ rather than of the α line of sodic plagioclase. In this fashion each of the new indices is formed from a different index regression line for natural

plagioclase, as is the case with high albite and uniaxial anorthite. But whereas only one index of each of the other forms is anomalous, this is true of two of the indices of orthorhombic anorthite.

No "physical" basis for these curious interrelationships between refractive indices of the various forms can be offered at present, yet one can hardly avoid supposing that there is one. Of the 8 required indices, only 2 differ from the observed values by much as 1 in the third place;[3] the possibility of such agreement arising from coincidence alone is certainly remote.

DISCONTINUITIES IN THE PLAGIOCLASE SERIES

The proposed discontinuities in the γ and α regression lines, An_{30} and An_{66} respectively, are reasonably close to the structural discontinuities recently proposed by Cole, Sörum, and Taylor at An_{32} and An_{70} mol per cent. (In weight per cent the C-S-T discontinuities are at An_{31} and An_{69}.) But the discontinuities in refractive index seem to be of a somewhat different type. The divisions based on structure could be shown as ordinates in figure 3, but it is clear from the figure that this would not hold for the refractive index grouping. Two of the three index regression lines pass unbroken through each boundary, one is not affected by either, and at the actual class boundary the optical properties are identical.

It is implicit in the approach taken here that composition is a function of refractive index. If the rate of change of refractive indices is in turn a function of structure, then the structure characteristic of the common sodic natural plagioclases evidently does not persist if enough anorthite is present to require a γ index much in excess of 1.551; similarly, the structure characteristic of calcic plagioclase does not persist if enough albite is present to require an α index much less than 1.562. In the first case the ensuing reorganization is such that γ follows the path characteristic of calcic plagioclase; in the second it is such that α follows the path characteristic of sodic plagioclase.

Refractive indices alone, of course, give little clue to the nature of the structural reorganization involved. Nothing in the refractive index variation is opposed to the suggestion that

[3] In all 8 cases, if the fourth place is not rounded out of the expected value the difference between expected and observed values is less than 1 in the third place.

plagioclases of intermediate composition are mixtures. If plagioclases in the range $30 < An < 66$ were actually submicroscopic mixtures of An_{30} and An_{66}, the variation of indices would probably be about like that shown in figure 3c. It would not be strictly linear, any more than would that for sodic or calcic plagioclase, but over such a short range the departure from linearity would in all likelihood be very small.

The relation between the sodic and calcic plagioclase index regressions remains to be discussed. It has already been suggested (Chayes, 1950) that natural calcic plagioclase is ordinarily the high temperature modification, while sodic plagioclase of the type suitable for high grade optical work is commonly the low temperature form. This view of the matter is supported by the finding that γ of high-temperature albite lies on the regression line of natural calcic plagioclase, but it is to be remembered that α of high-temperature albite is apparently the same as that of natural albite; perhaps the γ -index regression of calcic plagioclase is indicative of the high form only for compositions in the sodic plagioclase range.

The indices of anorthite formed in the standard quenching experiments (Merwin, cited in Bowen, 1912) are those of common natural anorthite, another indication that natural anorthite, and perhaps calcic plagioclases in general, are usually the high temperature modification. But a word of caution is again in order: no stable modification of anorthite other than the common variety is known in nature. Perhaps there is none, though from the symmetry of figure 3c one may hazard the guess that a series formed by extension of the sodic plagioclase α line may exist.

Even if we accept the extended calcic plagioclase γ line as defining a series of high temperature sodic plagioclases, the relation of this series to natural calcic plagioclase remains unclear. The α index of the new series certainly cannot be obtained by simple extension of the calcic plagioclase α line, for this line intersects the β line at a composition very near that at which the discontinuity in γ arises. At this composition our new high temperature andesine ought to be optically uniaxial, but no natural uniaxial plagioclase has ever been described. It happens that by reflecting the extended α line across β, or by rotating it about the uniaxial point through an angle equal to twice its inclination with the β line, we again arrive at the proper α index for high albite. At the other "uniaxial point"

(*ca.* An_{60}) formed by the intersection of the sodic-plagioclase γ line with β, operations similarly related to those already described will yield the indices of uniaxial and orthorhombic anorthite.

Derivation of the indices of the anomalous end members by operations at the "uniaxial points" is so involved that one is tempted to discard it, particularly since—as already shown—the same result can be achieved much more simply. But the whole trend of plagioclase research of the last two decades should make us wary of a too ready application of Occam's razor. Perhaps metastability arising from the high activation energy of the uniaxial forms provides a clue to the common occurrence of mixtures instead of homogeneous crystals in the intermediate composition range. At any rate, even if there are (at least) two temperature modifications over the entire composition range, it does not seem likely that either of the dominant temperature series is free of discontinuities in optical properties. If discontinuities in other properties are like those in refractive index, however, they may be extraordinarily difficult to detect. In the proposed high temperature sodic-plagioclase series, for instance, two of the three indices are identical with those of the natural low form at every composition, and at the supposed discontinuity all three are identical. Only at considerable distance from the discontinuity do differences in γ become large enough to detect, and this might well be true of other physical and chemical properties.

The notion that the commonly measured natural plagioclases are of two temperature modifications is directly opposed to Köhler's (1942) conclusion that they are invariably the low temperature form. Köhler's position seems to be based primarily on the fact that orientation of the indicatrix in a natural (nonvolcanic) crystal can almost always be changed by prolonged heating. This is not an infallable indication that the initial material is the low temperature form; if a successful method for transforming high into low albite is developed, one may be quite sure the reaction will not run at room temperature.

References

Becke, F., 1906. Die optischen Eigenschaften der Plagioklase: Min. pet. Mitt., vol. 25, pp. 1-42.

Bowen, N. L., and Tuttle, O. F., 1950. The system $NaAlSi_3O_8$—$KAlSi_3O_8$—H_2O: Jour. Geology, vol. 58, pp. 489-511.

Chayes, F., 1950. On the relation between anorthite content and γ-index of natural plagioclase: Jour. Geology, vol. 58, pp. 593-595.

Cole, W. F., Sörum, H., and Taylor, W. H., 1951. The structure of the plagioclase feldspars I: Acta Cryst., vol. 4, pp. 20-29.

Davis, G. L., and Tuttle, O. F., 1952. Two new crystalline phases of the anorthite composition, $CaO \cdot Al_2O_3 \cdot 2SiO_2$: Am. Jour. Sci., present vol.

Ernst, E., and Nieland, H., 1934. Plagioklase von Linosa, ein Beitrag zur Anemousitefrage: Min. pet. Mitt., vol. 46, pp. 93-126.

Fairbairn, H. W., *et al.*, 1951. A cooperative investigation of precision and accuracy in chemical, spectrochemical and modal analysis of silicate rocks: U. S. Geol. Survey Bull. 980.

Köhler, A., 1942. Die Abhängigkeit der Plagioklasoptik: Min. pet. Mitt., vol. 53, pp. 24-49.

———, 1950. Recent investigations on the feldspars: Jour. Geology, vol. 57, pp. 592-599.

Michel-Levy, A., 1895. Recherche des axes optique dans un minéral pouvant être considéré comme un mélange de deux minéraux déterminees: Soc. franç. minéralogie Bull., vol. 3, pp. 79-94.

Pockels, F., 1892. Ueber die Berechnung der optischen Eigenschaften isomorpher Mischungen aus derjenigen der gemischten reinen Substanzen: Neues Jahrb. BB 8, pp. 117-179.

———, 1906. Lehrbuch der Kristalloptik, B. F. Teubner Verlag, Leipzig, 519 pp.

Reinhard, M., 1931. Universal Drehtischmethoden, B. Wepf et Cie, Basel, 119 pp.

Tuttle, O. F., 1951. Origin of the contrasting mineralogy of extrusive and plutonic salic rocks: Jour. Geology, vol. 60, pp. 107-123.

———, and Bowen, N. L., 1950. High temperature albite and contiguous feldspars: Jour. Geology, vol. 58, pp. 572-583.

Wallerant, F., 1896. Calcul des constantes optique d'un melange de substance isomorphes, application aux feldspaths: Soc. franç. minéralogie Bull., vol. 19, pp. 169-207.

Wulff, G., 1902. Untersuchungen in Gebiete der optischen Eigenschaften isomorpher Krystalle: Zeitschr. Kristallographie, vol. 36, pp. 1-28.

Appendix A — Sources of the data

For permission to use nine as yet unpublished results I am indebted to my colleagues F. Kracek, T. Sahama, and K. Neuvonen. The data for these nine, all specially purified by Sahama and Neuvonen for use in calorimetric work, are as follows:

Locality	An	Analyst	α	β	λ
Varutrask	0.6	Zies	1.530	1.535	1.540
Amelia	0.0	Chadbourn ..	1.529	1.533	1.539
South Carolina	16.8	von Knorring.	1.538	1.543	1.545
Bakersville, N. C.	21.6	Chadbourn ..	1.539	1.544	1.547
Mitchell Co., N. C.	28.7	Chadbourn ..	1.543	1.548	1.550
Isle of Paul, Labrador	51.9	von Knorring.	1.555	1.558	1.562
Clear Lake, Utah	63.8	von Knorring.	1.562	1.566	1.571
Crystal Bay, Minn.	69.7	von Knorring.	1.565	1.568	1.574
Grass Valley, Cal.	92.6	von Knorring.	1.574	1.582	1.586

Indices of refraction were determined by K. Hytönen.

Professor Harry Hess has generously offered the following, also previously unpublished:

Locality	An	α	β	λ
Stillwater	75	1.5657	.....	1.5755
Rustenberg mine, Transvaal	76	1.5657	1.5705	1.5755
Stillwater	80	1.5675	.....	1.5780
Stillwater	86	1.5700	.....	.....
Stillwater	86	1.5713	1.5759	1.5814
Sittipunda	98	1.5751	.....	1.5884

Remaining data are culled from the literature and include nearly all those used by earlier workers in establishing the determinative charts now in use and their predecessors. References listed here are those from which the actual data have been drawn, and following each reference is a list of the feldspars described, together with their respective anorthite contents. Wherever there is text discussion of other material in a paper, the paper is also cited in the regular bibliography.

References

Becke, F., 1901. Tschermak's min. u. pet. Mit. *21,* 56. (Soboth 13)

———, 1921. Tschermak's min. u .pet. Mit. *35,* 31. (Kremstal 35)

———, and Goldschlag, M., 1918 Sitzungsber. Akad. Wiss. Wien, Math Kl. *127,* I, 473. (Mayeamo 38, St. Raphael 40)

Chudoba, K., 1925. Tschermak's min. u. pet. Mit. *38,* 88. (Rischuna)

———, and Jakob, J., 1933. Centralbl. Min. usw. 1. (Tamatave 54.3)

Duparc, L., and Gysin, M., 1926. Schweiz. min. u. pet. Mit. *6,* 255. (Spruce Pine 20.9, Inschitobel 2, Quebec 54.9)

Engels, A., 1937. Centralbl. Min. usw. 161. (Schirm 0.4)

Ferrucio, A., 1935. N. Jhrb. Min. *1,* 471. Abstract only. (Val Devoro 4)

Fischer, H., 1925. Zeit. Kryst. *61,* 226. (Amelia 2.9, Nadabula 0.9, Rischuna 0.7)

Fouque, F., 1894. Bull. soc. fr. de min., *17,* nos. 557, 558. (Mexico 19, Bakersville 22.2, Rochesauve 45, Santa Lucia 48, 48, Isle de Pico 50.8, Vellas 56.5, Capello 62, Mt. Somme 94)

Game, P. M., 1949. Min. Mag. *68,* 682 (Sultan Hamad 10.7, 17)

Grosspietsch, O., 1908. Tschermak's min. u. pet. Mit. *27,* 353. (Greenland 0.5, Moro Velho 0.5)

———, 1915. Tschermak's min. u. pet. Mit. *33,* 27. (Kamenoi Brod 56.3)

———, 1918. Sitzungsber. Akad. Wiss. Wien, Math-Nat Kl. I, *127,* 439. (Kremstal, 35)

Kozu, S., 1914. Rep. Tohoku Imp. Univ., Sendai, Japan, ser. 2, *2,* 1. (Miyakijima, Idzu 95.4)

———, 1915. Min. Mag. *17,* 189. (Rischuna)

Kratzert, J., 1921. Zeit. Krist. *56,* 465. (Vesuvius 97)

Krebs, B., 1921. Zeit. Krist. *56,* 386. (Rischuna 3.5 — no optics)

Lundegårdh, P. H., 1941, Bull. Geol. Inst. Univ. Upsala *28,* 415. (Bönskär 86)

Luziczkey, W., 1905. Tschermak's min. u. pet. Mit. *24,* 191. (Isle of Paul, Labrador 52)

Meen, V. B., 1933. Univ. Toronto Studies, Geol. Ser. *35,* 37. (Amelia 2.5, Pointe du Bois 0.8, Monteagle 5.7, Villeneuve 7.6, Monteagle 13.2, Hawk Mine 53.5, Clear Lake, Utah, 62.8, Crystal Bay, Minn., 76.2)

Merwin, H., in Bowen, N. L., 1912. Am. Jour. Sci. *33,* 551. (Synthetic anorthite)

Michel-Lévy, A., and Lacroix, A., 1890. Compte Rendus Acad. fr. *61,* 846. (Rochesauve 40, Bamle 14.3, Sainte Clement 90.9)

Miller, F. S., 1935. Am. Mineral. *20,* 139. (Pala Mtn. 95.1)

Offret, A., 1890. Bull. soc. min. fr. *13,* 648. (Bakersville 22)

Pagliano, G., 1937. Atti. Soc. Ital. Sci. Nat. Mil. *76,* 331. (Baveno 3.0)

Riva, C., 1902. Zeit. Krist. *35,* 361. (Cala Francesca 13)

Starrabba, F. Stella, 1927. Bull. dell' Acc. Gioenia di Sci. Nat. in Catania. Fasc. *57* ser. 2, 32. (Monti della Ciacca, Etna 89.7)

Tertsch, H., 1903. Tschermak's min. u. pet. Mit. *22,* 159. (Bakersville 22, Tvedestrand 25, Bamle 14.3)

Tsuboi, S., 1923. Min. Mag. *20,* 108. (Bakersville 24, Mayeamo 37, County Down 66)

———, Jap. J. Geol. Geog. *12,* 110. (Wadaki, Idu 97.9)

Vendl, M., 1922. Centralbl. Min. usw. A, 97. (Sajohaza 0.5, Beaume 2.2)

Viola, C., 1900. Zeit. Krist. *32,* 305. (Lakous, Crete 0)

Walker, T. L., and Parsons, A. L., 1927. Univ. Toronto Studies, Geol. Ser. *24,* 5. (Bytown 52)

Winchell, A. N., 1900. Am. Geol. *26,* 197. (Carlton Peak 59)

Geophysical Laboratory
Carnegie Institution of Washington
Washington, D. C.

TWO NEW CRYSTALLINE PHASES OF THE ANORTHITE COMPOSITION, $CaO \cdot Al_2O_3 \cdot 2SiO_2$

G. L. DAVIS AND O. F. TUTTLE

ABSTRACT. Two new crystalline phases of the composition $CaAl_2Si_2O_8$ are described, giving the optical properties and X-ray powder diffraction data. Their synthesis and stability are discussed. Comparisons are drawn with similar modifications of $BaAl_2Si_2O_8$.

INTRODUCTION

DURING the investigation of subsolidus phase relations in the system: albite—anorthite, an unknown phase appeared at temperatures near 1000° C. in compositions rich in lime feldspar. The unknown phase was found to be identical in optical and X-ray properties with one of the two principal phases of unknown composition crystallized by L. B. Wyckoff of the Research Laboratory of the Electrometallurgical Company of the Union Carbide and Carbon Corporation. This material, which was submitted by Wyckoff to L. H. Adams of the Geophysical Laboratory for examination, was prepared by fusing a large charge of several hundred grams of glass of the approximate composition of anorthite ($CaO:Al_2O_3 \cdot 2SiO_2$) at 2000° C. in a graphite crucible in a furnace with a nitrogen atmosphere. The melt was cooled slowly to 1250° and the charge was allowed to crystallize at this temperature. Crystallization resulted in segregation of the two crystalline phases in such a manner that it was possible to hand-pick the two for chemical analysis.

The two new phases will be called hexagonal (Donnay, 1952) and orthorhombic[1] $CaAl_2Si_2O_8$.

CHEMICAL COMPOSITION

The two phases crystallized by Wyckoff were separated by hand-picking under a binocular microscope and analyzed chemically by conventional methods. The results, with the theoretical composition of anorthite for comparison, were:

	Hexagonal phase	Orthorhombic phase	Anorthite
SiO_2	42.9	43.3	43.2
Al_2O_3	36.9	36.9	36.7
CaO	20.5	20.3	20.1
	100.3	100.5	100.0

[1] Laves, F., personal communication.

These analyses are the averages of duplicate determinations on 100 mg. samples. The composition is therefore essentially that of anorthite, $CaO \cdot Al_2O_3 \cdot 2SiO_2$.

GENERAL CHARACTER

The hexagonal phase crystallizes as spherulitelike masses consisting of transparent radiating basal plates. A perfect basal cleavage yields cleavage plates which are brittle and break with a conchoidal fracture. No evidence of twinning has been observed. It appears to have a hardness of 5 on the cleavage surface but a polished surface across the cleavage has a hardness of 6. The density determined on a 5 mg. fragment is 2.74.

The orthorhombic phase crystallizes as a massive mosaic of transparent equant crystals which show no evidence of crystal faces. Crushed fragments show a conchoidal fracture. The hardness is 6 and the density 2.70. This form has poor cleavage parallel to the optic plane. There are numerous inclusions aligned in planes parallel to the optic plane.

OPTICAL PROPERTIES

The optical properties of the two new phases are given together with those of anorthite for comparison:

	Hexagonal	Orthorhombic	Anorthite
2V	0	39°	77°
sign	+	—	—
n_ω	1.585	.....	.....
n_ϵ	1.590	.....	.....
n_α	.....	1.553	1.5755
n_β	.....	1.580	1.5832
n_γ	.....	1.584	1.5885

X-RAY DATA

Powder diffraction records were made on the Philips Wide-range Spectrometer. The values obtained are given in tables 1 and 2, which also present the results obtained by applying the method of indexing powder records proposed by C. Runge (1917) and recently generalized by T. Ito (1950). The radiation employed was CuKα with α_1 resolved at all angles above 32° (2θ). A .0007-inch nickel filter was used. In the tables, intensities are expressed relative to a strong line, not necessarily the strongest, and Q is the square of the reciprocal lattice

vector. The character of the powder pattern for the hexagonal phase indicates that the material examined was preferentially oriented.

The hexagonal material has the following lattice parameters: a = 5.110 ± .002 Å, c = 2 x 7.367 ± .002 Å, Z = 1. The calculated density is 2.77, which compares with 2.74 measured. This material has been studied by Donnay (1952) and assigned the space group *C 6/mmm*.

The orthorhombic phase has the unit cell dimensions a = 8.224 ± .006 Å, b = 8.606 ± .006 Å, c = 4.836 ± .005 Å, and Z = 2. The only systematic absences are for reflections with (h + k) odd in (hk0). A. J. Frueh, Jr., of the University of Chicago, has pointed out in a personal communication that

TABLE 1

Hexagonal Phase of $CaO \cdot Al_2O_3 \cdot 2\ SiO_2$

hkl	d(Å)	I*	2θ obs	2θ calc	Q obs	Q calc
002	7.37	85	12.01	12.01	.01842	.01842
100,010	4.43	7	20.05	20.06	.05099	.05105
$004\beta_1$	.....	5	21.77	21.76	.....	.....
102,012	3.80	30	23.43	23.45	.06937	.06947
004	3.68	100++	24.13	24.16	.07352	.07368
104,014	2.84	40	31.57	31.60	.12452	.12473
110	2.555	9	35.09	35.09	.15317	.15315
006	2.456	14	36.56	36.55	.16583	.16578
112	2.414	3	37.21	37.21	.17157	.17157
106,016	2.417	11	42.04	42.04	.21686	.21683
202,022	2.119	4	42.64	42.62	.22281	.22262
$008\beta_1$	.....	2	44.37	44.40	.....	.....
008	1.842	100+	49.45	49.44	.29487	.29472
116	1.770	9	51.58	51.57	.31905	.31893
108,018	1.701	1	53.86	53.86	.34594	.34577
210	1.658	1	56.35	56.35	.37577	.37577
212	1.501	2	60.76	60.75	.43110	.43103
118	1.495	14	62.04	62.06	.44736	.44787
300	1.475	3	62.96	62.95	.45963	.45945
1,0,10, 0,1,10	1.399	12	66.83	66.86	.51117	.51155
1,1,10	1.277	8	74.19	.....	.61323	.61365
2,0,10, 0,2,10	1.227	6	77.77	.....	.66432	.66470
1,0,12, 0,1,12	1.183	5	81.21	.....	.71394	.71417
308,038	1.152	1	83.95	.....	.75391	.75417
etc.						

a = 5.110 ± .002 Å, c = 2 × 7.369 ± .002 Å, Z = 1

* Specimen shows preferred orientation.

TABLE 2

Orthorhombic Form of $CaO \cdot Al_2O_3 \cdot 2\,SiO_2$

hkl	d(Å)	I	2θ obs	2θ calc	Q obs	Q calc
110	5.94	3	14.90	14.90	.02829	.02830
001	4.83	9	18.35	18.35	.04278	.04280
020	4.29	5	20.67	20.64	.05416	.05400
011	4.20	10	21.11	21.08	.05646	.05630
101	4.17	85	21.31	21.32	.05753	.05759
200	4.11	70	21.62	21.61	.05919	.05916
111	3.75	50	23.72	23.72	.07108	.07110
021	3.21	100	27.77	27.75	.09690	.09680
201	3.13	3	28.47	28.50	.10175	.10196
220	2.97	35	30.05	30.06	.11309	.11316
211	2.94	50	30.36	30.37	.11538	.11546
130	2.707	30	33.06	33.04	.13644	.13629
310	2.611	6	34.32	34.31	.14672	.14661
221	2.532	12	35.42	35.42	.15597	.15596
002	2.415	1	37.20	37.17	.17148	.17120
301	2.383	8	37.71	37.70	.17604	.17591
131	2.363	15	38.05	38.05	.17911	.17909
012	2.327	13	38.65	38.66	.18459	.18470
311	2.296	4	39.19	39.17	.18958	.18941
112	2.241	13	40.21	40.24	.19916	.19949
040	2.152	3	41.95	41.95	.21598	.21600
231	2.115	7	42.71	42.71	.22350	.22346
321	2.087	40	43.31	43.35	.22952	.22991
400	2.056	15	44.00	44.01	.23653	.23664
122	2.042	12	44.31	44.34	.23971	.23999
212	2.026	10	44.69	44.71	.24362	.24386
041	1.965	20	46.15	46.14	.25892	.25880
240	1.907	3	47.65	47.66	.27503	.27516
420	1.853	3	49.06	49.07	.29052	.29064
032	1.849	8	49.25	49.26	.29264	.29270
241	1.773	7	51.49	51.49	.31802	.31796
421	1.732	2	52.80	52.82	.33323	.33344
150	1.685	10	54.40	54.38	.35217	.35229
322	1.672	15	54.88	54.91	.35793	.35831
051	1.621	3	56.73	56.72	.38044	.38030
341	1.598	8	57.65	57.66	.39181	.39191
431	1.578	6	58.41	58.38	.40129	.40094
501	1.558	6	59.27	59.30	.41212	.41255
332	1.533	8	60.34	60.35	.42572	.42581
251	1.510	3	61.34	61.41	.43857	.43946
521	1.465	2	63.45	63.49	.46687	.46653
060	1.434	12	64.95	64.96	.48593	.48600
530	1.427	10	65.32	65.35	.49087	.49125
223	1.418	4	65.82	65.88	.49756	.49836
033	1.406	7	66.45	66.50	.50604	.50670

$a = 8.224 \pm .006$ Å, $b = 8.606 \pm .006$ Å, $c = 4.836 \pm .005$ Å, $Z = 2$

the space group is $P_{2_12_12}$ and that the absence (h + k) odd in (hk0) is only a pseudo-absence. These reflections are too weak to be observed in a powder pattern. The calculated density is 2.70 which agrees with the measured value.

LABORATORY INVESTIGATION

Orthorhombic $CaAl_2Si_2O_8$ apparently can be synthesized, in the absence of water vapor, only by crystallizing the glass at temperatures well below the liquidus. The largest yields have been obtained at temperatures just above the temperature at which the glass fails to crystallize. It was first observed in material obtained by crystallizing a glass of composition $Ab_{20}An_{80}$ at 1000° C. At 950° C. the glass crystallized essentially completely as the orthorhombic phase in four days. Glass of anorthite composition at 950° for four days gave some of the orthorhombic phase together with anorthite and the hexagonal modification. This glass failed to crystallize in four days at 890° C. By these methods a large yield of the orthorhombic form has never been obtained from anorthite glass. On the other hand, glasses having compositions in the range $Ab_{10}An_{90}$ to $Ab_{70}An_{30}$ crystallized predominantly as the orthorhombic form when held from two to four days between 950° and 1000° C. A small amount of the orthorhombic phase was detected in the poorly crystallized product when glass of composition $Ab_{80}An_{20}$ was heated at 1000° C. for twenty-one days.

The orthorhombic material crystallized from glasses rich in soda has noticeably lower refractive indices than the same phase crystallized from glass of anorthite composition, indicating considerable solid solution of $NaAlSi_3O_8$. The X-ray powder records confirm the existence of this solid solution which is shown by the change in the difference between 2θ (002) and 2θ (021) with increasing $NaAlSi_3O_8$.

Hexagonal $CaAl_2Si_2O_8$ has been synthesized only as a minor component of the crystalline product in compositions ranging from $Ab_{80}An_{20}$ to anorthite and its presence has been determined by X-ray powder patterns solely. It has not been identified optically. As in the case of the orthorhombic form, there is considerable solid solution with $NaAlSi_3O_8$ indicated by changes in the (004) spacing with increasing $NaAlSi_3O_8$.

A large yield of this phase has been obtained only by

repeating the conditions under which Wyckoff synthesized the materials in the course of his viscosity studies. A glass of anorthite composition heated to 2000° C. in a graphite resistor trough in a vacuum fusion furnace (Evans, 1935; Urry and Piggot, 1941) and quickly cooled to approximately 1200°, where it was allowed to crystallize, gave the hexagonal phase only. In this treatment there it some evidence that some of the silica is reduced. Possibly the slight compositional change may promote the growth of this phase.

COMPARISON WITH SIMILAR MODIFICATIONS OF $BaAl_2Si_2O_8$

Synthetic hexagonal $BaAl_2Si_2O_8$ has been reported by Ito (1950), and a structure has been proposed for this material. It was synthesized in an environment similar to that used for producing hexagonal $CaAl_2Si_2O_8$. An inversion of the high-low type has been reported for the hexagonal $BaAl_2Si_2O_8$ at 300° C. (Yoshiki and Matsumato, 1951). We have confirmed the existence of this inversion. Differential heating experiments show an absorption of heat beginning at 295° ± 5° C. Differential heating measurements on hexagonal $CaAl_2Si_2O_8$ failed to detect a heat effect up to 1200° C.

We have synthesized hexagonal $BaAl_2Si_2O_8$ by heating the oxides at 1500° C. for four days. However, longer heating caused it to change to celsian (monoclinic feldspar, $BaAl_2Si_2O_8$), a behavior like that of the hexagonal lime compound. Donnay (1952) reports that hexagonal $CaAl_2Si_2O_8$ is not isostructural with the barium compound, as described by Ito. However, hexagonal $CaAl_2Si_2O_8$ may be isostructural with the high temperature form of hexagonal $BaAl_2Si_2O_8$.

Paracelsian ($BaAl_2Si_2O_8$), described by L. J. Spencer (1942) is orthorhombic morphologically, and the possibility that this material is isostructural with orthorhombic $CaAl_2Si_2O_8$ was considered. More recently, Smith (1952) has found paracelsian to be monoclinic, departing only slightly from orthorhombic symmetry. There is no relation between the structure of paracelsian and the orthorhombic form of $CaAl_2Si_2O_8$ since they have completely different space groups, that of paracelsian being the pseudo space group *Pbnm* or *Pbn*. Paracelsian changes readily to celsian on heating, being similar in this respect to the orthorhombic lime compound.

STABILITY OF THE HEXAGONAL AND ORTHORHOMBIC $CaAl_2Si_2O_8$

Both the hexagonal and the orthorhombic forms change to anorthite on prolonged heating at the temperature at which they have been synthesized. The change takes place rapidly at high temperatures and becomes more difficult to produce as the temperature is lowered. However, in the presence of water vapor at 1000 kg/cm^2, both forms invert to anorthite at temperatures well below (700° C.) those at which no change can be detected when heated in the absence of water. Their possible stability at lower temperatures is being investigated by J. R. Goldsmith and E. G. Ehlers[2] of the University of Chicago.

The fact that these new phases have not been found in nature, in addition to the present lack of evidence for a stable temperature range of existence in the laboratory, suggests that they are unstable. High temperature modifications of silicates usually have higher symmetry than the low temperature forms. The symmetry relations of the three modifications of anorthite composition would suggest that the orthorhombic and hexagonal forms should be high temperature modifications but the rapid change of both phases to anorthite at high temperature appears to eliminate this possibility.

If further experiments at low temperature in the presence of fluxes fail to indicate a stable temperature range for the orthorhombic and hexagonal forms of $CaAl_2Si_2O_8$, it must be concluded that both are unstable modifications.

Laboratory studies of silicates crystallized from viscous glasses have repeatedly demonstrated that this environment promotes the formation of metastable and unstable phases. It is not surprising, then, that these unusual forms have been encountered in our studies of subsolidus relations of the feldspars. It is anticipated that other unstable phases will be discovered as our studies of subsolidus relations are extended to other silicate systems.

ACKNOWLEDGMENTS

Dr. N. L. Bowen has contributed not only many microscopic examinations of the crystallized products but also a continuous interest in the progress of this work. The preparations used

[2] Personal communication.

were those of J. F. Schairer. Encouragement and advice on the X-ray calculations were received from J. D. H. and G. Donnay.

References

Donnay, Gabrielle, 1952. Hexagonal $CaAl_2SiO_2O_8$: Acta Cryst., vol. 5, p. 153.

Evans, R. D., 1935. Apparatus for the determination of minute quantities of radium, radon and thoron in solids, liquids, and gasses: Rev. Sci. Inst., vol. 6, pp. 99-112.

Ito, T., 1950. X-ray studies on polymorphism, Maruzen Co., Ltd., Tokyo.

Runge, C., 1917. Die Bestimmung eines Kristallsystems durch Röntgenstrahlen: Physik. Zeitschr., vol. 18, pp. 509-515.

Smith, J. V., 1952. Single-crystal measurements on paracelsian: Am. Jour. Sci., present vol.

Spencer, L. J., 1942. Barium-feldspars (celsian and paracelsian) from Wales: Mineralog. Mag., vol. 26, pp. 231-245.

Urry, W. D., and Piggot, C. S., 1941. Apparatus for determination of small quantities of radium: Am. Jour. Sci., vol. 239, pp. 633-657.

Yoshiki, B. and Matsumato, K., 1951. High-temperature modification of barium-feldspar: Am. Ceramic Soc. Jour., vol. 34, pp. 283-286.

Geophysical Laboratory,
Carnegie Institution of Washington,
Washington, D. C.

THE SYMMETRY CHANGE IN THE HIGH-TEMPERATURE ALKALI-FELDSPAR SERIES

GABRIELLE DONNAY
AND
J. D. H. DONNAY

ABSTRACT—Accurate unit-cell dimensions are given for eleven synthetic alkali feldspars ranging from monoclinic $KAlSi_3O_8$ to triclinic $NaAlSi_3O_8$. Cell edges and angles are plotted against composition. The only discontinuity is found in the first derivative of the interaxial angle α at the point where the change of symmetry takes place. No two-phase region is observed. The phase transition is a high-order one and, for practical purposes, solid solution may be considered complete.

INTRODUCTION

THE phase diagram of the alkali feldspars (fig. 1), investigated by Bowen and Tuttle (1950), shows a complete series of solid solutions above 660° C. Two interesting features stand out: (1) Any composition crystallized above 660° C., if cooled rapidly, persists indefinitely at room temperature as a metastable phase. This metastability is unusual for a series in which sodium and potassium substitute for each other, since their ionic radii differ by considerably more than the usual tolerance of 15 per cent. (2) Since the potassium end-member is monoclinic and the sodium end-member is triclinic, the symmetry must change at some point in the series.

Bowen and Tuttle (1950) plotted the interplanar spacing $d(\bar{2}01)$ against composition and obtained a smooth curve, which they considered corroborative evidence for complete solid solution. This spacing, however, is not a function of all six cell dimensions (in the monoclinic case it is not a function of the cell edge b; in the triclinic case it depends neither on the cell edge b nor on the angles α and γ). Its continuity, therefore, does not by itself rule out the possibility of a break in the solid-solution series. Other quantities, such as cell volume and density, which are functions of all the cell dimensions, should be more conclusive. Inasmuch as the crystal structures of the high-temperature alkali feldspars are unknown, it is difficult to find better functions for the purpose. It was therefore decided to determine accurate cell dimensions for known compositions from pure potassium feldspar to pure sodium feldspar, to plot the corresponding

curves and to look for a discontinuity in any one of them. Since no single crystals were available, the powder method was used.

At the time this investigation was begun, the Geophysical Laboratory purchased a Philips back-reflection X-ray spectrometer. A good opportunity thus offered itself to test the potentialities of this instrument. Four unknowns in the monoclinic case and six in the triclinic case had to be determined from powder patterns that showed no usable peaks beyond $2\theta = 52°$ for Cu radiation. We aimed at developing a method that could be used in routine work, even though the desired accuracy was better than 0.1 per cent on cell edges and better than 0.1° on interaxial angles.

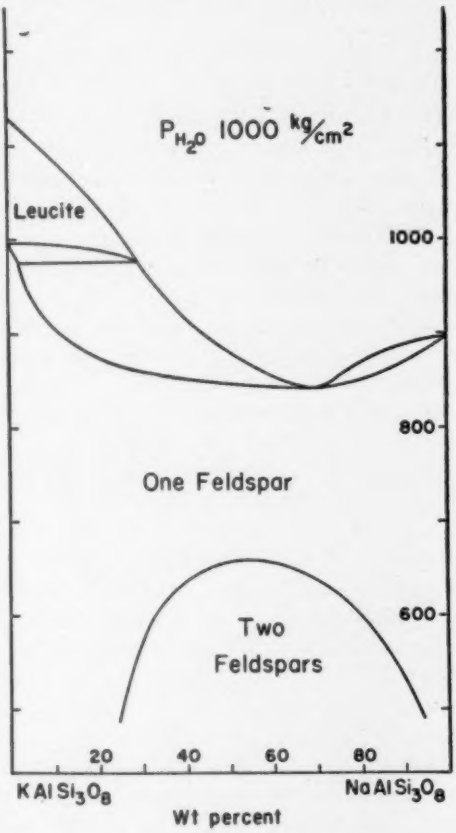

Fig. 1. Isobaric phase diagram of alkali feldspars, after Bowen and Tuttle.

After we had determined, for the synthetic material, the composition at which the symmetry change takes place, Dr. Tuttle supplied single crystals of natural high-temperature feldspars in the same composition range. We investigated these with a view to comparing the compositions at which the change of symmetry takes place in the synthetic and in the natural samples. This single-crystal work strikingly brought out the advantages of the powder method in the present study. The crystals commonly show either albite twinning or both albite and pericline twinning. Near the composition at which the symmetry changes, the angles α and γ are close to 90°. As a consequence pairs of X-ray reflections due to the two individuals of a twin merge into single spots, so that the Weissenberg photographs simulate monoclinic symmetry. This phenomenon is observed, for example, on crystals from Grande Caldeira, Azores. The powder pattern, however, shows perfect separation of 111 and $1\bar{1}1$, thus proving the triclinic character.

METHOD

Drs. Tuttle and Bowen report as follows on the preparation of the feldspar samples Ab_xOr_y which they supplied to us:[1] "Glasses of the chosen compositions were crystallized at a water pressure of 1000 kg/cm^2, for the lengths of time and at the temperatures shown in table 1. They were then cooled to room temperature in less than one minute and removed from the pressure apparatus for study."

TABLE 1

Temperatures and Lengths of Time at which Feldspars were Crystallized. Water Pressure 1000 kg/cm^2

Weight per cent Ab	0	20	40	50	60	65	66	70	80	90	100
Temperature (°C.)	700	800	800	700	800	800	700	800	800	800	800
Time (days)	1	1	4	?	1	4	9	9	3	2	5

Dr. L. H. Adams prepared all the charts on the Philips unit and developed a method of mounting the samples in lucite (to be described elsewhere). The instrumental setting that gives the most satisfactory results for the present purpose, as determined by Dr. Adams, is the following: multiplication factor, 8—that is, 400 counts per second, full scale; time constant, 4 seconds;

[1] The formula Ab_xOr_y signifies x weight per cent sodium feldspar and y weight per cent potassium feldspar.

divergent slit, 1°; receiving slit, 0.003 inch; scatter slit, 1°; scanning speed, ¼° per minute; and chart scale, 1 inch per degree.

Peak positions are read, to 0.005 inch, on a specially designed 3-foot ruler with vernier. The reading is taken at the mid-point of the peak width at approximately two-thirds of the peak height, an empirically determined value, which minimizes the interference of the α_2 peak and the effect of the detailed shape of the graph. The accuracy of the mid-point reading is estimated, as *peak quality q*, on a scale of 10 with 10 as the optimum. The resolution of the CuKα doublet begins, for most compositions, at about $2\theta = 28°$. Silicon calibration peaks at widely different 2θ angles are added both at the beginning and at the end of each pattern. The calibration correction of 2θ is found to be constant for a given chart and to vary only slightly (from $-0.03°$ to $+ 0.01°$) from chart to chart. To test reproducibility two charts were obtained from the same lucite mount of $Ab_{20}Or_{80}$. For peaks with $q = 3$, the 2θ readings agree within $\pm 0.01°$. Equally good reproducibility was obtained from the same sample, after it had been separated from the lucite of the mount and reheated to 600° C. for 24 hours.

The corrected 2θ values are converted to Q_{obs} by the use of a table (Donnay and Donnay, 1951*a*) which gives Q in terms of 2θ to 5 significant figures. It is known that

$$Q(hkl) = 1/d^2(hkl) = h^2a^{*2} + k^2b^{*2} + l^2c^{*2} + 2klb^*c^*\cos\alpha^* + 2lhc^*a^*\cos\beta^* + 2hka^*b^*\cos\gamma^*.$$

Approximate indexing was possible with the help of the known cell dimensions of the low-temperature forms. (It would have been easier to use the cell dimensions of the high-temperature natural feldspars, but the latter were not known at the time.) A peak due to only one reflection is called a *resolved peak*. Sharp resolved peaks are used to derive the values of the four monoclinic or the six triclinic reciprocal-lattice parameters that enter the expression of Q. All the Q(hkl) values are then calculated and the corresponding 2θ values read from the table.

The accuracy of the dimensions of the reciprocal cell can be estimated from the weighted average deviation $D = \dfrac{\sum_{i=1}^{N} q_i \left|2\theta_{obs} - 2\theta_{calc}\right|_i}{\sum_{i=1}^{N} q_i}$ and the absolute value of the

largest deviation $\Delta = 2\theta_{obs} - 2\theta_{calc}$. The number N of resolved peaks must be reasonably large to give D significance. For the compositions $Ab_{64}Or_{36}$ and $Ab_{65}Or_{35}$, this was unfortunately not the case (table 10). The necessity for taking Δ into consideration became apparent after a mistake was discovered in the indexing of the triclinic patterns (Donnay and Donnay, 1951*b*). Although D = 0.03° was reasonably satisfactory for the sodium end-member, there remained one resolved peak, 111, of quality 5, for which the deviation Δ = 0.18° was high. This discrepancy disappeared, D was reduced to 0.002° and Δ to 0.02°, after the pattern was re-indexed correctly. The conclusion is that no indexing can be considered reliable until the largest deviation has been reduced to a satisfactory value. In other words, the indexing can be wrong, even if only one 2θ value shows a large deviation.

To obtain a more quantitative estimate of the accuracy, the 2θ values were calculated for slightly different cell dimensions. An example of these calculations (table 2) demonstrates the sensitivity of the method. The estimated limits of error are ± 0.04 per cent for lengths and ± 0.01° for angles.

TABLE 2

Effect of Changes in Cell Dimensions on Weighted Average Deviation D and Maximum Deviation Δ for $Ab_{80}Or_{20}$

Cell Dimensions						Cell Vol.	Specific gravity	D for	
a	b	c	α	β	γ	V.	calc.	N=7	Δ
First trial									
8.243Å	12.927Å	7.140Å	92.27₅°	116.33₁°	90.16₀°	681.2Å³	2.585₃	0.037₄	0.085(q=10)
Second trial									
8.242	12.928	7.143	92.27₅	116.33₁	90.13₁	681.4	2.584₇	0.013₄	0.025(q=10)
Final values									
8.243	12.927	7.140	92.14₉	116.28₁	90.29₄	681.5	2.584₅	0.002₉	0.015(q=7)

Since the conversion of reciprocal cell to direct cell is somewhat tedious in the triclinic case, the calculation form is given (table 3) in the hope that it may be found useful by others. Having acquired some skill through considerable practice, we have reached the point where we can complete a monoclinic determination in about four hours and a triclinic one in seven to eight. This includes: reading the chart, obtaining reciprocal cell dimensions, computing 2θ for each reflection,

TABLE 3

Calculation Form for Conversion of Powder-Chart Data to Direct Cell Dimensions. Feldspar from Grande Caldeira

a^{*2}	.0180098	log a^{*2}	2.2555089	log a^*	1.1277544	$2b^*c^*\cos$	α^*	.0004667	
b^{*2}	.0059482	log b^{*2}	3.7743856	log b^*	2.8871928	$2c^*a^*\cos$	β^*	.0184770	
c^{*2}	.0243250	log c^{*2}	2.3860528	log c^*	1.1930264	$2a^*b^*\cos$	γ^*	.0002333	

a^*	.1342006	a^*N^*	.1203972	$2b^*c^*$	$.0240574_2$
b^*	.07712458	b^*N^*	$.0691918_5$	$2c^*a^*$	$.0418611_1$
c^*	.1559647	c^*N^*	.1399227	$2a^*b^*$	$.0207003_3$

		cos	sin	$\cos^2+\sin^2$ $10^7\Delta$		cos cos	sin sin
a^*	88.888_1	$.0193994_2$	.9998118	0.3	$\beta^*\gamma^*$	$.0049746_0$	.8972592
β^*	63.807_5	.4413882	.8973162	0.9	γ^*a^*	$.0002186_4$	.9997483
γ^*	89.354_2	$.0112703_2$	.9999365	0.2	$a^*\beta^*$	$.0085626_6$	.8971473

$$\cos(180^\circ-\alpha)=\frac{\cos\alpha^*-\cos\beta^*\cos\gamma^*}{\sin\beta^*\sin\gamma^*}$$

$$\cos(180^\circ-\beta)=\frac{\cos\beta^*-\cos\gamma^*\cos\alpha^*}{\sin\gamma^*\sin\alpha^*}$$

$$\cos(180^\circ-\gamma)=\frac{\cos\gamma^*-\cos\alpha^*\cos\beta^*}{\sin\alpha^*\sin\beta^*}$$

		cos	sin	$\cos^2+\sin^2$ $10^7\Delta$		sin sin
$180^\circ-\alpha$	89.078_8	$.0160765_1$	.9998708	0.7	$\beta\gamma$	.8973652
$180^\circ-\beta$	63.814_4	.4412806	.8973692	0.5	γa	.9998663
$180^\circ-\gamma$	89.827_1	$.0030180_{88}$	.9999955	0.9	$a\beta$	.8972533

$N^*=\sin\beta^*\sin\gamma^*\sin\alpha=\sin\gamma^*\sin\alpha^*\sin\beta=\sin\alpha^*\sin\beta^*\sin\gamma$

N^* $.8971432_7$ $.8971433_2$ $.8971432_6$

$N=\sin\beta\sin\gamma\sin\alpha^*=\sin\gamma\sin\alpha\sin\beta^*=\sin\alpha\sin\beta\sin\gamma^*$

N $.8971963_2$ $.8971962_2$ $.8971963_2$

$a=(\sin\alpha^*)/a^*N^*$ $b=(\sin\beta^*)/b^*N^*$ $c=(\sin\gamma^*)/c^*N^*$

$a^*=(\sin\alpha)/aN$ $b^*=(\sin\beta)/bN$ $c^*=(\sin\gamma)/cN$

				Check	$10^7\Delta$
a	8.304_{280}	aN	7.450569	a^* .1342006	0
b	12.968_{524}	bN	11.63532	b^* $.0771245_8$	0
c	7.146_{350}	cN	6.411679	c^* .1559647	0

α	90.921_2	$V^*=N^*a^*b^*c^*$	$V=N\ a\ b\ c$
β	116.185_6	V* .001 448 223	V 690.5015
γ	90.172_9	Check: $V^*V=1$	
		V*V 1.000 000 08	

MW 267.33

$SG=$ 6.6408 MW/V

SG 2.57_{10}

evaluating Δ and D, calculating the dimensions of the direct cell, its volume, and the specific gravity.

EXPERIMENTAL RESULTS

It turned out in the course of the investigation that the samples had not been quenched, in the strict sense of the word. The cell dimensions that we have determined are those of crystals at room temperature, not those that prevailed at the elevated temperature at which the material crystallized, as was first erroneously assumed (Donnay and Donnay, 1951*b*). The cooling was too rapid, however, for unmixing to take place, and the single-phase system remained a one-phase system. One could perhaps speak here of "quenching" in a thermodynamic sense; in this same sense, we are dealing with a metastable phase.

The reciprocal cell data obtained directly from the charts are given in table 4 and the reciprocal cell dimensions in table 5. The powder data yielded by four representative compositions, $KAlSi_3O_8$, $Na_{.61}K_{.39}AlSi_3O_8$, $Na_{.71}K_{.29}AlSi_3O_8$ and $NaAlSi_3O_8$, are given in tables 6 to 9. Figures 2 to 5 are reproductions of the corresponding powder charts. All results are summarized in table 10 and figure 6 which, for each sample, give cell dimensions, cell volume, specific gravity, interplanar spacings d(111) and d($1\bar{1}1$) with corresponding q values, D, N, and

TABLE 4

Reciprocal Cell Data Obtained from Synthetic Alkali Feldspar Charts

mol % Ab	a^{*2} (Å^{-2})	b^{*2} (Å^{-2})	c^{*2} (Å^{-2})	$2b^*c^*\cos\alpha^*$ (Å^{-2})	$2c^*a^*\cos\beta^*$ (Å^{-2})	$2a^*b^*\cos\gamma^*$ (Å^{-2})
0=Or	0.01669_{50}	0.00589_{00}	0.02407_{00}	———	0.01762_{40}	———
20.971	0.01696_{75}	0.00589_{25}	0.02403_{50}	———	0.01766_{75}	———
41.439	0.01737_{00}	0.00591_{63}	0.02411_{00}	———	0.01797_{00}	———
51.490	0.01762_{50}	0.00592_{43}	0.02416_{00}	———	0.01815_{50}	———
61.422	0.01787_{00}	0.00594_{50}	0.02422_{50}	———	0.01835_{00}	———
66.343	0.01798_{70}	0.00595_{00}	0.02427_{00}	———	0.01845_{00}	———
67.324	0.01802_{00}	0.00595_{25}	0.02429_{00}	0.000	0.01849_{50}	0.000
71.237	0.01814_{50}	0.00596_{85}	0.02434_{50}	0.00063_{50}	0.01860_{25}	0.00028_{10}
80.937	0.01831_{70}	0.00599_{58}	0.02445_{00}	0.00107_{50}	0.01876_{20}	0.00051_{00}
90.524	0.01855_{00}	0.00603_{10}	0.02459_{50}	0.00149_{00}	0.01901_{75}	0.00063_{00}
100=Ab	0.01870_{50}	0.00605_{40}	0.02471_{50}	0.00178_{00}	0.01920_{00}	0.00075_{50}

TABLE 5

Reciprocal Cell Dimensions of Synthetic Alkali Feldspars

mol % Ab	a^*(Å^{-1})	b^*(Å^{-1})	c^*(Å^{-1})	$\alpha^{*\circ}$	$\beta^{*\circ}$	$\gamma^{*\circ}$	10^3V^* (Å^{-3})
0=Or	0.12921$_0$	0.07674$_6$	0.15514$_3$	90	63.92$_2$	90	1.381$_8$
20.971	0.13025$_9$	0.07676$_9$	0.15503$_2$	90	64.05$_9$	90	1.394$_1$
41.439	0.13179$_5$	0.07691$_8$	0.15527$_4$	90	63.95$_6$	90	1.414$_2$
51.490	0.13274$_0$	0.07698$_2$	0.15543$_2$	90	63.89$_9$	90	1.426$_5$
61.422	0.13367$_0$	0.07710$_4$	0.15564$_4$	90	63.83$_4$	90	1.439$_0$
66.343	0.13411$_6$	0.07713$_6$	0.15578$_6$	90	63.79$_9$	90	1.446$_1$
67.324	0.13424$_0$	0.07716$_1$	0.15585$_0$	90.00	63.76$_8$	90.00	1.448$_6$
71.237	0.13469$_6$	0.07725$_3$	0.15602$_9$	88.48$_1$	63.73$_1$	89.22$_6$	1.455$_4$
80.937	0.13534$_0$	0.07743$_3$	0.15636$_5$	87.45$_6$	63.68$_3$	88.60$_6$	1.467$_1$
90.524	0.13623$_1$	0.07766$_0$	0.15682$_8$	86.49$_3$	63.57$_3$	88.29$_4$	1.483$_0$
100=Ab	0.13676$_6$	0.07782$_0$	0.15721$_0$	85.82$_8$	63.48$_1$	87.96$_7$	1.493$_2$

Δ with its q value. The data and observations on natural feldspars are presented in table 11.

Laves and Chaisson (1950) reported two reciprocal interaxial angles for synthetic albite prepared at 300° and 450°C. and unspecified water pressure. Their values, obtained from precession photographs, are: $\alpha^* = 86.15 \pm 0.1°$, $\gamma^* = 88.27 \pm 0.1°$. Ours are: $\alpha^* = 85.83 \pm 0.01°$ and $\gamma^* = 87.97 \pm 0.01°$, significantly lower than theirs. Could the difference in temperature and possibly water pressure at crystallization account for such a discrepancy?

The powder charts of the sodium-rich members show the latter to be triclinic. On the potassium side of the series, the charts have been indexed on the assumption of a monoclinic lattice. Powder data alone, of course, cannot prove that the symmetry is monoclinic; they yield information only on the cell geometry—all they tell us is that α and γ are equal to 90° within the limits of error. The inference that those samples for which $\alpha = \gamma = 90°$ are truly monoclinic rests on the following considerations: (1) Monoclinic symmetry is shown by our single-crystal photographs of natural high-temperature feldspars. (2) Natural sanidinized orthoclases are known to be monoclinic (Cole, Sörum, and Kennard, 1949). (3) It is highly unlikely that, if the symmetry were triclinic, *six* compositions would all have α and γ accidentally equal to 90°.

CONCLUSIONS

In the case of the synthetic feldspars, the composition at which the change of symmetry takes place corresponds, with-

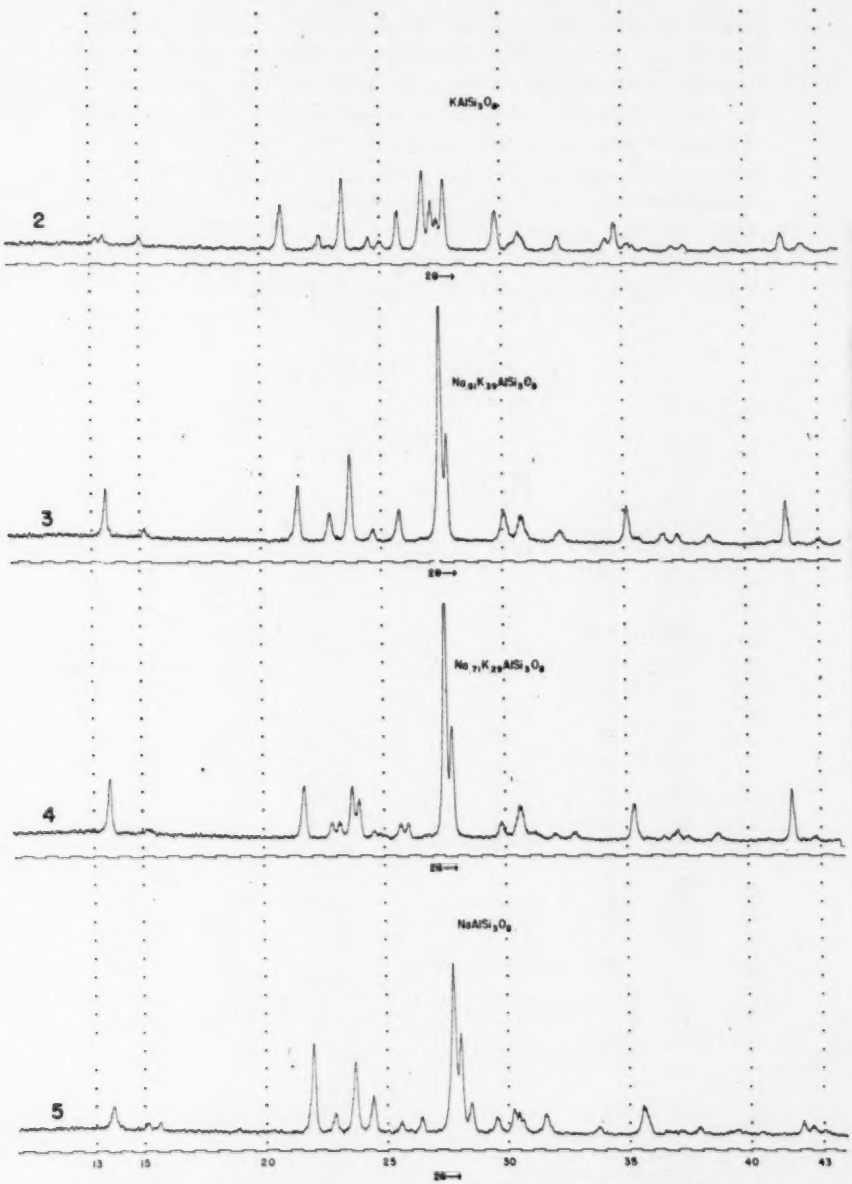

Figs. 2-5. Powder charts of (2) $KAlSi_3O_8$, (3) $Na_{.61}K_{.39}AlSi_3O_8$, (4) $Na_{.71}K_{.29}AlSi_3O_8$, (5) $NaAlSi_3O_8$.

in experimental errors, to an atomic ratio of sodium to potassium equal to 2:1. The symmetry change of natural high-temperature feldspars takes place at about the same value of the ratio (calcium + sodium) to potassium. (This is easily explained since, to a first approximation, the ionic radii of calcium and sodium may be assumed to be equal.) The 2:1 composition also coincides with the minimum melting point determined by Bowen and Tuttle (1950). These coincidences are fortuitous, as the symmetry-change composition varies rapidly with temperature (MacKenzie, 1952).

TABLE 6

Powder Data of $KAlSi_3O_8$

	q	$2\Theta_{obs}$	$2\Theta_{calc}$	hkl
	1R	13.31	13.31	110
	1	13.56 to 13.61	13.59	020
		——	13.74	001
	2R	15.095	15.095	111
		——	19.37	021
	8R	20.945	20.945	201
	3R	22.525	22.54	111
	1R	22.92 to 22.99	22.98	200
	10R	23.475	23.485	130
	4R	24.57	24.565	131
	3R	25.035	25.05	221
	8R	25.755	25.76	112
	9R	26.785	26.79	220
	9R	27.13	27.13	202
a_1—	6R	27.35	27.35	040
	10R	27.655	27.66	002
	8R	29.80	29.795	131
	1	30.465	30.43	222
	2	30.75	30.73	041
	1	30.92	30.93	022
		——	31.75	201
		——	31.91	311
	4R	32.34	32.34	132
	4	34.36	34.315	312
			34.67	221
	6	34.71	34.69	241
	peaks not sharp, 14 calculated reflections			

q	$2\Theta_{obs}$	$2\Theta_{calc}$	hkl
	——	40.89	151
1R	41.545 to 41.59	41.55	060
		41.76	313
peaks not sharp, 28 calculated reflections			
	——	50.64	062
		50.87	043
8	50.87	50.87	204
	——	50.94	171

$D = 0.345/85 = 0.004_1$, $N = 14$

$\Delta = 0.015$, $q = 3$

The curve of a shows a discontinuity in its first derivative. The same may possibly be true for d(111) and γ, but it is much less certain. All other curves, including those of cell volume and specific gravity, show no break at all (fig. 6). Within the limits of experimental accuracy, no region is found in which the monoclinic and triclinic forms coexist. For such a high-temperature two-phase region to escape detection by our method, it would have to be less than 1 atomic per cent wide. We are thus led to the conclusion that the phase transition is of second or higher order and that, for all practical purposes, the solid solution may be considered complete.

TABLE 7
Powder Data of $Na_{.61}K_{.39}AlSi_3O_8$

	q	$2\Theta_{obs}$	$2\Theta_{calc}$	hkl
	10	13.655	13.655	020
			13.67	110
		——	13.78	001
	2R	15.26	15.27	111
		——	19.45	021
	10R	21.58	21.585	20$\bar{1}$
	8R	22.92	22.915	111
	10	23.75	23.77	130
			23.79	200
	1R	24.73	24.745	13$\bar{1}$
		——	25.63	22$\bar{1}$
	7	25.80	25.83	112
	10	27.49	27.49	202
			27.51	040
			27.53	220
	10R	27.77	27.77	002
a_1—	6R	30.14	30.14	131
		30.72	30.79	222
		to 30.90	30.86	041
		——	31.04	022
	2R	32.45	32.45	132
		——	32.55	201
		——	33.00	31$\bar{1}$
			35.14	312
	7	35.20	35.20	24$\bar{1}$
			35.445	221
	1	35.54	35.59	112
			36.64	150
			36.65	240
	2	36.67	36.67	310
	1R	37.28	37.30	15$\bar{1}$
		——	38.09	203
	3	38.530	38.535	33$\bar{1}$
		——	38.895	113
		——	39.35	242
		——	39.455	042
		——	40.42	332
		——	40.64	223
		——	40.82	132
		——	41.245	151
	10	41.745	41.75	060
			41.78	330
		——	42.16	003
	peaks not sharp, 29 calculated reflections			
			50.87	062
	5	50.96	51.00	204
			51.07	043

$D = 0.145/40 = 0.003_6$, $N = 8$

$\Delta = 0.020$, $q = 1$

The ionic radii of sodium and potassium most commonly encountered in silicates are 0.98 and 1.33Å respectively, the difference between the two being 36 per cent of the smaller one. Let us call *effective radius* the radius increased by thermal motion. Applying the rule that a radius difference of 15 per cent is the upper limit for complete substitutional solid solution, we conclude that the effective radius of sodium increases more rapidly with temperature than that

TABLE 8

Powder data of $Na_{.71}K_{.29}AlSi_3O_8$

	q	$2\Theta_{obs}$	$2\Theta_{calc}$	hkl
			13.67	110
	9	13.70	13.68	020
			13.815	001
		——	13.83	110
	1	15.23	15.22	111
	1	15.39	15.40	1$\bar{1}$1
		——	19.23	021
		——	19.75	021
	10R	21.715	21.715	20$\bar{1}$
	4R	22.87	22.87	1$\bar{1}$1
	4R	23.19	23.19	111
	10R	23.71	23.71	130
	8	23.95	23.97	200
		to 24.01	23.995	130
	1R	24.625	24.625	13$\bar{1}$
		——	24.975	13$\bar{1}$
	4	25.715	25.71	112
			25.73	22$\bar{1}$
			25.78	221
	5R	26.005	26.02	112
			27.54	220
	10	27.565	27.565	040
			27.57	202
	10	27.84	27.84	002
			27.865	220
	1R	29.90	29.91	131
α_1—			30.59	04$\bar{1}$
	3	30.64	30.63	131
			30.685	222
		——	30.78	022
		——	31.06	222

q	$2\Theta_{obs}$	$2\Theta_{calc}$	hkl
peaks not sharp, 8 calculated reflections			
		35.255	312
		35.295	24$\bar{1}$
7	35.345	35.36	312
		35.37	24$\bar{1}$
		35.375	221
	——	35.56	1$\bar{1}$2
peaks not sharp, 25 calculated reflections			
	——	40.99	223
		41.80	330
8	41.835	41.84	060
	——	42.615	152

$D = 0.085/35 = 0.002_4$, $N = 7$

$\Delta = 0.015$, $q = 5$

Fig. 6. Cell dimensions, cell volume, calculated specific gravity and d(111) of synthetic high-temperature alkali feldspars. Note the differences in the scales of ordinates.

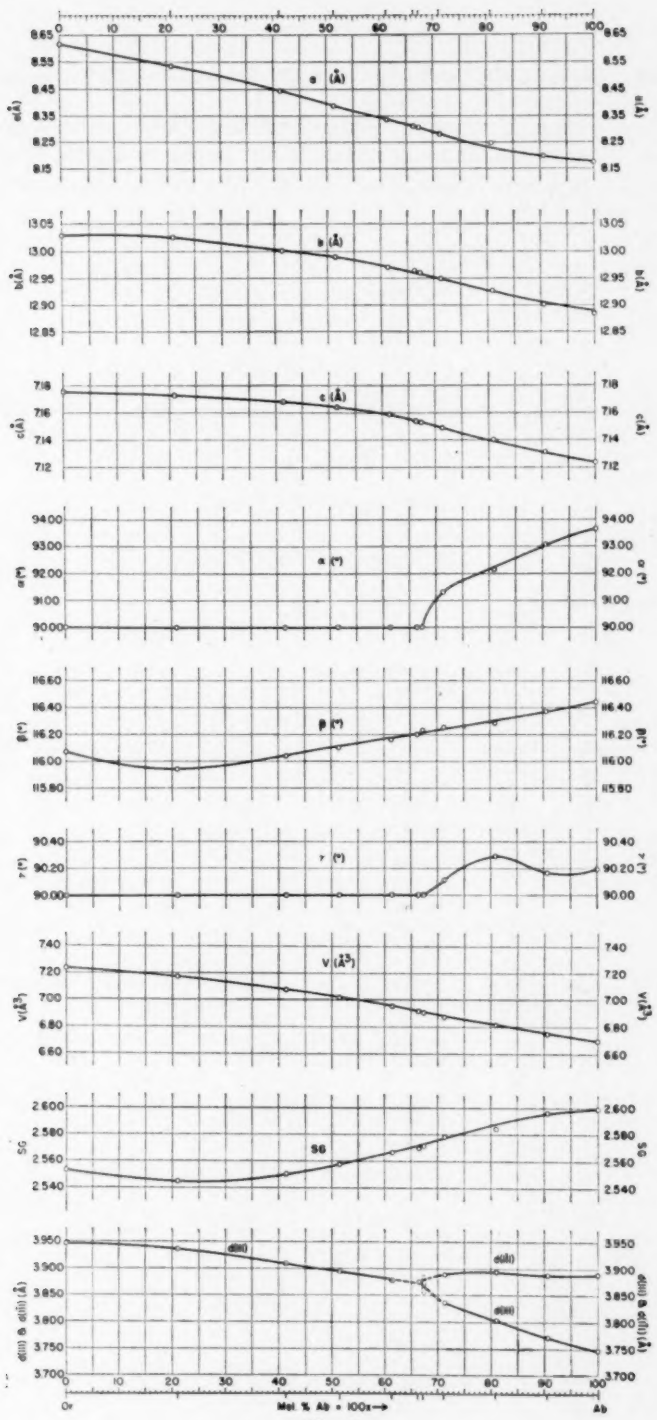

Fig. 6

of potassium. If e_T is the ratio of effective radius at temperature T to radius at room temperature, we have, at the lowest temperature where complete solid solution exists (above 660° ± 10°),

$$\frac{1.33\ e_T(K^+) - 0.98\ e_T(Na^+)}{0.98\ e_T(Na^+)} = 0.15\ ,$$

so that

$$e_T(Na^+) = 1.18 e_T(K^+)\ .$$

On cooling, the cell dimensions vary and, for a wide range

TABLE 9

Powder data of $NaAlSi_3O_8$

	q	$2\theta_{obs}$	$2\theta_{calc}$	hkl
			13.72	110
	5	13.78	13.78	020
	1	13.95	13.92	001
		——	14.15	110
	1R	15.175	15.155	111
	1R	15.69	15.68	111
		——	18.905	021
		——	20.35	021
	10R	21.975	21.975	201
	7R	22.87	22.87	111
	10	23.70	23.695	130
			23.745	111
			24.345	200
	8	24.445	24.455	130
			24.485	131
	2	25.57 to 25.71	25.475	131
			25.575	112
		——	25.95	221
		——	26.115	221
	2R	26.45	26.445	112
			27.64	220
			27.765	202
	10	27.77	27.77	040
	10R	28.055	28.055	002
	9R	28.515	28.515	220
	3R	29.57	29.56	131
	1	30.255 to 30.595	30.24	041
			34.44	022
a_1---			30.56	222

q	$2\theta_{obs}$	$2\theta_{calc}$	hkl
4	31.55 to 31.63	31.57	131
		31.63	222
	31.63	31.64	132
	——	32.09	041
	——	32.275	022
	——	33.245	201
		33.63	311
		33.75	311
2	33.775	33.755	132
	——	35.375	221
		35.51	312
		35.535	241
4	35.63	35.62	112
		35.79	241
	——	35.815	312
peaks not sharp, 26 calculated reflections			
	——	41.96	330
	——	42.01	152
3R	42.17	42.16	060
	——	42.455	313

$D = 0.100/46 = 0.002_2$, $N = 9$

$\Delta = 0.020$, $q = 1$

TABLE 10

Data on Synthetic High-Temperature Feldspars, $Na_xK_{1-x}AlSi_3O_8$

Monoclinic

Wt. % Ab	Mol. % Ab = 100 x	Molec. wt.	a	b	c	β	V	S.G. (calc.)	d(111) (obs.)	q (111)	d(111) (calc.)	D	N	Δ	
0	0	278.25	8.617Å	13.030Å	7.176Å	116.07,°	723.7Å^3	2.553_2	3.947Å	3	3.944Å	0.004°	14	0.015°	(q = 3)
20	20.971	274.87	8.537	13.026	7.173	115.94_1	717.3	2.544_8	3.936	9	3.936	0.005	17	0.020	(q = 1)
40	41.439	271.57	8.445	13.001	7.168	116.04_4	707.1	2.550_5	3.910	5	3.911	0.004	12	0.015	(q = 2)
50	51.490	269.96	8.389	12.990	7.164	116.10_1	701.1	2.557_0	3.895	4	3.896	0.003	7	0.010	(q = 8)
60	61.422	268.36	8.335	12.970	7.159	116.16_6	694.5	2.566_0	3.878	7	3.878	0.004	8	0.020	(q = 1)
65	66.343	267.57	8.310	12.964	7.154	116.20_1	691.5	2.569_5	3.875	1	3.873	0.003	3	0.010	(q = 1)

Triclinic

Wt. % Ab.	Mol. % Ab. = 100x	Molec. wt.	a	b	c	α	β	γ	V	S.G. (calc.)	d(111) (obs.)	q (111)	d(111) calc.	d(111) obs.	q(111)	d(111) calc.	D	N	Δ	
66	67.324	267.41	8.305Å	12.960Å	7.153Å	90.00_0°	116.23_2°	90.00°	690.6Å^3	2.571_4	3.850Å to 3.888	<1	3.871Å	3.850Å to 3.888	1	3.871Å	0.002°	2	0.005°	(q = 7)
70	71.237	266.78	8.279	12.949	7.149	91.31_2	116.25_9	90.11_3	687.1	2.578_5	3.835	4	3.835	3.888	4	3.888	0.002	7	0.015	(q = 5)
80	80.937	265.22	8.243	12.927	7.140	92.14_9	116.28_1	90.29_8	681.5	2.584_5	3.804	6	3.804	3.894	6	3.894	0.003	7	0.015	(q = 7)
90	90.524	263.67	8.197	12.901	7.131	93.06_9	116.37_7	90.16_3	674.3	2.596_4	not resolved	—	3.771	3.888	7	3.890	0.002	9	0.020	(q = 1)
100	100	262.15	8.172	12.884	7.123	93.64_9	116.44_7	90.19_2	669.7	2.599_9	not resolved	—	3.747	3.888	7	3.888	0.002	9	0.020	(q = 1)

V = cell volume
S.G. = specific gravity
q = peak quality
D = weighted average deviation
N = number of resolved peaks
Δ = largest deviation

of compositions, the symmetry goes from monoclinic to triclinic (MacKenzie, 1952). This is taken as evidence that *displacive*[2] changes are taking place in the structure, that is to say that ions will gradually change their positions as the effective ionic radii shrink and strain sets in. The crystal structure of a feldspar is pervaded by a framework of strong Si-O and Al-O bonds, which is responsible for the stability of the edifice. The alkali ions, being the largest cations and those that shrink most, will be responsible for the strain. Indeed the bonds under the greatest strain are the Na-O and K-O bonds and, if these were the main bonds to hold the structure together, the structure could be expected to collapse. As it is, however, the strong Si-O and Al-O bonds should absorb the strain and the weaker alkali-oxygen bonds should remain unbroken. In other words, *ordering* is not likely to occur. We set out to test this experimentally.

In the low-temperature form studied by Taylor, Darbyshire, and Strunz (1934), as well as in the sanidinized orthoclase studied by Cole, Sörum, and Kennard (1949), the four alkali

TABLE 11

Data and Observations on Natural High-temperature Feldspars

Composition* Wt. per cent			Locality	Thermal treatment	Observations	
Ab	An	Or		°C.	symmetry	twinning
47.0	3.8	49.2	Sparling Gulch Colorado	heated to 900 for 6 hours	monoclinic	.....
56.2	0.8	43.0	Mitchell Mesa Texas	heated to 900 for 12 hours	monoclinic	.....
57.8	2.0	40.2	San Juan Colorado	heated to 900 for 21 hours	monoclinic	.....
61.4	6.1	32.5	Kenya East Africa	heated to 900 for 18 hours	triclinic	albite
66.5	1.8	31.7	Grande Caldeira Azores	heated to 900 for 22 hours	triclinic	albite
61.8	10.1	28.1	Kenya East Africa	heated to 900 for 18 hours	triclinic	albite and pericline
69.5	7.5	23.0	Ropp Nigeria	heated to 900 for 5 hours	triclinic	albite and pericline
75.5	1.2	23.3	Victoria Australia	heated to 900 for 24 days	triclinic	.....

*Data supplied by W. S. MacKenzie.

[2] Terminology of M. J. Buerger (1948).

ions occupy a special 4-fold position (000; ½ ½ 0) ± (x0z) in the C-centered monoclinic cell and a general 4-fold position (000, ½ ½ 0) ± (xyz) in the C-centered triclinic cell. Assuming their distribution in the high-temperature form to be the same, one would predict a superstructure due to ordering at the composition $Na_{.50}K_{.50}AlSi_3O_8$ where sodium would occupy ±(x0z) and potassium would occupy ±(x+½, ½, z) so that the lattice would change to primitive. We did not observe any such ordering in the powder patterns. Reflections due to ordering, in the present case those with $(h + k)$ odd, are bound to be very weak, however, and could easily have passed unnoticed on the powder charts. For this reason, we decided to take single-crystal pictures. We selected a natural feldspar, with composition close to $Ab_{50}Or_{50}$, from Sparling Gulch (table 11). A single crystal was homogenized by heating and then cooled to dry-ice temperature for 36 hours. A precession photograph of this crystal showed no evidence of ordering. Attempts to induce ordering by cooling the crystal during exposure were equally unsuccessful. Another crystal was annealed for seven months at 1090° and then examined by X-rays. Evidence of ordering was never observed. Indeed, the stable system at room temperature consists of two disordered phases, in each of which the concentration of solute alkali ion is small, so that there is considerably less strain energy. Before these phases can be obtained by unmixing, the metastable phase must first be reheated below the solvus (Tuttle, 1951).

The phase transition could not have been predicted from the symmetry inversion alone, for symmetry is different from other properties such as specific heat, energy, or entropy, which are usually considered in thermodynamics. Any one of these properties indicates that a phase transition is taking place whenever it, or one of its derivatives, shows an observable discontinuity. A symmetry change, in all rigor, is a discontinuous phenomenon, but we may not be able in every case to ascertain the exact point (composition or temperature, as the case may be) at which the discontinuity occurs. Indeed, monoclinic symmetry is the limiting case of triclinic symmetry. As long as an atom A lies on a mirror plane, or a pair of equivalent atoms BB′ lie astride it, the symmetry is monoclinic. If A moves out of the plane by an *infinitesimal* distance *dy*, or if B and B′ move unequally from the plane by an infinitesimal

amount, the plane ceases to be a mirror and the symmetry becomes triclinic. The energy change accompanying such structural changes will also be infinitesimal and the energy function will not show any discontinuity. Thus *physically* a symmetry change may be continuous and need not be accompanied by a phase change.

ACKNOWLEDGMENT

We wish to thank Dr. O. F. Tuttle for a critical reading of our manuscript.

REFERENCES

Bowen, N. L., and Tuttle, O. F., 1950. The system $NaAlSi_2O_8$-$KAlSi_3O_8$-H_2O: Jour. Geology, vol. 58, pp. 489-511.

Buerger, M. J., 1948. The role of temperature in mineralogy: Am. Mineralogist, vol. 33, pp. 101-121.

Cole, W. F., Sörum, H., and Kennard, O., 1949. The crystal structures of orthoclase and sanidinized orthoclase: Acta Crystallographica, vol. 2, pp. 280-287.

Donnay, G., and Donnay, J. D. H., 1951*a*. Tables for the interpretation of X-ray diffraction data giving the square of the reciprocal lattice vector to 5 decimals in terms of the deviation angle 2Θ for every hundredth of a degree from 10.00° to 49.99° for $CuK\alpha$ and from 25.00° to 69.99° for $CuK\alpha_1$: Crystallographic Laboratory of The Johns Hopkins University, Baltimore. Limited edition.

———, and ———, 1951*b*. Unit-cell dimensions of synthetic high-temperature alkali feldspars determined from their powder patterns (abstract): Am. Cryst. Assoc., Program and Abstracts of the Winter Meeting, February 1951, pp. 32-33.

Laves, F., and Chaisson, U., 1950. An X-ray investigation of the "high"-"low" albite relations: Jour. Geology, vol. 58, pp. 584-592.

MacKenzie, W. S., 1952. The effect of temperature on the symmetry of high-temperature soda-rich feldspars: Am. Jour. Sci., present volume.

Taylor, W. H., Darbyshire, J. A., and Strunz, H., 1934. An X-ray investigation of the feldspars: Zeitschr. Kristallographie, vol. 87, pp. 464-498.

Tuttle, O. F., 1951. Studies in feldspar equilibria at the Geophysical Laboratory, Washington: Mineralog. Mag., vol. 29, pp. 757-758.

GEOPHYSICAL LABORATORY
CARNEGIE INSTITUTION OF WASHINGTON
WASHINGTON, D. C.

CRYSTALLOGRAPHIC LABORATORY
THE JOHNS HOPKINS UNIVERSITY
BALTIMORE, MARYLAND

ON THE GRANULITES OF LAPLAND

PENTTI ESKOLA

With contributions by Einar A. O. Nordenswan

"We still know very little about rocks."

—N. L. Bowen privately to the writer about 1922.

ABSTRACT. The granulites of Lapland are garnet-bearing acid quartz-feldspar rocks and mostly hypersthene-bearing intermediate, basic, and ultrabasic rocks forming sharply bounded bands in the former. Twenty rock analyses and 13 mineral analyses are given, and a granulite norm is proposed to show the critical minerals of the granulite facies. Specific properties of the granulite minerals are described. A greater part of the granulites is chemically aluminous rock, suggesting original argillaceous character. Graphite-granulites show a composition like that of sapropelic sediments; their carbon is supposed to be of organic origin. The basic granulites are interpreted as metamorphic volcanic or hypabyssic rocks, while more coarse-grained and homogeneous quartz-dioritic rocks are assumed to be primary magmatic. The granulite facies appear to be identical with that facies represented by the charnockites, the specific characteristics of the foliated granulites being due to their tectonic history.

INTRODUCTION

HORACE, in *De Arte Poetica*, says a literary product should ripen nine years before it is given publicity. This paper more than fulfills this requirement, as the first draft of it was written a score of years ago. Fortunately it was not published at that time for my views on the granulite have since undergone a thorough metamorphism! The present paper is based partly upon field observations made by me in the summers of 1924, 1926, and 1932, those made by E. Nordenswan in 1925 and 1926, and partly upon chemical analyses carried out by the latter in 1926-28. I spent the field season of 1932 in Lapland together with my pupil and friend, Dr. Th. G. Sahama, who in 1936 published his study on the petrofabrics of the granulites. It was planned that the late Dr. Erkki Mikkola would complete the field survey and prepare a structural investigation of the granulites. He did much to this end (Mikkola, 1932, 1941). The accompanying map is copied chiefly from him. Kranck (1936) published a valuable tectonic sketch on the granulites.

The publication of my results has been delayed because my views on the genesis of the granulites, briefly outlined in an early paper (Eskola, 1932), were not definite enough,

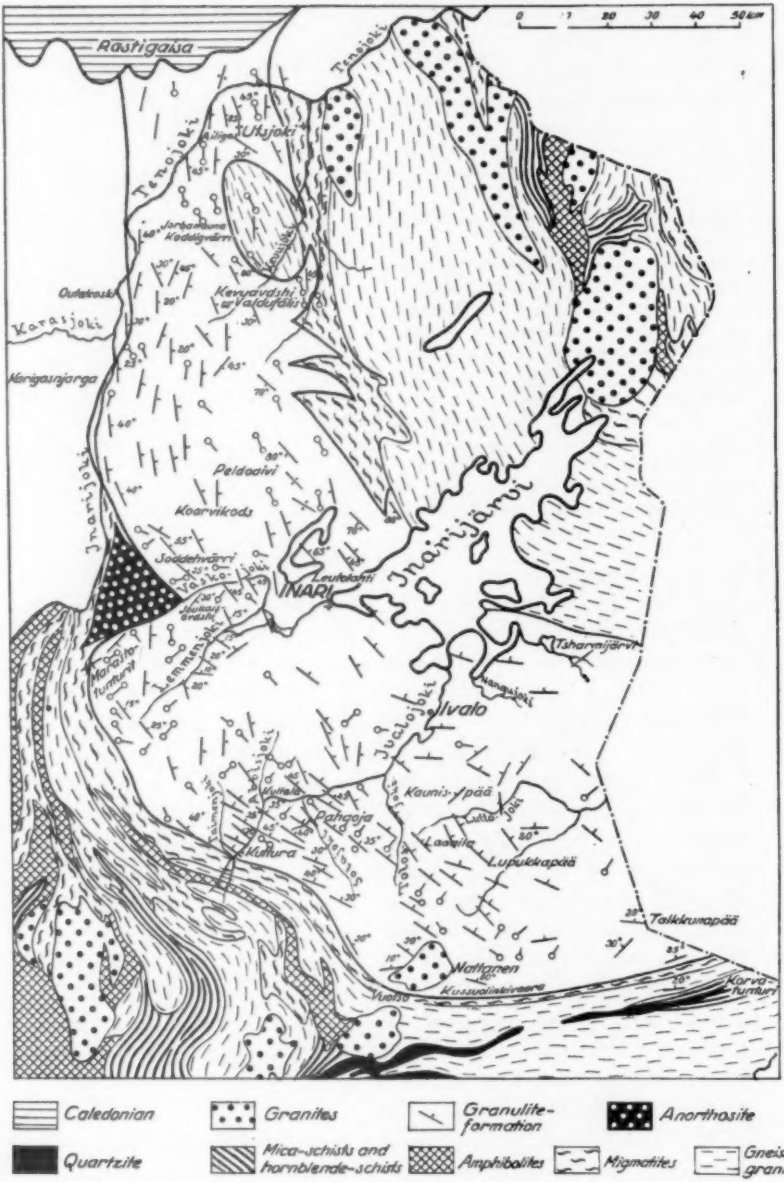

Fig. 1. Geological map of the granulite area of Lapland.

and because I wanted to await Mikkola's results. Since the death in 1940 of this pioneer of Lapland's geology, field work has been carried out in the last few years by the Geological Survey. Mr. O. Helovuori especially has augmented the field observations on the granulites.

For the present investigation I revised the material and studied microscopically the thin sections made for E. Mikkola, Th. G. Sahama, and P. Eskola—about 450 in all. Much is still to be done, beginning with a more detailed field survey, but it is hoped that the present results may throw some light upon the genesis and the facies of granulites and the charnockite suite of rocks as a whole, which at present attract the interest of a wide circle of petrologists.

GEOLOGY OF THE GRANULITE FORMATION

The granulites of Lapland occupy an area of more than 15,000 square kilometers, or about 30 times as much as the similar granulites in Saxony. The Lappish area has the shape of a huge arch, about 300 kilometers long and from 40 to 60 kilometers broad (fig. 1) in its northern part striking north-south and in the north diving under the lower Paleozoic at the Gaisa mountains (Rastigaisa) and in the southeast continuing into Soviet territory.

The land-forms of the granulite area are characterized by round-contoured highlands rising from 500 to 650 meters above sea-level and mostly above the timber line. These naked fields (Swedish *fjäll*) are covered by thin but continuous glacial drift. Many rivers, such as the Ivalojoki, the Tenojoki, and the Kevujoki, have deep V-shaped valleys some 200 meters deep, the floors of which are covered with moraines indicating the pre-glacial origin of the valleys. Most of the fresh outcrops are found along the rivers and in small clean-washed canyons (Lappish *avdshi*) eroded by glacifluvial currents (fig. 2).

Like the granulites in Saxony, lower Austria, Ceylon, etc., the Lappish granulites are banded garnetiferous quartz-feldspar rocks with bands of more basic, mostly garnet-free and hypersthene-bearing material, in part identical with charnockites of the charnockite provinces (figs. 3, 4). The strike of the foliation (see map, fig. 1) is remarkably conformable to the arched massif, dipping mostly at low angles toward the center of the arch, or east and north. Near the inner side

of the arch the dips are steep and frequently overturned to west and south. The lineation on the map, marked chiefly according to Sahama (1936) is in the northern part mostly horizontal parallel to the northerly strike, or pitches at low angles. Further south, where the prevailing strike turns toward southeast and east, the lineation is commonly parallel to the banding and foliation at right angles to the strike.

The structure of the complex gives the impression of overthrust toward west and south. The bordering schists, which further south have a north and south trend (Mikkola, 1941) have been turned parallel to the contact and have assumed the same northerly and easterly dips as the granulites. The boundary zone is most interesting petrologically. In the east at Korvatunturi (known to every child in Finland as the supposed home of Santa Claus!) sheared gneisses, kyanite and staurolite schists may be found along with many occurrences of ultrabasic rocks (Mikkola and Sahama, 1936), enstatite rock or sagvandite, quartzites, and other extreme rocks, including the large mass of anorthosite at Vaskojoki in the west. These formations will not be treated in this paper, but it is important to note that a large part of the bordering rocks are chemically quite different from the granulites, so the latter cannot possibly be products of metamorphism from them, although they are older than the emplacement of the granulites. The postkinematic Nattanen granite (Mikkola, 1928) is younger than the granulite.

The granulite area is renowned as a gold-bearing tract (Fircks, 1906). Placer gold has been washed for more than 70 years, especially on the Ivalojoki and its southern affluents. In recent years the Lemmemjoki valley and the area near the southern boundary of the granulite have also been worked, but the results have never been remarkable. A number of gold-bearing—though not workable—veins have been found. These are composed of carbonates of the siderite-magnesite series, quartz, pyrite, and secondary hematite and limonite. The main strike of the veins is at right angles to the strike of the granulite.

Fig. 2. Kevuavdshi, canyon carved by glaciffuvial waters in an elevated peneplain.

Fig. 3. Banded granulite at the northwestern end of Marastotunturi. Banding due to varying garnet content.

Fig. 4. Acid granulite with sharply bounded sill-like bands of darker norite-granulite (HyPla). East of the upper course of Sotajoki.

Fig. 2

Fig. 3

Fig. 4

The granulites, furthermore, are intersected by dikes of granite-porphyry, quartz-syenite-porphyry, and diabase (or trap). The following types of granulites may be distinguished:

Light massive granulite.—Sparse garnets dispersed in a granoblastic quartz-feldspar mass (figs. 5, 11). Biotite absent or present only in traces.

Light foliated granulite.—Small sparse garnets almost or perfectly biotite free (foliation marked by parallel orientation of thin quartz plates) (figs. 6, 12). Remarkably enough, this type may alternate as narrow bands with the massive type and, in fact, the granoblastic mass between the quartz plates is also of the non-foliated type.

Field granulite.—Usually biotite-bearing, with abundant garnets, up to 2 cm. in diameter, in a quartz-feldspar mass (fig. 7). Foliation marked by oriented biotite or by alternation of different bands. May contain cordierite.

Granitic granulite.—Coarse-grained, with big garnets, containing biotite and often cordierite (fig. 8). May be migmatic, with fragments of darker granulites (fig. 9).

Noritic and quartz-noritic granulites.—Gray, mostly garnet-free plagioclase-pyroxene rocks, sometimes hornblende-bearing, more or less distinctly foliated, common in all parts of the area as bands and lenses in the lighter types (figs. 4, 26).

Pyroxene-dioritic and granodioritic granulites. Like the former type but less foliated and coarser in grain, occurring as larger masses near the inner contact of the arch (fig. 29).

Ultrabasic granulite. Dark bands and fragments in the lighter types, peridotitic or pyroxenitic in composition (figs. 10, 13).

Fig.5. Massive biotite-free granulite from Kultalan sauna, analysis 15. Dark spots garnets. 0.9X.

Fig. 6. Foliated biotite-free granulite with oriented platy quartz (grey); black spots garnets. From Ivalojoki west of Kultala. 0.7X.

Fig. 7. "Field-granulite" from Palsi, 1 km east of the mouth of Sotajoki. Dark spots garnets surrounded by biotite as augen. 0.7X.

Fig. 8. "Garnet granite," granite-like granulite, from Mahlattinuora, Inarijärvi. Black spots garnets surrounded by black biotite. 0.7X.

Fig. 9. Coarse-grained granulite with a fragment of biotite-rich rock. Dark rounded spots big garnets and small spots biotite. Middle course of Sotajoki. 0.7X.

Fig. 10. Inclusions of pyroxenite in pegmatitic granulite and digested noritic granulite near Karigasnjarga at Tenojoki.

Fig. 5

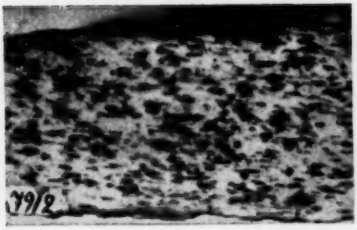

Fig. 6

Fig. 8

Fig. 7

Fig. 9

Fig. 10

THE GRANULITE NORM

The mineral composition of a rock, as a function of the physical conditions during its crystallization, defines its mineral facies. I have defined the granulite facies (Eskola, 1939) as comprising rocks for which, at basaltic bulk composition, the association of hypersthene and plagioclase, and, at granitic bulk composition, quartz, feldspars, and almandine-pyrope garnet are typomorphic, while ilmenite is the titanium mineral in basic and rutile in the acid rocks. Amphiboles and micas do not belong to the granulite facies.

The norm of the CIPW classification is an idealized mineral composition most closely agreeing with the mode in the pyroxene-hornfels facies. Each facies might have its own "facies norm" but this is not practicable because the constituent minerals are too variable in composition. For the granulite facies, however, an idealized *granulite norm* is suggested by the actual minerals.

Excessive alumina in the granulites results in the crystallization of garnet and is allotted with an equal amount of (Mg, Fe, Mn) SiO_3 for pyrope-almandite, which may be understood as a compound of corundum, enstatite, and ferrosilite, $Al_2O_3 \cdot$ (Mg, Fe) SiO_3. Cordierite may occur instead of garnet but does not belong to the granulite facies proper and need not be taken in the norm. If there is still an excess of alumina it forms sillimanite and is calculated as $Al_2O_3 \cdot SiO_2$. TiO_2 in the hypersthene-free granulites occurs as rutile and is put as *ru* in the norm. In hypersthene-bearing granulites rutile has never been observed and the titania not present in the silicates enters into the iron ore as ilmenite. As presumably only ilmenite and not rutile is in equilibrium with hypersthene, TiO_2 in the hypersthene-bearing rocks is allotted to FeO to form ilmenite in the granulite norm. For the garnet-free granulites the granulite norm is identical with the CIPW norm.

Fig. 11. Massive granulite from Palsi at Ivalojoki. Crossed Nicols, 20X.

Fig. 12. Foliated granulite with platy quartz (white). Gray = saussuritized plagioclase and garnets (high relief). One Nicol, 14X.

Fig. 13. Olivine-hornblende-granulite, peridotitic. Analysis I. One Nicol, 20X.

Fig. 14. Acid granulite from Lupukkapää. Analysis 20. Gas(?) inclusions in quartz. Crossed Nicols, 20X.

Fig. 15. Rutile needles in platy quartz in granulite from Kaktsavärri. One Nicol, 107X.

Fig. 16. Hair-antiperthite in plagioclase-granulite. The orthoclase "hairs" are cut obliquely. Habmarastinoaivi near Ailigas. One Nicol, 40X.

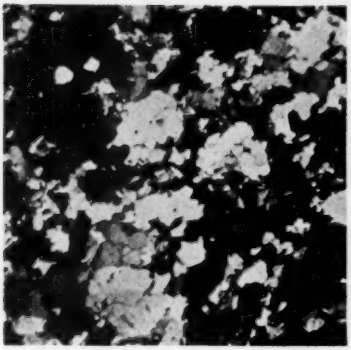

Fig. 11

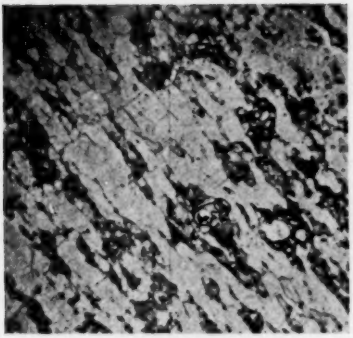

Fig. 12

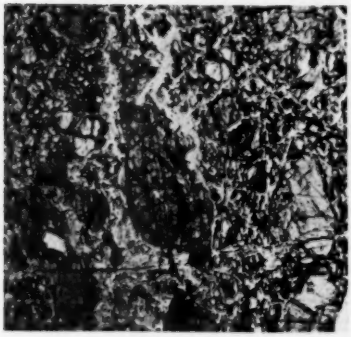

Fig. 13

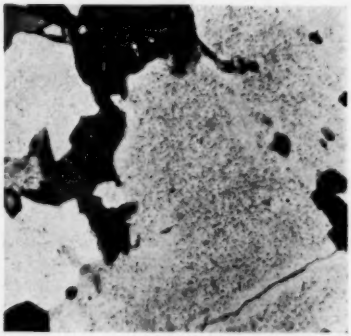

Fig. 14

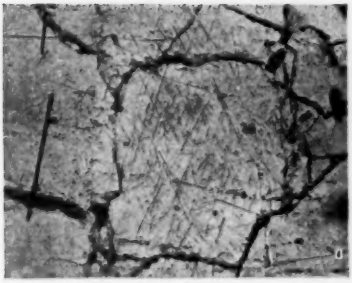

Fig. 15

Fig. 16

THE MINERALS OF THE GRANULITES

All the rocks of the granulite facies are granulites. They are characterized by their chief mineral components; the word granulite need not be mentioned and, for the sake of brevity, the mineral names are designated by symbols formed of the first two or more letters. The minerals are given in the order of their abundance. Thus, instead of "plagioclase-hypersthene-garnet-granulite," we write "PlaHyGa." When accessory minerals are mentioned also, their symbols are printed in small type; e.g., a sillimanite- and rutile-bearing granulite: QuaOrPlaGa:SillRuMa (Ma = magnetite which may contain ilmenite or hematite).

Twenty analyses of granulites are given in tables 1 and 2. In the following text the numbers refer to the analyzed rocks.

Quartz is first in abundance in the acid granulites, sometimes forming more than 90 per cent of the rock. The inner parts of the grains may contain minute inclusions (gas?), as in the analyzed (20) rock from Lupukkapää (fig. 14), and very commonly needles of rutile (fig. 15).

Plagioclase varies widely in composition. Some values from the analyzed rocks illustrate the range of variation: PlaHy (4) Pahaoja An_{70}; PlaDiHy (5) Härkäselkä An_{62}; PlaDiHoHy (2) Koddigvärri An_{52}; PlaDiHy (3) west of Abbisjoki An_{49}; PlaQuaHy (6) Sotajoki An_{41}. Values around An_{40} were found optically to be most common in the PlaQuaHy:s. In the acid granulites the plagioclase is usually between An_{25} and An_{30}, and rarely less than An_{20}. In the red gneiss (16) from Sotajoki the plagioclase is An_7, but this is not a true granulite.

Fig. 17. Undulating extinction in orthoclase, the first stage in the process of microclinization. A band of sillimanite across the slice. Banded granulite from roadside between Inari and Leutolahti. Crossed Nicols, 28X.

Fig. 18. Undulating extinction in orthoclase showing the first signs of quadrille-structure in hypersthene-granitic granulite (OrMiQuaPlaHyDiMa). Jonlaki near Talkkunapää. Crossed Nicols, 40X.

Fig. 19. Hair-perthite, the same slice as Fig. 17, with one Nicol, 40X.

Fig. 20. Hair-perthite in aplitic granulite from Sotajoki. One Nicol, 40X. Cross sections of "hairs" near the upper margin.

Fig. 21. Sillimanite porphyroblasts and a band of biotite in acid granulite from Tolosjoki. One Nicol, 20X.

Fig. 22. Sillimanite band in granulite from Joukaisavdshi. One Nicol, 28X.

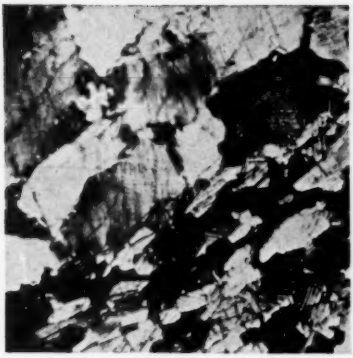

Fig. 17

Fig. 18

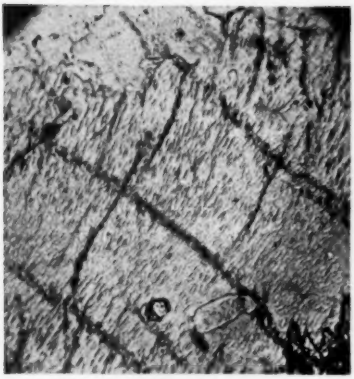

Fig. 19

Fig. 20

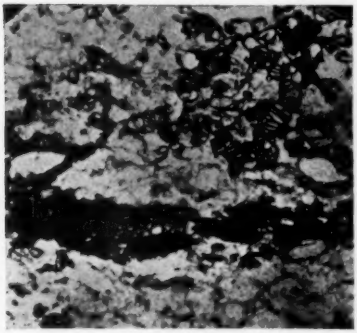

Fig. 21

Fig. 22

TABLE 1

Hypersthene-bearing Granulites

	1.	2.	3.	4.	5.	6.	7.	8.	9.	10.
SiO_2	41.82	48.39	48.73	51.60	52.03	59.21	76.85	62.38	52.11	38.10
TiO_2	0.49	2.08	3.70	0.37	2.27	2.01	0.33	0.64	0.77	0.35
Al_2O_3	2.34	12.88	11.78	16.59	16.39	17.51	12.96	17.66	18.08	21.22
Fe_2O_3	4.90	2.83	5.67	0.50	0.82	1.93	—	1.50	1.04	0.91
FeO	6.00	11.63	11.32	6.37	9.13	4.49	1.22	3.71	9.19	6.83
MnO	0.15	0.33	0.28	0.08	0.17	0.06	0.03	0.32	0.07	0.11
NiO	0.05	0.00	—	—	—	—	—	—	—	—
MgO	28.23	6.85	4.61	14.42	7.04	3.81	0.11	3.27	8.37	2.43
CaO	7.65	11.84	9.13	8.03	8.78	5.87	3.32	4.52	5.20	7.05
BaO	0.00	0.01	0.02	0.01	0.03	0.016	0.08	—	—	0.016
Na_2O	0.19	2.09	3.33	1.32	2.14	3.26	3.60	3.46	2.93	2.38
K_2O	0.40	0.45	0.77	0.48	1.21	1.86	1.08	1.58	1.63	0.90
P_2O_5	0.07	0.17	0.13	0.00	0.06	0.05	0.09	0.43	—	0.04
Cr_2O_3	0.29	0.02	0.00	0.14	0.10	0.00	0.00	—	—	0.02
V_2O_5	—	0.00	—	—	—	—	—	—	—	—
ZrO_2	—	—	—	0.00	0.00	0.02	—	—	—	0.00
CO_2	1.53	—	—	—	—	—	—	—	—	—
S	0.03	—	0.21	0.12	0.04	0.15	—	—	—	0.11
H_2O+	5.17	0.59	0.28	0.30	0.30	0.36	0.27	0.36	0.38	0.34
H_2O-	0.43	0.06	0.06	0.04	0.05		0.09		0.04	0.08
	99.74	100.22	100.02	100.37	100.56	100.60	100.03	99.83	99.81	100.88
Sp. gr.	2.97	—	3.10	3.02	3.04	2.82	2.67	—	—	2.92

TABLE 1 (*Cont.*)

Granulite norms

		1	2	3	4	5		6	7		8	9	10
	qu	—	—	1.96	—	2.47		13.61	43.57		19.40	—	16.89
	or	2.34	2.67	4.56	2.84	7.12		10.95	6.39		9.34	9.62	5.28
	ab	1.62	19.75	28.14	11.15	18.08		27.56	30.44		29.12	24.63	20.12
	an	4.34	24.33	14.83	37.78	31.44		27.52	15.85		22.41	25.85	34.89
di	wo	9.78	13.88	12.36	0.86	4.91		0.55	0.08	ga cor	2.04	2.05	3.56
di	en	7.90	6.95	6.38	0.61	2.79		0.38	0.01	ga en	4.08	3.91	3.92
di	fs	0.70	6.63	5.64	0.17	1.97		0.12	0.08	ga fs	2.53	2.80	8.29
hy	en	22.20	8.21	5.05	32.06	14.72		9.07	0.26		4.03	13.67	2.11
hy	fs	1.97	7.82	4.45	9.40	10.55		3.02	1.68		2.57	9.77	4.46
ol	fo	27.94	1.29	—	2.17	—		—	—		—	2.23	—
ol	fa	2.75	1.37	—	0.71	—		—	—		—	1.84	—
	mt	7.12	4.11	8.24	0.72	1.18		2.80	—		2.18	1.51	1.32
	il	0.93	3.95	7.02	0.70	4.31		3.81	0.62		1.22	1.46	0.67
	cm	0.43	0.03	—	0.20	0.16		—	—		—	—	—
	ap	0.17	0.40	0.30	—	0.13		—	0.20		1.01	—	0.10
	cal	3.48	—	0.40	—	—	FeS_2	0.28	—		—	—	0.20

The analyst is indicated by initials after the number:

E.N. = Einar Nordenswan; N.S. = Naima Sahlbom; A.H. = Aarto Huhma.

1. E.N. OlHoSerp (Fig. 1, Pl. 1), Abbisjoki, Ivalojoki.
2. E.N. PlaDiHoHy : Ma. Koddigvärri.
3. E.N. PlaDiHy : Ma, W. of Abbisjoki, Ivalojoki. Band in 7.
4. E.N. PlaHy : BiHoDiMa. Pahaoja, Sotajoki.
5. E.N. PlaHyDi : BiOrMa. Härkäselkä, between Ivalojoki and Laanila.
6. E.N. PlaQuaHy : BiMa. Sotajoki.
7. E.N. PlaQuaHy, W. of Abbisjoki, Ivalojoki. In contact with 3.
8. N.S. PlaQuaGaHy : Ma. W. of Kultala, Ivalojoki. (Hackman, 1905).
9. A.H. PlaHyGa : Bi. Kevuavdshi, Kevujoki.
10. E.N. PlaQuaGaHy, Sotajoki.

TABLE 2

Hypersthene-free Granulites

	11.	12.	13.	14.	15.	16.	17.	18.	19.	20.
SiO_2	49.83	59.5	72.52	72.70	68.01	78.75	73.98	76.13	80.67	85.46
TiO_2	1.39	0.2	2.01	Trace	1.39	0.23	Trace	0.21	0.42	0.63
Al_2O_3	18.35	16.9	12.58	16.20	16.25	12.20	14.93	11.32	10.17	6.44
Fe_2O_3	2.88	3.3	0.04	—	1.46	0.49	0.26	0.64	0.74	0.64
FeO	16.78	9.9	5.05	1.36	3.32	0.46	0.34	3.07	1.93	2.51
MnO	0.25	0.2	0.04	0.02	0.07	Trace	0.00	Trace	Trace	0.03
MgO	6.86	4.2	2.02	0.05	1.55	0.02	0.36	1.86	1.14	0.78
CaO	1.32	1.9	1.24	1.54	3.36	0.48	1.92	1.33	0.93	1.10
BaO	—	—	0.065	0.06	0.03	0.05	—	—	—	0.04
Na_2O	1.09	1.4	1.94	3.18	2.89	3.65	3.14	2.16	1.47	1.60
K_2O	1.09	1.8	2.30	5.19	2.04	3.89	5.07	3.51	2.41 (9?)	1.02
P_2O_5	Trace	—	0.00	—	0.00	0.00	0.00	Trace	Trace	0.04
Cr_2O_3	—	—	0.00	—	0.00	0.00	—	—	—	0.00
ZrO_2	—	0.1	—	Trace	Trace	Trace	—	—	—	—
S	—	0.2	—	0.04	0.09	—	—	—	—	—
H_2O+	0.85	0.3	0.23	0.15	0.18	0.20	0.11	0.50	0.20	0.24
H_2O-			0.04	0.02	0.09	0.08				0.04
	100.69	99.9	100.07	100.51	100.73	100.50	100.11	100.73	100.08	100.57
Sp. gr.	—	—	2.85	2.65	2.79	2.63	—	—	—	2.73

TABLE 2 (*Cont.*)

Granulite norms

		11	12	13	14	15	16	17	18	19	20
	qua	12.67	26.1	40.65	29.59	32.58	41.17	31.32	42.36	56.90	66.90
	or	6.45	10.6	13.56	30.72	11.68	22.97	30.02	20.57	14.29	6.00
	ab	9.22	12.1	16.40	26.88	24.63	30.87	26.72	18.34	12.46	13.41
	an	6.53	9.4	6.28	7.64	16.68	2.47	9.45	6.67	4.62	5.45
	sill	—	2.4	5.10	0.76	—	0.15	—	—	2.72	—
ga	cor	12.93	7.7	4.11	2.08	2.04	0.91	0.71	1.53	1.73	0.71
ga	en	16.50	10.4	5.01	0.12	3.00	0.05	0.90	4.65	2.83	0.81
ga	fs	28.43	15.8	6.03	2.53	3.96	0.84	0.41	5.15	2.94	1.70
hy	en	0.54	—	—	—	0.90	—	—	—	—	1.12
hy	fs	0.96	—	—	—	0.92	—	—	—	—	2.38
	mt	3.33	4.9	0.05	—	2.09	0.72	0.37	0.93	1.07	0.93
	ru	1.39	0.2	2.01	—	1.39	0.23	—	0.21	0.42	0.63
			FeS_2 0.4								

11. N.S. GaQuaBiCord: Ma (Laanilite), Laanila. (Hackman, 1905).
12. Geometr. QuaGaPlaBiOrCordSi: PyMaZi, Sotajoki mouth.
13. E.N. QuaGaPlaOr, Luttolouhos near Laanila.
14. E.N. PlaOrQuaGa, Luttolouhos near Laanila.
15. E.N. PlaQuaGaOr: SillMaHemRu, Kultalan sauna, Ivalojoki.
16. E.N. QuaPlaOr: BiMa (Red gneiss), Sotajoki.
17. N.S. QuaOrGaPla, Kakslauttanen near Laanila. (Hackman, 1905.)
18. N.S. QuaPlaOrGa: Bi, Ivalojoki. (Hackman, 1905.)
19. N.S. QuaPlaOrGa: SillRu, Laanilauttanen near Laanila. (Hackman, 1905.)
20. E.N. QuaPlaOrGa, Lupukkapää.

In PlaQuaHy (7) west from Abbisjoki it is An_{34}, in cordierite-granulite (12) from Sotajoensuu An_{40}, in PlaQuaGaOr (15) from Kultalan sauna An_{39}. Examples of uncommon compositions will be given in the section on the granulites as rocks.

The plagioclases in the granulites are homogeneous and show no zoning. Twinning lamellae are frequently present but not very numerous.

Antiperthite is common, especially in andesines. It is of two types—the potash feldspar present as short homoaxial inclusions partly bounded by crystal faces, or as fine short hairs, the hair-antiperthite (fig. 16).

Potash feldspar in the granulites appears to be primarily orthoclase, unlike that in most Archaean rocks of Finland. This was concluded from the straight extinction in sections $\perp$ (010). In many thin sections of coarse-grained cordierite- and garnet-bearing rocks of granitic appearance, e.g., from Mahlattinuora on Lake Inarijärvi and from the roadside northeast of Ivalo, the orthoclase is clear and free from perthite, like adularia, and similar potash feldspar was also met in foliated and more fine-grained biotite-free granulites with platy quartz. In other specimens the orthoclase is otherwise similar but contains hair-like perthite threads. The first stage of alteration of the clear orthoclase into microcline appears in the form of undulating extinction (fig. 17). Gradually extremely fine twinning lamellae appear in the most strained parts of the crystals, and finally the whole crystal is cross-hatched microcline (fig. 18), while other specimens display only well developed quadrille structure.

This type of development of the cross-grating is strikingly different from that observed in Archaean pegmatites and granites in which untwinned microcline becomes cross-grated starting from edges or boundaries and the twinning lamellae are at once as large as they ever will grow (Eskola, 1951, p. 40). The microclinization of orthoclase in the rapakivi is similar. The development of microcline from strain shadows seems to be specific for the granulite facies. It appears to be due to deformation of the rock, but it is strange that unchanged clear orthoclase often occurs in the foliated granulites whose parallel orientation of the quartz plates and other manifestations of schistosity are believed to be a result of shearing and overthrusting. We can hardly avoid the conclusion that

the crystallization of orthoclase has occurred after the overthrust movements, or that the main deformation was pre-crystalline.

One of the most specific characteristics of granulites is the occurrence of *hair-perthite*. The plagioclase threads, which in the perthite of common granites are comparatively thick and often have curved and tapering flame-like forms (*flame-perthite*) are here like extremely thin, short hairs (figs. 19, 20). In transmitted light under the microscope they give a curious light effect resembling opalescence. As a rule, the hair-perthite grains have a clear and hairless border zone. This hair-perthite occurs in the same way both in the foliated fine-grained granulites and in the coarse-grained granite-like and migmatic rocks.

Sillimanite. On the calculation of the granulite norms from the actual analyses, all the granulites with normative sillimanite proved to contain modal sillimanite. The sillimanite occurs as porphyroblasts of stout prism shape showing rhombic cross-sections and cleavage cracks on (010) (fig. 21). In many cases such cross sections show anomalous, and so far unexplained, inclined extinction. Fibrolitic sillimanite is found enclosed in cordierite and in the shear zones of granulite.

Biotite. This is quantitatively an important constituent in the coarse-grained and granitic granulites and in the field-granulites. All cordierite granulites seem to have biotite, whereas it is lacking in many granulites containing sillimanite porphyroblasts or platy quartz.

Cordierite. As a chief constituent cordierite is found locally in all parts of the granulite area. In the pegmatitic metatect of migmatic varieties it occurs in places as beautifully translucent bluish crystals showing polysynthetic lamellar twinning. A fine occurrence is exposed on the roadsides between the church of Inari and Leutolahti (fig. 33). In general the cordierite-granulites are coarse-grained. The mineral was never observed in biotite-free varieties nor in schistose granulites containing platy quartz.

The analysis of cordierite from cordierite granulite at the mouth of the Sotajoki (analysis 29) shows 69 mol per cent Mg compound. The refringence in other cordierites is not noticeably higher, as is the case in the very iron-rich cordierites

described by Shibata (1936, quoted by Folinsbee, 1941*a*) from some Japanese pegmatites. Therefore it is not probable that cordierites unusually rich in iron occur in the granulites. All show the normal characteristics of cordierite, such as pinitization along cracks, yellow pleochroic halos around zircon inclusions, and sillimanite fibers as inclusions.

Garnet.—This is represented by analyses 30-33 (table 4). As shown, the [Fe] : [Mg] ratio increases only a little with increasing acidity of the rocks. Even in the garnets from the most acid granulites this ratio is lower than that in the garnets from rocks of the amphibolite facies, including basic rocks. This is clearly apparent from table 5 which shows the indices of refraction of garnets from different rocks of the granulite and amphibolite facies determined by the prism method. Thus the granulite garnets show a wider diadochy of Fe^{2+} and Mg than do the amphibolite garnets, but in the diadochy of Ca and (Fe, Mg) there is no difference and the percentages of CaO in both are less than in the eclogite garnets.

[Fe] : [Mg] ratio in the mafic minerals.—This varies characteristically as may be seen by comparing the analyses in tables 3 and 4 and figure 34. It appears to decrease in the series garnet-hypersthene-hornblende-diopside-cordierite. For one and the same mineral species and for the bulk of the rock the iron : magnesium ratio varies without apparent relation to the acidity of the rocks in contradistinction to normal series of igneous rocks. Thus four rocks, 2-5, all of noritic composition, show rather different ratios.

Folinsbee (1941*b*) says garnets associated with cordierite contain from 15 to 25 per cent pyrope. The garnet of the

---

Fig. 23. Graphite-granulite. Scales of graphite and grains of pyrite, black; small crystals of sillimanite in high relief. Ivalojoki between Abbisjoki and Kuttura. One Nicol, 25X.

Fig. 24. Same as Fig. 22 with crossed Nicols. In the center a grain of cordierite showing polysynthetic twinning.

Fig. 25. Graphite-granulite. Scales of graphite and grains of pyrite, black. Laanioja near Laanila. One Nicol, 25X.

Fig. 26. Hypersthene-hornblende-granulite from Koddigvärri. Analysis 2. Crossed Nicols, 20X.

Fig. 27. Hypersthene-granulite with alternating hypersthene and plagioclase-quartz bands. Valdufälis. One Nicol, 15X.

Fig. 28. Same as Fig. 27 with crossed Nicols. A long quartz plate in the middle.

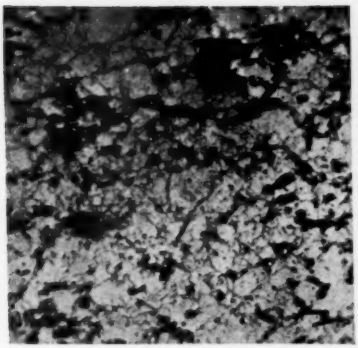

Fig. 23

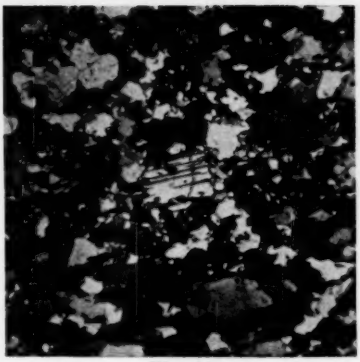

Fig. 24

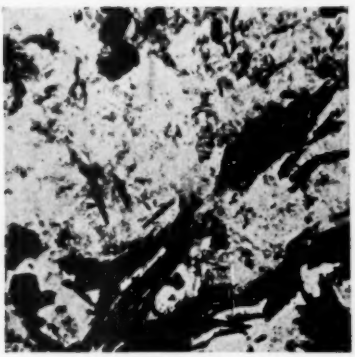

Fig. 25

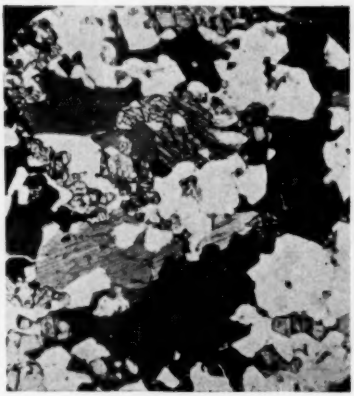

Fig. 26

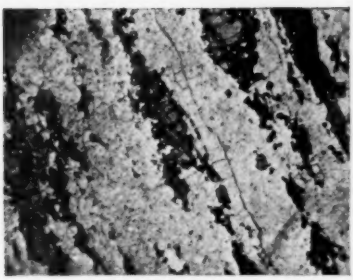

Fig. 27

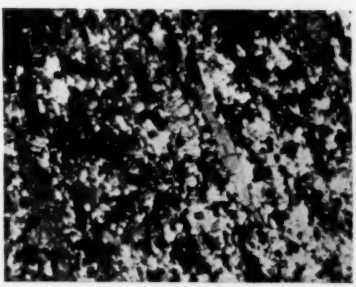

Fig. 28

TABLE 3

Pyroxene, Amphibole, Cordierite

	21.	22.	23.	24.	25.	26.	27.	28.	29.
SiO_2	55.12	52.87	46.91	49.28	48.94	51.96	50.40	42.24	54.63
TiO_2	0.32	0.49	0.51	0.46	1.40	0.80	0.74	2.76	0.00
Al_2O_3	1.25	0.68	8.26	4.51	0.45	2.18	1.79	10.47	29.32
Fe_2O_3	1.26	2.00	3.02	2.61	0.24	1.43	2.21	4.04	1.13
FeO	11.96	20.89	19.88	23.13	30.97	8.85	12.99	16.06	5.15
MnO	0.20	0.29	0.20	0.24	0.76	0.21	0.48	0.28	0.02
MgO	29.10	22.13	20.02	19.65	15.36	14.49	11.02	9.22	7.82
CaO	0.40	0.89	0.34	0.00	1.82	20.25	20.61	11.23	0.00
Na_2O	—	—	0.10	—	—	—	—	1.44	—
K_2O	—	—	0.06	—	—	—	—	0.89	—
Cr_2O_3	0.16	0.04	—	Trace	0.00	0.11	0.01	0.05	—
H_2O+	—	—	0.30	—	—	—	—	} 0.72	} 0.82
H_2O-	—	—	0.03	—	—	—	—		
	99.77	100.28	99.63	99.88	99.94	100.28	100.25	99.40	98.89
Sp. gr.	3.323-3.340	3.49	3.42-3.51	3.525-3.540	3.571-3.662	3.484-3.510	3.414-3.437	3.260-3.272	n.d.
α	1.677	1.710	1.705	1.704	1.718	1.693?	1.699	1.677	1.540
β	1.688	1.720	n.d.	1.715	1.727	n.d.	1.708	1.686	1.545
γ	1.691	1.724	1.716	1.721	1.734	n.d.	1.726	1.693	1.552
2V	—88°	—60°	n.d.	—60°	—56°	+60°	+60°	—60°	—77°

Analyses by E. Nordensvan (E.N.) and A. Huhma (A.H.)

21. E.N. Hypersthene from 4 (table 1) Pahaoja.
22. E.N. Hypersthene from 5 (table 1) Härkäselkä.
23. A.H. Hypersthene from 9 (table 1) Kevuavdshi.
24. E.N. Hypersthene from 10 (table 1) Sotajoki.
25. E.N. Hypersthene from 2 (table 1) Koddigvärri.
26. E.N. Diopside from 5 (table 1) Härkäselkä.
27. E.N. Diopside from 2 (table 1) Koddigvärri.
28. E.N. Hornblende from 2 (table 1) Koddigvärri.
29. E.N. Cordierite from 12 (table 2) Sotajoki mouth.

cordierite-granulite (analysis 33), however, contains 39 per cent pyrope as a consequence of the wider diadochy of Mg and Fe in the granulite facies.

Hornblende.—Not infrequently hornblende occurs in all parts of the area in association with typomorphic minerals of the granulite facies. It is of the greenish brown strongly pleochroic type common also in other granulite and charnockite districts of the world. Analysis 28 shows its composi-

TABLE 4

Garnets

	30 from 9, Kevuavdshi (A.H.)	31 from 15, Kultala (E.N.)	32 from 10, Sotajoki (E.N.)	33 from 12, Sotajoensuu (E.N.)
SiO_2	36.35	39.17	39.50	39.05
TiO_2	1.72	0.26	0.29	0.42
Al_2O_3	22.97	21.70	21.00	20.42
Fe_2O_3	—	4.98	4.30	7.31
FeO	24.72	22.45	22.15	23.63
MnO	0.64	0.32	0.80	0.38
MgO	11.80	10.43	9.74	8.97
CaO	1.87	1.07	2.96	0.72
H_2O+				
H_2O-				
	100.07	100.38	100.74	100.90
Sp. gr.	3.766-3.836	4.046-3.973	4.016-3.823	4.071-3.971
n_D	1.76	1.7868	1.7793	1.7848

TABLE 5

Refringence of Garnets

Rocks of Granulite Facies		Rocks of Amphibolite Facies	
	n_D		n_D
Acid granulite Inari	1.7930	Granite, Turku	1.804
" " Vävypää	1.7860	Aplite, Helsinki	1.821
" " Lutto	1.7835	Amphibolite, Kalvola	1.810
" " Luottama	1.7864	Cord. granite, Lemu	1.813
" " Kuivakuru	1.7829	Cord.-anthoph. rock,	
" " Louhioja	1.7772	Träskböle	1.806
" " Ivalo	1.783	Granite, Helsinki	1.8176
" " Palsi	1.785	Granite, Turku,	
Laanilite (analysis 11)	1.7915	Pispanpelto	1.8129
		Chlorite schist, Outokumpu	1.803

tion which, compared with the granulite pyroxenes, is characterized by higher TiO_2 and Fe_2O_3 and a notable alkali content. In the ultrabasic granulites the hornblende is much lighter in color and almost non-pleochroic, as in the rock from Abbisjoki (analysis 1). The occurrence of common green hornblende, again, is a reliable criterion that the rock in question belongs not to the granulite but to the amphibolite facies.

Olivine.—This is found only in the ultrabasic granulites. It is, according to analysis 1, $Fo_{89}Fa_{11}$, or normal for peridotitic rocks.

Hypersthene.—The typical femic mineral in granulites is most common in rocks of noritic or dioritic composition (analyses 2-6) but occurs also in acid quartz-rich (analysis 7) and aluminous garnet-bearing (analyses 8-10) rocks. The analyses (21-25) indicate various [Mg] : [Fe] ratios but otherwise have rather uniform composition, normal for orthorhombic pyroxenes excepting the remarkably high percentages of alumina in the garnet-bearing, i.e., highly aluminous, granulites. Aluminous hypersthenes, containing up to 9.39 per cent Al_2O_3 have been recorded by Groves (1935) from charnockites in Uganda (cf. Hess, 1941). In the Lappish hypersthenes the atomic number of Si is almost identical to that of Fe + Mg. Half of the aluminum must therefore replace silicon within the SiO_4-tetrahedra and the other half (Mg, Fe^{2+}). We see here an extended diadochy of cations just as in the granulite garnets (cf. Ramberg and De Vore, 1951).

According to Quensel (1951) the hypersthenes in the basic charnockites of the Varberg district in Sweden are more strongly pleochroic than those in the intermediate types. In the granulites of Lapland many—perhaps most—acid types, on the contrary, have most intensely colored hypersthenes, but it is hard to see any regularity in this respect. Hypersthene 21 from a basic granulite is pale colored, almost non-pleochroic, as is also 22, whereas 23 and 25 from basic and 24 from acid granulite are strongly pleochroic and Quensel's characteristics, α purple violet, β pale reddish yellow, γ pale green, are applicable. Nor is the pleochroism dependent upon the tenor of ferric iron, for 24, almost devoid of Fe_2O_3, is strongly pleochroic. The problem of the colors of hypersthenes remains

unsolved. An apparent oblique extinction was observed in some hypersthenes (Quensel, 1951).

Diopside.—The composition of the two clinopyroxenes analyzed (26, 27) appears best in figure 34 and shows a small excess of (Mg, Fe)SiO_3 over the diopside ratio, possibly due to admixture of hypersthene. In all thin sections of diopside-bearing granulite rocks this mineral is faintly greenish, non-pleochroic (cf. Hess, 1949).

Ilmenite-magnetite.—In most granulites analyzed the TiO_2 content is greater than in the mafic minerals analyzed. From this it is concluded that the iron ore present contains part of the TiO_2. Similarly the high Fe_2O_3 percentage in many rocks indicates the presence of magnetite or hematite, though in other rocks the ore may be pure ilmenite. This mineral has not yet been analyzed as it deserves, i.e., to prove or disprove the plausible guess that the ilmenite may contain geikielite. Hematite has been found in many acid granulites.

Sulfides.—Pyrite, pyrrhotite, and locally chalcopyrite occur in minute amounts in some of the rocks analyzed. Larger amounts of sulfides are found in granulite at the margin of the area near the mouth of Taimenjoki. They are also found in the graphite-bearing rocks.

Rutile.—This regular titanium mineral in the acid granulites occurs as irregularly shaped grains, sometimes elongated in the plane of schistosity. It is dark reddish brown, usually appearing almost opaque unless inspected with the aid of the condsenser in strong light. It remains to be investigated whether it contains tantalum and niobium (strüverite) or just Fe_2O_3 (nigrin). Rutile also occurs as minute needles enclosed in quartz (fig. 15).

Apatite.—A common minor constituent in garnet-free intermediate and basic granulites. Its almost total absence in the acid granulites is striking. This may be partially understood from the fact that acid granulites contain another phosphate mineral, viz., monazite.

Monazite.—This occurs in minute egg-like grains of greenish yellow tint. During the gold-washing trials by dredge in Ivalojoki some hundred grams of monazite-bearing tailings

consisting of monazite, rutile, zircon, etc. (see below under 1) were collected. They were analyzed by Dr. L. Lokka with the following result (2). If, in all of these, 29.24 per cent of lanthanides are present in the monazite, their percentages are as given under (3).

	(1)		(2)	(3)
Monazite	55.0	ThO_2	1.98	6.7
Rutile	41.5	Cerium earths	26.11	89.3
Zircon	2.5	Yttrium earths	1.15	4.0
Garnet	1.0			
			29.24	100.00

Zircon.—This is a common though very sparse minor constituent. Exceptionally high in zircon was a MiQuaHoZiTiPlaGa found near the mouth of Abbisjoki. *Spinel* as small rounded grains occurs in many acid granulites.

Many minerals not belonging to the granulite facies are found in them in small amounts as products of alteration, such as *muscovite*, *epidote*, *chlorite*. Meionite-rich *scapolite* replacing plagioclase was found on the middle course of the Ivalojoki, in the Marastotunturit, at Joukaisavdshi and at Utsapadda Creek in the northernmost fields. On the eastern slopes of Marastotunturit, scapolite also occurs as vein-like segregations, according to information from Mr. O. Helovuori. *Graphite* occurs in many granulites as an important constituent. Barrel-shaped crystals of *corundum* were found among the tailings in the placers at Lemmenjoki.

THE GRANULITES AS ROCKS

The granulites have no relict textures or structures preserved of either igneous or sedimentary rocks. In the early stages of this study I tried, by variation diagrams and other means, to find relations between the different rocks of the granulite complex that are known to be characteristic of differentiation series in igneous rock complexes. The results were disappointing. The question now is: have the granulites any primary features preserved in their chemical composition, either of igneous or sedimentary rocks, that might help toward the understanding of their genesis? Or is, perhaps, their variation due solely to metamorphic differentiation under the control of tectonic processes?

We have first to look at the individual rock analyses and next to the mineral components studied microscopically. We take first the acid granulites (table 2) which make up the major part of the complex and in which the intermediate and basic granulites form sharply bounded bands and lenses.

The varieties extremely rich in garnet and cordierite with low amounts of quartz and feldspars called *laanilite* (Hackman, 1905, analysis 11), differ in their bulk composition from any normal igneous or sedimentary rocks and are presumably local products of metamorphic differentiation (cf. Tuominen and T. Mikkola, 1950).

Cordierite granulites (12), like the laanilite, vary greatly in bulk composition but form larger masses and, as a whole, show the chemical characters of argillaceous sediments. This is even more the case with the garnet-rich and commonly sillimanite-bearing field granulites, probably the most abundant of the granulite types, represented by analysis 13.

Analysis 14 shows the characteristic alkali percentages of *ideal granites* but shows at the same time a considerable excess of Al_2O_3. Therefore, if their alkali content is primary, the rocks might be guessed to have assimilated shales or to have been derived from liparitic tuffs subjected to some degree of weathering. On the other hand, it must be noted that such light granulites frequently grade over into aplitic granulites devoid of garnet, and analysis 17 conforms in all respects with ideal granites.

The red gneiss (16) occurs as lenticular bands in the granulites and presumably is formed by later intrusion into them. They are mineralogically aplitic and are supposed to stand in genetic connection with the dykes of pegmatite.

The mode of occurrence of the chemically varying *quartz-rich granulites* (19 and 20) chiefly suggests enrichment in silica during precrystalline shearing, but for some outcrops displaying thicker layers, arkosic sandstone would seem the most plausible primary material. It is noteworthy, however, that no pure quartzites are on record though they are very common in Lapland outside the granulite area.

The compositions of the acid granulites analyzed do not afford any conclusive evidence of their origin. There are, however, significant mineral assemblages, especially the *graph-*

ite-granulites. A specimen from the bank of Ivalojoki above the mouth of Abbisjoki is a granoblastic PlaQuaSillPyrrhGraBiCord (figs. 23, 24). The sillimanite is abundant but the crystals are small sized, as are those of cordierite also, developed as twins or as triplets with polysynthetic lamellae and showing yellow pleochroic halos. This rock possesses a typical argillaceous bulk composition with a large excess of alumina and is at the same time, in its carbon and sulfur content, suggestive of having been originally a sapropelic sediment. The black schists, common in all Precambrian formations, are similar in their bulk composition and their carbon is mostly fine-grained graphite. It has lately been proved in many cases by determination of the isotope ratio C^{12}/C^{13} that their carbon is of organic origin (Rankama, 1948). The isotope ratio in the graphite from the Lappish granulites will, of course, be determined as soon as possible. We can predict a positive result with considerable assurance.

Graphite-bearing granulite is quite common. At Laanioja, near Laanila, graphite occurs in a PlaQuaGaGraPyrrh as still larger scales (fig. 25). The advanced recrystallization of the carbon is eloquent evidence of the high grade of metamorphism.

Exceptionally high in alumina are many *sillimanite-rich bands* in granulites, e.g., at Joukaisavdshi (fig. 22). Very sillimanite-rich granulites were also found at Kevuavdshi, QuaSillGaPla, and on Koarvikods. Such sillimanite- and quartz-rich rocks may approach in composition the khondalite of India and Ceylon (Adams, 1929), and some of the sillimanite-rich granulites may be supposed to have consisted originally of kaolin, whereas in other cases metamorphic differentiation is more probably responsible for their present composition.

Sometimes much Al is bound with Ca in plagioclase, as at Saddehvärri in a medium-grained hornfels-like QuaPlaGa, which was studied in thin sections from two specimens. In one of these the rock is QuaPlaGa: BiRuMa, the plagioclase showing in a section $\perp$ PM an extinction angle of 40° (bytownite). The other thin section exhibits two different bands, one half of the section containing plagioclase whose refringence equals that of quartz (about An_{30}) while the other half is bytownite with much quartz.

Near the occurrence of graphite-granulite at Ivalojoki, just described, there are several outcrops of diopside-rich gneiss,

PlaQuaDi, with anorthite-rich plagioclase. These rocks no doubt possess the composition characteristic of high grade metamorphic derivates from lime-rich sediments. At Ailigas on the Tenojoki River narrow bands of DiPlaQuaHy, and at Jorbamauna a one-meter thick band of HyDiPlaQua : Ma, were found in granulite. In the latter, narrow bands of hypersthene and diopside alternate.

It is probably significant that granulites extremely rich in alkalies, either soda or potash, have not been found. The granulite richest in potash is from the Kistuskäidi at Tenojoki, OrQuaGa : SillBiMa.

Ultrabasic granulites, represented by analysis 1 (table 1) of the rock from the mouth of Abbisjoki (fig. 13), are mostly olivine-bearing and peridotitic in composition. Many occurrences were found in the southern boundary zone, such as at Kussuolinkivaara and one kilometer north of Vuotso. Various other ultrabasics, such as sagvandite (enstatite-rock), spinel-actinolite rock, etc., are known from this zone (E. Mikkola and Sahama, 1936). An inclusion in granulite at Joukaisavdshi is HoDiOl : Pla, another west of Lake Paltonjärvet, OlHyHo with light green Ho. Other occurrences are pyroxenites, e.g., near Karigasnjarga on the Teno River. The rock here is mainly composed of coarse-grained clinopyroxene. Garnet-pyroxenite, HyHoGa : SillQuaPlaMa, with brown hornblende, is exposed on the northwesterly summit of Pirkkoaivi near Ailigas. It forms a dyke-like band, 3 meters thick, in granulite and grades over into gabbro with big crystals of garnet.

The ultrabasics studied occur in the manner of breccias (fig. 10). At Karigasnjarga the pyroxenite forms angular blocks in pegmatitic granulite, composed of large crystals of quartz in a granular quartz-feldspar mass. It grades over into normal granulite, QuaPlaGaBi, with platy quartz, and augen of plagioclase. The narrow band of granulite, again, is bounded by noritic HyHoPlaDi in which the Pla = An_{60} and contains occasional augen-like phenocrysts of feldspar. The brecciation of the ultrabasics is a regular phenomenon, though in places less basic varieties also are brecciated. The cementing granulite behaves like an eruptive rock.

Among the *basic granulites* the PlaHy and PlaHyQua rocks are most common and, next to the acid granulites, quantitative-

ly most important (analyses 4, 5, 6). They occur as bands from a few centimeters to some hundred meters in thickness, and with hair-sharp contacts (fig. 4). Though the contacts are frequently exposed, the whole length of the bands rarely is visible. In the shore-cliffs of the Tenojoki at Ailigas several lenticular bands are seen to taper out at both ends. One of them is 3 m. long and 10 cm. in maximum thickness, another 1.6 m. long and 14 cm. thick. Apparently their maximum elongation is in the direction of lineation. Some of them have pegmatitic segregations in their center and they often contain garnets. In the southern boundary zone of the granulite area near Vuotso several bands have been exposed during prospecting work, and they too have proved to taper out at both ends (according to O. Helovuori). As the compositions of the bands agree with those of basalts, andesites, and dacites, possibly contaminated with the invaded aluminous granulites, it might be concluded that the bands were originally flows or sills of volcanic material or of dolerite which have been metamorphosed in the granulite facies and thinned out and shattered by the shear. This interpretation is, in principle, analogous to that applied to granulitic and charnockitic basic rocks by several recent investigators (cf. Quensel, 1951).

Other basic rocks contain more femic lime resulting in diopsidic pyroxene besides hypersthene (2, 3). In some rocks from the banks of the Ivalojoki near Kuttura the amount of diopside indicates lime-proportion higher than that encountered in normal basalts or gabbros and the rocks may correspond with marly sediments. The majority of the basic granulites, however, could very well be metamorphites derived from volcanic or hypabyssal rocks, as could the acid hypersthene-bearing granulite such as 7 of enderbitic composition (Tilley, 1936). The almandine-bearing HyPla rocks like 8, 9, 10, belong chemically to a common type of lavas and instrusives hybridized by contamination with clayey sediments.

The inner boundary zone of the granulite arch east of Ivalo is characterized by hypersthene-bearing rocks of a coarser grain, earlier called *hypersthene diorites*. East of the present frontier of Finland such a rock underlies a wide area, mapped by E. Mikkola who called it charnockite. A more correct name might be enderbite. From my own limited study of this area, I would judge it to be a coherent abyssal instrusion. The

rock from near Tsharmijärvi is PlaQuaHyBi: HoMa (fig. 29), another from the mouth of Nangujoki is PlaQuaGaBi, with no Or, and one from Gaisvaara is PlaQuaHy. Farther east, at Jonlaki, were found potash-rich rocks, OrQuaHyPla. As appears from these examples, the minerals follow the rules of the granulite facies.

Migmatic and granitic rocks occur in many parts of the granulite area, but more especially near the inner boundary of the arch. A rock from Kolhuselkä is, in the size of the mineral grains and their corroded boundaries, like the best coarse-grained granites from southern Finland, a QuaOrPlaGaBi. But the minerals are different. The orthoclase is somewhat disturbed in its extinction, the first sign of alteration into microcline, and its perthite is a most typical meager hair-perthite; it may be without perthite and adularia-like.

The migmatic granulites may be described with the aid of photographs. For the first example may be taken an outcrop on the roadside east of Ivalo between Nangujoki and Tsharmijärvi, 314 kilometers from Rovaniemi. The neighboring rock is the widely distributed hypersthene-quartz-diorite, or enderbite. In figure 31, we see this rock in a comparatively well-preserved condition, a PlaQuaHy with indistinct lighter and more coarse-grained bands which consist of the same materials as the main rock. Near by, the rock contains phenocrysts (nowadays often called porphyroblasts) of the same andesinic plagioclase as the charnockite and grades over into pegmatitic segregations in which phenocryst-like plagioclases are still seen (fig. 32). Resorbed inclusions of enderbite have been preserved. No potash feldspar is present nor are other materials proving considerable difference in bulk composition from the enderbite, except biotite and quartz, which may be more abundant. Biotite occurs also as large scales. Hypersthene occurs even in the coarsest pegmatite (fig. 30). Under the microscope it is seen to have altered partly into biotite. The mobilization of the pegmatitic material also appears in a vein- or dyke-like occurrence visible in the photograph.

Banded migmatic cordierite-granulite was studied along the roadside between Inari and Leutolahti (fig. 33). It is QuaOrGaPlaSillCordMaSpin. Its undulous orthoclase is shown in figure 17. The cordierite in the coarse-grained metatect is bluish and translucent.

Different stages of migmatization of granulites were studied at Joukaisavdshi in rock surfaces clean-washed by glacifluvial waters (figs. 35-39). The granulite occurs also as the fine-grained biotite-free type with platy quartz. More common is a field granulite type with garnet augen and biotite streaks (fig. 35). In figure 36 is seen incipient migmatization and folding with preservation of the granulitic banding and minerals. Figure 37 shows banded and sheared granulite in which the metatect veins in one layer have turned transversely. At more advanced stages the rock becomes either a "wild migmatite" (fig. 38) or segregates vugs of "porphyry-pegmatite" (fig. 39), like those shown in figure 32. The dark bands of noritic granulite are still traceable as fragments with phenocrysts. Also the acid granulite is in part thus preserved, though more like "ghostly fragments." This pegmatite contains well preserved hypersthene in apparent equilibrium, and the biotite forms large scales.

THE GRANULITE FACIES

The granulite facies (Eskola, 1939; Turner and Verhoogen, 1951) was defined to comprise the minerals; sillimanite, almandite-pyrope, hypersthene, diopside-hedenbergite, plagioclase, calcite, quartz, olivine, ilmenite, rutile. Instead of or besides sillimanite, kyanite may occur but it has never been observed with certainty in the Lappish granulites, although it is abundant in the schists of the contact zone at Korvatunturi.

I have said that cordierite is alien to the granulites proper. The present analysis of cordierite (29) shows a [Mg]: [Fe] ratio never observed in the granulite garnets. Sillimanite + hypersthene should therefore be expected instead of pyrope-rich garnet, and this assemblage has in fact been observed, though rarely, e.g., in a HyHoGaSillQua:$_{\text{PlaMa}}$ from Pirkkoaivi near Ailigas. But cordierite also is very common and

Fig. 29. "Hypersthene-quartz-diorite" or "enderbite," PlaQuaHy:$_{\text{BiHoMa}}$, from near Tsharmijärvi. Crossed Nicols, 20X.

Fig. 30. Hypersthene-bearing pegmatite, QuaPlaHyBiMa, roadside 314 kilometers from Rovaniemi. Crossed Nicols, 14X.

Fig. 31. Incipient migmatization of "charnockite." Loc. as Fig. 29.

Fig. 32. Hypersthene-bearing "porphyry-pegmatite" in migmatized "charnockite." Loc. as above.

Fig. 33. Incipient migmatization of cordierite-granulite showing primary banding. Roadside between Inari and Leutolahti.

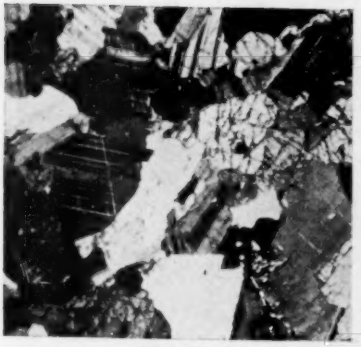

Fig. 29

Fig. 30

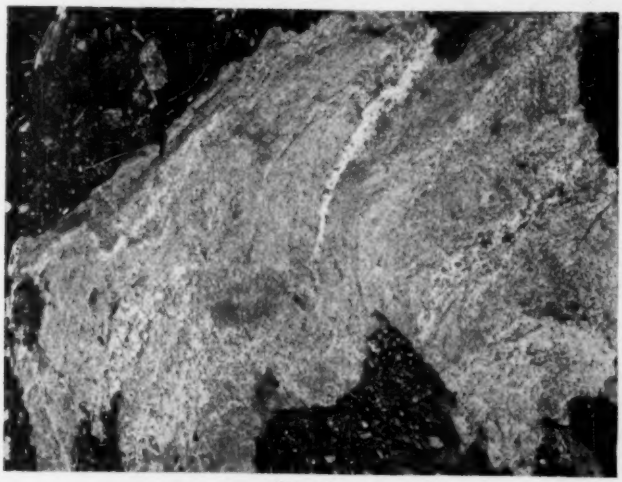

Fig. 31

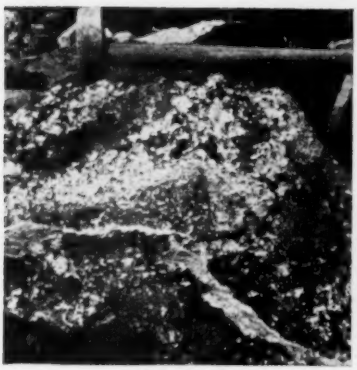

Fig. 32

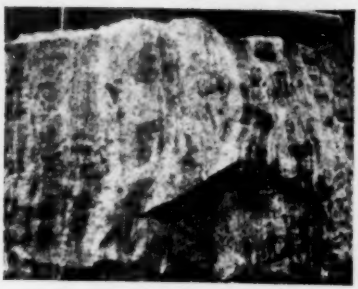

Fig. 33

often alternates with layers of cordierite-free granulites. Observation of the mineral parageneses would point to the existence of a subfacies in which cordierite is typomorphic. As far as is known, it is always accompanied by biotite. Moreover, the cordierite appears to be antagonistic to platy quartz. Many features would seem to indicate that cordierite is in itself stable under the TP conditions of the granulite facies but that its formation in sheared rocks is checked by its antistress nature. On the other hand, as this cannot be said of biotite, with which the cordierite is commonly associated, the alternative hypothesis that cordierite and biotite belong to a subfacies stable at next lower temperatures is also worth considering.

The biotite in most cases occurs around garnet and in its pressure-shadows, being obviously a product of alteration of this mineral. But it occurs also as a regular constituent in the quartz-feldspar mass and in that case cannot be regarded as a posterior product, although it no doubt is always a late mineral in the rocks.

The brownish green hornblende, so common in the granulites and charnockites all over the world and encountered in all parts of the Lappish granulite area, is also in apparent equilibrium with hypersthene, etc. Turner (1951, p. 476) alludes to the possibility that the occurrence of this hornblende in the granulites is due to the presence of (OH). This idea would also apply to the biotite. In general, the dryness of the granulite minerals could then be interpreted as depending upon

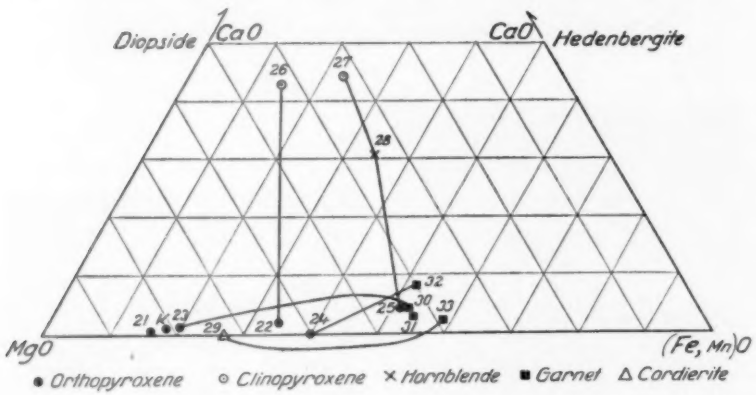

Fig. 34. Molecular ratios of mafic minerals.

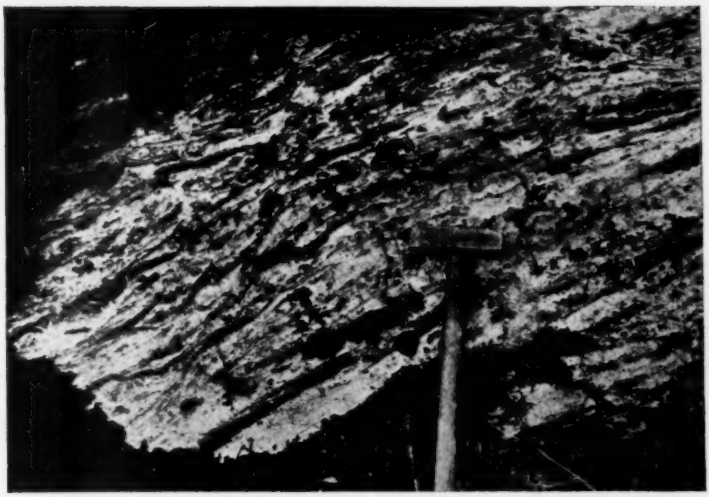

Fig. 35. Granulite with large garnets and biotite bent around the augen of garnet and stretched along the strike. Joukaisavdshi.

Fig. 36. Incipient migmatization and folding of granulite. Joukaisavdshi.

the accidental dryness of the material and not at all upon the physical conditions. Regarding this matter, however, I agree with Ramberg (1949) who says it is the high temperature that prevents the formation of hydrated minerals in the granulites. Of course the free water can escape during the recrystallization and can be squeezed out during shearing; this is probably the reason why the highly foliated granulites have not developed biotite or hornblende as secondary minerals on cooling, like the less sheared granulites.

It is rather surprising that rocks of the amphibolite facies often alternate with granulites. Examples of this are quite common in the valley of Ivalojoki, near the southern contact of the area, and in the northernmost fields. Such rocks in many cases show no relict features from the granulite facies. Their granoblastic texture is very similar to that of the granulites, but the minerals are strikingly different: common green hornblende, sphene instead of rutile or ilmenite, and flame-perthite in acid rocks instead of hair-perthite. This fact is hard to understand, but it must have important significance. The vivid variation of properties across the strike is remarkable in other respects as well, e.g., of sheared and non-sheared bands, and of cordierite- and biotite-bearing bands within normal granulites.

Quensel (1951) objects to classifying the granulites in the same facies with the charnockites, but he cannot refer to any point of divergence other than "the typical xenomorphic-granular texture combined with a banded structure, indicating the cooperation of directed stress in contrast to the only occasionally granular flow structure in the charnockitic rocks." Textural differences, however, are not a legitimate basis for separation of mineral facies. The critical minerals are the same and the differences may be accounted for by differences in material or in tectonic history. The hypersthene-bearing granulites are mineralogically identical with the charnockites. The garnet content of the acid granulites is due to their richness in alumina, often much greater than that which in granitic rocks may enter into the micas. There may be, also, minor differences

Fig. 37. Transversal banding in migmatic granulite. Joukaisavdshi.

Fig. 38. Venitic migmatite in granulite. Joukaisavdshi.

Fig. 39. "Porphyry-pegmatite" in migmatic granulite. Joukaisavdshi.

in the mineral facies. Thus the pyroxene-gneiss complex in Western Uusimaa (Parras, 1941) agrees in the typomorphic minerals with the granulite facies in the wider sense except for the presence of scapolite as a stable constituent, while scapolite in the Lappish granulites occurs only as a posterior product.

The cordierite-garnet-gneisses, or kinzigites, very common in southern Finland, are stable members of the charnockite suite and may be identical with our cordierite-granulites except

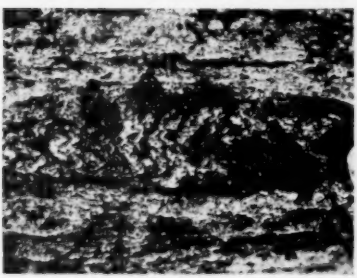

Fig. 37

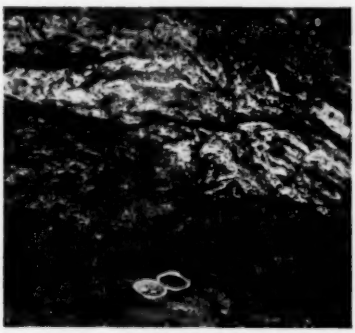

Fig. 38

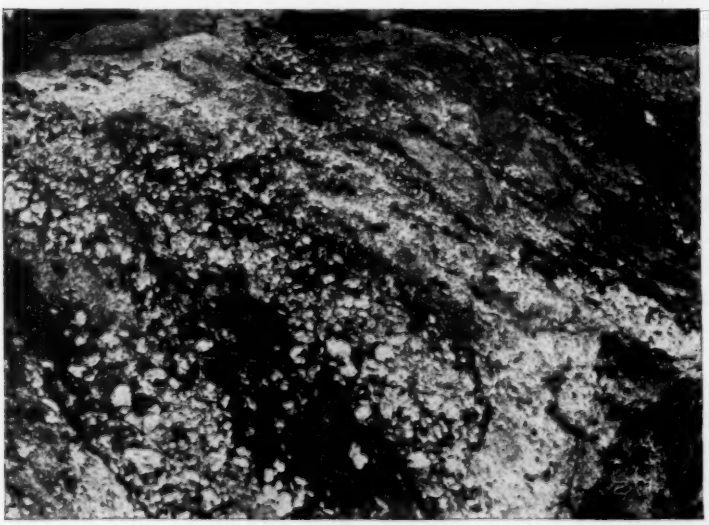

Fig. 39

for the composition of the garnet, but nearly similar almandite-cordierite-gneisses are also stable in the amphibolite facies. The kinzigites thus have a very wide range of stability, a fact that may explain their wide occurrence in the roots of ancient mountains.

GENESIS OF THE GRANULITES

Earlier I (Eskola, 1932) regarded the granulite complex as a "hyperkinematic intrusion." After a closer study of the rocks I can no longer cling to this idea but must consider the interpretation given by J. Lehmann as early as 1884 in his classic treatise. Similar conclusions were later reached in studies of the granulites by Scheumann (1925, 1936) and Adams (1929), for the charnockites by Stillwell, Groves (1935), Rama Rao, Quensel (1951), and many others, whose theories agree in explaining the granulites and the charnockites as metamorphic rocks derived from various primary materials.

The main part of the acid garnet-bearing granulites have chemical characteristics agreeing closely with those of different Al-rich residual and hydrolysatic sediments. Very significant is the occurrence of graphite- and sulfide-bearing aluminous rocks, which, in all probability, are ancient bituminous sediments containing organogenous carbon. The ultrabasic granulites are chemically like peridotites, also, as regards the content of nickel and chromium. The greater part of the basic granulites, again, is similar to igneous rock, varying from basalts or dolerites to andesites and dacites. Their sharp boundaries against the acid granulites seem to warrant the belief that diffusion across the boundaries has not been sufficient to obliterate the original differences, although considerable migration of elements has no doubt taken place. The granulite complex comprises rocks of most primary types, though pure quartzites and limestones are absent.

From the principle of mineral facies it is presupposed that the mineral composition of a rock depends only upon the attendant physical conditions and concentration of the components. It is therefore to be expected that the same mineral assemblages may form by primary crystallization of magmas as well as by metamorphic recrystallization in the solid state. Convergences of magmatic and metamorphic mineral development are common in many pairs of rocks, as e.g., in gabbro

and pyroxene-hornfels, hornblende-gabbro and amphibolite. From theoretical considerations it is quite possible that the final crystallization of a magma may take place at the same temperature as metamorphic recrystallization (Eskola, 1921, 1939). The feldspar-pyroxene assemblage in rocks of the granulite facies is certainly one that can be expected to crystallize from magmas, provided they are rather poor in water, as has been the case with those magmas from which, e.g., many dolerite sills have crystallized.

Field evidence makes a magmatic intrusive mode of origin of the charnockitic or enderbitic rocks in the Lappish granulite belt most probable and, as far as my own scanty—and E. Mikkola's much more extensive—observations go, they show none of the features that eventually compelled me to accept the metamorphic interpretation. In the same way I have the impression from field observation of the charnockitic rocks of Western Uusimaa (Parras, 1941) and the Turku district (Anna Hietanen, 1947) that parts of these rocks are magmatic, although in these areas sedimentogeneous and volcanogeneous rocks are much more obvious, and more variegated, than in the Lappish granulite area. A detailed discussion of these phenomena, however, must be postponed.

From this viewpoint the migmatic pegmatite at 314 km. from Rovaniemi would be interpreted as a last crystallized portion of the enderbite magma still under the conditions of the granulite facies, while the metatect of similar migmatite at Joukaisavdshi would be interpreted as having crystallized from palingenic magma formed by partial anatexis from rocks already metamorphosed into granulites. Contrary to Ramberg, I do not believe that structures like those depicted in figures 35-39 have originated by metamorphism in the solid state.

ACKNOWLEDGMENTS

Mr. Einar A. O. Nordenswan has carried out 24 and Mr. Aarto Huhma 3 chemical analyses for this study. The former also, for two summers, made field observations and collected specimens from the Ivalojoki Valley. Professor Th. G. Sahama allowed me to use his thin sections.

Professor Aarne Laitakari, Director of the Geological Survey of Finland, permitted me to use the notes, maps, and thin sections of the late state geologist, Dr. Erkki Mikkola.

Mrs. Toini Mikkola carried out the determinations of the indices of refraction and optic axial angles in pyroxenes, hornblende, and cordierite. Mr. O. Helovuori gave me useful information from recent observations in the granulite area. Mr. Erkki Viluksela made the following photographs: Figures 5-9, 12, 14-20, 22, 23-25, 27-30. Mrs. Lyyli Orasmaa drew the map and the diagram, figures 1 and 34.

To all the persons mentioned, and to many others who have aided my work, I wish to express my gratitude.

References

Adams, F. D., 1929. The geology of Ceylon: Canadian Jour. Research, vol. I, pp. 425-511.

Eskola, Pentti, 1921. The mineral facies of rocks: Norsk geol. tidsskr., vol. 6, pp. 143-194.

————,1932. On the origin of granitic magmas: Min. pet. Mitt., vol. 42, pp. 455-481.

————, 1939. Die metamorphen Gesteine: *In* Barth, Tom. F. W., Correns, Carl W., Eskola, Pentti, Die Entstehung der Gesteine, Julius Springer, Berlin, pp. 263-407.

————, 1951. Around Pitkäranta: Ann. Acad. Sci. Fenn., Ser. A, III, no. 27.

Fircks, Curt, 1906. The occurrence of gold in Finnish Lapland: Comm. géol. Finlande Bull. 17, 35 pp.

Folinsbee, R. E., 1941*a*. Optic properties of cordierite in relation to alkalies in the cordierite-beryl structure: Am. Mineralogist, vol. 26, pp. 485-500.

————, 1941*b*. The chemical composition of garnet associated with cordierite: Am. Mineralogist, vol. 26, 50-53.

Groves, A. W., 1935. The charnockite series of Uganda, British East Africa: Geol. Soc. London Quart. Jour., vol. 91, pp. 150-207.

Hackman, Victor, 1905. Die chemische Beschaffenheit von Eruptivgesteinen Finnlands und der Halbinsel Kola: Comm. géol. Finlande Bull. 15, 143 pp.

Hess, H. H., 1941. Pyroxenes of common mafic magmas: Am. Mineralogist, vol. 26, pp. 515-535, 573-594.

————, 1949. Chemical composition and optical properties of common clinopyroxenes: Am. Mineralogist, vol. 34, pp. 621-666.

Hietanen, Anna, 1947. Archean geology of the Turku district: Geol. Soc. America Bull., vol. 58, pp. 1019-1084.

Kranck, E. H., 1936. Zur Tektonik der Lappländischen Granulite: Comm. géol. Finlande Bull. 115, pp. 373-386.

Lehmann, J., 1884. Untersuchungen über die Entstehung der altkrystallinischen Schiefergesteine mit besonderer Bezugnahme auf das Sächsische Granulitgebirge, Erzgebirge, Fichtelgebirge und Bairisch-Böhmische Mittelgebirge, Bonn, 278 pp.

Mikkola, Erkki, 1928. Über den Nattanengranit im finnischen Lapplande: Fennia 50, no. 12, 22 pp.

————, 1932. On the physiography and late-glacial deposits in Northern Lapland: Comm. géol. Finlande Bull. 96, 88 pp.

———, 1941. Suomen geologinen yleiskartta, The general geological map of Finland, Lehdet—Sheets B7—C7—D7, Muonio-Sodankylä-Tuntsajoki, Kivilajikartan selitys—Explanation of the map of rocks, Suomen Geologinen Toimikunta.

———, and Sahama, Th. G., 1936. The region to the south-west of the "Granulite Series" in Lapland and its ultrabasics: Comm. géol. Finlande Bull. 115, pp. 357-371.

Parras, Kauko, 1941. Das Gebiet der pyroxen führenden Gesteine im westlichen Uusimaa: Geol. Rundschau, Band 32, pp. 484-507.

Quensel, Percy, 1951. The charnockite series of the Varberg district on the south-western coast of Sweden: Arkiv för Min. och Geol., Band 1, no. 10.

Ramberg, H., 1949. The facies classification of rocks: Jour. Geology, vol. 57, pp. 18-54.

———, and De Vore, George, 1951. The distribution of Fe^{++} and Mg^{++} in coexisting olivines and pyroxenes: Jour. Geology, vol. 59, pp. 193-210.

Rankama, Kalervo, 1948. New evidence of the origin of pre-Cambrian carbon: Geol. Soc. America Bull., vol. 59, pp. 387-416.

Sahama, Th. G., 1936. Die Regelung von Quarz und Glimmer in den Gesteinen der finnisch-lappländischen Granulitformation: Comm. géol. Finlande Bull. 113, 119 pp.

Scheumann, K. H., 1925. Die Gesteins- und mineralfazielle Stellung der Metakieselschiefergruppe der südlichen Randzone des sächsischen Granulitgebirges: Akad. Wiss., Abh. Math.-phys. Kl. der Sächs, Band 39.

———, 1936. Über eine Gruppe bisher wenig beachteter Orthogneise des Granulitgebirges und deren Einschlichtung: Min. pet. Mitt., vol. 47, pp. 403-469.

Tilley, C. E., 1936. Enderbite, a new member of the charnockite series: Geol. Mag., vol. 73, pp. 312-316.

Tuominen, Heikki V., and Mikkola, Toivo, 1950. Metamorphic (Mg,Fe) enrichment in the Orijärvi region as related to folding: Comm. géol. Finlande Bull. 150, pp. 67-92.

Turner, F. J., and Verhoogen, Jean, 1951. Igneous and metamorphic petrology: McGraw-Hill Book Co., New York.

Geological Institute of the University
Helsinki, Finland

ORTHOPYROXENES OF THE BUSHVELD TYPE, ION SUBSTITUTIONS AND CHANGES IN UNIT CELL DIMENSIONS*

H. H. HESS

ABSTRACT. The *a*, *b* and *c* dimensions of the unit cell of a number of orthopyroxenes of the Bushveld type were measured. The variation in size with substitution of Fe^{+2} for Mg^{+2} and Al^{+3} for Mg^{+2} and Si^{+4} are given. The optical properties N_γ, 2V and birefringence have been revised and density determinations made on a number of samples. For ordinary orthopyroxenes of the Bushveld type with 2¾ per cent R_2O_3, unit cell dimensions, N_γ, birefringence and density vary as linear functions within the limits of accuracy of the observations and thus appear to obey Vegard's Law. The quantities present of all of the main constituents of these pyroxenes, Mg, Fe, Al and Ca, can be determined from optical property and unit cell measurements without chemical analysis. It is suggested, other things being equal, that the Al content may increase with pressure and should be further investigated as potential means of assessing depth of crystallization.

INTRODUCTION

THE pyroxenes were among the first of the silicate structures to be worked out (Warren and Bragg, 1928; Warren and Modell, 1930). Crystallographically the pyroxenes may be divided into two main groups: orthorhombic, those with enstatite structure; and monoclinic, those with diopside structure. Besides these, Foster (1951) has recently examined a phase he calls protoenstatite which is unstable and difficult to preserve at low temperature. Atlas (1952) suggests an orthorhombic symmetry for this phase differing from enstatite in space group. The natural Ca-poor monoclinic pyroxenes, pigeonites, have not thus far been investigated by X-ray methods. The writer has just begun such a study but the results are not far enough along to draw conclusions other than that the clinoenstatite and pigeonite powder diffraction patterns appear to be the same. The pyroxene group shows a remarkable range in composition and a great diversity of possible ion substitutions. Nevertheless it is uniquely regular in its chemistry, invariably satisfying exactly the general formula $(X, Y)_2 Z_2O_6$ where X equals an ion such as Mg^{+2}, Fe^{+2} or Ni^{+2}, Y equals an R^{+3} ion, and Z equals Si^{+4} or Al^{+3}.

The present paper is purely an exploratory research to

*Princeton Investigations of Rock Forming Minerals, No. 7.

determine variation in unit cell dimensions with the substitution of various ions in the pyroxene structure. Where practicable a correlation with optical properties and density will be attempted. It is hoped that such data may lead to a better understanding of subsolidus equilibria and that possibly some ion substitutions sensitive to pressure might be found. While an increasing number of geologic thermometers are being discovered we are woefully lacking in geologic barometers at present.

In this paper the plutonic orthopyroxenes of the Bushveld type have been investigated (Hess and Phillips, 1940). These have fine diopsidic exsolution lamellae parallel to (100) and are characteristic of slowly cooled plutonic igneous rocks and some high temperature metamorphics. Slow cooling probably has permitted a high degree of ordering and exsolution of the lamellae has removed almost all of the Ca^{+2} ions. This is indicated by the percentage of the total volume occupied by the lamellae compared to the bulk CaO content and by Atlas' experimental demonstration (1952).

CELL DIMENSION DETERMINATIONS

The measurements of cell dimensions were made on powders with a North American Philips X-ray spectrometer using iron radiation at 35 kv and 10 Ma, scan speed 1° in 8 minutes, chart speed 2 inches for 1°, time constant 8 seconds, angular aperture 4°, receiving slit 0.006 inch and goniometer radius 17 cm. The measurements are reproducible to approximately 0.01°. Spacings are based on Fe $K\alpha_1 = 1.93597$ Å. Calibration of the instrument was based on silicon assuming $a = 5.43062$ Å, and quartz, assuming $a = 4.9131$ Å, $c = 5.4046$ Å. The error in cell dimension measurements on these pyroxenes is about $\pm$ 0.003 Å.[1] The more magnesian pyroxenes were also measured using Cu radiation based on $K\alpha_1 = 1.54050$ Å as a check on measurements with Fe radiation.

The *a* and *b* dimensions were measured initially on 12,0,0 and 060 and checked on several of the following, 14,5,0, 650, 250, 610, and 420. The length of *c* was measured on 004 and

[1] A large portion of this error is related to the slight departure of the surface of the sample from being a perfect plane. The amount of this error is estimated by comparison of values for several Si and quartz standards. Some portion of the error may be related to the thickness of the plate irradiated or in homogeneities in distribution of the powdered material in the area irradiated.

using a predetermined *a* value on 202 and 502 and in some cases 521, 531, or 11, 3, 1 using a predetermined *a* and *b*. In some of the samples quartz or silicon as an internal standard was mixed with the material to be determined; in others a correction was made from a curve based on similarly prepared Si or quartz standards.

In order to obtain results of the requisite accuracy the upper surface of the sample must be a flat, smooth plane. Slight curvature introduces considerable error. The powdered samples were pressed down on a glass slide with another glass slide so that they covered an area of 2 cm^2 and were about 0.5 mm. thick. A thin liquid bakelite solution was allowed to seep into the powder and spread evenly over the whole slide. The solvent was removed by leaving the sample in an oven at 60° C. for about two hours, adding additional bakelite solution after one hour to assure that the whole slide was smoothly covered. The slide was then heated at 80° C. for about 24 hours. Once hardened, the sample was ground on a flat lap to a thickness of about 0.1 mm. If a thicker layer of bakelite is allowed to remain, stresses set up by its contraction will often break the slide.

A reconnaissance traverse on the goniometer was run on each sample at 2 minutes per degree and ½ inch per degree on the chart paper for the range of 2θ from 150° to 20° to choose the best peaks for measurement and locate them approximately.[2] The selected peaks were then examined at the slower speed and larger chart interval mentioned above. Each peak was run four to six times with successive recordings one above the other on the chart paper. From this the center of the peak could be found easily with 0.01° accuracy or better in many cases. Weak peaks not readily discernible from background in a single run can also be found by this method.

X-RAY RESULTS

Orthopyroxenes of the Bushveld type were chosen to begin the investigation because they are available as natural phases over almost the whole range of Mg-Fe variation and show

[2]All peaks of sufficient intensity to recognize were indexed by the writer for one sample following the method given by Henry, Lipson, and Wooster (1951, p. 178). The writer is indebted to G. L. Davis for indexing the pattern of one sample by a similar method. Three or four lines which could not be indexed were found in each case. The explanation for these is not apparent and they are being investigated further.

an almost constant amount of minor constituent ions. Ca has been almost completely removed by exsolution of the diopside-hedenbergite lamellae.[3] Na and K are virtually absent. The R_2O_3 content in most samples is very close to 2¾ per cent by weight and consists predominantly of Al_2O_3. Ti and Ni are present in minute amounts and the Mn content is small except in the iron-rich end of the series. The solid line curves, figure 1, represent the variation in *a*, *b*, and *c* from enstatite to orthoferrosilite with approximately 2¾ per cent R_2O_3 present. The effect of Ca in volcanic orthopyroxenes is being investigated by Kuno and will be reported elsewhere.

The substitution of Fe for Mg in the structure results in a regular increase of the size of all three dimensions, *a*, *b*, and *c*, but is comparatively smaller for *c* than for the other two. These increases are linear within the accuracy of present measurements and may be expressed by the equations below for the common suite of Bushveld type orthopyroxenes containing 2¾ per cent R_2O_3.

$$a = 18.228\ \text{Å} + .00205\ (100 - \text{mg})\ \text{Å}$$
$$b = 8.805\ \text{Å} + .00255\ (100 - \text{mg})\ \text{Å}$$
$$c = 5.185\ \text{Å} + .00073\ (100 - \text{mg})\ \text{Å}$$
$$\text{where mg} = 100\ Mg^{+2}/Mg^{+2} + Fe^{+2} + Fe^{+3}$$

Enstatite from the Shallowater meteorite analyzed by Foshag is very close to pure $MgSiO_3$. Measurement of the dimensions of this pyroxene as compared to the others of the En-Of natural series which contain 2¾ per cent R_2O_3 shows that the *c* dimension is smaller, the *b* dimension larger, and the *a* is unchanged. On the other hand a bronzite (Mg_{89}) from Ross' and Foster's (1951) suite of minerals from peridotite xenoliths in basalt with a little over 4 per cent R_2O_3 of which 3½ per cent is Al_2O_3 shows the *c* dimension the same as for normal series, the *b* dimension considerably smaller, and the *a* unchanged. I am indebted to S. S. Goldich for an orthopyroxene from a volcanic with 8½ per cent R_2O_3, mostly Al_2O_3, analyzed by Oslund. This has *c* the same as for the normal series, *b* strikingly smaller, and *a* unchanged (all compared to Kuno's curves for dimensions of volcanic hypersthenes). The *b* evidently decreases regularly with the substitution of the smaller Al^{+3} or

[3] The volume of the lamellae is about 6 per cent of the sample and apparently is too small to produce recognizable peaks in the records.

other R^{+3} ions. The *c* dimension seems to be affected by small amounts of Al^{+3} but after R_2O_3 reaches something less than 2¾ per cent by weight, further increase is not observed in *c*. The substitution of the larger Al^{+3} ion for the smaller Si^{+4} ion at first increases the length of the $-SiO_3$ chains but larger amounts of Al^{+3} possibly cause the $-SiO_3$ chains to zigzag in the (010) plane. Zigzag in this plane is further suggested by the lack of change of *a*, though the Mg^{+2} ions are being replaced by smaller Al^{+3} ions and the conspicuous contraction of *b*.

It may be noted in figure 1 that the curve for *b* of highly aluminous orthopyroxenes is nearly a horizontal line and approximately equal to *b* for pure $MgSiO_3$. This suggests that the value, $b = 8.810$ Å, perhaps is the minimum value to which the *b* dimension may contract for such an orthopyroxene structure. It also suggests that this may represent the maximum amount of R_2O_3 which the structure can accommodate for a given Mg/Fe ratio. More analyses of highly aluminous orthopyroxenes are needed to investigate this further.

TABLE 1

Approximate Interionic Distances

VI Coordination			
Mg^{+2} ..... O^{-2} = 2.1 Å		Al^{+3} ..... O^{-2} = 1.9 Å	
Fe^{+2} ..... O^{-2} = 2.15Å		Cr^{+3} ..... O^{-2} = 2.0 Å	
Ca^{+3} ..... O^{-2} = 2.3 Å		Fe^{+3} ..... O^{-2} = 2.05Å	
IV Coordination			
Si^{+4} ..... O^{-2} = 1.62Å		Al^{+3} ..... O^{-2} = 1.72Å	

In the magnesian orthopyroxenes one might expect the small Al^{+3} ions would substitute for Mg^{+2} ions inasmuch as they are smaller than the Fe^{+2} ions. If at the same time Al^{+3} were substituted for Si^{+4}, a small net decrease in volume might be expected, judging from table 1. There is a suggestion from geological evidence that pressure may favor the reaction $MgMgSiSiO_6 \rightarrow MgAlAlSiO_6$. The orthopyroxene analyses (Ross and Foster, 1951) from peridotite inclusions in basalts thought to be brought up from the peridotite substratum have

Index to Samples in Figure 1

Number		Locality	Rock	Classification	Source
1*	Sh	Shallowater Meteorite	Meteorite	Probably High Temperture	Foshag (1940)
2†	W26	Webster, N.C.	Pyroxenite	Bushveld Type Plutonic Igneous	R. Miller (1951)
3a‡	RF1	Inclusion in basalt	Peridotite	Bushveld Type Ultramafic Igneous	Ross & Foster (1951)
5†	7666	Bushveld	Pyroxenite	Bushveld Type Plutonic Igneous	E. Sampson
6a‡	Bonin	Bonin Is.	Basalt	Volcanic	Kuno
8	EB38	Stillwater Complex	Norite	Bushveld Type Plutonic Igneous	Hess
9a‡	Al-Hy	.....	....	Volcanic	Goldich
11†	EB130	Stillwater Complex	Gabbro	Bushveld Type Plutonic Igneous	Hess
12‡	EB41	Stillwater Complex	Gabbro	Bushveld Type Plutonic Igneous	Hess
13a‡	DOM1	Dominica, B.W.I.	Andesite	Volcanic	Hess
15†	K-9	Kasimine, near Osaka, Japan	Ferrogabbro	Bushveld Type Plutonic Igneous	Kuno
16a*	——	Greenland	....	.....	Ramberg & De Vore, (1951)
17†	K-11	Je-ho-shen, S. Manchuria	Eulysite	Metamorphic	Kuno

* Chemical analysis in literature. † Chemical analysis in Table 2. ‡ Chemical analysis to be published elsewhere.

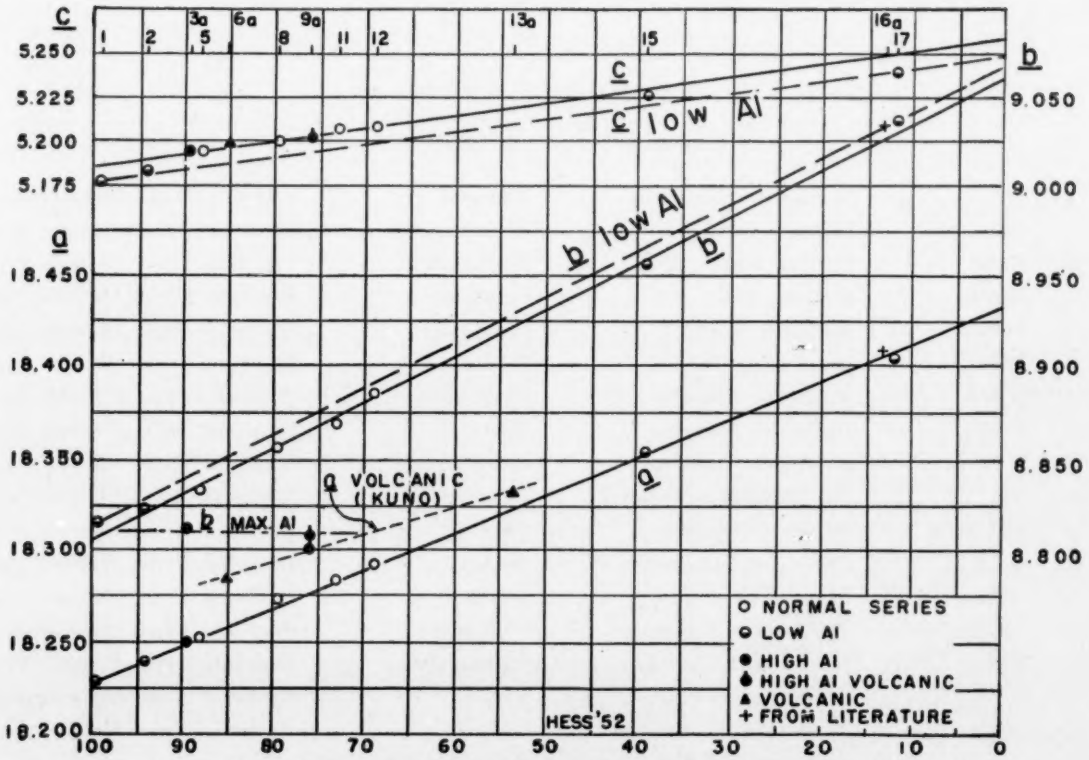

Fig. 1. Cell dimensions a, b and c for various orthopyroxenes. Units on scale along base of chart are in molecular per cent En or more exactly as

$$\frac{100\ Mg^{+2}}{Mg^{+2}+Fe^{+2}+Fe^{+3}+Mn^{+2}}.$$

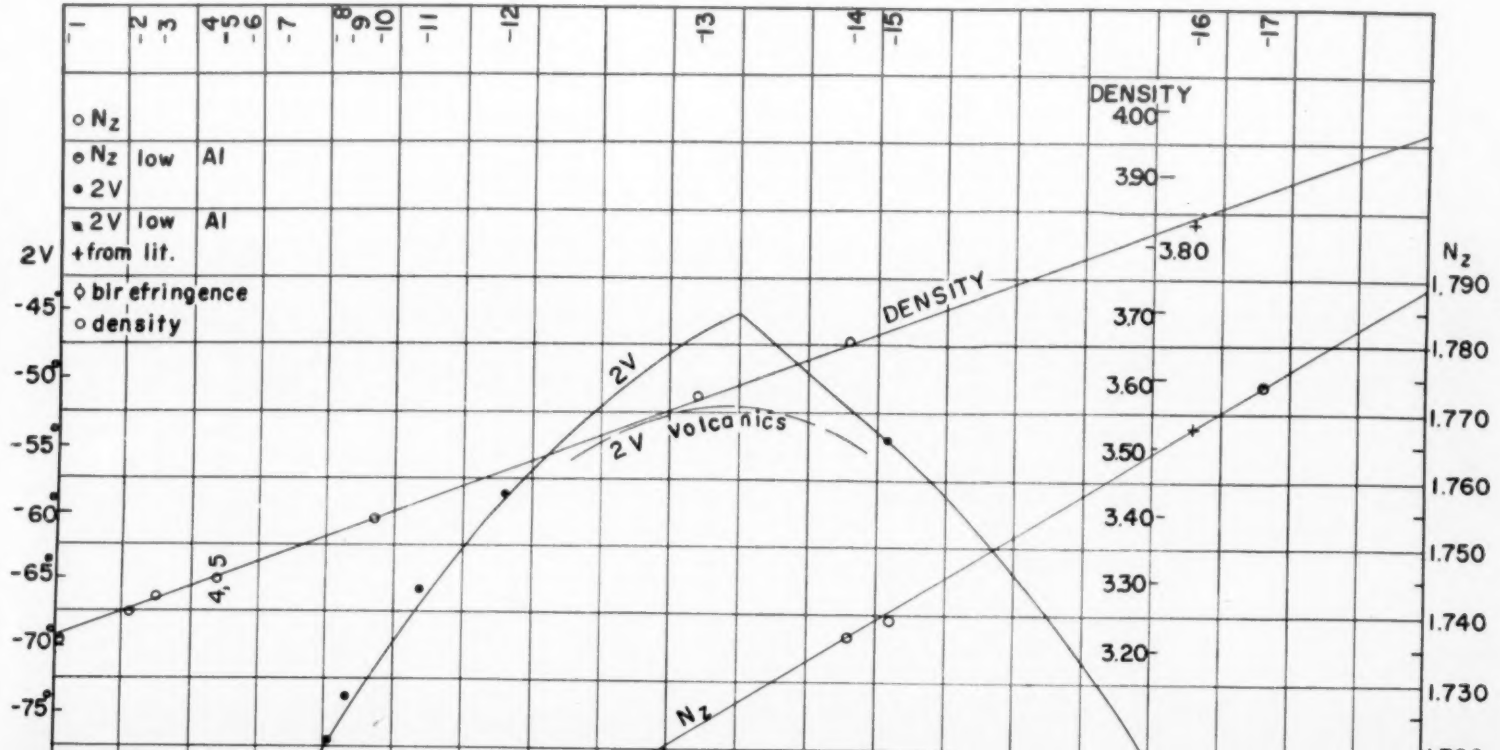
-1
-2 -3
4 -5 -6
-7
-8 -9 -10
-11
-12
-13
-14
-15
-16
-17
○ Nz
○ Nz low Al
• 2V
▪ 2V low Al
+ from lit.
◊ birefringence
○ density
2V
-45
-50
-55
-60
-65
-70
-75
DENSITY
4.00
3.90
3.80
3.70
3.60
3.50
3.40
3.30
3.20
Nz
1.790
1.780
1.770
1.760
1.750
1.740
1.730
DENSITY
2V
2V Volcanics
4, 5
Nz

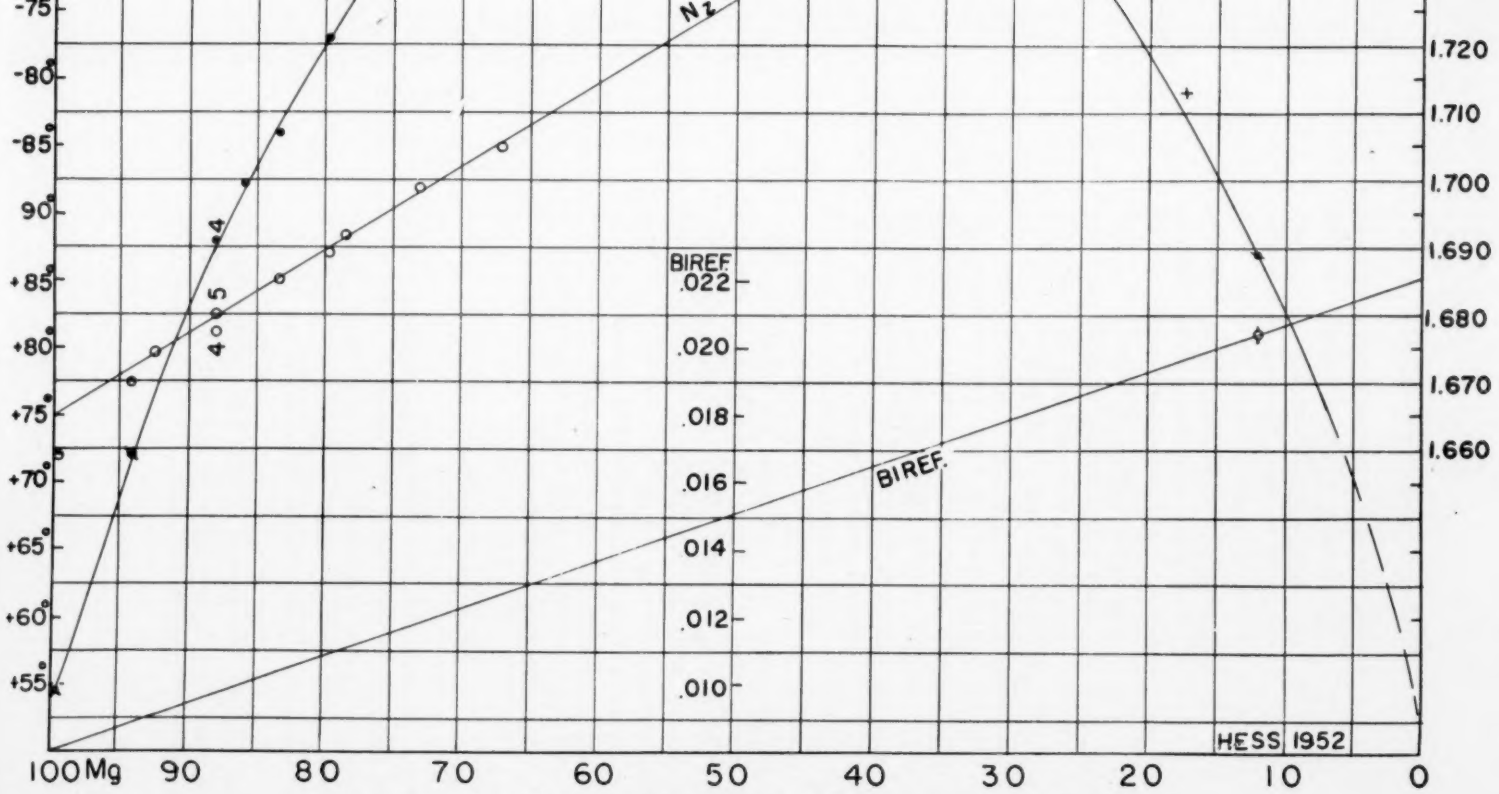

Fig. 2. Curves for optical properties and density of orthopyroxenes of the Bushveld type.

Index to Samples in Figure 2

	Number	*Locality*	*Rock*	*Classification*
1	Sh	Shallowater Meteorite	Meteorite	Probably High Temperature
2	W26	Webster, N.C.	Pyroxenite	Bushveld Type, Plutonic Igneous
3	B323	Shulaps Range, B.C.	Pyroxenite	Bushveld Type, Plutonic Igneous
4	W26B	Webster, N.C.	Pyroxenite	Bushveld Type, Plutonic Igneous
5	7666	Bushveld Complex	Pyroxenite	Bushveld Type, Plutonic Igneous
6	7704	Great Dyke, S.R.	Pyroxenite	Bushveld Type, Plutonic Igneous
7	EB13	Stillwater Complex	Pyroxenite	Bushveld Type, Plutonic Igneous
8	EB38	Stillwater Complex	Norite	Bushveld Type, Plutonic Igneous
9	EB32a	Stillwater Complex	Gabbro	Bushveld Type, Plutonic Igneous
10	374	Bay of Islands Complex	Pyroxenite	Bushveld Type, Plutonic Igneous
11	EB130	Stillwater Complex	Gabbro	Bushveld Type, Plutonic Igneous
12	EB41	Stillwater Complex	Gabbro	Bushveld Type, Plutonic Igneous
13	5718	Saranac Lake, N.Y.	Norite	Bushveld Type, Plutonic Igneous
14	12700	Pallavaram, Madras	Charnockite	Bushveld Type, Metamorphic
15	K-9	Near Osaka, Japan	Ferrogabbro	Bushveld Type, Plutonic Igneous
16	....	Tunaberg, Sweden	Eulysite	Bushveld Type, Metamorphic
17	K-11	Je-ho-shen, S. Manchuria	Eulysite	Bushveld Type, Metamorphic

conspicuously more Al^{+3} than orthopyroxenes from rocks almost identical chemically which have crystallized near the surface. Admittedly this could also be an effect of higher temperature of crystallization at depth, but in either case a clue as to depth of crystallization might be forthcoming. Similarly orthopyroxene phenocrysts which come to the surface in lavas generally have more R_2O_3 than found in even-grained intrusives where crystallization has occurred at relatively shallow depth. It would be most interesting to compare the orthopyroxene phenocrysts of lavas with the groundmass orthopyroxenes of the same flow, though this has not been done.

The Cr^{+3} and Fe^{+3} ions are too large to substitute for Si^{+4} and no doubt would produce a similar but proportionately smaller effect than Al^{+3} in substituting for Mg^{+2} or Fe^{+2}. If Al^{+3} were to substitute for Si^{+4} and Cr^{+3} for Mg^{+2} little or no change in volume would result, judging from the values given in table 1. The Cr^{+3} content is in all cases so much lower than the Al^{+3} in natural orthopyroxenes that no measure can be made of the specific effect of Cr^{+3}. Much the same is true in the case of Fe^{+3}.

The comparatively large Ca^{+2} ion cannot fit into the orthopyroxene structure at low temperature judging from the exsolution effects observed. At the high temperature of crystallization of magmas it enters the structure in small amounts ($CaO = 1.65$ per cent $\pm$ 0.3 per cent in ordinary igneous orthopyroxenes). If the large Ca^{+2} ion is retained in the structure, the most conspicuous effect is expansion of the structure in the *a* direction in contrast to contraction of the structure in the *b* direction when a small ion is substituted.

OPTICAL PROPERTIES

Various optical properties and densities were measured on 17 analyzed samples. The results are summarized in figure 2. All but one of these (the Shallowater meteorite enstatite No.1) are orthopyroxenes of the Bushveld type. Number 1 is nearly pure natural $MgSiO_3$ and is included for comparison and discussion.

Both the N_z and density curves are straight lines within the limits of accuracy of measurement and chemical analysis of the samples. The N_z value for Al-poor enstatite falls below

the curve for the Bushveld type orthopyroxenes with normal content of R_2O_3.

The optic angle curve departs slightly from that given in Poldervaart (1950) in that it shows an abrupt change of direction at $Mg_{50}Fe_{50}$. In order to determine more accurately the shape of the optic angle curve a plot was made of 2V against N_z, figure 3. The curve for optic angle in figure 2 was drawn by plotting 2V values taken from figure 3 below the corresponding points on the N_z curve. This permitted the use of a number of samples for which there were no chemical analyses. The approximate optic angle curve for volcanic hypersthenes is given as a dashed line in figure 2 for comparison with those of the Bushveld type. The difference between the two optic angle curves may possibly be accounted for by the effect of Ca^{+2} retained in the quickly cooled volcanic hypersthenes but expelled from the slowly cooled Bushveld type.

Ca^{+2} does not seem to affect the N_x index of refraction appreciably. Values for volcanic orthopyroxenes and those of the Bushveld type fall along the same straight line. Al^{+3} increases N_z somewhat, approximately 0.001 per weight per cent of Al_2O_3, while the same amount of Al_2O_3 increases $2V_x$ by a little less than 1° and decreases birefringence by about 0.0001.

The regular increase in birefringence from enstatite to Mg_{50} Fe_{50} is well established from data in the literature. One point was measured at Mg_{12} Fe_{88} in order to find out whether this trend continued to the iron-rich end of the series. Apparently this curve is also a straight line.

Inasmuch as analyses at hand give very few points in the iron-rich region, Sundius' (1932) excellent data for the Tunaberg eulite are plotted in figure 2. Similarly Ramberg and De Vore's (1951) X-ray data for their eulite, "XYZ," are plotted in figure 1.

APPLICATION OF VEGARD'S LAW

Sahama and Torgeson (1949) studied the thermochemistry of the orthopyroxene series and found no heat of mixing. They concluded, therefore, that the orthopyroxenes represent ideal mixed crystals. Ramberg and De Vore (1951) plotted data for N_z and cell dimensions *a* and *b* and concluded from the curvature of the graphs thus obtained that the orthopyroxenes are not ideal mixed crystals and do not obey Vegard's Law.[4] They

[4] The present writer expresses no opinion as to the validity of this general concept.

point out that Sahama's and Torgeson's points lie close to the Mg and Fe end members of the series and thus might not be sensitive to departures from Vegard's Law. The present investigation strongly suggests that the curves for N_z, birefringence, density and cell dimensions are all straight lines, thus supporting Sahama and Torgeson and disagreeing with Ramberg and De Vore. It seems very probable that the curvature found by the latter authors is the result of the presence of variable amounts of minor ions which they did not consider, particularly Al^{+3} and Ca^{+2}. Random samples of orthopyroxenes will generally give greater quantities of these two ions in orthopyroxenes of intermediate compositions and thus account for Ramberg's and De Vore's observations.

TABLE 2

Chemical Analyses of Orthopyroxenes of the Bushveld Type

	2 W26	5 7666	8 EB38	11 EB130	15 K9	17 K11	
SiO_2	57.73	55.94	55.20	53.67	49.43	46.56	
Al_2O_3	.95	1.61	1.50	1.65	.38	.23	
Cr_2O_3	.46	.45	.07	.06	—	—	
Fe_2O_3	.42	.97	.84	1.14	.04	.20	
FeO	3.57	7.15	11.86	15.30	34.91	48.10	
MnO	.08	.19	.28	.33	1.19	.15	
MgO	36.13	32.12	28.14	25.37	12.96	3.70	
NiO	.35	.07	.07	.05	—	—	
CaO	.23	1.48	1.93	1.81	.71	.77	
Na_2O	—	.00	—	—	.02	.04	
K_2O	—	.00	—	—			
H_2O+	.52	.09	.30	—	—	—	
H_2O-	.04	.00	.06	.09	—	—	
TiO_2	.04	.11	.22	.29	.17	.03	
	100.52	100.18	100.47	99.76	99.81	99.78	
Analyst	L. C. Peck				Tada Huzimoto	Konishi	
N_z	1.6700	1.6802	1.6893	1.6979	1.7390	1.7738	± .0005
$2V_z$	107¾°	92°	77°	68¼°	54¼°	93°	± ½°
Biref.	—	—	—	—	—	.0205	± .0002
a in Å ...	18.239	18.251	18.273	18.284	18.353	18.404	± .003Å
b in Å ...	8.823	8.834	8.856	8.870	8.954	9.038	
c in Å ...	5.184	5.193	5.199	5.207	5.226	5.239	
$\frac{100\ Mg^{+2}}{Mg^{+2}+Fe^{+2}+Fe^{+3}+Mn^{+2}}$	94	88	79¾	73	39	12	
Density g/cc	3.249/ /24°C	3.302/ /22½°C	—	—	—	—	

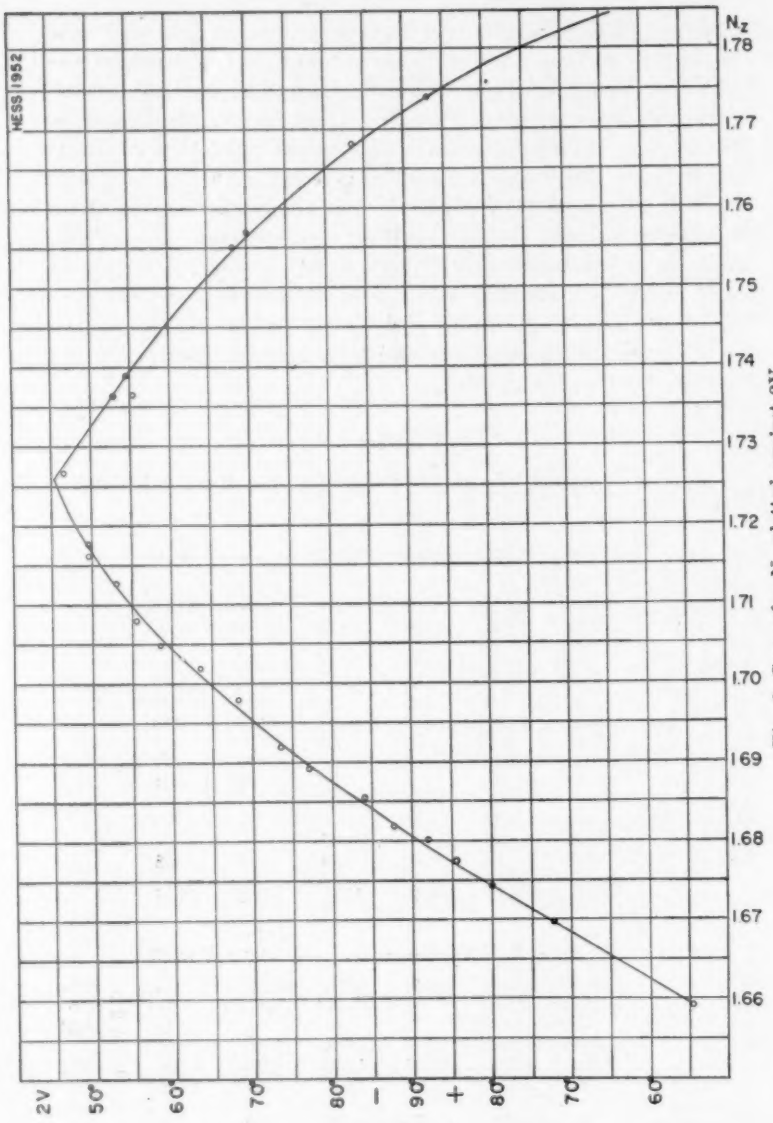

Fig. 3. Curve for N_z plotted against 2V.

DENSITY OF NATURAL ENSTATITE

Values given for the density of enstatite show considerable variation, so the measured and calculated values for the Shallowater enstatite are given as follows:

$$\delta = \frac{M\ n}{V\ N_0}$$

δ = density
M = molecular weight = 201.057
n = number of molecules in unit cell = 8
V = volume unit cell = 18.230 x 8.815 x 5.177 Å
= 831.931 Å^3 at 23°C.
N_0 = Avagadro's number = 6.023 x 10^{23}

			ionic ratios
SiO_2	59.92		
FeO	.38	Si	.9977
MgO	39.51	Fe	.0072
CaO	.32	Mg	.9799
		Ca	.0057
Foshag (1940)	100.32	O	2.9881

f (assuming 6 oxygens in formula) $= \frac{2.9881}{6} = .49802$

$$\frac{100.32}{.49802} = 201.057 = M$$

$$\delta_c = \frac{201.057 \times 8}{831.931 \times 6.023 \times 10^{23}} = 3.2104 \text{ at } 23°C.$$

δ_0 = 3.209 ± .003 at 27° C. measured by M. N. Bass by flotation in clerici solution

TABLE 3

Additional Unit Cell Measurements

	1 Sh	3a RF1	6a Bonin	9a Al-Hy	12 EB41	13a DOM-1
a in Å	18.230	18.250	18.285	18.300	18.293	18.333
b in Å	8.815	8.812	8.843	8.807	8.887	—
c in Å	5.177	5.192	5.198	5.201	5.208	—
N_z	1.6592	—	—	1.7015	1.7050	1.7230
$2V_z$	125.5°	—	—	76.5°	58.5°	52°
Biref.	—	—	—	.0105	—	—
$\frac{100\ Mg^{+2}\ *}{Mg^{+2}+Fe^{+2}+Fe^{+3}+Mn^{+2}}$ ..	99½	89½	85	76	69	53½
Density ..... g/cc	3.210/23°	—	—	3.412/25°	—	3.570/24°
Comments	No R_2O_3 Meteorite	R_2O_3=4% Plutonic	Normal Volcanic	R_2O_3=8½% Volcanic	Normal Plutonic	Normal Volcanic

* Based on chemical analysis.

DISCUSSION OF RESULTS

It was thought that the *c* dimension would not be changed by substitution of a larger Fe^{+2} for a smaller Mg^{+2} because this dimension would be controlled by the $—SiO_3$ chains. The measurements made indicate that this supposition is incorrect. Similarly it was thought that substitution of the larger Al^{+3}_{iv} for the smaller Si^{+4}_{iv} would increase the length of the chains and hence *c*. The measurements show that this supposition is also incorrect. The substitution of a large cation such as Ca^{+2} or a small cation such as Al^{+3}_{vi} for Mg^{+2} might have been expected to increase or decrease respectively *both a* and *b*. Measurements show that the larger ion only increases *a* and the smaller ion only decreases *b*. These are the empirical results. Explanation of them in terms of structure is beyond the scope of this investigation. In a sense these results are fortunate inasmuch as they make it possible to estimate the amount of Ca^{+2} and Al^{+3} present and also determine the Mg : Fe ratio as a revision of the value obtained from N_z and 2V modified for the effect of the indicated Al^{+3} and Ca^{+2}. These four ions plus Si^{+4}, which may be calculated by difference, represent all of the major constituents of orthopyroxenes. One may, therefore, determine the chemical composition of such pyroxenes with reasonably good accuracy without chemical analysis.

ACKNOWLEDGMENTS

This study has been carried out in close cooperation with H. Kuno who has been making similar measurements on the volcanic suite of orthopyroxenes. Many fruitful ideas evolved from comparison of results and discussion of the problems encountered. I wish to express my indebtedness to Kuno and to thank him for supplying three of the samples used. Support for this research was obtained from the Higgins Trust funds allotted to Princeton University for which I am duly grateful. I wish to thank G. L. Davis of the Geophysical Laboratory for assistance in setting up the X-ray goniometer and for helpful advice on techniques of measurement. C. McAneny assisted in making some of the measurements and in instrument calibration.

I also wish to thank A. F. Buddington, S. S. Goldich, E. P. Henderson, R. Miller, C. S. Ross and M. Foster for supplying

analyzed samples of orthopyroxenes, and W. R. Foster for synthetic clinoenstatite. I am also indebted to H. S. Yoder for critically reading the manuscript.

References

Atlas, L., 1952. The polymorphism of $MgSiO_3$ and solid state equilibria in the system $MgSiO_3$-$CaMgSi_2O_6$: Jour. Geology, vol. 60, pp. 125-147.

Foster, W. R., 1951. High temperature X-ray diffraction study of the polymorphism of $MgSiO_3$: Am. Ceramic Soc. Jour., vol. 34, pp. 255-259.

Foshag, W. F., 1940. The Shallowater meteorite; a new aubrite: Am. Mineralogist, vol. 25, pp. 779-786.

Henry, N. M. F., Lipson, H., and Wooster, W. A., 1951. The interpretation of X-ray diffraction photographs, The Macmillan Company, New York.

Hess, H. H., 1949. Chemical composition and optical properties of common clinopyroxenes, part I: Am. Mineralogist, vol. 34, pp. 621-666.

———, and Phillips, A. H., 1940. Optical properties and chemical composition of magnesium orthopyroxenes: Am. Mineralogist, vol. 25, pp. 271-285.

Kuno, H., in press. Study of orthopyroxenes from volcanic rocks: Am. Mineralogist.

Miller, R., 1951. The structure and petrology of the Webster-Addie ultrabasic ring, Jackson County, N.C. Unpublished thesis, Princeton University.

Poldervaart, Arie, 1950. Correlation of physical properties and chemical composition in the plagioclase, olivine, and orthopyroxene series: Am. Mineralogist, vol. 35, pp. 1067-1079.

Ramberg, H., and De Vore, G., 1951. The distribution of Fe^{++} and Mg^{++} in coexisting olivines and pyroxenes: Jour. Geology, vol. 59, pp. 193-210.

Ross, C. S., and Foster, M. D., 1951. Studies of minerals in dunites and in olivine-rich inclusions in basaltic rocks (abst.): Geol. Soc. America Bull., vol. 62, pp. 1472-1473. (Complete paper in press, Am. Mineralogist.)

Sahama, Th. G., and Torgeson, D. R., 1949. Some examples of application of thermochemistry to petrology: Jour. Geology, vol. 57, pp. 255-262.

Sundius, N., 1932. Über den sogenannten Eisenanthophyllit der Eulysite: Sveriges geol. undersökning Årsbok 26, ser. C, no. 374.

Warren, B. E., and Bragg, W. L., 1928. The structure of diopside $CaMg(SiO_3)_2$: Zeitschr. krystallographie, vol. 69, pp. 168-193.

———, and Modell, D. I., 1930. Structure of enstatite $MgSiO_3$: Zeitschr. krystallographie, vol. 75, pp. 1-14.

Princeton University
Princeton, New Jersey

TWINNING FREQUENCY IN FELDSPAR PHENOCRYSTS FROM A QUARTZ LATITE SILL AT SIERRA BLANCA, TEXAS

EARL INGERSON*

ABSTRACT. Study of some 1500 sanidine phenocrysts from a quartz latite sill in Texan Mountain, Trans-Pecos, Texas, shows the following abundances of (1) untwinned crystals, (2) Carlsbad, (3) Manebach, and (4) Baveno twins, respectively: from a zone near the upper contact: (1) 84.35%; (2) 8.5%; (3) 6.9%; (4) .25%; from the center of the sill: (1) 94.3%; (2) 3.3%; (3) 2.4%; (4) not observed. The average size of the phenocrysts near the top of the sill is larger than that of those near the center; the twinned crystals are significantly larger than the untwinned ones in both places. These facts are tentatively explained as due to (1) somewhat earlier initiation of crystallization of twinned crystals, (2) floating of early formed phenocrysts, and (3) greater tendency for nuclei to develop twinning in the more disturbed contact zones. Chemical data support the idea that the twinned crystals began crystallizing, on the average, slightly ahead of the untwinned ones.

INTRODUCTION

HUFFINGTON (1943) has described the geology of the Northern Quitman Mountains in Hudspeth County, Texas. His geologic map covers the area as far east as the town of Sierra Blanca, south of the Southern Pacific Railroad.

Texan Mountain, immediately southwest of the town, consists almost entirely of the Cox and Finlay formations of early Cretaceous age. Figure 1 is an index map showing the location of the area, and figure 2 gives the details of the geology of Texan Mountain. The exposed part of the Cox formation in Texan Mountain is about 500 feet thick and is composed mostly of white to reddish-brown quartzite with thin layers of dense gray limestone and purple to greenish shales. The mountain is a tilted fault block; the strata strike about N. 55° W. and dip 27° SW. The top and backslope are covered by the Finlay formation, overlying the Cox; only the lower 100 feet of the Finlay, consisting of gray limestone with a few thin layers of sandstone, is here exposed.

Along the northeast face of Texan Mountain three porphyritic sills are exposed. The uppermost and lowermost contain abundant phenocrysts of potash feldspar that weather out of the matrix more or less readily, but only in the lowermost sill

*Publication authorized by the Director, U.S. Geological Survey.

are the phenocrysts well enough formed so that the type, or absence, of twinning can be determined by megoscopic inspection. The middle sill is only slightly porphyritic. The two lower sills are 40 to 50 feet thick. The uppermost one is about the same thickness where it is entirely within the Cox formation, but near the center of the northeast face of Texan Mountain it cuts across to the contact between the Cox and Finlay formations. At this point the sill is well over 100 feet thick.

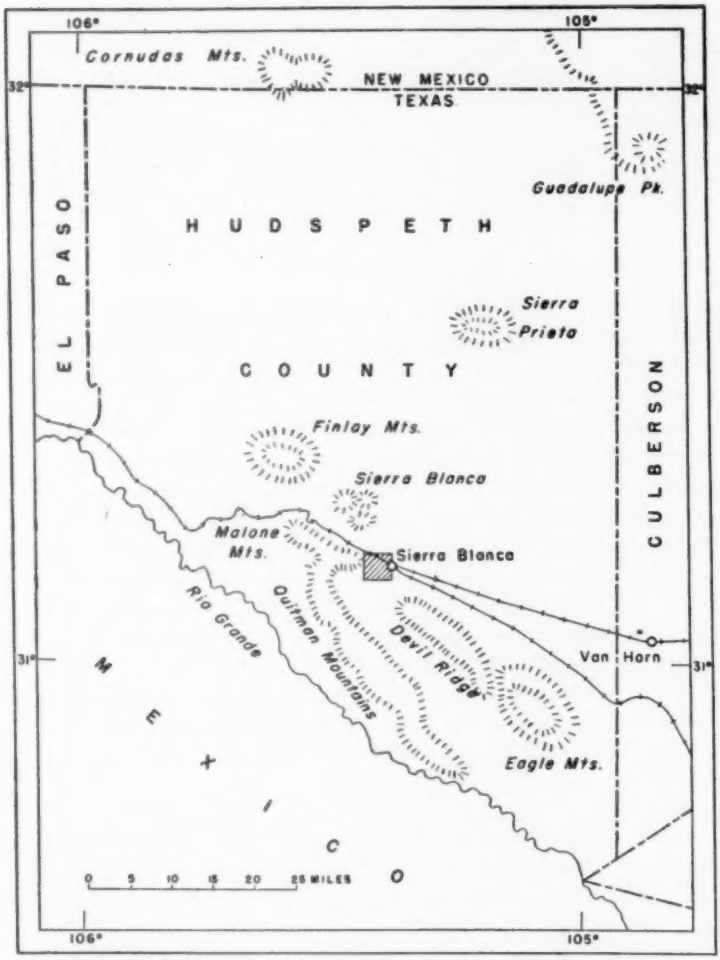

Fig. 1. Index map showing location of the area described.

The lowermost sill has been intruded into the lowest exposed quartzite beds of the Cox formation. The sill crops out at and near the break in slope at the northeast foot of Texan Mountain. The sill is composed of a light gray porphyritic rock with abundant phenocrysts of both potash feldspar and plagioclase. The crystals of potash feldspar are slightly pink on a freshly broken surface and are as much as 1.5 cm. in diameter. The plagioclase crystals are white to cream-colored and are mostly less than 3 mm. in their greatest dimension (fig. 3). Altered hornblende phenocrysts are much less conspicuous than the feldspars; the longest are about 3 mm. Quartz can be found by aid of a hand lens only with considerable difficulty. The groundmass is aphanitic.

In thin section the plagioclase was determined as oligoclase, about An_{20}. The hornblende is completely altered to calcite, chlorite, and magnetite. Quartz is present as rare phenocrysts less than a millimeter in diameter, but most of the quartz is present as nests of smaller grains that grade into the groundmass, which is composed largely of a very fine felt of feldspar microlites in which quartz grains up to about 0.25 mm. in diameter occur. The quartz appears to have grown around the feldspar microlites as the last primary mineral to crystallize. Figure 3 shows a typical hand specimen of the rock, and figure 4 is a photomicrograph from a thin section.

Table 1 gives the chemical composition, norm, and mode of the sill rock. The CIPW symbol is II·4·2·(3)4. According to Johannsen's (1931) classification the rock would be a rhyodacite, but a more common name that applies equally well is quartz latite.

Some 1500 sanidine phenocrysts were collected from the lowermost sill near its southeastern extremity for a statistical study of twinning. These were for the most part weathered out so as to be entirely free of the matrix. They were collected in two groups: (1) 1148 from a zone near the top of the sill and (2) 371 from a zone near the center of the sill, which at this point is about 40 feet thick.

PROPERTIES OF SANIDINE PHENOCRYSTS

Crystallography.—Most of the crystals are untwinned, but the three common monoclinic feldspar twin types—Carlsbad, Manebach, and Baveno—are all present. In addition to these twin types and simple single crystals there are also irregular

TABLE 1

Analysis, Norm, and Mode of Quartz Latite from Texan Mountain

Chemical Analysis*			Norm		Mode	
Oxide	Found	Less $CaCO_3$ and H_2O	Mol.	%	Min.	%
SiO_2	63.48	67.97	Q	23.52	Sanidine	14.1
Al_2O_3	15.35	16.44	or	26.13	Oligoclase	13.9
Fe_2O_3	2.70	2.89	ab	34.58	Hornblende‡	8.8
FeO	0.77	0.82	an	3.89	Quartz	3.4
MnO	0.07	0.08	ce†	0.75	Groundmass	59.8
MgO	1.10	1.18	C	3.26		100.0
CaO	3.42	0.93	hy	3.06		
Na_2O	3.85	4.12	mt	0.70	S. G. = 2.593	
K_2O	4.16	4.45	hm	2.40		
TiO_2	0.63	0.67	il	1.22		
P_2O_5	0.16	0.17	ap	0.31		
CO_2	2.00	—				
H_2O+	1.60	—		99.82		
H_2O-	0.55	—				
BaO	0.26	0.28				
Sum	100.10	100.00				

*W. W. Brannock, analyst.
†Celsian.
‡Completely altered. See text.

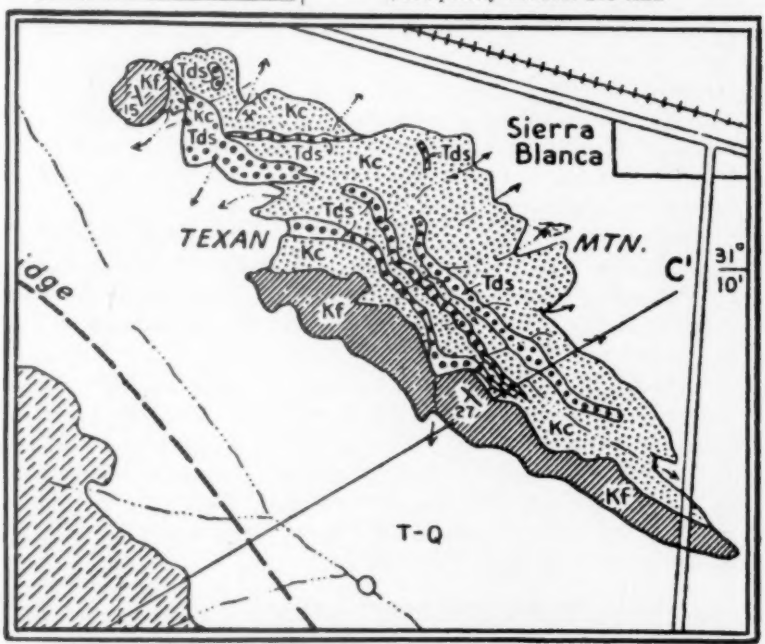

Fig. 2. Geology of Texan Mountain (after Huffington: Geol. Soc. America Bull., 1943, vol. 54, plate 1, *facing* p. 987). Scale 2 in. = 1 mi.
Kc, Cretaceous Cox formation.
Kf, Cretaceous Finlay formation
Tds, Tertiary dikes and sills

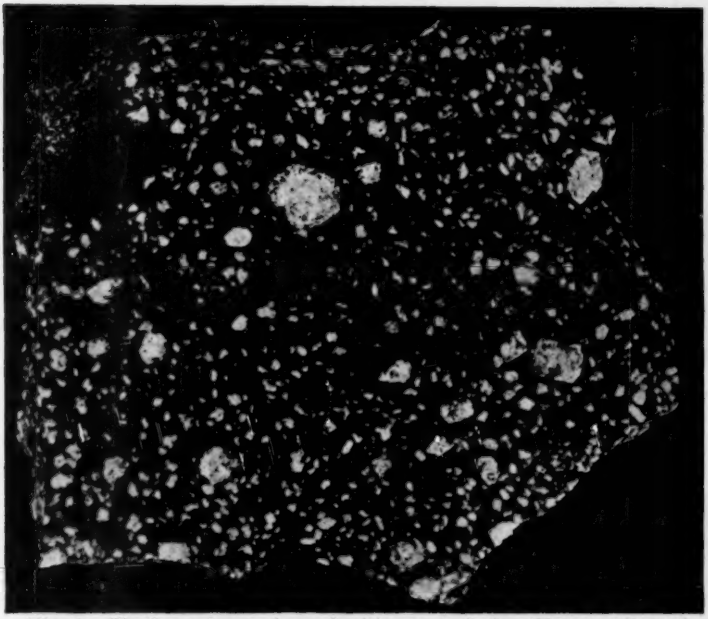

Fig. 3. Hand specimen of porphyritic quartz latite (X5/6). All of the phenocrysts larger than about 3 mm. are sanidine; most of the smaller ones are oligoclase.

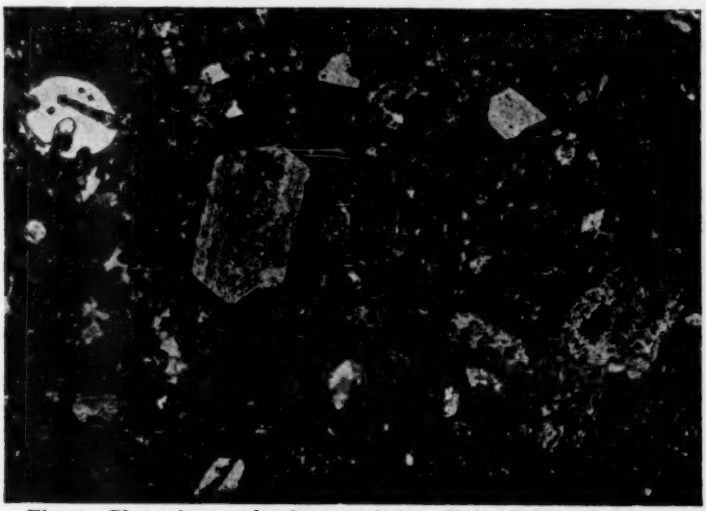

Fig. 4. Photomicrograph of quartz latite (X14). Palette-shaped grain in upper left is quartz; large crystal near center, oligoclase; mottled area at lower right, altered hornblende.

combinations of crystals and parallel growths. The latter show re-entrant angles that make many of these crystals resemble Carlsbad or Manebach twins in which the two individuals are unequally developed. It was necessary to make and study a

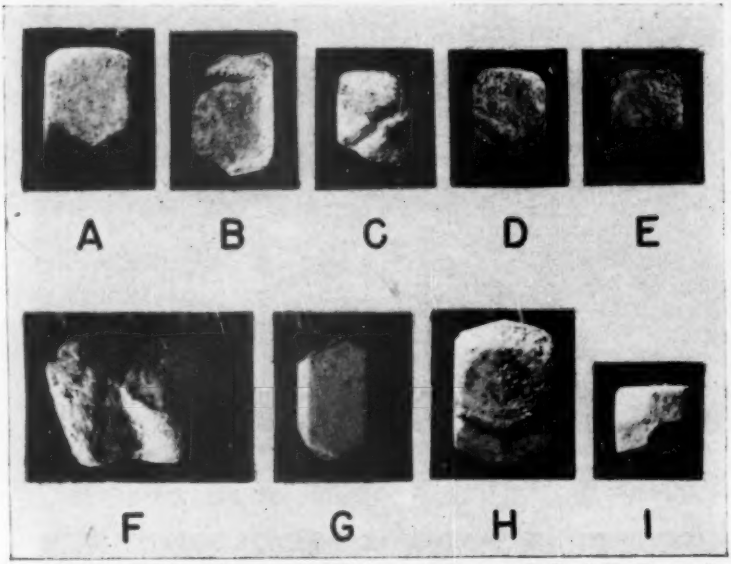

Fig. 5. Sanidine phenocrysts (X2). A, single crystal; B, C, D, E, parallel intergrowths; F, irregular intergrowths; G, Carlsbad twin; H, Manebach ⊥ (001); I, Manebach ⊥ *a*.

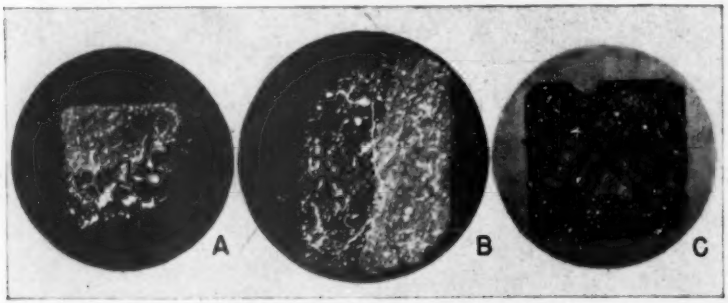

Fig. 6. Photomicrographs of sanidine crystals, all sections (standard thickness) ca. parallel (100), *c*-axis vertical. Crossed Nicols (X3). A, Manebach twin; B, Carlsbad twin; C, parallel intergrowth, crystal resembled modified Carlsbad twin (note re-entrant at top) but showed no twinning in thin section.

number of thin sections from this group to be sure that the crystals were not twinned. Figure 5 shows crystals from the various groups and figure 6 is a series of photomicrographs of Carlsbad and Manebach twins and a parallel growth, all with the same orientation. The three Baveno twins mentioned in table 2 were positively identified as such, but the faces are not clear and sharp enough to be readily distinguishable in a photograph.

These phenocrysts are simple crystallographically. The prominent forms that determine the shapes of the crystals, both twinned and untwinned, are {010}, {001}, {110} and {20$\bar{1}$}. These are the only forms observed on the Manebach twins; {11$\bar{1}$} and {130} were observed on a very few Carlsbad twins. On the untwinned crystals {130} is rarely observed; {11$\bar{1}$} is common but varies a great deal in development, being completely absent from some crystals and developed as prominently as {110} on others.

The untwinned crystals and Baveno and Manebach twins are dominantly elongate parallel to the a-axis and have their shapes determined largely by {010} and {001}. The Carlsbad twins are elongate parallel to the c-axis and their shape is controlled dominantly by {110} and {010}. (See figures 5, 7, and 8.)

Optical Properties.[1]—The sanidine is cryptoperthitic. Its indices of refraction are α 1.520, β almost equal to γ = 1.526. Extinction, X $\wedge$ 001 = 3° to 5°. Dispersion, inclined, distinct, $\rho > v$. Optic plane normal to {010}. 2V was determined on the Universal stage; the average of eight determinations on eight thin sections of different crystals is 26.6°. Individual measurements ranged from 25° to 30°. Three measurements on sections about three times standard thickness gave 26°, 27°, and 28°. There is some variability in 2V, but 27°, negative, appears to be a good average value.

FREQUENCY OF TWINNING AND RELATIVE SIZES OF TWINNED AND UNTWINNED CRYSTALS

Carlsbad twins are the most abundant variety, Manebach are slightly less abundant, and Baveno twins are quite rare. The percentages of the various twin types, as well as of un-

[1] Indices of refraction, dispersion, and extinction angle determined by Jewell J. Glass.

twinned crystals, for the top and center of the sill are shown in table 2. Also shown are average weights of the different types of crystals.

Rosenbusch (1925, pp. 657-659) says that in monoclinic potash feldspar, Carlsbad twinning is by far the most common, Baveno is much less common, and Manebach twinning is very rare.

Iwasaki (1899) has described quartz-orthoclase veins cutting quartz diorite dikes near Shinano, Japan, in which most of the crystals of the orthoclase are Baveno twins. Untwinned crystals are much less abundant than the twins, only two being observed in one group of 50 crystals.

In sanidine phenocrysts from the Bearpaw Mountains, Pecora[2] found Carlsbad twinning to be dominant, the Baveno quite common, and the Manebach very rare. Baveno twins are more abundant in the pegmatites than in higher temperature facies such as dikes.

The generalization by Rosenbusch and the other examples cited suggest that the high proportion of Manebach twins in the Texan Mountain sill is quite unusual. It might be well to study this occurrence in more detail and to compare it with other localities for genetic implications.

The 1148 crystals collected near the top of the sill contain 15.5 per cent of twinned crystals; the 371 from the center of the sill, 5.7 per cent. Figures 7 and 8 are histograms showing size distribution of the different groups of crystals from the two parts of the sill. These histograms and table 2 show two things about the size distribution: (1) The crystals near the top of the sill are larger than those from the central part, and (2) the average size of the twinned crystals is significantly larger than that of the untwinned crystal.

These observed facts may possibly be explained in the following manner: (1) If some of the early formed phenocrysts had floated to the top of the magma chamber in which crystallization began, the average size of the crystals near the top of the chamber would be larger than that of the ones farther down, because the early formed crystals had more time to grow and probably grew more rapidly as they approached the cooler overlying rocks. It is logical to assume that during intrusion of the sill these larger crystals would tend to stay toward the

[2]W. T. Pecora, personal communication.

TABLE 2

Twinning in Feldspar Phenocrysts

		Single Crystals	Parallel growths	Irreg. Combinations	Carlsbad Twins	Manebach Twins	Baveno Twins	Undetermined	Totals
Upper 4 feet of sill	No. xls	843	109	4	98	79	3	12	1148
	%	73.4	9.5	0.35	8.5	6.9	0.25	1.1	100.0
	Av. wt.	0.48g	0.56g		0.63g	0.62g			
Center of sill	No. xls	308	32		12	9		10	371
	%	83.0	8.6		3.3	2.4		2.7	100.0
	Av. wt.	0.39g	0.56g		0.54g	0.34g			

top of the invading magma. Some of the segregation might be destroyed by local turbulence, but some of it would be expected to remain. (2) Other things being equal, the amount of twinning that develops in crystals is commonly a function of the amount of mechanical disturbance experienced by the nuclei during

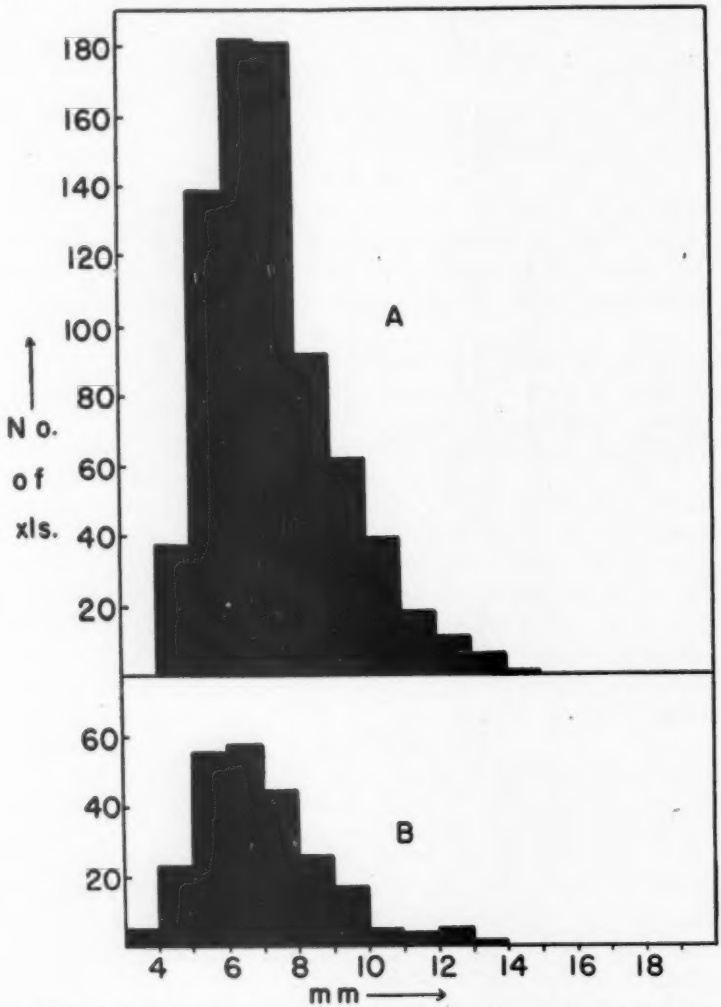

Fig. 7. Histograms showing greatest-length distribution of sanidine phenocrysts. A, untwinned crystals from top of sill, elongate parallel to a-axis ; B, untwinned crystals from center of sill, elongate parallel to a-axis.

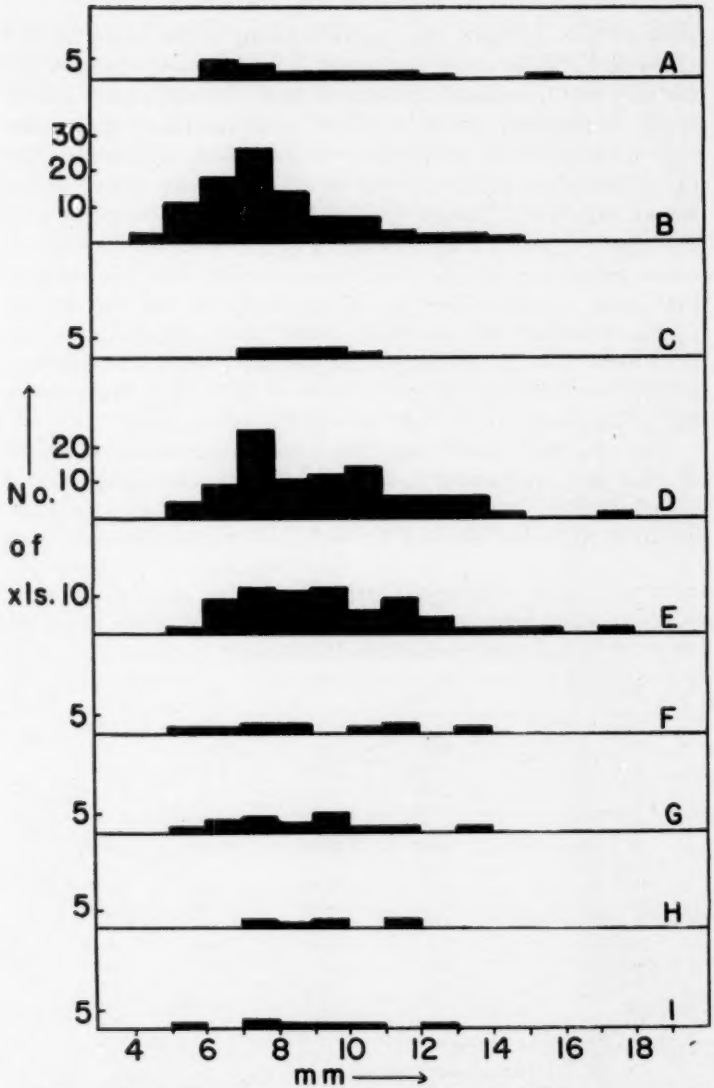

Fig. 8. Histograms showing greatest-length distribution of sanidine phenocrysts. From top of sill: A, untwinned crystals, elongate parallel to c-axis; B, parallel growths, elongate parallel to a-axis; C, parallel growths elongate parallel to c-axis; D, Carlsbad twins, elongate parallel to c-axis; E, Manebach twins, elongate parallel to a-axis. From center of sill: F, untwinned crystals, elongate parallel to c-axis; G, parallel growths, elongate parallel to a-axis; H, Carlsbad twins, elongate parallel to c-axis; I, Manebach twins, elongate parallel to a-axis.

growth. For example, the quartz crystals in the veins formed in the tectonically active belt of the Sierra Nevada in California are very highly twinned, whereas those in veins developed quietly in the tectonically stable portions of the Brazilian Shield contain a much higher proportion of untwinned individuals. The early formed feldspar crystals in the sill under consideration would have had a longer time to be subjected to mechanical disturbance, which may explain why the twinned individuals are of larger average size than the untwinned ones. The crystals that were forming near the discontinuity at the top of the magma chamber were probably under more differential stress than were those in the central part of the chamber, which may explain why the percentage of twinned crystals is higher near the upper contact of the sill than in its central part.

The idea that the twinned crystals formed somewhat ahead of the untwinned ones is supported by spectrographic and chemical data. The spectrographic analyses (table 3) show significantly more Rb and Li in the untwinned crystals, and

TABLE 3

Spectrographic Analyses* of Latite Porphyry and Sanidine Phenocrysts

El.	1	2	3	4
Mn	0.04	0.02	0.02	0.03
Fe	2.0	0.4	0.4	0.4
Ga	0.002	0.002	0.001	0.001
Cr	0.001	—	—	—
V	0.007	—	—	—
Sc	0.0006	—	—	—
Y	0.005	0.002	0.002	0.001
La	0.01	—	—	—
Ti	0.4	0.07	0.07	0.08
Zr	0.02	0.006	0.006	0.005
Be	0.0001	—	—	—
Mg	0.2	0.04	0.04	0.04
Sr	0.1	0.1	0.1	0.1
Ba	0.2	1.0	1.0	1.0
Li	0.01	0.0008	0.0006	0.0006
Rb	0.04	0.07	0.04	0.04

*E. L. Hufschmidt, analyst.

Lab. number	*Description*
1. 52-350 SCW	Quartz latite.
2. 52-351 SCW	Sanidine; untwinned crystals.
3. 52-352 SCW	Carlsbad twins.
4. 52-353 SCW	Manebach twins

Looked for but not found: Cu, Ag, Pt, Mo, W, Ge, Sn, Pb, As, Sb, Bi, Zn, Cd, Tl, In, Co, Ni, Yb, Nb, Ta, U, Cs, B.

calculations from the chemical analyses (table 4) show about 0.5 per cent more of the albite molecule in the twinned crystals. Both of these relations would be expected if the twinned crystals started crystallizing earlier and at a higher temperature. More albite goes into solid solution in potash feldspar at higher temperatures. Later formed crystals would be expected to contain slightly more of the rare elements such as Li and Rb because these elements concentrate in the rest magma during crystallization.

CONCLUSIONS

1. Early formed crystals in sills appear to have a greater tendency to twin than do later crystals of the same minerals. This may be due in part to the higher temperature, but mechanical disturbance is probably a more important factor.

2. There is a higher incidence of twinning near the contacts, which may be brought about by the greater differential motion and the resulting more intense differential stresses to which the growing crystals are subjected.

3. It is probable that (1) and (2) can be applied to other types of bodies such as stocks, border zones of batholiths, and veins. For example, quartz crystals near the edge of a quartz vein are commonly more highly twinned than the crystals near

TABLE 4

Analyses of Sanidine Phenocrysts*

Oxide	1	2	3
SiO_2	64.62		
Al_2O_3	18.54		
Fe_2O_3	0.41		
CaO	0.21		
Na_2O	2.46	2.55	2.51
K_2O	11.57	11.59	11.46
BaO	1.24		
Sum	99.57		
or:ab†	76.7:23.3	76.1:23.9	76.2:23.8

1. 52-351-SCW; single crystals.
2. 52-352-SCW; Carlsbad twins.
3. 52-353-SCW; Manebach twins.

* W. W. Brannock, analyst.

† W. S. MacKenzie, of the Geophysical Laboratory, using as a criterion the value of the d-spacing of the (201) planes as determined on an X-ray spectrometer (Bowen and Tuttle, 1950), determined this ratio to be 71:29. The material was heated to 900° C. to homogenize it before the measurements were made.

the center of the vein. It is almost certain that the relatively untwinned crystals grew at a lower temperature and under more quiescent conditions than the ones near the contacts of the vein.

4. Careful chemical and spectrographic studies can provide an indication of relative ages of different crystals of the same mineral. Further study and careful evaluation of all the factors involved should make it possible, in certain instances at least, to extend this interpretation to different mineral species.

5. It appears that there are no theoretical grounds at present on which to predict, or explain, the relative abundance of different types of twinning in a mineral for any given set of conditions. Kalb (1924) believes that high temperature favors the formation of Carlsbad twins, that as the temperature falls the incidence of Carlsbad twinning decreases and Baveno twinning increases, and that almost all of the crystals that form at still lower temperatures are untwinned. He does not, however, cite experimental evidence for this interpretation. It is based on geologic occurrence and mineral association. Other factors doubtless affect the amount and kind of twinning; so the rule, while probably valid in general, cannot be considered thoroughly established or to be strictly applicable to all occurrences.

Careful evaluation of the chemical and physical conditions under which the phenocrysts formed in the examples cited above, studies of other occurrences, and correlative laboratory work on crystal growth and twinning might give an empirical basis for predicting the order of abundance of the different types of twins in a given situation.

References

Bowen, N. L., and Tuttle, O. F., 1950. The system $NaAlSi_2O_6$—$KAlSi_2O_6$—H_2O: Jour. Geology, vol. 58, pp. 489-511.

Huffington, R. M., 1943. Geology of the Northern Quitman Mountains, Trans-Pecos, Texas: Geol. Soc. America Bull., vol. 54, pp. 987-1047.

Iwasaki, C., 1899. On the orthoclase crystals from Shinano, Japan: Am. Jour. Sci., 4th ser., vol. 8, pp. 157-158.

Kalb, Georg, 1924. Die Kristalltracht des Kalifeldspates in minerogenetischer Betrachtung: Centralbl. Mineralogie, pp. 449-460.

Johannsen, Albert, 1931. A descriptive petrography of the igneous rocks, Vol. I, University of Chicago Press, Chicago.

Rosenbusch, H., 1925-27. Mikroskopische Physiographie [der Mineralien und Gesteine], 5th ed., by E. A. Wülfing and O. Mügge. Vol. I. Schweizerbart'sche Verlagsbuchhandlung, Stuttgart.

U. S. Geological Survey
Washington, D. C.

SIGNIFICANCE OF VARIATION IN THE HIGH-LOW INVERSION OF QUARTZ

M. L. KEITH AND O. F. TUTTLE

ABSTRACT. The high-low quartz inversion of some 250 quartz specimens has been studied by a differential thermal method. The method does not permit determining the exact temperature at which the inversion would take place under equilibrium conditions, but the measured temperature is probably not greatly different from the equilibrium value. The difference between the inversion temperatures of various quartz specimens can, however, be determined to within ± 0.1° when the heat absorption is rapid (approximately 90 per cent of all specimens studied).

Differences between the inversion temperatures of natural quartz samples vary over a range of 38° C. and the inversion of synthetic quartz varies over a range of 160° C. However, over 95 per cent of all natural specimens examined invert on heating within a range of 2.5° C.

Variations found in the inversion temperature are believed to be the result of solid solution of small amounts of ions other than Si^{4+} and O^{2-}. That conjecture is supported by inversion studies on synthetic quartz. For example, synthetic quartz grown in the presence of germanium has an inversion-break 40° C. *above* the normal range for quartz, whereas quartz grown in the presence of lithium and aluminum has the inversion temperature *lowered* by as much as 120° C. Spectrochemical analysis of natural quartz with different inversion temperatures shows variations in the amounts of minor elements and this variation is in turn accompanied by changes in the cell dimensions as measured by X-ray methods.

The amount of solid solution is influenced by the temperature of growth and therefore the inversion temperature can be used as an indication of the relative temperature of formation of samples of quartz which grew in similar chemical environments. A general relationship between the inversion temperatures and the occurrence of natural quartz is derived from comparison of occurrences for which approximate formation temperatures can be inferred. For example, quartz from rhyolites, where the presence of glass indicates high temperature, inverts at lower temperatures than quartz from veins or from cavities in limestone where geologic evidence indicates a lower temperature of formation.

There are, however, numerous exceptions to this relationship and the temperature differences in the inversion can generally be taken to indicate only that the quartz is in some way different. In other words, the inversion can in most cases be used only as a "finger-print" method of comparing quartz from various sources and for the study of zoning within rock bodies; in these applications it has proven to be potentially useful. A large proportion of the following report is a preliminary "finger printing" of quartz from various rock types.

INTRODUCTION

QUARTZ occurs in a great variety of associations and is second only to the feldspars in abundance in the accessible part of the earth's crust; it is a major constituent of the predominant igneous rocks, and because of its resistance to weathering processes it is more abundant than feldspar

in clastic sedimentary rocks. Despite its abundance and wide distribution, little effort has been made to study the differences in the properties of quartz which result from the variety of environments in which it grows and recrystallizes. There is a tendency to regard quartz as a pure substance with negligible differences in composition and properties. Chemical analyses indicate that departures from the ideal composition are small, relative to the variations from pure end-members in other minerals; the quartz structure has indeed exceptionally low tolerance for most ions other than Si^{4+} and O^{2-}. However, the amounts of foreign ions present and the magnitude of structural differences are not necessarily a measure of their importance in petrologic deduction. Any measurable variation in a common mineral such as quartz is potentially a key to significant information regarding geologic processes; it was with this in mind that a detailed study was undertaken of the high-low inversion of quartz from various sources.

One of the fundamental characteristics of quartz is that it exists in two crystalline modifications: low quartz (or α quartz) below and high quartz (or β quartz) above a transformation temperature which has been considered by many to be a constant, or variable only within very narrow limits. Sosman (1927, p. 116) gave $573^\circ \pm 1^\circ$ for the rising temperature inversion, a figure based largely upon the work of Bates and Phelps (1927), but he recognized that the inversion point may not be constant for all kinds of quartz. C. N. Fenner (1913), who was one of the few investigators to use powdered samples and quartz from geologically different sources, obtained a wider range of results.

The high-low inversion was first noted by Le Chatelier in 1889, and it has since been studied by numerous investigators (see Sosman, 1927), most of whom used selected clear transparent quartz in the form of plates or single pieces of other shapes. Samples consisting of single, shaped pieces are convenient, of course, for measurements involving location of the high-low transformation by observation of the abrupt change of volume or of optical properties, but one practical result of the choice of such method is to limit the investigation to large clear crystals, that is, mainly to quartz which has grown in open cavities in pegmatites and veins. By contrast, adequate study has not been given to the fundamental properties of

quartz which occurs disseminated as a major constituent of the most common rocks.

The investigation here reported has grown out of the demonstration by Tuttle (1949*a*) that the inversion temperature of quartz differs in samples of contrasted origin. The ease and precision of determination of the relative inversion temperature have been increased and a sufficiently large number of different samples has been studied to allow some correlation between the inversion and the types of rocks from which the quartz was obtained.

The studies followed two avenues of approach, one being the investigation of inversion characteristics of quartz synthesized under known conditions of pressure, temperature, and chemical environment, the other consisting of studies on the inversion of suites of natural quartz from different sources.

METHOD OF MEASUREMENT

The inversion-break temperature and characteristics were determined for granular samples of quartz (sized to $-35 + 200$ mesh) by recording the accompanying heat effect on a potentiometer chart in such a way that it can be scaled for temperature. In order to make precise determinations for a large number of samples without repeated thermocouple calibration as a separate operation, a differential thermal method was developed whereby the quartz is heated together with reference materials having solid-state transformations that take place at known temperatures, and which therefore serve as fixed points and in effect allow calibration as an integral part of each run.

The differential thermal method gives a graphical record of the thermal effect due to inversion of a sample under specific conditions of sample size, heating rate, and placing of the thermocouple. By keeping those conditions constant, and by the use of a reference sample heated under identical conditions at the same time as the "unknown" sample, it is possible to choose comparable points on the thermal curves and to obtain a comparison temperature for the inversion of an "unknown" sample in relation to that of a reference sample. On the basis of preliminary runs it was found that a point at the intersection of the base line produced with a line drawn along the first straight portion of the differential thermal

curve (see fig. 5) is both reproducible and easily located. The temperatures of points located in that manner are used throughout in order to compare the inversion of different samples.

The differential thermal method does not give directly the true inversion temperature defined as that temperature at which the high and the low forms can coexist in equilibrium. An analysis of the relationship between the thermal effect and the inversion under idealized conditions shows that the true inversion temperature (under equilibrium conditions) probably lies somewhere in the range between the temperatures of completion of the thermal effect on heating and on cooling. For purposes of the present study, however, the inversion temperature as precisely defined is less significant than comparison of different samples of quartz. Therefore no attempt was made to determine the true inversion temperature; recorded temperatures in all cases are those determined by the method of straight-line intersection and are referred to as comparison temperatures or inversion-breaks.

The apparatus is shown in a schematic diagram in figure 1. The sample of "unknown" quartz is packed into No. 1 of four symmetrically disposed chambers[1] in a silver sample block of cylindrical shape. Chamber No. 2 of the silver block is packed with a granular sample of cryolite, Na_3AlF_6, which has a reversible high-low inversion about 10° below that of quartz. Chamber No. 3 contains one of two samples of reference quartz which were run repeatedly so that the temperature of the thermal effect is accurately known. Chamber No. 4 is packed with a sample of specially purified K_2SO_4 which has a reversible inversion about 10° above that of quartz. Both cryolite and K_2SO_4 have heats of transformation several times greater than that of quartz.

The four chambers of the sample block are capped by mullite insulators and connected by a four-junction differential thermocouple, one junction in each, made of 90Pt 10Rh versus 60Au 40 Pd (Vines and Wise, 1941).[2] The E.M.F.'s of alternate junctions are opposed so that the resultant E.M.F. across b-c of figure 1 is zero when the four samples are at the same temperature. An additional AuPd lead is connected to the

[1] Dimensions of cylindrical chambers: diameter 5 mm., length 8 mm. Average weight of granular quartz sample used, 300 mg.

[2] This thermel has an E.M.F. which changes about 56 μv per degree, in the range in which it was used.

junction which projects into chamber No. 1, so that the sample temperature can be obtained independently from a reading of the E.M.F. across a-b of figure 1.

The silver sample block is suspended in a refractory tube at the hotspot of a vertical nichrome-wound furnace, whose heating rate is controlled by a motor-driven rheostat, shown

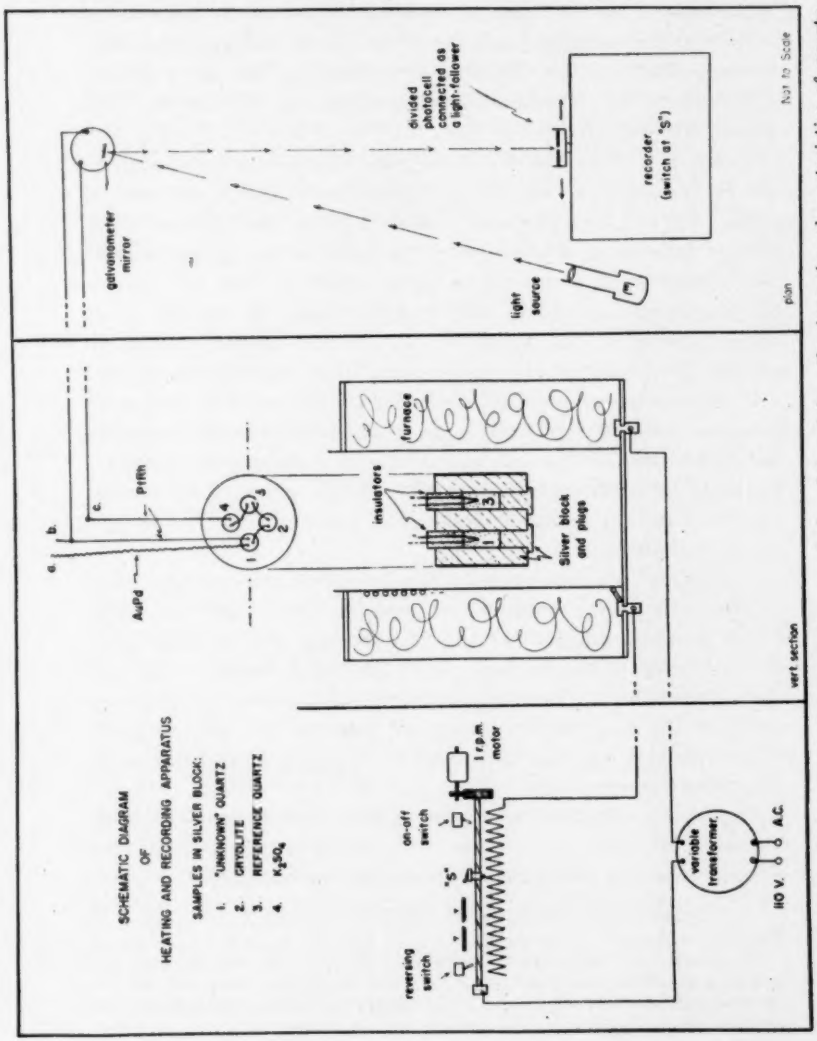

Fig. 1. Schematic diagram of the apparatus used for determining the inversion characteristics of quartz.

schematically in the left-hand part of figure 1. The rheostat motor-drive assembly serves also to actuate three control switches: a reversing switch and an on-off switch by means of which the length of the heating and cooling cycle can be pre-set, and a microswitch "s" that turns on the recorder for short periods which can be selected by adjustment of the tracks T-T, beveled so that one of them is by-passed by the microswitch on the heating cycle, the other on the cooling cycle. The heating rate can be adjusted by changing the drive gears. Throughout the investigation a heating rate of 0.5° to 0.7° per minute was used.

Leads b-c, from the four-junction differential thermocouple, are connected to a sensitive galvonometer (right-hand part of figure 1) and a light spot reflected from the galvanometer mirror falls on a divided photocell which is supported on the pen assembly of a recording potentiometer.[3] The two halves of the divided photocell are opposed and the output leads are connected to the amplifier unit of the recorder so as to actuate the potentiometer motor drive when one-half the photocell receives more illumination than the other. The photocell and pen assembly thus becomes a light-follower and records the deflections of the galvanometer. At a fixed galvanometer-to-photocell distance the sensitivity can be adjusted by changing the external damping resistance and the shunt resistance of the galvanometer.

A routine determination of the inversion temperature of a sample of quartz contained in chamber No. 1 of the silver block involves simply starting the heating and cooling cycle by switching on the rheostat drive. Without further attention the sample and reference materials are heated and cooled through the temperature range of interest and the recorder is switched on at the appropriate time to record the heat effects of the inversions.

Figure 2 shows three examples of the chart records obtained. Those illustrated are records of inversions on cooling; the records of rising temperature inversions are similar.[4]

[3] Brown Instrument Company, Potentiometer 153 x 12 V — x — 30, 0-10 millivolts.

[4] It should be noted that the apparent difference of sign between the quartz heat effect and those of K_2SO_4 and cryolite is due only to the arrangement of the differential thermocouple. The falling temperature inversions of quartz, K_2SO_4, and cryolite are all exothermic.

The topmost record of figure 2 shows the difference in inversion temperature between two samples of contrasted quartz. In this case the two samples, F3-14[5] and F3-44, are the ones used as standard or reference materials. If F3-44 be considered as an "unknown" for purposes of an example, it will be seen that the temperature of its inversion break can be obtained from a curve drawn through points representing the inversion-breaks of K_2SO_4, quartz F3-14, and cryolite. In practice, the fixed points are used to determine the chart scale for a given run, in terms of degrees per inch, and then the temperature difference between the reference quartz and the "unknown" quartz is scaled off the chart. The heating rate is not exactly linear throughout the interval used, but the departure from linearity is small and essentially constant from run to run.

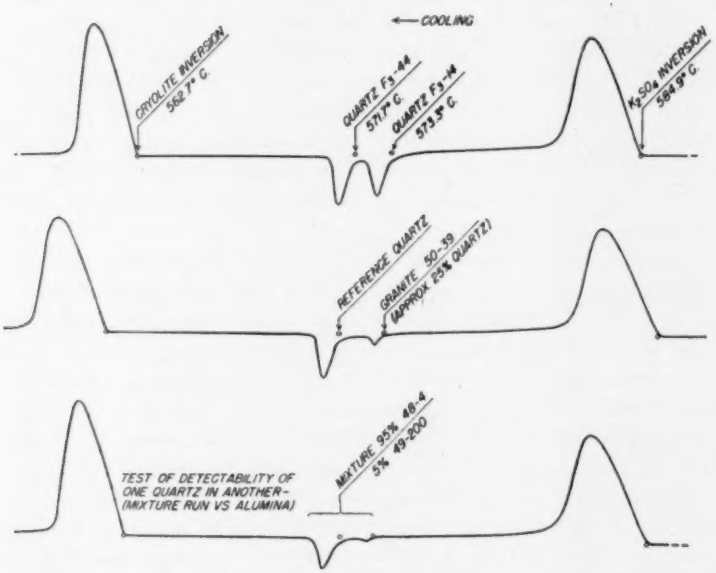
← COOLING
CRYOLITE INVERSION 562.7° C.
QUARTZ F3-44 571.7° C.
QUARTZ F3-14 573.5° C.
K_2SO_4 INVERSION 584.9° C.
REFERENCE QUARTZ
GRANITE 50-39 (APPROX 25% QUARTZ)
TEST OF DETECTABILITY OF ONE QUARTZ IN ANOTHER- (MIXTURE RUN VS ALUMINA)
MIXTURE 95% 48-4 5% 49-200

Fig. 2. Chart records illustrating thermal curves for inversion on cooling (rising-temperature records are similar). The inversion-break temperature is taken as the beginning of the heat effect, defined as the intersection of a line drawn through the first straight portion of the thermal curve with the base line.

[5] Inversion temperatures and localities of all samples are listed in the appendix.

The middle record of figure 2 shows the heat effect obtained from a sample of crushed granite estimated to contain about 25 per cent of quartz. Trial runs showed that no error of temperature determination is introduced by using a crushed sample of quartz-bearing rock instead of the separated quartz. The inversion temperatures of some of the samples of granite quartz were determined in this way in order to obviate the necessity of separating the quartz.

The lower limit of detectability of quartz mixed with another mineral, or of one kind of quartz in another kind, was tested by runs made on a mixture of two finely ground samples of natural quartz. The lower record of figure 2 shows that 5 per cent of one is easily detectable in another of different inversion temperature.

The 90 Pt 10Rh versus 60 Au 40Pd thermel was calibrated at the melting point of ice, at the melting point of zinc (419.5°),[6] and at the thermal break of the inversion of purified K_2SO_4 (rising temperature 583.5°, falling temperature 584.9°).[7] At the same time the inversion-break temperatures of a sample of natural cryolite and of two selected samples of quartz were determined in terms of the scale established by the primary fixed points. The secondary fixed points so obtained, for subsequent use as reference temperatures, are as given in table 1.

Subsequent tests showed that with use, the E.M.F. of the PtRh—AuPd thermocouple has a slow drift to lower readings. The K_2SO_4 is subject to some kind of slow change—probably due to recrystallization—upon repeated heating through its inversion, and it was therefore renewed at intervals. However, the cryolite and quartz standards show no change with repeated heating and cooling over some months of use. Over a period of two years eleven check runs were made by heating reference samples F3-14 and F3-44 together. The results of measurements of the temperature difference between their inversion-breaks can be expressed as 1.55° ± .05° on heating, and 1.61° ± 0.11° on cooling. Further confirmation of the constancy of the fixed points was obtained by the substitution of fresh

[6] National Bureau of Standards, melting point sample 43.

[7] Sample of K_2SO_4 whose inversion previously had been determined with a carefully standardized Pt versus PtRh thermel, by J. S. Burlew, Geophysical Laboratory. Inversion-break temperatures were obtained by the same construction used for the quartz curves.

samples for used samples of the standard materials at intervals. In addition, a check on the scale of temperature was provided by later runs made on quartz kindly supplied by Dr. Phelps of the Bureau of Standards from two of the crystals used by him in an earlier investigation (Bates and Phelps, 1927). Table 2 is a comparison of our data for solid cylinders of quartz, with the data of Bates and Phelps (1927, table 2) for parts of the same quartz crystals investigated by them in the form of thin plates.

On the basis of repetitive tests, it is estimated that the

TABLE 1

Inversion-Break Temperature of Reference Materials

Material	Rising temperature inversion-break °C.	Falling temperature inversion-break °C.
Cryolite, Na_3AlF_6 Ivigtut, Greenland	563.0	562.7
Quartz F3-14 Carrara, Italy	573.6	573.3
Quartz F3-44 rose quartz, source unknown	572.1	571.7

TABLE 2

Inversion-Break Temperature of Two Crystals Previously Studied at the National Bureau of Standards

Sample	Rising temperature inversion-break		Falling temperature inversion-break	
	Present investigation (cylinder)	Values given by B. & P. (plate)	Present investigation (cylinder)	Values given by B. & P. (plate)
Crystal B of Bates & Phelps No. 49-196	573.5	573.4* 573.3	572.0	572.0
Crystal C of Bates & Phelps No. 49-197	573.6	573.35	571.8	571.8

* Two determinations given.

precision (reproducibility) of the inversion data is ± 0.1°. A lower degree of precision must be assigned to data for a few samples of sluggishly inverting quartz which required grinding and which were not directly compared with reference materials heated at the same time.

EFFECT OF STATE OF DIVISION OF SAMPLES

There are pronounced differences between the inversions of samples composed of single pieces of a crystal and samples of the same mass composed of granules, and probably very slight differences among granular samples of different, very fine-grain sizes. Table 3 gives data on the inversion-break temperature of cylinders of quartz cut from single crystals, as compared with that of part of the same quartz samples in granular form (size — 35 + 200 mesh).

It will be observed that the inversion of a single piece of quartz in cylindrical form is retarded relative to the inversion of the equivalent granular sample, both on heating and on cooling. For the samples tested the average inversion lag of the cylinders is 0.9°. There is some evidence that similar retardation is inherent in large single pieces of quartz of other than cylindrical shape. Sample 49-195, part of Bates and Phelps crystal A (1927, table 2) was not large enough to permit the preparation of a cylinder to fit the silver sample block. In granular form, the sample reaches the inversion-break at 572.9° on heating and has a double thermal effect beginning at 573.2° on cooling; those figures are to be compared with Bates and Phelps data for the inversion of a thin plate of crystal A, 573.3° on heating and 572.3° on cooling. The fact that the data of Bates and Phelps (and of other investigators who have used single, shaped pieces of quartz), generally show the falling temperature inversion-break as from 1° to 2° lower than the rising temperature inversion-break suggests that the lag is a phenomenon associated in part with superheating and undercooling of large monocrystalline samples.

It is suggested in explanation that inversion in either direction probably begins around centers of local strain, such as might be found around inclusions, which "trigger" the inversion because the structure there is distorted toward greater similarity to the alternate form. The idea that inversion may be initiated at a number of different places in a crystal and not

TABLE 3

Comparison Between the Inversion of Cylinders and Equivalent Granular Samples

Sample	Rising Temperature Inversion-Break °C. (a) Granular sample	(b) Cylinder	(b)–(a)	Falling Temperature Inversion-Break °C. (c) Granular sample	(d) Cylinder	(c)–(d)
F3-21	571.8	572.3	0.5	572.0	572.0	0
49-194	572.2 571.6	---* 573.2	1.6	573.1 ---	571.9	1.2
49-196	--- 527.7	573.5	0.8	573.5 572.3	572.0	1.5
49-197	573.1	573.6	0.5	573.0	571.8	1.2
49-198R	573.2 572.0	573.3	1.3	573.2 ---	572.5 572.0	0.7
49-202	573.6	574.3	0.7	573.5	573.0	0.5
Mean difference between the inversion of a cylinder and the inversion of the equivalent granular sample			0.9			0.9

* The bracket symbol indicates a double inversion. For closely overlapping doubles, generally only the beginning can be determined—that is, the lower inversion-break on heating, the higher inversion-break on cooling.

necessarily simultaneously, is not new; it is supported by the observations of Wright, Mügge, and others, quoted by Sosman (1927, pp. 120, 121) that at the inversion temperature reflection signals from all faces become hazy and divide into multiple reflections which move relative to one another and then rejoin to form a sharp single reflection above the inversion. Imperfections which may act as inversion triggers include foreign ions which are not a good fit in the structure at temperatures near the inversion, inclusions of liquid or gas or of other minerals, and irregularities on grain surfaces.

According to the above concept, a relatively large, smooth-surfaced piece of a pure and nearly perfect crystal would have few inversion triggers and might be expected to superheat in one direction and undercool in the other, past the temperature at which it will invert if inversion triggers are supplied by surface irregularities produced when the sample is crushed to granular condition.

The chart records show other striking differences between the inversion of cylinders and granular samples. The cylinders invert very rapidly and give sharp peaks on the differential thermal records, whereas granular samples invert less abruptly and the records exhibit complexities which are reproducible and characteristic of a given sample.

The observed differences between granular samples and solid pieces prompted an investigation of possible differences among different grain-size fractions of a sample of quartz. Table 4 gives comparative data for inversion-break temperatures of four size-fractions of a sample of vein quartz (No. F3-40).

All of the results are within the error of measurement ($\pm$ 0.1° C.) with the exception of the falling temperature

TABLE 4

Inversion-Break Temperatures vs. Grain Size

Grain Size in Millimeters	Rising temperature inversion-break ° C.	Falling temperature inversion-break ° C.
0.5 to 0.15 (−35 + 100 mesh) ...	573.5	573.5
0.15 to 0.07 (−100 + 200 mesh) .	573.5	573.4
0.07 to 0.02 (−200 mesh, washed)	573.5	573.5
Less than 0.02 (elutriated)	573.6	573.7

inversion-break of the finest size-fraction, which is slightly higher. A series of tests on another sample (49-122) gave similar results. The effect of state of division in extremely fine sizes probably is deserving of a separate investigation for its possible bearing on theories of the structure of crystal surfaces. In that connection it may be noted that Stahl (1951) found some differences in the inversion temperature depending upon the kind and amount of adsorbed gas on the surfaces of a finely ground quartz sample.

It may be concluded, however, that differences of grain size of a sample of quartz do not have an appreciable effect on the inversion within the range of particle size (— 35 + 200 mesh) used for the routine measurements.

FACTORS THAT MAY INFLUENCE THE INVERSION TEMPERATURE

The temperature of any polymorphic transformation can be influenced by compositional changes in the material and by physical change in the crystals or their environment. Compositional variations by solid solution may cause the inversion temperature to be raised or lowered, depending on the solubility relations of the "impurity" in the high and low temperature modifications in the "inversion interval." This relation can be illustrated by theoretical equilibrium diagrams (fig. 3). Figure 3A illustrates the change of inversion temperature under equilibrium conditions when the solubility is greater in the high temperature modification than in the low form and 3B shows the relationships when the solubility is greater in the low temperature form.

Figure 3A is drawn for a case in which the solubility continues to increase in the high form at temperatures above the inversion interval. Theoretically the solubility above the inversion may either increase or decrease. In the case shown, crystals grown above the inversion (assuming total composition to the right of HI) would, under equilibrium conditions, unmix some of the "impurity" as the temperature is lowered and the composition of the high form would change along the line IH. At the temperature (and composition) of H the inversion would begin. Consider, now, a crystal whose composition is represented by E. Under equilibrium conditions if this crystal is heated to a temperature at E, inversion to the high form will begin. The first material to appear as the high

form will have a composition represented by F and as the temperature is raised the low form will change composition along the curve EG while the high form changes composition along FD. At a temperature corresponding to G the inversion will be completed and the high form will have a composition D. On cooling through the inversion these relations will be reversed.

Solid solution, then, requires, under equilibrium conditions, compositional changes during inversion and the high and low forms must coexist throughout a finite temperature range. It seems unlikely that the heating rates utilized in the present study would permit quartz to obey in detail these equilibrium requirements when heating or cooling through the inversion interval because of the compositional changes demanded. However, quartz grown in the presence of lithium and aluminum has the temperature of inversion lowered as the temperature of growth is increased (see p. 220). Also inversion temperatures of quartz grown at different temperatures in the presence of germanium are raised, and the lower the temperature of growth the higher the inversion (see specimens Q1-1C and Q1-2A in the appendix). Thus, the general requirement of raising or lowering of the temperature of inversion with increased solubility in the low or high form appears to be obeyed.

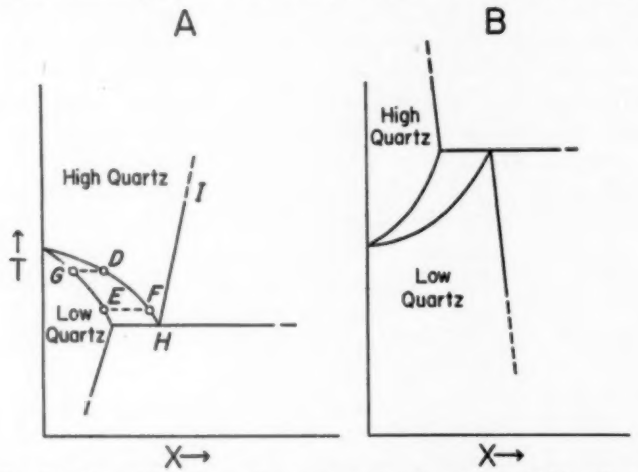

Fig. 3. Theoretical phase diagrams illustrating the probable effect of solid solution on the quartz inversion for cases in which A, solubility of the "impurity" (e.g., Li + Al) is greatest in the high temperature form; and B, solubility of the "impurity" (e.g., Ge), is greater in the low temperature modification.

In the case of lithium and aluminum the solubility increases at temperatures above the inversion and on cooling through the inversion interval it is likely that the composition is to the right of the point H (fig. 3A) and the inversion takes place at a temperature that would probably be represented by a metastable extension of the curve DFH to lower temperatures.

Inversion temperatures can be influenced by variations in hydrostatic pressure and in the case of quartz this effect has been investigated by Gibson (1928) and recently by Yoder (1950). The inversion temperature is raised approximately 1° C. by each 40 atmospheres pressure.

Inversion temperatures can also be influenced by directed pressure. This effect has apparently not been investigated, but it undoubtedly varies with crystallographic direction and will tend to raise the inversion temperature if the net effect of the resultant stress in the crystal acts in such a manner that the volume increase on changing to the high modification is opposed. If the directed pressure tends to increase the volume, the inversion temperature will be lowered.

Studies of the inversion of novaculite and chert (see page 244) indicate that directed pressure is operative in altering the inversion temperature. For example, no heat effect could be discovered in two novaculite specimens until the material was fine-ground to a size approaching that of individual crystal units. This has been interpreted as being the result of differential stresses being set up, on heating, in coarse grains that are made up of a mosaic of fine grains, because of the variation of the coefficient of expansion with crystallographic direction.

This effect can apparently also be operative in changing the inversion character of single crystals with strong development of lineage structure, as such specimens may show a greater heat effect after being fine-ground (see p. 246). The smaller heat effect before grinding is attributed to the effect of differential stresses being set up at lineage boundaries by slight misorientation of adjacent lineage units.

THE INVERSION OF SYNTHETIC QUARTZ GROWN AT DIFFERENT TEMPERATURES

Synthesis of quartz under controlled conditions is difficult and time consuming except under special conditions. In certain

environments—for example, in sodium hydroxide-water solutions—growing of quartz is relatively easy at temperatures above 300° C. and pressures above 5000 psi (pounds per square inch), but when the chemical environment is changed and the alkali omitted, the rate of growth is exceedingly slow.

Two sets of experimental syntheses were carried out, however. In the first set the initial materials were crushed pure silica glass, sodium hydroxide and water; no quartz seed plates were used. Runs were made in a stainless steel pressure vessel with a seal slightly modified from that used by P. W. Bridgman (see Tuttle, 1949*b*). Temperature was maintained to ± 5° C., and pressure was maintained at 15000 psi by means of a pump with a gauge-operated on-off control. Each run was of five to twelve days' duration. Samples of quartz obtained from a series of such runs consisted of small clear crystals of about 2 mm. maximum length. Investigation of the inversion characteristics of the quartz revealed that in the system Na_2O—SiO_2—H_2O there is apparently a general inverse relationship between the temperature of growth of quartz and the temperature at which it inverts on cooling (fig. 4). A plot of growth-temperature versus rising-temperature inversion-break is less regular and suggests a discontinuity at about 590°C., which is the temperature of inversion at the pressure under which the quartz was grown (Yoder, 1950). It would be desirable to have additional data on quartz grown between 300° and 500°. Two runs in that temperature range yielded quartz but the product is almost entirely a fine-grained mosaic intergrowth which apparently formed by direct crystallization of the silica glass used as source material, rather than by solution of silica glass and concurrent crystallization of quartz. The fine-grained quartz mosaic does not give a measurable heat effect in the inversion range until it is ground to a size approaching that of the crystal units of the mosaic. Even in that condition the inversion is very sluggish and difficult to measure precisely. The inversion characteristics are much the same as those of natural novaculite which has a similar fine-grained mosaic texture (see p. 244).

A series of quartz syntheses at a pressure of 4000 psi was left incomplete for the same reason—namely, that at temperatures around 400° C. the silica glass crystallizes directly to a fine-grained mosaic intergrowth of quartz and does not

go into solution rapidly. It is probable that syntheses from silica gel as initial material would avoid the difficulty encountered with silica glass.

In a second set of experiments quartz was grown in the presence of some ions which can be incorporated in larger amounts than sodium in the quartz structure (ionic radii nearer to Si^{4+}). In three runs a previously prepared glass containing about 93 per cent silica and 7 per cent germania was substituted for the silica glass as source material. Quartz grown at 600° C. and 15000 psi from germania-bearing source material has a sluggish inversion which begins at 591° ± 2° on both heating and cooling; that is, about 18° above the mean inversion temperature of natural quartz. Quartz grown

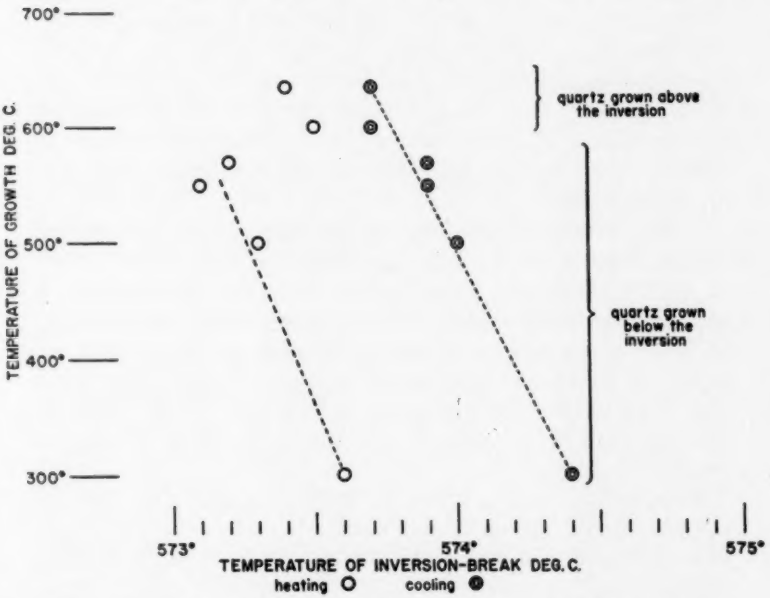

Fig. 4. Inversion results on quartz grown under controlled conditions. All samples were synthesized at 15000 psi in a stainless steel pressure vessel charged with silica glass, sodium hydroxide and water. Sample numbers of synthetic quartz: (°C.) 635, Q1-1D
600, 49-156
568, 49-162
550, 49-161
500, 49-157
300, 48-107

at 500° and 400° from the germania glass apparently is even more abnormal; the thermal curve of the 500° sample shows a change of slope at about 623° C., while the 400° sample either does not invert or it inverts so slowly that a thermal effect could not be detected with maximum amplification.[8] X-ray patterns of the 400° sample mounted in an X-ray goniometer furnace (G. L. Davis, Geophysical Laboratory), suggest a very gradual inversion which begins at a temperature of about 640° on heating. The higher inversion temperature and more sluggish inversion of the samples grown below the inversion indicate that Ge^{4+} can proxy for Si^{4+} in greater amounts in the low than in the high quartz structure.

A pressure run at 500° C., in which glass of molecular proportion $Li_2O \cdot Al_2O_3 \cdot 12SiO_2$ was used as source material, produced quartz (sample No. Q1-2B) which inverts so slowly that the thermal effect is below the limit of detectability with the apparatus. By means of an X-ray goniometer furnace (H. A. McKinstry, Pennsylvania State College) the inversion on heating was located at 550° ± 15°. Unit cell dimensions of both the high and the low form are slightly larger than that of normal quartz.

A sample of the same bulk composition prepared by sintering the finely ground component oxides for 15 hours at 1300° C. (F. A. Hummel, Pennsylvania State College) exhibits a similar slow inversion at a still lower temperature, 463° ± 15° on heating, located by plotting the peak shifts obtained by means of the X-ray goniometer furnace. It should be noted that both of the above samples, Q1-2B and 50-217, contain β spodumene in an amount approximately equal to that of the quartz phase.

Roy and Osborn (1949, p. 2089) suggest the possible stabilization of high quartz at room temperature by incorporation of lithium, and they refer to the demonstration of Winkler (1948) that the lithium ion is of just the right size to fit into "holes" in the high quartz structure. The present data are in close agreement with the observation of F. A. Hummel (1951, p. 238) who made thermal expansion tests on sintered lithia-alumina-silica mixtures similar to sample 50-217 and reported a sluggish inversion at a temperature

[8] At maximum amplification the thermal peak due to inversion of a normal quartz is more than 3 feet high in the plane of the recorder chart.

between 400° and 500°. The observed lowering of the inversion temperature caused by lithium and aluminum suggests that near the inversion those elements can be incorporated in larger amounts in high than in low quartz.

Another sample of synthetic quartz (49-141) with abnormal inversion characteristics was kindly supplied by Dr. James Schulman from a suite prepared during his investigation (Schulman *et al.*, 1949) of the crystallization of silica. The sample consists of a mixture of 100 mols of silica and 1 mol of calcium carbonate which had been fired for 3 days at 1150°. It exhibits an extremely sluggish inversion which is barely detectable and is spread out over such a wide range of temperature that it was not considered feasible to measure the temperature at which inversion begins.

Much additional work will be required in order to determine in detail the relationships between inversion characteristics and conditions of growth of synthetic quartz. The present data support the evidence offered by data on natural quartz in two respects: first, that the temperature of growth has a measurable effect on the temperature of inversion of quartz, and second, that the differences of inversion temperature as well as the extreme slowness of inversion of some samples are due primarily to solid solution.

SPECTROCHEMICAL ANALYSES OF QUARTZ WITH DIFFERENT INVERSION CHARACTERISTICS

Spectrochemical analyses have been made on a few quartz specimens to see what chemical variations in minor element content could be found and whether they were related to inversion differences. The analyses were kindly carried out by K. J. Murata of the United States Geological Survey, L. H. Ahrens of the Massachusetts Institute of Technology, and H. L. Lovell of Pennsylvania State College.

The first material selected for study was taken from two zones of a large clear quartz crystal of oscillator grade from Brazil that showed two peaks on the differential thermal curve. The two peaks were found to be related to two zones in the crystal which, after irradiation by X-ray, developed color banding that permitted separation into two fractions (fig. 5). Spectrochemical analyses gave the following results:

	Fe	Mg	Al	Ca	Inversion-break Temperatures ⌐Heating¬	⌐Cooling¬
Core zone	.00X	.00X	.00X	.00X	572.8	572.2
Outer zone ...	not detected	.000X	.000X	.00X	573.6	573.4

The following elements were looked for but were not detected: Cu, Ni, Sn, Pb, Ge, Ti, Zn, Mn, Cd, B, Be, Co, Ba, Sr, Ga, In, Tl, Ag, Bi, Y, La, Zr, Cr, V, Re, Th, U, W, Cb, and P. No data were obtained for the alkalies. The differences are not great, but the core zone does show significantly larger amounts of Fe, Mg, and Al than does the outer zone. This suggests that the core may have grown at a higher temperature than the outer zone and that greater amounts of impurities were incorporated at the higher temperature with the result that the inversion-break temperature is lowered. Substitution of Al^{3+} and Mg^{2+} probably would have an effect similar to that caused by substitution of Al^{3+} and Li^{+} (see p. 220).

Spectrochemical results on four samples with different inversion characteristics are shown in table 5. Sample F3-17 has a normal slightly high inversion-break temperature, 48-4 has a low inversion-break temperature on heating and cooling, F3-18 has an extreme difference between heating and cooling inversion-break temperatures, and 49-148 has an extremely low, barely detectable slow inversion spread out over a range of about 20° C.

The table shows that F3-17, which has the highest temperature inversion-break, with a normal strong heat effect, has a greater amount of Cu, Ti, and Mg than the others. The concentration of Li, Na, and K is greatest in 49-148 which has the lowest and most sluggish inversion of all the investigated samples of natural quartz. Specimens 48-4 and F3-18 contain a smaller amount of lithium than 49-148 and the lithium content of F3-17 is below the limit of detectability.

In view of the effect of Li and Al on the inversion temperatures of synthetic quartz (see previous section) it is suggested that the unusually low inversion temperature of 49-148 may be due to solid solution of that type. The low values for the inversion-break temperature of 48-4 and F3-18

may also be a result of that substitution. An idealized substitution formula can be written as $Li_X(Al_XSi_{1-X})O_2$.

Germanium was not looked for in these specimens, but it is reported as being below the detectable limit in the two zones of the previously mentioned crystal. The experiments on synthetic quartz show, however, that germanium can be incorporated (see p. 219) in the quartz structure, probably by substitution for silicon, and the effect of substitution is to raise the inversion temperature.

The most probable general relationship between the amount

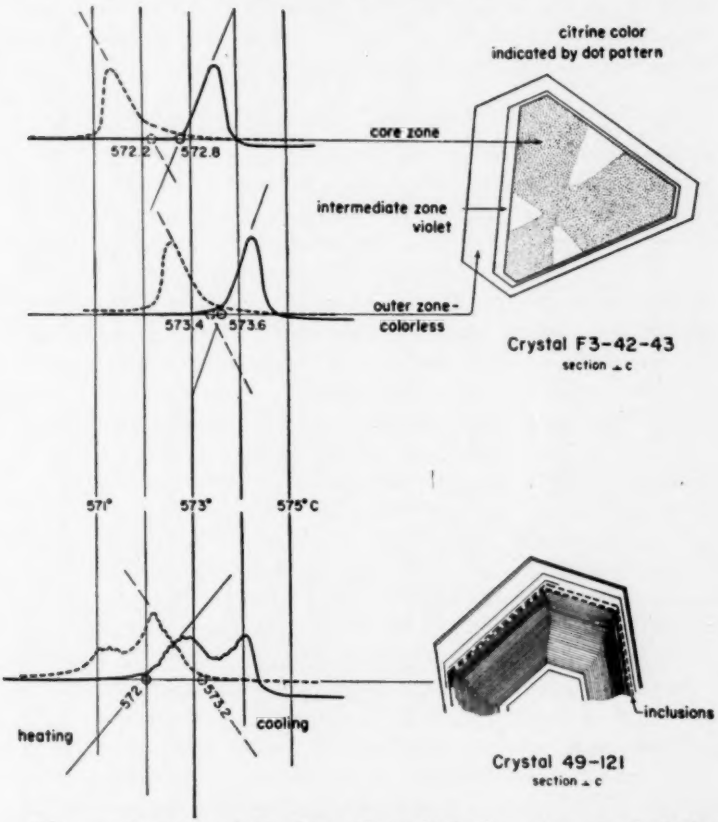

Fig. 5. Character of the heat effect obtained on two zoned single crystals. Crystal F3-42-43 was separated into two fractions as illustrated and the inversion of each fraction is shown (solid lines = thermal effect on heating, dashed lines = thermal effect on cooling).

TABLE 5

Spectrochemical Analyses*

Sample No.†	Cu	Ti	Mg	B	Li	Na	K	Inversion-break Temperatures Deg. C. Heating	Cooling
F3-17	.01 – .001	.01 – .001	.01 – .001	Not sought	Not detected	.0001 – .0005	Not detected	573.6	573.4
48-4	~ .0001	Not detected	< .001 ?	Not sought	.001 – .005	.0001 – .0005	Not detected	571.8	571.9
F3-18	~ .0001	Not detected	< .001 ?	~ .001	.001 – .005	.0001 – .0005	Not detected	570.3	573.2
49-148	< .0001	Not detected	< .001 ?	~ .002	.1 – .01	.03 – .001	.005 – .0005	536.	Not detected

* Al is present in all samples (.01 – .001 per cent), but 49-148 is estimated to have about four times as much as F3-18. Ba and Fe are reported in small amounts in all four samples.

Ag, V, and Sr are doubtful trace constituents (possible electrode impurities); Mn, Cr, Co, Ni, Pt group, In, Ga, Zr, La, Nd, Y, Be, Rb, and Cs were looked for but not found. Ge and Au were not detected in F3-18 and 49-148 (not looked for in the other two specimens).

The limit of detectability for Li, Na, and K is .0001 per cent, for Rb and Cs, .0003 per cent.

† See appendix for localities.

of lithium and aluminum solid solution and the change of inversion is shown in the theoretical equilibrium diagram, figure 3A, and the probable effect of germanium solid solution is represented by figure 3B.

Consideration of ionic radii and valence requirements suggest other elements that may have a limited solubility in the quartz structure. For example: Mn^{4+}, Ti^{4+}, S^{4+} and Se^{4+} are theoretical possibilities. Also, in addition to the Al^{3+} substitution discussed above, other small trivalent ions might occupy Si^{4+} positions, providing such substitutions were accompanied by incorporation of Li^{+} or Na^{+} or perhaps small bivalent ions in the "holes" in the quartz structure in the required proportion to balance the valence requirements.

VARIATION OF OTHER PHYSICAL PROPERTIES OF QUARTZ

X-ray studies.—Variation of the (234) spacing of 23 quartz specimens, most of which show unusual inversion properties, has been measured in the back reflection region using a Philips Geiger Counter X-ray Spectrometer and a General Electric XRD-3 spectrometer.

The (234) spacing was chosen for three reason: first, the reflection is strong and usually sharp; second, preliminary examination indicated that this reflection shows marked variation from sample to sample; and third with $Cu_{k\alpha}$ radiation the (234) reflection was the highest 2θ that can be utilized with the available instrument.

No attempt was made to determine the absolute value of the (234) spacing with high accuracy for any of the specimens examined. However, the instrument was roughly calibrated by mixing silicon powder with the quartz and measuring the relative positions of the $(642)_{\beta}$ reflection of the silicon and the $(240)_{\alpha_1}$ reflection of quartz. The 2θ value of the $(642)_{\beta}$ reflection was taken as 147.15°.

Differences between the (234) spacings of the quartz samples studied are reproducible to ± 0.01° 2θ for samples with sharp reflections. More diffuse reflections are somewhat less well located, but the maximum error is less than ± 0.03° 2θ between any two values given for 2θ.

Results are shown in table 6. The greatest variation in the (234) spacing was found to be 0.41° 2θ, or .00067 Å. Cell dimensions were calculated for two extreme specimens of

natural quartz, F2-16 and 49-148, using the (234) and (240) reflections, with the following results:

	a	c
F2-16	4.9131	5.4036
49-148	4.9172	5.4069

The differences in cell dimensions strongly support the hypothesis that solid solution of foreign atoms is responsible for the observed differences in inversion properties of quartz. The extreme cell dimension difference corresponds to a density difference between F2-16 and 49-148 of 0.006, and that in turn corresponds to a difference in mean index of refraction of approximately .001. Unfortunately specimen 49-148 is fibrous and its indices of refraction cannot be measured with the accuracy necessary to check the theoretical difference between the two samples.

TABLE 6

Variation in the (234) Spacing of Quartz*

Specimen No.	Source	2θ	d	Inversion-break temperature — Heating °C.	Inversion-break temperature — Cooling °C.
F2-16	Quartz vein	153.57	.79120	573.3	573.2
49-25	Phenocrysts from rhyolite	153.56	.79122	572.4	572.7
F3-34	Novaculite	153.56	.79122	573.7	573.8
F3-38	Cavity in dolomite	153.56	.79122	573.6	573.5
49-183	Geode in limestone	153.55	.79123	573.6	574.0
F2-2	Novaculite	153.55	.79123	573.7	574.3
F3-17	Quartz vein	153.55	.79123	573.6	573.4
49-141	Synthetic	153.55	.79123	not located	
49-103	Welded rhyolite tuff	153.54	.79125	572.8	572.5
F2-14	Cavity in limestone	153.54	.79125	573.5	573.5
F3-21	Phenocryst from rhyolite	153.53	.79126	571.8	572.0
F3-18	Unknown	153.53	.79126	570.3	573.2
49-29	Cavity in lead-silver ore	153.53	.79126	570	574
48-4	Zoned pegmatite	153.51	.79130	571.8	571.9
F2-1	Chert from limestone	153.49	.79133	573 ± 2	573 ± 2
49-142	Unknown	153.47	.79137	571.7	574.2
Q1-1B	Germanium-bearing synthetic	153.30	.79164	not located	
Q1-1C	Germanium-bearing synthetic	153.28	.79167	623 ?	....
49-28	Pegmatite	153.26	.79170	545	564
49-148	Unknown	153.21	.79179	536	....
Q1-2A	Germanium-bearing synthetic	153.16	.79187	592	591

* See appendix for localities.

Color varieties, and change of color upon heating.—The present inversion studies have been related primarily to geologic occurrence of the quartz samples and we have not made an extensive comparison of the inversion of color varieties of quartz. Three examples of rose quartz have sharp inversions with inversion-breaks below 572.9°, while one example of amethyst has an inversion-break at 572.3° on heating and 573.4° on cooling. The inversion of smoky quartz varies with geologic occurrence. Two examples of blue quartz associated with titanium-bearing minerals, and examples of quartz containing inclusions of tourmaline, rutile, and actinolite respectively, show high inversion-breaks in the range 573.2° to 573.6°.

Many of our samples of originally colorless quartz develop a pale color upon being heated through the inversion; most common are tints of yellow and brown. On the other hand, a few samples which were originally colored (e.g., smoky and citrine quartz), are paler after the inversion run.

No detailed analysis of the color phenomena or of possible correlation with inversion characteristics has been attempted, but a few extremes may be noted. Strong yellow color develops in some samples from zoned pegmatites in the Black Hills, South Dakota, as well as in quartz from two veins in the same district. McIntyre Mine samples develop different tints of yellow and brown. A cluster of tabular yellow crystals from Hot Springs, Arkansas, is blue-gray after being heated through the inversion, while a specimen of "Cat's Eye" (originally orange yellow), described as secondary after crocidolite, develops a strong red color after heating.

Lack of color or extremely pale color after heating through the inversion may be one criterion of purity of quartz. Those which remain colorless or nearly so include many of the crystals from Brazil and Arkansas and all those from vugs in limestone, with one exception—sample F3-14 from the Carrara marble in Italy, which has a very pale green color after being heated.

Variation in oxygen isotope ratios.— An investigation[9] of oxygen isotope ratios in quartz, to be reported at a later

[9] M. L. Keith and G. L. Davis, Geophysical Laboratory, in cooperation with M. A. Tuve and J. B. Doak, Department of Terrestrial Magnetism, Carnegie Institution of washington.

date, shows measurable variation in the $O^{18} : O^{16}$ ratio in natural quartz samples of different geological history.

DIFFERENCES OF INVERSION TEMPERATURE WITHIN SINGLE CRYSTALS

Large single crystals of quartz are most commonly found in open spaces or formerly open spaces in quartz veins or in pegmatites; some occur in cavities in sedimentary rocks, notably in limestones. Those from pegmatites and veins are mostly non-uniform. They are generally zoned, although in many cases the zoning is not apparent upon casual examination. One of the most striking results of the earlier part of the investigation was the discovery that many single crystals show more than one high-low inversion. Sample F3-42-43, a clear and colorless crystal of "oscillator grade" quartz from Brazil, was selected for use as a standard in preliminary runs. Upon detailed study it was found to give two distinct heat effects on inversion. The double inversion, the first encountered in this study, was very puzzling until a section of the crystal was irradiated with X-rays,[10] with resultant development of a citrine color in alternate prism face loci of the core, and amethystine color in a narrow intermediate zone, while the outer zone remained clear (fig. 5). The two principal zones were separated and studied individually; each gave a single heat effect, the quartz from the core inverting at the lower temperature, that from the outer zone inverting at the higher temperature. Spectrographic analyses of the quartz from the two zones are reported on page 222.

A large crystal (12.5 inches long) of Brazilian quartz, kindly supplied by Earl Ingerson of the U.S. Geological Survey, was cut in half parallel to crystallographic "c" and was sampled by drilling and slicing pieces from different parts of the crystal and then crushing each for study. The results of inversion test on the four samples so obtained are shown by reproduction of the differential thermal curves in figure 6. The crystal apparently contains at least three different kinds of quartz. A small slice of sample "R," cut normal to a rhombohedral face, was exposed to an X-ray beam for 30 hours with the resultant development of two

[10] Cu radiation, $\lambda = 2.54$ Å

principal color bands and narrower, alternately paler and darker bands of a smoky violet color, similar to those obtained by Frondel (1945) in quartz oscillator plates irradiated with X-rays. The banding is parallel to crystal faces and obviously represents zonal growth. No attempt was made to separate contrasted quartz in this case, but it seems reasonable to infer that the two principal color bands developed by irradiation probably can be correlated with the broad double inversion.

A third sample worthy of special mention is part of a crystal[11] from Hot Springs, Arkansas, which was used by R. E. Gibson (1928) for a study of the effect of pressure on the high-low inversion, and which he kindly made available for this investigation. The crystal was originally color-

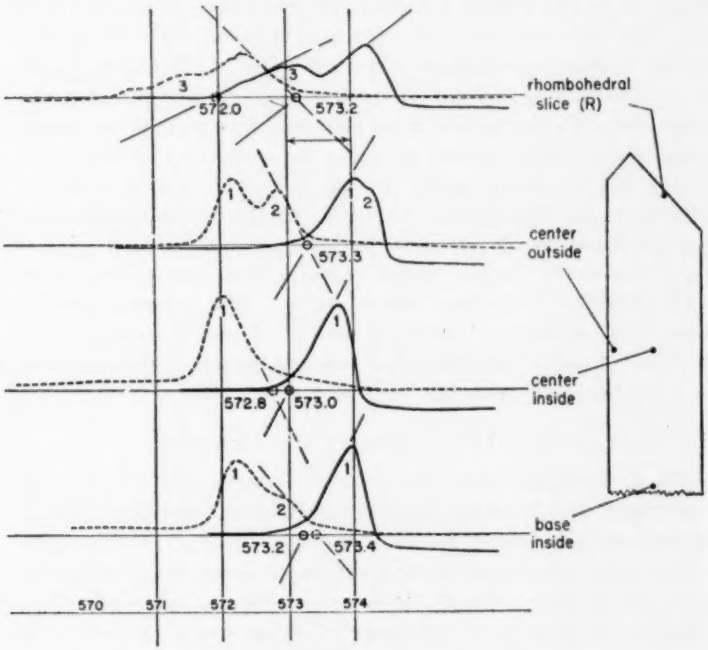

Fig. 6. Differential thermal curves of samples taken from different parts of a large (12.5" long) quartz crystal from Brazil (solid line curves = heating, dashed-line curves = cooling). See text for discussion of results.

[11] Sample 49-121 U. S. National Museum No. 83660.

less and clear except for a phantom outlined by a thin double line of inclusions faintly visible in a slice cut normal to crystallographic "c." Upon irradiation with X-rays the core of the crystal, inside the line of inclusions, developed a closely spaced zonal banding in smoky shades, while the outer rim remained nearly colorless except for a few thin smoky zones parallel to the prism faces. Figure 5 shows the appearance of part of the slice after irradiation. A tracing of the chart record of the inversion is included to show the complex multiple inversion with two principal composite peaks.

Comparison of records of inversion of monocrystalline quartz cylinders with those of equivalent granular samples (table 3), shows that when a solid piece composed of two different kinds of quartz is heated through the inversion, both inversions are retarded and they take place at temperatures which are closer together than those obtained when the different kinds of quartz are separated from one another by crushing. In some cases the monocrystalline piece exhibits a single inversion peak while the equivalent granular sample has a double peak (table 3). Probably many of the instances described in the literature of shattering of quartz crystals and slices upon passing through the inversion are the result of strains caused by inclusion in the test piece of more than one growth zone with different inversion temperatures. The present studies show that in many instances zoning of single crystals can be inferred from the differential thermal curves of the inversion of representative granular samples.

QUARTZ FROM GRANITES AND RHYOLITES

On a statistical basis the inversion temperatures of quartz from granites is different from quartz of rhyolites. These differences are shown figure 7 which is a plot of inversion-break temperatures on heating versus inversion-break temperatures on cooling. All of the inversion breaks are single; the common complexity of inversion of large single crystals and of some quartz from zoned pegmatites is completely absent in quartz from granite and rhyolite.

The samples of quartz from rhyolites used in this study are mainly from western United States localities. Granites included in the study are from various North American localities, including the New England States, Texas, South Dakota,

Wyoming, and Colorado (see appendix for localities). The inversion of one sample of quartz from a rhyolite (heating inversion-break 573.6° C.) is well outside the main group of values of rhyolite quartz inversion temperatures. This specimen is from Judith Peak, Montana. The quartz in some samples of Pike's Peak granites and in granite from three localities in Maine inverts at temperatures outside the main group of points representing granite-quartz, and closer to the mean inversion of rhyolite quartz. Quartz from the Pike's Peak granite shows a wide variation in inversion-break temperature from one specimen to another.

Despite the exceptions, the results are taken to indicate a significant difference between the environment of final

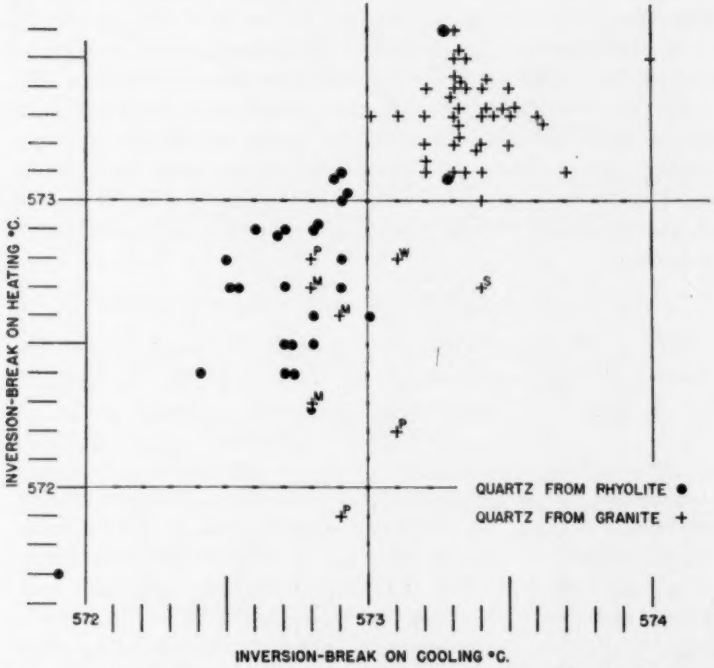

Fig. 7. Inversion of quartz from granites and rhyolites. The higher temperature of inversion of most of the granitic quartz studied is believed to indicate that the quartz recrystallized at relatively low temperatures. M = granites from three localities in Maine: North Sullivan, Jonesport, and Wallace Cove. P = Pike's Peak granite. W = granite from Westwood, Mass. S = White Silver Plume granite from Colorado, sample 49-55.

crystallization of "granite-quartz" and "rhyolite-quartz." The explanation of the difference may lie in a study of the effects of recrystallization. It is likely that rhyolite-quartz as well as granite-quartz crystallizes under abyssal conditions; however, it is probable that granites generally recrystallize in the late stages of magmatic activity when pressure is raised owing to concentration of volatile constituents in progressively smaller intercrystalline volume (Tuttle, 1952). During that stage, early-formed quartz phenocrysts probably are made over so as to take on properties attendant upon crystallization in an environment of lower temperature and high pressure. An investigation is being undertaken with the objective of discovering whether more than one kind of quartz may be found in border zones or offshoots of granite, where recrystallization may have been incomplete.

No attempt was made in the present study to select or distinguish different types of granite based upon possible differences of origin. It may be noted, however, that most of the granites studied to date are massive and equigranular rather than gneissic. A collection is being made for further investigation of granitic rocks which appear from field evidence, structure, or texture to have developed by replacement processes.

INVERSION STUDIES ON QUARTZ FROM PEGMATITES

The quartz from unzoned pegmatites is characterized by sharp uncomplicated differential thermal peaks, in contrast to the quartz of zoned pegmatites, the inversion peaks of which are in many cases double, complex, or asymmetric. Further, the inversion temperatures of quartz from "simple" pegmatites fall in a comparatively narrow temperature range, whereas the range of inversion temperatures of quartz from zoned pegmatite is nearly as great as that of all other types of quartz combined. For example, of fourteen specimens collected from simple pegmatites in which no zoning was apparent, only one has an inversion-break temperature on cooling at a temperature below 573.0° C., whereas nearly one-half of the inversions of quartz from zoned pegmatite fall below that value.

The complex inversion curves encountered for a high proportion of the samples from zoned pegmatites are believed to be due to the presence of more than one kind of quartz, perhaps

indicating in some cases replacement of one kind of quartz by another. The differences in inversion temperature are thought to be due primarily to unusual concentrations of some rare elements in zoned pegmatites and to temperature variation of different stages of deposition of quartz, resulting in varying degrees of solid solution of elements which are absent or present in very small amount in other rock types studied.

Figure 8 illustrates the relationship between the inversion-break on heating and on cooling for quartz from the complex pegmatites and shows the range of inversion temperatures. The only type of quartz studied that falls consistently outside this range of temperatures is quartz from cavities in limestone (see fig. 12). Quartz from granites, rhyolites, and quartz veins all fall within the range shown here for the zoned pegmatites.

Variation in shape of the differential curves can be seen in figures 9 and 10. Quartz from the Helen Beryl mine (fig. 10) illustrates the general nature of the differential curves; not one of the specimens studied from this pegmatite has a single, sharp, uncomplicated peak. Specimen 48-10, which is perhaps

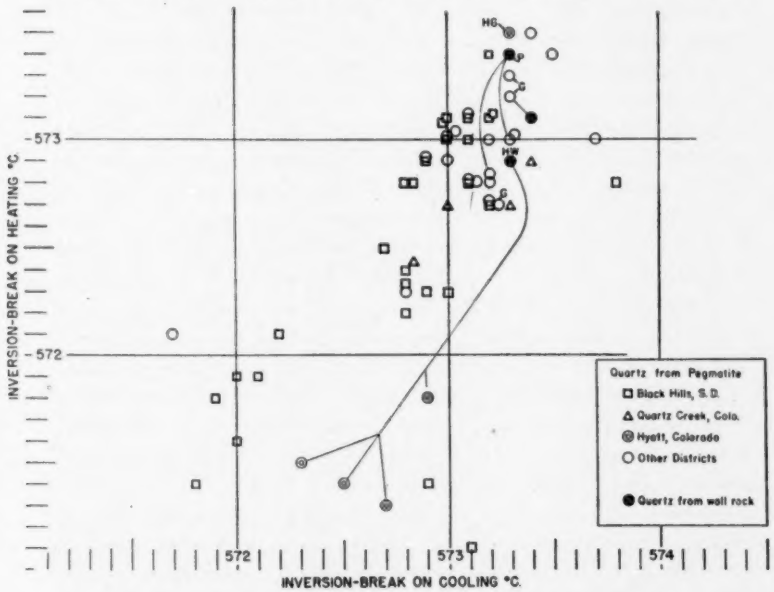

Fig. 8. Inversion temperature of quartz from pegmatites. (See text for discussion of results.)

the nearest approach to a single peak, has a small amount of quartz that inverts at a higher temperature than the bulk of the sample on cooling through the inversion. Sample number 48-5, which is a white quartz from the core zone, is particularly interesting because it is obviously composed of at least two distinct types of quartz and a glance at inversion curves for the other samples shows that specimen 48-6, gray quartz from the core zone, and 48-9 from the perthite-quartz-2 mica zone probably represent components of 48-5. A mixture of 48-6 and 48-9 in the proportions indicated by relative thermal peak heights gave a differential curve which is reproduced below 48-5 for comparison. An explanation of the intermixture of gray core quartz with quartz from an outer zone is not obvious. Replacement of the core by quartz 48-6 would seem to be the most likely possibility, but an extensive sampling of the entire pegmatite and detailed correlation of inversion data with field data would be necessary to check that possibility.

Detailed study of quartz from different zones of several pegmatite masses brings out some comparable variations of the inversion. The inversion of quartz from the New York and Helen Beryl pegmatites, Custer County, South Dakota, is shown graphically in figures 9 and 10 in which the differential thermal curves are reproduced and related to sketches of the respective pegmatites. The zonal arrangements of these two pegmatites are not strictly parallel; there are some appreciable differences in their mineralogy. There is, however, a general similarity in the sequence of changes of the quartz inversion from wall zone to intermediate zones to core zone. The similarity is brought out by study of figures 9 and 10 in conjunction with figure 11, in which the temperature of the inversion-break is plotted for the various zones designated by the zone numbers of Cameron and co-authors (1949, p. 68). Part of their table of sequence of mineral assemblages in pegmatites of the Black Hills is reproduced in table 7. Considering the rising-temperature inversion first, it will be noted that quartz from the wall zone (albite-quartz-muscovite) in both cases has an inversion-break at 572.5° ± 0.2°,[12] while the quartz of intermediate zones inverts at lower temperatures and some samples

[12] Data are for the first heat through the inversion range. Some samples from Helen Beryl pegmatite exhibit a shift of inversion temperatures after the initial run. The shift probably is due to exsolution, although there is no direct evidence that such is the case.

exhibit overlapping double inversions. In both cases samples from the core zones, predominantly quartz, exhibit double or asymmetric thermal inversion curves indicative of the presence of two different kinds of quartz. The falling temperature inversion curves show similar complexities which apparently are due to intermingling in varying proportions of two kinds of quartz, one of which inverts near 573° and the other at or below 572°.

At both the New York Mine and Helen Beryl Mine the youngest pegmatitic material is microcline (or perthite) plus quartz, which forms fracture-controlled replacement zones. The late-stage quartz is predominantly of a low-inverting variety.

Quartz samples were obtained also from various zones of the Hugo pegmatite, near Keystone, South Dakota, and data for those zones which correspond to recognized zones of the New York or Helen Beryl pegmatites are shown in figure 11. No

TABLE 7*

Sequence of Mineral Assemblages, Black Hills, South Dakota

Zone No.	Mineral Assemblages	New York	Helen Beryl	Hugo
(1)	Plagioclase-quartz-muscovite	X†	X	X
(2)	Plagioclase-quartz	X		X
(3)	Quartz-perthite-plagioclase, with or without muscovite	X	X	X
(4)	Perthite-quartz	(?)‡	X	
(5)	Perthite-(or microcline-) quartz-plagioclase-amblygonite-spodumene	(?)	X	X
(6)	Plagioclase-quartz-spodumene (6a)§..	X		X
(7)	Quartz-spodumene		X	X
(8)	Lepidolite-plagioclase-quartz	(?)		
(9)	Quartz-microcline	(?)		X
(10)	Microcline-plagioclase-lithia micas-quartz			X
(11)	Quartz	X		

* After E. N. Cameron, R. H. Jahns, A. H. McNair, and L. R. Page, (1949).

† X indicates mineral assemblage recognized in zones.

‡ (?) indicates mineral assemblage has been recognized, but is poorly exposed or developed.

§ 6a, in which spodumene is not an essential mineral, is considered as a variant of assemblage 6.

complex double inversions were encountered in samples from the Hugo; the low inverting quartz found at the other two occurrences seems to be entirely absent and the variations from one zone to another are less extreme. Nevertheless, it will be noted that the sequence of changes is similar. The plot of rising temperature inversion-break shows that wall-zone quartz inverts at a comparatively high temperature, and that the inversion is lowered in successive intermediate zones and rises again as the core of the pegmatite mass is approached.

Samples of quartz from a few other zoned pegmatites have been studied, (see fig. 8) but no other complete suites were collected to represent a succession of zones from the walls inward. Zones in a pegmatite in the Hyatt District of Colorado apparently correspond most nearly to zones 3 and 4 of the Black Hills sequence (table 7,) but are not strictly comparable. Samples of the Hyatt pegmatite quartz exhibit single inversions at temperatures of 571.4° to 571.8° on heating and 572.4° to 572.9° on cooling.

In summary, quartz from zoned pegmatites may have complex inversion curves such as those found for samples from the Helen Beryl pegmatite, or simple inversion curves such as those for samples from the Hyatt and Hugo pegmatites. The complex pegmatites such as the Helen Beryl and New York mines may owe their complicated quartz to large scale replacement which is lacking in the Hugo and Hyatt. Quartz from the country rock of the zoned pegmatites is usually considerably different from the pegmatite quartz; this is in contrast to the unzoned pegmatites where wall rock quartz and pegmatite quartz have nearly identical inversion relations (see p. 238).

Zoned pegmatites from the Black Hills, South Dakota, show a regular sequence of changes in the character of the quartz from wall zone to intermediate zones to core zone, and the sequence is recognizable from one pegmatite to another in spite of some differences in mineral proportions and the absence of some zones in one pegmatite mass, and other zones in another pegmatite mass. In respect to the existence of a general sequence of zones common to a whole petrographic province, the data presented here are in agreement with those of Cameron and co-authors (1949, pp. 67, 68).

Comparison of quartz from pegmatites and adjacent wall rocks.—Inversion-break temperatures of quartz from unzoned

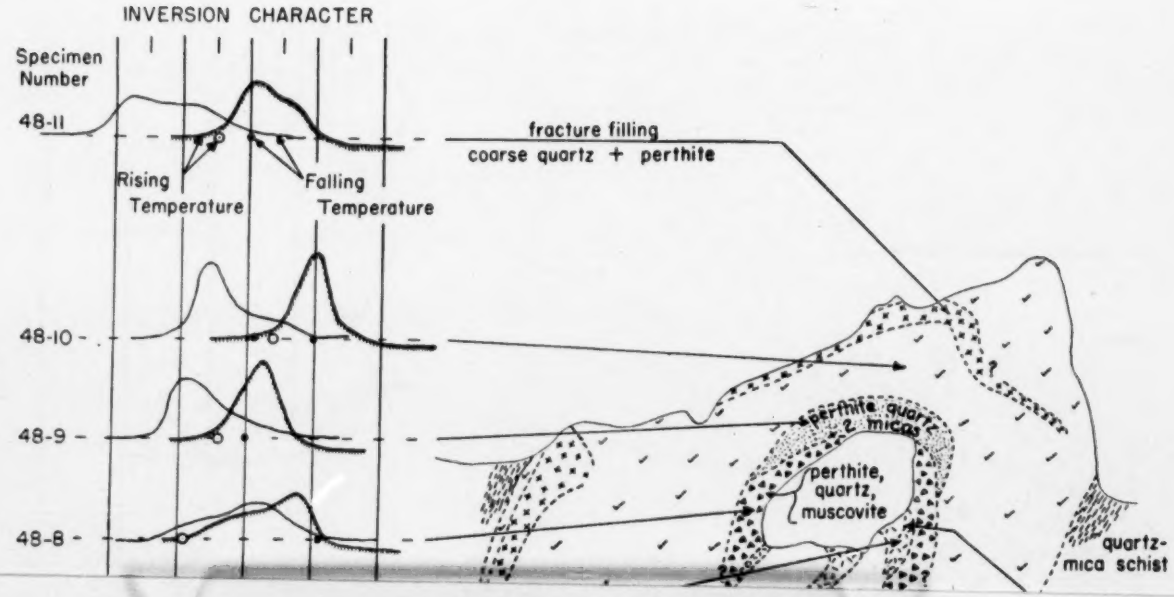
INVERSION CHARACTER
Specimen Number
48-11
Rising Temperature
Falling Temperature
fracture filling
coarse quartz + perthite
48-10
48-9
48-8
perthite quartz & micas
perthite, quartz, muscovite
quartz-mica schist

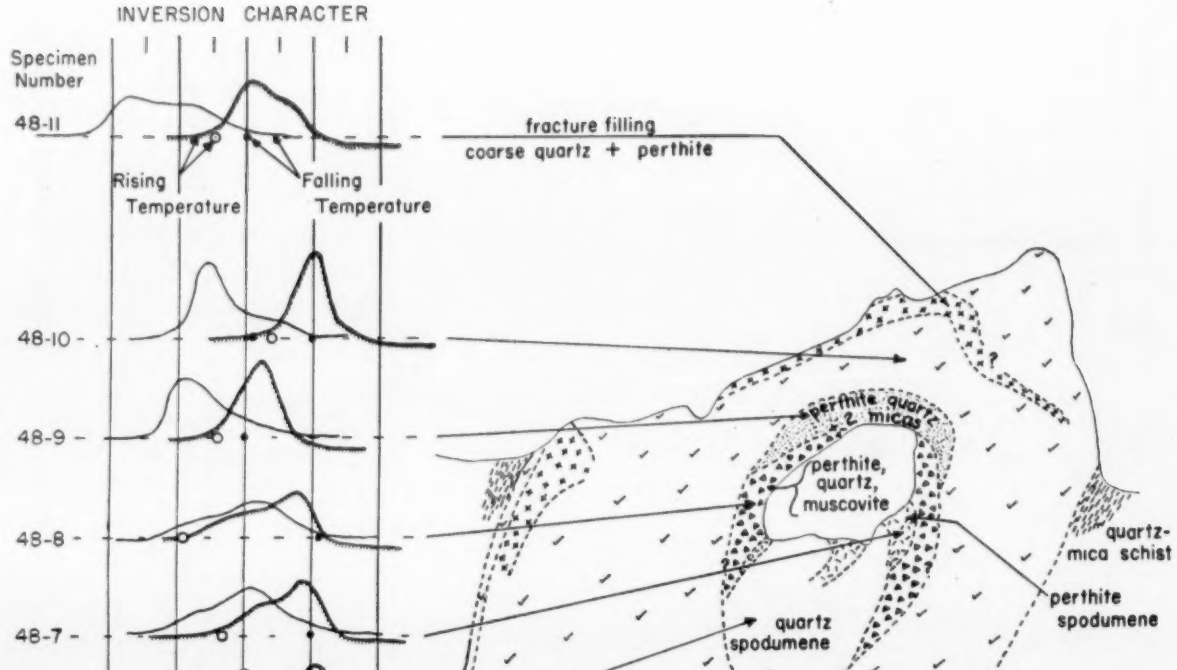
INVERSION CHARACTER
Specimen Number
48-11
Rising Temperature
Falling Temperature
fracture filling
coarse quartz + perthite
48-10
48-9
48-8
48-7
perthite quartz & micas
perthite, quartz, muscovite
quartz-mica schist
perthite spodumene
quartz spodumene

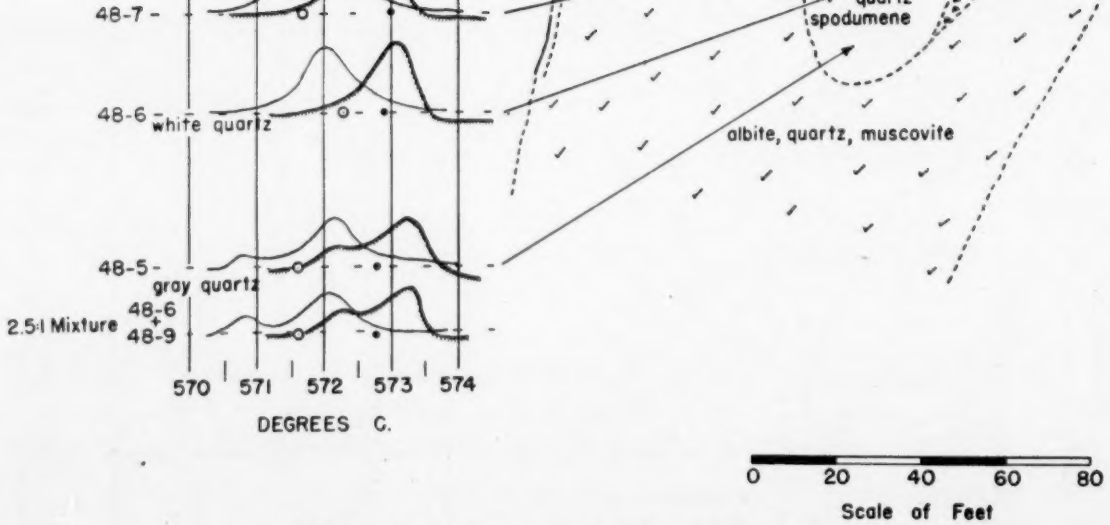

Fig. 10. Quartz inversion results on samples from the Helen Beryl Mine pegmatite, Custer County, S. D., shown in relation to a vertical section after M. H. Staatz and J. J. Norton of the U. S. Geological Survey. At least four different types of quartz can be recognized and each sample shows evidence of containing more than one type of quartz.

complex double inversions were encountered in samples from the Hugo; the low inverting quartz found at the other two occurrences seems to be entirely absent and the variations from one zone to another are less extreme. Nevertheless, it will be noted that the sequence of changes is similar. The plot of rising temperature inversion-break shows that wall-zone quartz inverts at a comparatively high temperature, and that the inversion is lowered in successive intermediate zones and rises again as the core of the pegmatite mass is approached.

Samples of quartz from a few other zoned pegmatites have been studied, (see fig. 8) but no other complete suites were collected to represent a succession of zones from the walls inward. Zones in a pegmatite in the Hyatt District of Colorado apparently correspond most nearly to zones 3 and 4 of the Black Hills sequence (table 7,) but are not strictly comparable. Samples of the Hyatt pegmatite quartz exhibit single inversions at temperatures of 571.4° to 571.8° on heating and 572.4° to 572.9° on cooling.

In summary, quartz from zoned pegmatites may have complex inversion curves such as those found for samples from the Helen Beryl pegmatite, or simple inversion curves such as those for samples from the Hyatt and Hugo pegmatites. The complex pegmatites such as the Helen Beryl and New York mines may owe their complicated quartz to large scale replacement which is lacking in the Hugo and Hyatt. Quartz from the country rock of the zoned pegmatites is usually considerably different from the pegmatite quartz; this is in contrast to the unzoned pegmatites where wall rock quartz and pegmatite quartz have nearly identical inversion relations (see p. 238).

Zoned pegmatites from the Black Hills, South Dakota, show a regular sequence of changes in the character of the quartz from wall zone to intermediate zones to core zone, and the sequence is recognizable from one pegmatite to another in spite of some differences in mineral proportions and the absence of some zones in one pegmatite mass, and other zones in another pegmatite mass. In respect to the existence of a general sequence of zones common to a whole petrographic province, the data presented here are in agreement with those of Cameron and co-authors (1949, pp. 67, 68).

Comparison of quartz from pegmatites and adjacent wall rocks.—Inversion-break temperatures of quartz from unzoned

pegmatites are nearly the same as the inversion-break temperature of quartz from the wall rocks. Table 8 illustrates this similarity in five samples studied.

The complex pegmatites on the other hand may show rather large differences (see, for example, the Hyatt pegmatite, fig. 8) between the pegmatite quartz and the quartz from the

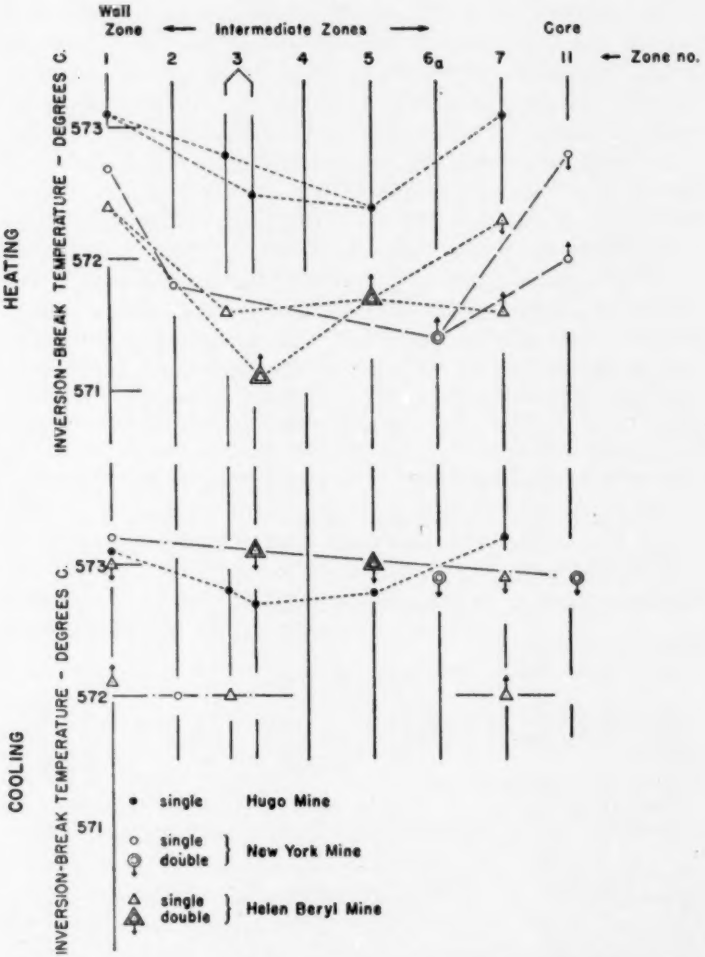

Fig. 11. Sequence of change of inversion temperatures from wall-zone to intermediate zones to core, in zoned pegmatites of the Black Hills, S. D.

adjacent wall rock. Some investigators have suggested that a relationship exists between mineral assemblages in pegmatite and enclosing wall rock. Cameron and co-authors (1949, p. 8) refer to the common occurrence of sheet-mica bearing pegmatites in mica schists but conclude that no generalizations as to associations of wall-rock and pegmatite are justified by present knowledge. Ramberg (1949) reports that pegmatites in southwest Greenland represent metamorphic facies which correspond with those in the surrounding wall rock. He very kindly supplied for this study three specimens of pegmatite and one specimen of schistose country rock. Two of the specimens of pegmatite were classified by Ramberg as representing high temperature and low temperature facies respectively, on the basis of the composition of the contained garnet. Quartz from both of the above two specimens has a rising-temperature inversion-break at the same temperature, 573.3°, within the error of measurement, while quartz from the third pegmatite specimen, unclassified as to facies, has a lower inversion-break (572.7°). It must be concluded that the inversion of quartz cannot be used as an indicator of whatever variation of con-

TABLE 8

Inversion-Break Temperature of Quartz From Unzoned Pegmatites

Locality	Pegmatite quartz		Adjacent wall rock	
	Specimen No.	Temperature °C.	Specimen No.	Temperature °C.
S. W. Greenland	49-151	*H 573.2	49-155	H 573.1
		*C 573.3		C 573.4
Sylvan Lake, Black Hills, South Dakota	48-17	H 573.1	48-18	H 573.3
		C 573.0		C 573.0
Needles Highway, Black Hills, South Dakota	48-19	H 573.1	48-20	H 573.3
		C 573.0		C 573.1
1 mile S. W. Keystone, Black Hills, South Dakota	48-23	H 572.9	48-24	H 573.0
		C 572.9		C 573.4
Head Harbour Island, Maine	F3-9A	H 572.2	F3-9B	H 572.2
		C 572.5		C 572.3

*H - inversion-break on heating.

C - inversion-break on cooling.

ditions produced compositional differences in the garnet of the Greenland pegmatite specimens. Quartz from the specimen of country rock from a location adjacent to the specimen designated as high temperature pegmatite has inversion-breaks at 573.1° on heating and 573.4° on cooling. Points representing the inversion-breaks of pegmatite quartz and that of quartz from adjacent country rock are joined by a line and marked G on figure 8. It will be noted that the two points are not far apart on the scale of inversion of pegmatite quartz.

Points representing the relative inversion temperatures of quartz from wall rock and adjacent granite at the Hyatt pegmatite, Colorado, are marked HW and HG respectively on figure 8 and lines are drawn from HW to points which represent the inversion of quartz from the several zones of the Hyatt complex pegmatite. Another example is from the Pike's Peak region of Colorado, 2.5 miles west of Lake George. Gneissic wall rock of a pegmatite body at that locality contains quartz with an inversion represented by the point P on figure 8 and lines are drawn to points which represent the inversion of quartz from the wall zone and core zone of the pegmatite.

The few examples listed here do not support the concept of a consistent relationship between wall rock quartz and pegmatite quartz, except for the simple unzoned pegmatites. It should be pointed out, however, that thorough and widespread sampling of a variety of wall rocks and pegmatites would be required in order to demonstrate or disprove a relationship, and the problem is complicated by "within-pegmatite" variations and by the probable introduction of pegmatite-quartz into surrounding rocks.

VEIN QUARTZ

Determination of inversion characteristics was made for thirty samples of vein quartz from different localities; the data are summarized in figure 12. It will be noted that the range of inversion-break temperatures of most of the samples is from 572.2° to 573.5° on heating and from 573.0° to 573.8° on cooling, a range considerably more restricted than that for quartz from zoned pegmatites. In addition to the Kirkland Lake, Ontario, samples which are discussed below, the two points which fall outside the above range represent quartz from the McIntyre Mine in Ontario. Point C represents a

surface vein sample of quartz which appears to be pseudomorphic after calcite, while point S represents a younger quartz which forms a ladder structure of veinlets crosscutting the early vein quartz on the 1750 foot level. The younger quartz has a rising temperature inversion-break about 1° lower than that of early quartz at the same sample location.

Number 10 vein at the McIntyre Mine was sampled over a vertical range of over 4000 feet. It was found that the inversion temperature changes very little with depth; rising temperature inversion-breaks for a single sample from each level are as follows: 1250 foot level, 572.7°; 1875 foot level, 572.7°; 2875 foot level, 572.9°;[13] 3875 foot level, 573.0°; 4475 foot level, 573.0°; 5375 foot level, 572.9°. No investigation was made of possible variation of inversion with distance from the porphyry intrusives, nor of possible differences in the quartz from one vein to another.

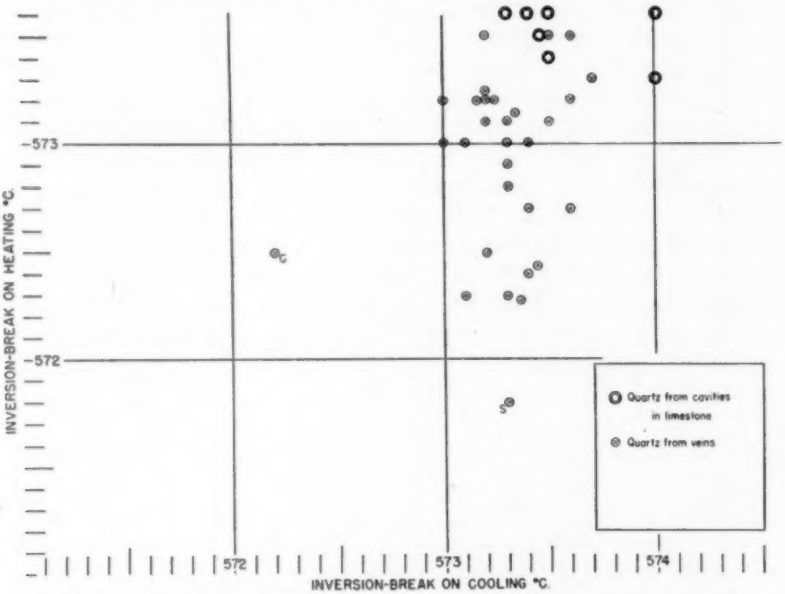

Fig. 12. Inversion of quartz samples from cavities in limestone and from quartz veins. C = sample 48-105, vein quartz which appears to be pseudomorphic after calcite. S = younger quartz, sample 48-102B, which cuts across earlier vein quartz at the McIntyre Mine, Ont.

[13] One sample taken 1400 feet to the east, on the 2875 foot level, has an inversion temperature of 572.4°.

Three series of samples of vein quartz were obtained from different levels of the Wright-Hargreaves and Teck-Hughes gold mines at Kirkland Lake. All of the Kirkland Lake samples have extremely sluggish inversions and require fine grinding in order to make it possible to measure the inversion with sufficient accuracy. It was found that fine grinding of the samples results in a sharper inversion and therefore all test samples of the Kirkland Lake group were ground in a sintered alumina mortar to pass a 325-mesh screen.[14] Figure 13 shows the relationship between the rising temperature inversion-breaks and depth of sample below the surface. Samples from the South vein at Wright-Hargreaves show inversion breaks at temperatures which increase with depth, from a minimum of 571.9° at 1000 foot depth to a maximum of 572.9° at a depth of 6150 feet. The Teck-Hughes samples and samples from the North vein at Wright-Hargreaves exhibit a decrease of inversion temperature with increasing depth to a depth of 3000 to 4000 feet; at deeper levels there is a reversal of trend and the inversion temperature increases with depth.[15] The falling-temperature inversions (table 9) exhibit a very slight change with depth; for each sample the falling temperature inversion-break takes place at a higher temperature than the rising temperature inversion-break.

The sluggishness of inversion of quartz samples of the Kirkland Lake suite is probably owing in part to the effect of strains developed in a mosaic of differently oriented grains, since the inversion is sharpened when the grains are separated by fine grinding. However, the inversion of even the fine-ground samples is sluggish in comparison with most natural quartz and that sluggishness as well as the variation of the inversion temperature with sample depth is attributed to solid solution in the quartz structure, controlled by different conditions of temperature and pressure at different depths of vein formation. It should be emphasized that lateral variations, which remain to be investigated, may be as great or greater than the observed variations in a vertical direction.

[14] Because of this treatment of samples, the Kirkland Lake data are not considered comparable with other data for vein quartz and are therefore not included in figure 12.

[15] Samples from the 2500 foot level of the Teck-Hughes have an exceptionally slow inversion. The first heating run gave a result of 571.7°, but subsequent repeat tests gave variable results between 571.7° and 572.0°.

Preliminary spectrochemical analysis[16] by H. L. Lovell of one Kirkland Lake sample (49-174) shows appreciable amounts of Mg, Al, and Ba, in addition to the alkalies. Micro inclusions are abundant and it is therefore impossible to say which of the reported elements are incorporated in the quartz structure on an atomic scale. It is possible that quantitative spectro-

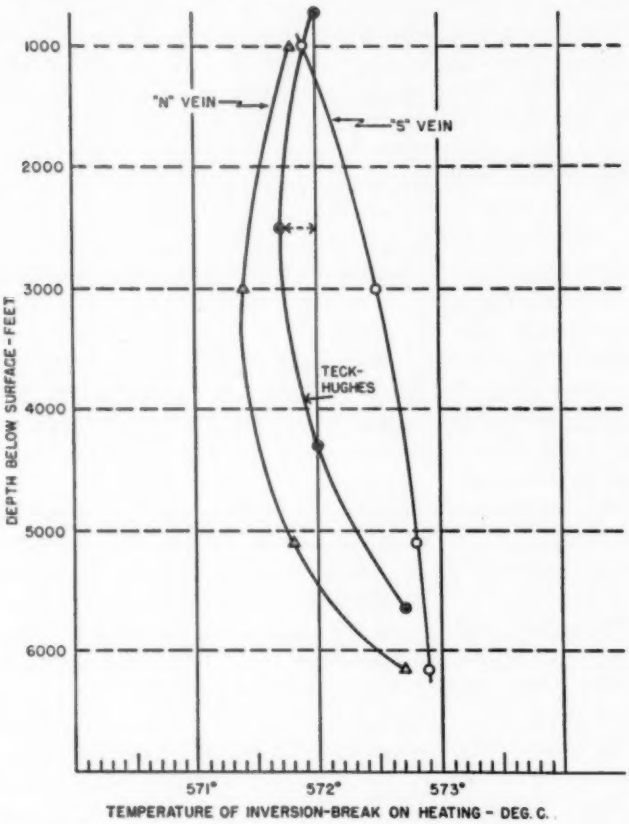

Fig. 13. Inversion of quartz from different depths of the Teck-Hughes Mine and from the North vein and South vein of the Wright-Hargreaves Mine, Kirkland Lake, Ontario.

[16] Spectrochemical analysis, Sample 49-174 (estimated per cent): Cu .001, Ti .0005 to .001, Mg .004, Al .008, Fe .0008, Ba .008, Ag .0002, Li .001, Na .001, K .002, Sr .001, V .0003, B .001.

Not detected: Rb, Cs (?), Ge, Au, Mn, and Be. Allowance has been made for some Mg as an electrode impurity.

analysis of samples from different depths would bring out a relationship between compositional change and change of inversion temperature.

Two samples, from the 200 foot level and the 1800 foot level, respectively of the Pamour mine in the Porcupine District of Ontario, have the same inversion-break temperature (572.5° on heating, 573.2° to 573.3° on cooling). Similarly, two samples from the Normetal Mine in Western Quebec show no appreciable change of inversion temperature from the surface down to a depth of 3240 feet. The Normetal samples have an inversion-break at 573.2° on heating, and at 573.9° to 574.0° on cooling.

It is possible that a regional study of variations in the inversion of vein quartz would bring out zonal relationships or a correlation with structural features. It may also be suggested, on the basis of the preliminary results mentioned above on the Kirkland Lake samples, that within one vein system a useful correlation might be made between the inversion temperature and other variable characteristics of the vein material, as, for example, the relative proportions of sulfides, the average gold content, and the ratio of gold to silver. Such a study would require extensive sampling and precise fixing of sample locations on assay plans and sections.

QUARTZ FROM CAVITIES IN LIMESTONE

Among the most consistently high inversion temperatures (considering both heating and cooling inversions) which were encountered in natural quartz are those of quartz crystals

TABLE 9

Falling Temperature Inversion-Break vs. Depth Below Surface

Depth Below Surface (feet)	Wright-Hargreaves		Teck-Hughes
	North Vein °C.	South Vein °C.	°C.
730	....	....	574.5
1000	574.0	574.4	....
2500	....	....	574.3
3000	574.1	574.2	....
4300	....	....	574.2
5100	574.3	574.2	....
5625	....	....	574.1
6150	574.4	574.1	....

from cavities in limestone and marble. Those which have been examined in this study differ from most other large single crystals investigated in that they have no pronounced zonal development and have essentially single, uncomplicated inversions which take place within a comparatively narrow range: inversion-breaks 573.3° to 573.6° on heating, and 573.3° to 574.0° on cooling. Except for one sample from a geode in limestone (Keokuk, Iowa, inversion-break 573.3° on heating, 574.0° on cooling) the heating and cooling inversion-breaks are less than 0.5° apart. Inversion data for samples of this group are plotted in figure 12, along with inversion data for vein quartz. The crystals found in vugs in limestone probably grew at relatively uniform low temperature.[17] It is expected that they will be found to be among the purest samples of natural quartz.

INVERSION CHARACTERISTICS OF NOVACULITE AND CHERT

Early in the investigation it was found that novaculite and chert did not produce a measurable heat effect on heating through the inversion temperature despite the fact that the X-ray indicated that they were quartz. This was puzzling until it was discovered that the novaculite specimens (F2-2 and F3-34) would produce a measurable heat effect after grinding to a size approaching that of the individual grains (1 to 7 microns).[18] Suppression of the heat effect in polycrystalline fragments is attributed to differential stresses set up in a mosaic of differently oriented grains. Such differential stresses probably have the effect of raising the inversion temperature of some individual crystal units, and therefore of spreading out the heat effect over a considerable range of temperature. This is probably similar to the effect of hydrostatic pressure, except that the resultant raising of the inversion temperature varies from grain to grain and depends on the stress environment around each crystal unit (see p. 217).

[17] Some of the doubly-terminated crystals which occur in cavities in dolomitic limestone in Herkimer Co., N. Y., contain angular inclusions of two kinds of hydrocarbon: a pale yellow variety which melts at 70° to 80° C. and a brown variety which melts at 200° to 220° in contact with the yellow one. (See sample 51-6 and compare F3-38 and 49-202.)

[18] Size range determined by estimates made with the microscope (micrometer ocular), and by measurements made on electron photomicrographs of a collodion replica of a fracture surface of Arkansas novaculite: the arithmetic mean of 75 measured mean grain diameters is 2 microns.

In the present study three specimens of microcrystalline quartz were investigated: two of chert (F2-1 and 49-36) and one of petrified wood (F3-20); all were found to give no detectable thermal effect in coarse granular condition. In finely ground form, samples 49-36 and F3-20 gave a weak thermal effect, measurable with maximum galvanometer sensitivity; inversion begins at about 573.4° C. on heating and from 1.0° to 1.5° higher on cooling. Sample F2-1 does not give a measurable thermal peak, even in fine-ground condition, but the inversion can be located approximately from a change of slope in the differential thermal record, and probably takes place within one degree of the temperature recorded for the other two specimens.

SOME GENERAL OBSERVATIONS ON THE CHARACTER OF THE INVERSION

Significance of the shape of the differential thermal curve.—The differential thermal curves of natural quartz specimens are highly variable in height and shape; some are double or complex owing to intermixture of more than one kind of quartz with different inversion temperature (e.g., see figs. 5, 6, 9, and 10), others are asymmetric or flat-topped, probably owing to the quartz having grown in progressively changing environment, and others show weak heat effects.

Height of the differential thermal curve can be affected by (1) change in the heat of inversion, (2) solid solution, and (3) directed pressure. It is unlikely that the heat of inversion is greatly different from one specimen to another because compositional variations are small. Solid solution, on the other hand, may have a pronounced influence on the height of thermal peaks without large variation in composition by increasing the temperature range over which the high and low forms can coexist. Evidence for that lies in the low broad thermal peaks due to inversion of synthetic quartz grown in the presence of ions which can be incorporated in the quartz structure. M. J. Buerger's analysis of the phenomena of displacive transformation (in Smoluchowski *et al.*, 1951, p. 190), should be qualified to the extent that displacive transformations do not take place at high speed if there is appreciable solid solution in the structure. Solid solution also affects the peak height indirectly, since compositional zoning has the effect of spreading the in-

version over a range of temperature. Directed pressures were also found to be effective in lowering the magnitude of the thermal effect in quartz specimens which are not broken down into monocrystalline fragments. Fine grinding of those specimens materially increases the heat effect. The novaculites and cherts offer examples of that type of suppression of the heat effect (see preceding section). Directed pressure may also be operative in suppressing the heat effect in single crystals in which structural imperfections such as lineage or block structure are pronounced.

Extreme differences in peak heights can be illustrated by the thermal curves for specimens F3-38 and 49-29. Sample F3-38 has a strong sharp absorption of heat at the rising temperature inversion, giving a maximum deflection of approximately 40 mm. with normal galvanometer sensitivity, whereas specimen 49-29 has a broad weak heat effect with a maximum deflection of only 2 mm. Both specimens are clear, doubly terminated crystals; the only visible difference between them is the strong development of lineage in 49-29 and the absence of such imperfections in F3-38. The pronounced misorientation within the crystals of 49-29, as evidenced by the lineage structure probably is in part responsible for the weak heat effect because fine grinding of the quartz increases the height of the differential peak considerably. This difference in the heat effect is probably due to differential stresses set up within the grains of sample 49-29 on heating; non-uniform stress probably causes the inversion to take place at different temperatures in differently stressed lineage units. This is not surprising when it is realized that a change in hydrostatic pressure of only 4 atmospheres will change the inversion temperature by a measuable amount.

Normal and abnormal inversions—Approximately 70 per cent of all the natural quartz specimens studied show an inversion-break on heating within the range 572.5°-573.5° C. The total range for natural quartz is 38° C., from a minimum temperature of 536° C. (Sample 49-148) to a maximum of 573.8° C. (Sample 49-146). The total range found for synthetic quartz is about 160° C.

As inversion-break temperatures depart from the "normal" range (573.2° ± 0.6° C.) the general tendency is for the

thermal peaks to be low and broad. For example, all specimens with inversion-break temperatures below 571.5° have a low thermal peak, and the inversion is spread out over a range of temperature.

Two extreme samples deserve special mention as neither gives a measurable thermal effect in a size coarser than 200 mesh. One of them (49-28) is from a vug in pegmatite in the Tenmile Range, Summit County, Colorado. In finely ground condition it begins to invert at a temperature of about 545° on heating, and at about 564° on cooling. Both the heating and cooling inversions are very slow; the total range of temperature over which the quartz continues to invert is estimated at more than 15° on heating and slightly less than 15° on cooling (heating rate 0.6° per minute). The second sample (49-148) is pale green drusy quartz from Bernfjord, Iceland, details of the occurrence of which are unknown. In finely ground condition it begins to invert at a temperature of about 536° on heating, and continues to invert very slowly over a range of almost 20°. The beginning of the cooling inversion thermal effect has not yet been established.

CONCLUSIONS

The primary cause of the observed variation in temperature of the high-low inversion of quartz is believed to be solid solution of ions other than Si^{4+} and O^{2-}. The amount of solid solution is not known, but it must be very small in comparison with the amounts of solid solution in other common rock-forming minerals (see p. 217). The general effect of solid solution has been studied by synthesizing quartz in the presence of ions such as Ge^{4+} and Al^{3+} plus Li^{+}, which are possible candidates for solid solution. In the first case the inversion temperature of the quartz was raised by as much as 40° C. and in the second it was lowered by approximately 120° C. The inversion temperature in both cases is related to the temperature of growth. In the germanium-bearing quartz the inversion temperature is raised by lowering the temperature of growth and in the presence of lithium and aluminum the inversion is lowered by raising the temperature of growth. Theoretical explanations of these relationships are discussed with the aid of equilibrium diagrams.

Solid solution in natural quartz has been studied by spectro-

chemical analysis of quartz having different inversion temperatures and the results suggest that lithium may be important in lowering the inversion of natural quartz. Other minor elements found in quartz are: Ti, Al, Fe, Mg, Ca, Ba, Na, K, Cu, B.

Examination of synthetic and natural quartz by means of the X-ray spectrometer shows that the (234) spacing varies appreciably from one sample to another with different inversion-break temperatures. The corresponding changes in cell dimensions offer convincing evidence for solid solution as the cause of the inversion variations.

Certain fine-grained forms of quartz, such as novaculite and chert, produce no heat effect when examined in coarse grain size (—35 + 200 mesh), but grinding to a size near that of the individual crystal units results in a measurable heat absorption upon heating through the inversion. Suppression of the heat effect in coarser sizes is believed to be the result of differential stresses set up in fine-grained mosaics because of the random or nearly random orientation of the individual crystals which expand differently when heated. (The coefficient of expansion of quartz perpendicular to "c" is approximately twice as great as in a direction parallel to "c.") The resultant effect on the inversion temperature is probably similar to the effect of hydrostatic pressure, the amount of increase in the temperature of inversion depending on the stress environment of each individual crystal unit. The result is a "spreading out" of the heat effect, thus accounting for the apparent absence of a thermal effect before fine grinding.

Results on natural quartz may be summarized as follows:

(1) The inversion of quartz from most of the granites studied is different from that of quartz from rhyolites and related welded tuffs and intrusive porphyries, and it is concluded that there is a significant difference between the environments of final crystallization of granite-quartz and rhyolite-quartz. The difference may be owing primarily to the effects of late-stage recrystallization in granites. Further studies are being made with the object of throwing light on the problem of the origin of granites of different types.

(2) Quartz from unzoned pegmatites has inversion characteristics similar to those of quartz from granites, but quartz

from zoned pegmatites is quite different and shows wide variations, even within a single pegmatite mass. Within one area, such as the Harney Peak region, South Dakota, there is a similarity in the sequence of change of inversion characteristics of the quartz from wall zone to intermediate zones to core zone. Moreover, some zones contain intimate intermixtures of more than one kind of quartz.

(3) Variation of the inversion of quartz in veins offers promise of providing a useful tool for the study of zonal relationships. It may be noted that the largest variation with depth is found in vein quartz which has a sluggish inversion attributable to appreciable solid solution in the quartz structure. Therefore preliminary investigation of inversion characteristics of quartz from a specific vein or vein system may indicate whether zoning may be amenable to study by means of measurements of variation of the inversion.

(4) The inversion temperature of samples of natural quartz investigated varies over temperature range of about 38°; a frequency plot of measured inversion temperatures shows, however, that most quartz inversions take place within a much narrower range, with a frequency maximum for the rising-temperature inversion-break at 573.1° to 573.2° and a frequency maximum for the falling temperature inversion-break at 573.3° C. Approximately 70 per cent of all specimens studied have an inversion-break on heating at temperatures between 572.5° and 573.5° C.

(5) Many large single crystals of natural quartz are zoned, although the zoning may not always be evident upon casual examination, without pretreatment by irradiation or etching. Different growth zones comonly exhibit different inversion characterististics; if quartz with uniform properties is desired a sample should be cut from a single growth zone. It should be possible to grow synthetic quartz with uniform properties throughout a crystal, providing that seed plates are prepared from synthetic quartz grown under the same conditions and that growth conditions are kept constant. It may further be suggested that synthetic quartz can be grown with specific desired properties, such as a suppressed or sluggish inversion, by adding to the growth solution elements such as germanium, or

lithium plus aluminum, which can be incorporated in the quartz structure.

(6) It has been suggested that the high-low inversion of quartz be used as a fixed point on the thermometric scale (Bates and Phelps, 1927-28). The present study confirms the fact that the inversion is highly reproducible and therefore suitable for a temperature standard. However, it is obvious from the present work that a specific sample must be used; it is suggested that certain precautions be taken in selecting a reference quartz: the quartz should have a single sharp inversion that remains unchanged with repeated runs, the inversion temperature should be invariant within a large bulk sample, and the material should be ground to approximately 200 mesh to minimize superheating and undercooling. It may be noted that specimen F3-40, from one of the numerous quartz veins which cut gneissic rocks in and around Washington, D. C., has a suitable sharp inversion.

(7) It is concluded that the temperature of the high-low inversion of quartz cannot be used as an indication of the temperature of formation for rocks of widely different chemical composition. The inversion is a sensitive indicator of changing conditions of quartz growth, however, and within one chemical environment, as within one vein or one intrusive body or within a group of rocks of very similar bulk chemical composition, variation of the inversion temperature can be used to study zonal relationships and variations in the conditions of final crystallization of quartz.

ACKNOWLEDGMENTS

The writers are indebted to a number of colleagues for suggestions and constructive criticism, particularly to N. L. Bowen and J. W. Greig of the Geophysical Laboratory, and to E. F. Osborn of The Pennsylvania State College.

Spectrochemical analyses were made by L. H. Ahrens of the Massachusetts Institute of Technology, K. J. Murata of the U.S. Geological Survey, and H. L. Lovell of The Pennsylvania State College. Measurements with an X-ray goniometer furnace were made by G. L. Davis of the Geophysical Laboratory and H. A. McKinstry of The Pennsylvania State College.

Valuable assistance in obtaining suitable quartz specimens for

study was furnished by Felix Chayes of the Geophysical Laboratory, Clifford Frondel of Harvard University, E. P. Henderson and W. Foshag of the U.S. National Museum, F. P. Phelps of the Bureau of Standards, F. A. Hummel of The Pennsylvania State College, W. H. Newhouse and Hans Ramberg of the University of Chicago, D. R. Hale of the Brush Development Company, A. C. Walker of the Bell Telephone Laboratories, R. H. Thomas of Rutgers University, James Schulman of Naval Research Laboratory, R. E. Gibson of Applied Research Laboratories, Johns Hopkins, D. F. Hewitt of the Ontario Department of Mines, R. C. E. Bray, K. Griffin, H. G. Skavlem, E. S. Moore, H. Hopkins, R. D. Macdonald and Louis Moyd, associated with mining and exploration companies in Ontario and Quebec, and by L. W. Currier, Earl Ingerson, Dean Kent, A. H. Koschman, J. J. Norton, W. T. Pecora, C. S. Ross, M. H. Staatz, W. Thurston, and Ogden Tweto of the U. S. Geological Survey.

References

Bates, F. J., and Phelps, F. P., 1927-28. The new fixed point on the thermometric scale: Nat. Bur. Standards, Sci. Papers, vol. 22, pp. 315-327.

Cameron, E. N., Jahns, R. H., McNair, A. H., and Page, L. R., 1949. Internal structure of granite pegmatites: Econ. Geology Pub. Co., Monograph 2.

Fenner, C. N., 1913. The stability relations of the silica minerals: Am. Jour. Sci., 4th ser., vol. 36, pp. 331-384.

Frondel, C., 1945. Effect of radiation on quartz: Am. Mineralogist, vol. 30, pp. 432-446.

Gibson, R. E., 1928. The influence of pressure on the high-low inversion of quartz: Physical Chem. Jour., vol. 32, pp. 1197-1210.

Hummel, F. A., 1951. Thermal expansion properties of some synthetic lithia minerals: Am. Ceramic Soc. Jour., vol. 34, pp. 235-239.

Le Chatelier, H., 1889. Sur la dilatation du quartz: Acad. Sci. Paris Comptes rendus, vol. 108, pp. 1046-1049; vol. 109, pp. 264-266.

Ramberg, H., 1949. Facies classification of rocks: a clue to the origin of quartzofeldspathic massifs and veins: Jour. Geology, vol. 57, pp. 18-54.

Roy, Rustum, and Osborn, E. F., 1949. The system lithium metasilicate—spodumene—silica: Am. Chemical Soc. Jour., vol. 71, pp. 2086-2095.

Schulman, J. H., Claffy, E. W., and Ginther, R. J., 1949. Some observations on the crystallization of silicic acid: Am. Mineralogist, vol. 34, pp. 68-73.

Smoluchowski, R., Mayer, J. E., Weyl, W. A., *et al.*, 1951. Phase transformations in solids, John Wiley and Sons, Inc., New York.

Sosman, R. B., 1927. The properties of silica: Am. Chemical Soc. Monograph 37.

Stahl, P., 1951. Influence of adsorbed gas on the polymorphic transformation of quartz: Acad. Sci. Paris Comptes rendus, vol. 232, pp. 1669-1670.

Tuttle, O. F., 1949*a*. The variable inversion temperature of quartz as a possible geologic thermometer: Am. Mineralogist, vol. 34, pp. 723-730.

———, 1949*b*. Two pressure vessels for silicate water studies: Geol. Soc. America Bull., vol. 60, pp. 1727-1729.

———, 1952. Significance of the mineralogical differences between extrusive and plutonic salic rocks: Jour. Geology, vol. 60, pp. 107-124.

Vines, R. F., and Wise, E. M., 1941. The platinum metals and their alloys, Internat. Nickel Co., New York.

Winkler, H. G. F., 1948. Synthese und Kristallstruktur des eukryptits, $LiAlSiO_4$: Acta Crystallographica, vol. 1, pp. 27-34.

Yoder, H. S., Jr., 1950. High-low quartz inversion up to 10,000 bars: Am. Geophys. Union Trans., vol. 31, pp. 827-835.

Department of Earth Sciences
The Pennsylvania State College
State College, Pennsylvania

Geophysical Laboratory
Carnegie Institution of Washington
Washington, D.C.

Appendix

Description and Inversion Data for Samples of Natural and Synthetic Quartz Examined

NOTE. Samples are listed in several series according to original designations in the following order: F2, F3, Q1, and a series for each of the years 1948 to 1951 inclusive. H = inversion-break on heating; C = inversion break on cooling. The inversion-break is defined as the intersection, on the differential-thermal record, of the base line with a line drawn along the first straight portion of the thermal peak due to inversion.

Sample No. and Source		H (°C.)	C (°C.)	Remarks
F2-1	Marathon, Texas	573 ± 2	573 ± 2	Chert from Maravillas limestone. No thermal peak detected. Inversion located from change of slope of differential thermal curve.
F2-2	Marathon, Texas	573.7	574.3	Novaculite, fine ground. Very slow inversion.
F2-12	Sierra Blanca, Texas	571.8	572.9	Crystal from granite-limestone contact zone.
F2-13	Kens'ngton, Md.	573.3	573.7	Quartz vein containing apatite.
F2-14	Lemont, Centre Co., Pa.	573.5	573.5	From cavity in limestone.
F2-15	Yosemite National Park, near long tunnel	573.4	573.4	Granite.
F2-16	Lake Toxaway	573.3	573.2	Geophysical Laboratory; stock of crushed vein quartz.
F3-9A	Wallace Cove, Head Harbour Island, Maine	572.2	572.5	From cavity in pegmatite.

APPENDIX (cont.)

Sample No.	Source	H (°C.)	C (°C.)	Remarks
F3-9B	Wallace Cove, Head Harbour Island, Maine	572.2	572.3	Granite. First run.
		572.3	572.8	Second run. (Note change.)
F3-10	Bradbury, Maine	572.8	573.2	Pegmatite.
F3-11	Minot, Maine	572.3	572.8	Pegmatite.
F3-12	Brazil	573.0 572.4	573.5 572.9	Citrine quartz. Double inversion which merges to single on repeat runs.
F3-13	Switzerland	573.6	573.4	Twisted smoky crystal from limestone.
F3-14	Carrara, Italy	573.6	573.3	From cavity in marble.
F3-15	Guanajuato, Mexico	572.3	573.4	Amethystine crystal.
F3-16	Brazil	573.6	573.4	Easily twinned crystal. (From C. Frondel.)
F3-17	Brazil	573.6	573.4	Easily twinned crystal. (From C. Frondel.)
F3-18	Cripple Creek, Colo.	570.3	573.2	Harvard Museum, No. 83118. Drusy incrustation on either barite or celestite, later dissolved away leaving hollow molds. Slow inversion.
F3-19	Keokuk, Iowa	573.3	574.0	From geode in limestone. Crystals show strong lineage.

APPENDIX (cont.)

Sample No. and Source		H (°C.)	C (°C.)	Remarks
F3-20	Geophysical Laboratory collection ..	573.4	574.9	Petrified wood. Very slow inversion in fine-ground sample.
F3-21	Geophysical Laboratory collection ..	571.8	572.0	Quartz (prism faces absent); from rhyolite.
F3-33A	Brazil	573.5	573.2	Clear zone of crystal.
F3-33B	Brazil	573.4	573.3	Smoky zone of crystal.
F3-34	Arkansas	573.7	573.8	Novaculite, fine ground; no heat effect from coarse-grained sample.
F3-35	New Mexico	573.1	572.9	From rhyolite tuff.
F3-36	Guanajuato, Mexico	572.7	572.5	From rhyolite.
F3-37	Colorado	572.5	572.7	From rhyolite.
F3-38	Herkimer Co., N. Y.	573.6	573.5	From cavity in dolomitic limestone.
F3-39	Hot Springs, Arkansas	573.3 570.8	573.3	Double inversion on heating.
F3-40	Soapstone Creek, Washington, D. C.	573.5	573.5	Quartz vein.
F3-41	Synthetic (C. N. Fenner)	572.8	573.2	From $NaWO_4$ melt, 90 hours at 800° C.
F3-42	Brazil	573.6	573.4	Outer zone of crystal.

APPENDIX (cont.)

Sample No.	Source	H (°C.)	C (°C.)	Remarks
F3-43	Brazil	572.8	572.2	Core zone of crystal—citrine colour after irradiation with X-rays.
F3-44	Harvard Museum	572.1	571.7	Rose quartz.
Q1-1A	Synthetic: silica glass + NaOH, stainless steel bomb	573-575	574	15000 psi, 400° C., 7 days. No inversion found. tergrowth, probably from recrystallization of silica glass. Weak heat effect.
Q1-1B	Synthetic: 7% GeO_2, 93% SiO_2 glass + NaOH, stellite bomb	....	....	15000 psi, 400° C., 7 days. No inversion found.
Q1-1C	Synthetic: 7% GeO_2, 93% SiO_2 glass + NaOH, stellite bomb	623 ±	....	15000 psi, 500° C., 5 days. From change of slope of differential thermal curve.
		640 ±	....	From X-ray data—very slow inversion.
Q1-1D	Synthetic: silica glass + NaOH, stainless steel bomb	573.4	573.7	15000 psi, 635° C., 3 days.
Q1-2A	Synthetic: 7% GeO_2, 93% SiO_2 glass + NaOH; stellite bomb	592	591	15000 psi, 600° C. Weak heat effect, sluggish inversion.

APPENDIX (cont.)

Sample No. and Source		H (°C.)	C (°C.)	Remarks
Q1-2B	Synthetic: $Li_2O \cdot Al_2O_3 \cdot 12\ SiO_2$ glass + NaOH; stellite bomb	550 ± 15		15000 psi, 500° C., 10 days. Product — quartz + β spodumene. Inversion located by X-ray goniometer furnace. Thermal peak below limit of detectability.
Q1-2C	Synthetic: silica glass, alkalies + Be, Al, Ti, Ge, Mn, V, Mo, Sn, and Zr	572	578	15000 psi, 500° C., 20 days. Fine ground, very sluggish inversion.
Q1-2D	Synthetic: silica glass, alkalies + Be, Al, Te, Ge, Mn, V, Mo, Sn, and Zr	576	580	15000 psi, 650° C., 20 days. Very sluggish inversion.
48-1	New York pegmatite, Custer Co., S. D.	572.7	573.2	Wall zone: albite, quartz, muscovite + some black tourmaline.
48-2	New York pegmatite, Custer Co., S. D.	572.8 572.0	572.9	White glassy quartz, central core; small amount of low-inverting quartz.
48-3	New York pegmatite, Custer Co., S. D.	571.4	572.9	White quartz adjacent to cleavelandite; fracture filling, possibly equivalent to zone 6a. Flat-topped thermal curve.

APPENDIX (cont.)

Sample No. and Source	H (°C.)	C (°C.)	Remarks
48-4 New York pegmatite, Custer Co., S. D.	571.8	571.9	Zone 2, albite-quartz, about 5 feet south of the cleavelandite zone.
48-5 Helen Beryl pegmatite, Custer Co., S. D.	572.5 571.6	572.9	White quartz from quartz-spodumene central core (zone 7). Double inversion with rising temperature inversions farther apart on successive repeat runs.
48-6 Helen Beryl pegmatite, Custer Co., S. D.	572.3	572.9	Gray quartz from central core.
48-7 Helen Beryl pegmatite, Custer Co., S. D.	.... 571.7	573.0	Perthite-spodumene zone, probably zone 5. Double inversion.
48-8 Helen Beryl pegmatite, Custer Co., S. D.	.... 571.1	573.1	Zone of quartz, large perthite, albite, muscovite (zone 3b). Double inversion.
48-9 Helen Beryl pegmatite, Custer Co., S. D.	571.6	572.0	Zone of quartz, large perthite, albite, biotite. (Zone 3a.)
48-10 Helen Beryl pegmatite, Custer Co., S. D.	.... 572.4	573.0	Wall zone; fine-grained albite, quartz, biotite. Double inversion.

APPENDIX (cont.)

Sample No. and Source		H (°C.)	C (°C.)	Remarks
48-11	Helen Beryl pegmatite, Custer Co., S. D.	.... 571.5	572.0	Perthite-quartz fracture-filling. Double inversion.
48-12	New York pegmatite, Custer Co., S. D.	571.9	572.1	Microcline-quartz pegmatite at north end of main mass.
48-13	New York pegmatite, Custer Co., S. D.	572.3	572.8	Small lens of pegmatite west of main mass.
48-15	Custer Co., S. D.	573.2	573.2	Small quartz vein in schist, near the New York pegmatite.
48-16	Custer Co., S. D.	573.3	573.4	Schistose country rock.
48-17	Sylvan Lake, Black Hills	573.1	573.0	Unzoned pegmatite; quartz, perthite black tourmaline, in granite.
48-18	Sylvan Lake, Black Hills	573.3	573.0	Muscovite granite.
48-19	Needles Highway, Black Hills, S. D.	573.1	573.0	Unzoned pegmatite in Harney Peak granite.
48-20	Needles Highway, Black Hills, S. D.	573.3	573.1	Harney Peak granite.
48-21	2 miles north of Keystone, Black Hills, S. D.	573.2	573.2	Quartz vein in amphibolite and schist.

APPENDIX (cont.)

Sample No. and Source		H (°C.)	C (°C.)	Remarks
48-22	Grizzly Bear Campground southwest of Keystone, S. D.	573.0	573.0	Pegmatite: perthite, quartz, muscovite, + some black tourmaline. Quartz is rose coloured in part.
48-23	1 mile south of Keystone, S. D.	572.9	572.9	Unzoned pegmatite.
48-24	1 mile south of Keystone, S. D.	573.0	573.4	Coarse grained granite.
48-25	1 mile northeast of Mt. Rushmore, Black Hills, S. D.	573.4	573.2	Small quartz-rich pegmatite.
48-26	Northeast of Mt. Rushmore, S. D. .	572.8	572.8	Pale rose quartz from perthite, quartz, muscovite pegmatite cutting Harney Peak granite.
48-27	Northeast of Mt. Rushmore, S. D. .	573.2	573.0	White quartz pod in granite.
48-28	Northeast of Mt. Rushmore, S. D. .	573.1	573.3	Harney Peak granite.
48-29	Hugo pegmatite, Keystone District, S. D.	572.8	572.9	Zone 3a: quartz, perthite, albite.
48-30	Hugo pegmatite, Keystone District, S. D.	573.1	573.1	Wall zone: quartz, muscovite.
48-31	Hugo pegmatite, Keystone District, S. D.	572.4	572.8	Zone 5: perthite, quartz, cleavelandite, amblygonite.

APPENDIX (cont.)

Sample No. and Source		H (°C.)	C (°C.)	Remarks
48-32	Hugo pegmatite, Keystone District, S. D.	573.1	573.2	Zone 7: quartz, spodumene.
48-33	Hugo pegmatite, Keystone District, S. D.	573.0	573.1	Quartz, microcline zone.
48-34	Hugo pegmatite, Keystone District, S. D.	572.8	573.1	Core zone: cleavelandite, microcline, lithia mica.
48-35	Hugo pegmatite, Keystone District, S. D.	572.5	572.6	Zone 3b: quartz, perthite, albite.
48-36	2 miles north of Hill City, Black Hills, S. D.	573.2	573.2	Quartz vein in schist.
48-37	Etta Mine, Black Hills, S. D.	572.3	573.0	Quartz core of spodumene-rich pegmatite.
48-40	2 miles west of Hill City, Black Hills, S. D.	572.3	573.1	Quartz vein containing andalusite.
48-48	Laramie Mountains, Wyo.	573.0	573.0	Quartz vein within large dyke of leuco-granite cutting hornblende schist.
48-77	Snowy Range, west of Laramie, Wyo.	573.0	573.2	Unzoned quartz-feldspar pegmatite in marble.
48-82	Snowy Range, west of Laramie, Wyo.	573.4	573.5	Quartz-ankerite vug in fine-grained blue marble.

APPENDIX (cont.)

Sample No. and Source		$\frac{H}{(°C.)}$	$\frac{C}{(°C.)}$	Remarks
48-97	Porcupine District, Ont., McIntyre Mine	572.7	573.5	No. 10 vein in porphyry, 1250-ft. level.
48-98	Porcupine District, Ont., McIntyre Mine	572.7	573.4	No. 10 vein in porphyry; 1875-ft. level.
48-99	Porcupine District, Ont., McIntyre Mine	572.9	573.3	No. 10 vein in porphyry; 5375-ft. level.
48-100	Porcupine District, Ont., McIntyre Mine	573.0	573.3	No. 10 vein in porphyry; 4475-ft. level.
48-101	Porcupine District, Ont., McIntyre Mine	573.0	573.1	No. 10 vein in porphyry; 3875-ft. level.
48-102A	Porcupine District, Ont., McIntyre Mine	572.7	573.6	No. 12 vein in basalt, early quartz. 1750-ft. level.
48-102B	Porcupine District, Ont., McIntyre Mine	571.8	573.3	Younger quartz which forms a ladder structure in quartz 48-102A.
48-103	Porcupine District, Ont., McIntyre Mine	573.0	573.4	No. 10 vein, 2875-ft. level, 2000 feet west of No. 11 shaft.
48-104	Porcupine District, Ont., McIntyre Mine	572.4	573.4	No. 10 vein, 2875-ft. level, 600 feet west of No. 11 shaft.

APPENDIX (cont.)

Sample No.	Source	H (°C.)	C (°C.)	Remarks
48-105	Porcupine District, Ont., McIntyre Mine	572.5	572.2	Surface vein, quartz apparently pseudomorphic after carbonate.
48-107	Synthetic: silica glass, Na(OH), stainless steel bomb	573.6	574.4	15000 psi, 300° C., 3 days.
49-2	Moorfield mine, Amelia Co., Virginia	573.0	573.0	Pegmatite: quartz, albite, muscovite, microcline.
49-4	Nelson County, Virginia	573.0	573.7	Blue quartz containing oriented rutile needles.
49-5A	Potomac Gold Mine, Montgomery Co., Md.	573.2	573.3	Milky quartz from dump.
49-5B	Potomac Gold Mine, Montgomery Co., Md.	573.5	573.6	Sugary gray quartz from dump.
49-6	Marble Falls, Texas	573.0	573.0	Unzoned pegmatite.
49-7	Marble Falls, Texas	572.8	573.1	Pegmatite.
49-8	Big Thompson Canyon, about 3 miles above Drake, Colorado	572.7	573.2	Pegmatite: quartz, feldspar, muscovite.
49-9	Hyatt pegmatite, Larimer Co., Colorado	573.5	573.3	Granite at 50 ft. from pegmatite contact.
49-10	Hyatt pegmatite, Larimer Co., Colorado	573.2	573.6	Small quartz vein in granite, about 150 ft. from pegmatite mass.

APPENDIX (cont.)

Sample No. and Source		H (°C.)	C (°C.)	Remarks
49-11	Hyatt pegmatite, Larimer Co., Colorado	571.4	572.5	Wall zone: fine-grained quartz, perthite, muscovite, + black tourmaline and about 1% of beryl.
49-12	Hyatt pegmatite, Larimer Co., Colorado	571.3	572.6	Second zone: coarse perthite and quartz.
49-13	Hyatt pegmatite, Larimer Co., Colorado	571.8	572.9	Third zone: plagioclase, quartz, muscovite + large beryl crystals.
49-14	Hyatt pegmatite, Larimer Co., Colorado	571.5	572.3	Fourth zone, (core ?): white perthite colored by manganese oxide dendrites; minor quartz.
49-15	Hyatt pegmatite, Larimer Co., Colorado	572.9	573.3	Schistose country rock.
49-17	Jacque Mt., Summit Co., Colorado ..	572.9	572.8	Phenocrysts of "Lincoln" porphyry.
49-19	Pearl Creek valley, Holy Cross quad., Eagle Co., Colorado	572.5	572.7	Phenocrysts from "Elk" porphyry.
49-21	Wilfley Mine, Summit Co., Colorado	572.5	573.8	Quartz crystals from vug in rock sample from dump.
49-22	Sheep Mt., Summit Co., Colorado ..	572.6	572.8	Phenocrysts from "Lincoln" porphyry. Jagged thermal curve.

APPENDIX (cont.)

Sample No. and Source		H (°C.)	C (°C.)	Remarks
49-25	Chalk Mt., about 1 mile west of Climax, Lake Co., Colorado	572.4	572.7	Phenocrysts from rhyolite (nevadite).
49-26	Chalk Mt., Lake Co., Colorado	572.9	572.7	Smoky quartz phenocrysts from Chalk Mountain rhyolite.
49-28	Between peak 10 and Crystal Peak, Tenmile Range, Summit Co., Colorado	545.0	564.0	(Fine ground sample.) Quartz from vug in pegmatite.
49-29	Col. Sellers Mine (Pb-Ag ore or in Pennsylvanian limestone), Elk Mt., Summit Co., Colorado	570.0	574.0	Quartz in vugs in ore zone; very slow inversion.
49-31	Climax to Leadville highway, 6 miles from Climax, Colorado	572.7	572.7	Phenocrysts from "Lincoln" porphyry.
49-32	Ranch Creek Rd., near Camp Hale, Eagle Co., Colorado	572.6	573.0	Phenocrysts from "Pando" porphyry.
49-33	Camp Hale, Eagle Co., Colorado ...	572.4	572.7	Phenocrysts from porphyry of "Elk Mountain" type.
49-35	Cataract Creek road, Eagle Co., Colorado	572.4	572.4	Phenocrysts from pink "Lincoln" porphyry.
49-36	Radio-Ridge, Eagle Co., Colorado ..	573.4	574.4	Jasperoid chert, replacement mass in Mississippian limestone. Slow inversion, weak thermal effect in fine ground sample.

APPENDIX (cont.)

Sample No. and Source		H (°C.)	C (°C.)	Remarks
49-37	Between Kokomo and Wheeler Junction, Summit Co., Colorado ..	572.7	572.9	Quartz monzonite porphyry.
49-38	Between Kokomo and Wheeler Junction, Summit Co., Colorado ..	572.3	573.3	2-in. quartz vein in porphyry.
49-39	Between Kokomo and Wheeler Junction, Summit Co., Colorado ..	572.9	573.0	Unzoned quartz-feldspar pegmatite.
49-40	Excelsior Mine, Summit Co., Colorado	572.3	573.4	White quartz associated with siderite and galena. Slow inversion; possibly double.
49-41	2.6 miles west of Lake George, Colorado	572.8	573.2	Zoned pegmatite, sample from quartz-albite wall zone.
49-42	2.6 miles west of Lake George, Colorado	573.0	573.3	Core zone; massive quartz + microcline, perthite, muscovite, biotite.
49-44	2.6 miles west of Lake George, Colorado	573.4	573.3	Gneissic wall rock of pegmatite.
49-45	2.6 miles west of Lake George, Colorado	572.8	573.1	Quartz intergrowth with albite replacing microcline, central zone.
49-47	3 miles north of Cripple Creek, Colorado	571.9	572.7	Pike's Peak granite.

APPENDIX (cont.)

Sample No. and Source		H (°C.)	C (°C.)	Remarks
49-50	Cripple Creek, Colorado	573.1	573.1	8-in. pegmatite dyke in granite.
49-55	4.5 miles south of Jefferson, South Park Area, Colorado	572.7	573.4	White "Silver Plume" granite.
49-56	Southwest part of Twp. 8 S, Range 75 W., South Park Area, Colorado	573.1	573.2	Pink "Silver Plume" granite.
49-60	10 miles southwest of Hartsell, South Park Area, Colorado	573.4	573.3	Granite.
49-61	19 miles southwest of Hartsell, South Park Area, Colorado	573.1	573.3	Granite.
49-62	5 miles east of Aspen, Route 82, Colorado	573.1	573.4	Granite or granodiorite.
49-63	Black Canyon of the Gunnison River, Colorado	573.5	573.4	Unzoned pegmatite: quartz, graphic granite, minor muscovite and biotite.
49-66	Quartz Creek District, Gunnison Co., Colorado	573.3	573.6	Quartz crystals from vug in pegmatitic granite.
49-67	Quartz Creek District, Gunnison Co., Colorado	572.9	573.4	Quartz with muscovite inclusions from fine-grained pegmatite half-mile west of Brown Derby Mine.

APPENDIX (cont.)

Sample No. and Source		H (°C.)	C (°C.)	Remarks
49-68	Quartz Creek District, Gunnison Co., Colorado	572.7	573.3	Graphic granite from same locality.
49-69	Quartz Creek District, Gunnison Co., Colorado	573.2	573.3	Wall rock: coarse biotite granite.
49-70	Brown Derby Mine, Quartz Creek District, Gunnison Co., Colorado	572.7	573.0	Wall zone at base of gently dipping pegmatite.
49-71	Brown Derby Mine, Quartz Creek District, Gunnison Co., Colorado	572.4	572.8	Zone of curved lepidolite + topaz.
49-94	Campground, east fork of San Juan Road, 11 miles east of Pagosa Springs, Colorado	572.3	573.4	Quartz associated with chalcedony; amygdules in basic lava.
49-95	Highway near Los Alamos, Sandoval Co., New Mexico	573.1	572.9	Quartz from welded rhyolite tuff.
49-97	Banco Bonito glass flow, Jemez Mts., New Mexico	572.9	572.8	Phenocrysts from obsidian.
49-98	Highway 4, at entrance to East Jemez Forest Camp, New Mexico	573.0	572.9	Quartz from domed rhyolite plug ("Domite").
49-103	8 miles northwest of Cochiti, Jemez Mts., New Mexico	572.8	572.5	Quartz from welded rhyolite tuff.

APPENDIX (cont.)

Sample No. and Source		H (°C.)	C (°C.)	Remarks
49-105	Between Blake and Valle Grande, Jemez Mts., New Mexico	573.1	572.9	Welded tuff containing quartz and iridescent feldspar.
49-106	Between Eagle Nest Lake and Ute Park, northern New Mexico	572.9	572.7	Phenocrysts from intrusive porphyry.
49-119	Pamour Mine, Porcupine District, Ont.	572.5	573.2	Vein quartz, 200-ft. level.
49-120	Pamour Mine, Porcupine District, Ont.	572.5	573.3	Vein quartz, 1800-ft. level.
49-121	Hot Springs, Arkansas, National Museum No. 83660	573.2 572.0	573.2	Crystal used by R. E. Gibson. Thermal peak double and jagged.
49-122	Brazil	573.1	572.8	Size –35 + 80 mesh.
		573.0	572.7	Size –80 + 200 mesh.
		573.0	572.9	Size –200 mesh washed free of finer sizes which remain suspended in 8-in. water column longer than 5 minutes.
		573.1	573.0	Elutriated fines.
49-123	Teck-Hughes Mine, Kirkland Lake, Ont.	572.0	574.5	(Fine ground sample.) Main vein, 730-ft. depth, very slow inversion.

APPENDIX (cont.)

Sample No. and Source		$\frac{H}{(°C.)}$	$\frac{C}{(°C.)}$	Remarks
49-124	Teck-Hughes Mine, Kirkland Lake, Ont.	572.0	574.2	(Fine ground sample.) 36R branch vein, 4300-ft. depth, very slow inversion.
49-125	Teck Hughes Mine, Kirkland Lake, Ont.	572.7	574.1	(Fine ground sample.) South branch of main vein, 5625-ft. depth, very slow inversion.
49-126	Normetal Mine, Western Quebec ...	573.2	573.9	(Fine ground sample.) Vein quartz from surface.
49-127	Normetal Mine, Western Quebec ...	573.2	573.9	(Fine ground sample.) Vein quartz from 3240-ft. depth.
49-128	Laramie Mts., Wyoming	573.3	573.3	Quartzite inclusion in anorthosite.
49-131	Synthetic (G. W. Morey)	573.3	574.0	From silica glass, 15000 psi, 500° C., 3 weeks.
49-132	Marble Falls, Texas	573.1	573.2	Quartz separated from granite.
49-133	San Cristobal Quad.; San Juan Mts., Colorado	572.9	572.6	Smoky quartz from Hinsdale rhyolite.
49-134	Synthetic: Bell Telephone Laboratory: Na_2Co_3 + Na (OH)	573.4	573.2	15000 psi, 383° C.
49-135	Synthetic: Bell Telephone Laboratory: Na_2Co_3 + Na (OH)	573.4	573.2	15000 psi, 390° C.

APPENDIX (cont.)

Sample No.	Source	H (°C.)	C (°C.)	Remarks
49-136	Synthetic: Bell Telephone Laboratory: Na_2CO_3 + Na (OH)	573.3	572.9	Pressure less than 15000 psi, 300° C.
49-137	Lisbon, Md.	572.3	573.4	Vein quartz.
49-141	Synthetic: (J. Schulman) silicic acid + $CaCO_3$	?	?	Heated 3.5 days at 1150° C., very sluggish inversion.
49-142	Blue Hill, Delaware Co., Pennsylvania	571.7	574.2	Green quartz (sample finely ground), very slow inversion. No heat effect in coarse granular sample.
49-143	Brazil	573.5	573.5	Single clear crystal.
49-144	St. Lawrence Co., New York	573.1	573.3	From dolomite, prism faces missing from quartz crystals.
49-145	Amelia Co., Virginia	573.5	573.3	Crystal with tourmaline inclusions.
49-146	Brazil	573.8	573.3	Crystal with rutile inclusions.
49-147	Paris, Maine	572.5	572.3	Milky quartz.
49-148	Bernfjord, Iceland	536	....	Pale green quartz, extremely slow inversion.
49-149	Hot Springs, Arkansas	573.1	573.2	Tabular yellow crystals, double inversion on cooling.

APPENDIX (cont.)

Sample No. and Source		H (°C.)	C (°C.)	Remarks
49-150	Synthetic: silica glass + Na (OH)	....	....	15000 psi, 300° C., product is fine grained mosaic with very sluggish inversion.
49-151	Southwest Greenland	573.2	573.3	Pegmatite containing quartz, K feldspar, Mg, Ti, Mn garnet + biotite. Classed as high-temperature facies by Hans Ramberg (1949).
49-153	Southwest Greenland	573.3	573.3	Garnet-bearing pegmatite, classified as low-temperature facies by Hans Ramberg.
49-154	Southwest Greenland	572.7	573.2	Pegmatite containing plagioclase, K feldspar, biotite; unclassified as to facies.
49-155	Southwest Greenland	573.1	573.4	Schistose country rock adjacent to 49-151. Lower heating inversion obtained on repeat run.
49-161	Synthetic: silica glass + Na (OH)	573.1	573.9	15000 psi, 550° C.
49-162	Synthetic: silica glass + Na (OH)	573.2	573.9	15000 psi, 568° C.
49-163	Synthetic: silica glass + Na (OH)	573.3 ?	573.7 ?	15000 psi, 395° C., fine-grained mosaic with very slow inversion. No thermal effect until sample was finely ground.
49-164	Synthetic: silica glass + Na (OH)	573.2	573.8	4000 psi, 400° C. Fine grained mosaic with slow inversion. No thermal effect until sample was finely ground.

APPENDIX (cont.)

Sample No. and Source		H (°C.)	C (°C.)	Remarks
49-171	Wright-Hargreaves Mine, Kirkland Lake, Ont.	571.9	574.4	Fine ground sample from south vein, 1000-ft. level. Sluggish inversion.
49-172	Wright-Hargreaves Mine, Kirkland Lake, Ont.	571.8	574.0	Fine ground sample from north vein, 1000-ft. level. Sluggish inversion.
49-173	Wright-Hargreaves Mine, Kirkland Lake, Ont.	572.5	574.2	Fine ground sample from south vein, 3000-ft. level. Sluggish inversion.
49-174	Wright-Hargreaves Mine, Kirkland Lake, Ont.	571.4	574.1	Fine ground sample from north vein, 3000-ft. level. Sluggish inversion.
49-175	Wright-Hargreaves Mine, Kirkland Lake, Ont.	572.8	574.2	Fine ground sample from south vein, 5100-ft. level. Sluggish inversion.
49-176	Wright-Hargreaves Mine, Kirkland Lake, Ont.	571.8	574.3	Fine ground sample from north vein, 5100-ft. level. Sluggish inversion.
49-177	Wright-Hargreaves Mine, Kirkland Lake, Ont.	572.8	574.2	Fine ground sample from No. 60 vein, 5100-ft. level. Slugg'sh inversion.

APPENDIX (cont.)

Sample No. and Source		H (°C.)	C (°C.)	Remarks
49-178	Wright-Hargreaves Mine, Kirkland Lake, Ont.	573.2	574.7	Fine ground sample from No. 8 vein, 5100-ft. level. Sluggish inversion.
49-179	Wright-Hargreaves Mine, Kirkland Lake, Ont.	572.8 572.9 572.8 572.9	574.1 574.1 574.1 574.0	Fine ground sample from south vein, 6150-ft. level. Sluggish inversion. (Repeat runs.)
49-180	Wright-Hargreaves Mine, Kirkland Lake, Ont.	572.7	574.4	Fine ground sample from north vein, 6150-ft. level. Sluggish inversion.
49-181	Ceylon	573.6	573.3	Single crystal with actinolite inclusions.
49-182	Striegau, Silesia, Germany	573.5	573.3	Smoky quartz, jagged thermal curve.
49-183	Keokuk, Iowa	573.6	574.0	Crystals from geode.
49-184	Ballard Mine, Cherokee Co., Kansas	571.3 570.4	573.6	Quartz associated with sphalerite; overlapping double inversion.
49-185	Manitoba	572.9	572.9	Rose quartz from pegmatite.
49-186	New York City	573.2	573.2	Iridescent vein quartz.
49-187	Cumberland, England	571.7 569.9	573.2	Quartz intergrown with hematite; overlapping double inversion.

APPENDIX (cont.)

Sample No. and Source		H (°C.)	C (°C.)	Remarks
49-188	Culpepper Co., Va.	573.4	573.5	Blue quartz.
49-189	Minas Geraes, Brazil	573.0	573.1	Green quartz with fuchsite.
49-190	Globe, Arizona	573.4	574.0	Quartz associated with malachite, chrysocolla and calcite; geode in limonite.
49-191	Bahia, Brazil	573.6	573.3	Single crystal with orange red phantom.
49-192	Little Pipestone, Jefferson Co., Montana	573.5	573.5	Smoky quartz with tourmaline.
49-193	Brazil	573.6	573.7	"Cat's-Eye" quartz secondary after crocidolite.
49-194	Brazil	572.2 571.6	573.1	Granular sample from single crystal; double inversion.
		.... 573.2	571.9	Cylinder cut from same crystal.
49-195	Brazil (Bates and Phelps, crystal A)	572.9	573.2 572.4	Granular sample, double inversion on cooling.
49-196	Brazil (Bates and Phelps, crystal B)	573.5	572.0	Cylinder.
		.... 572.7	573.5 572.3	Crushed cylinder, double inversion.

APPENDIX (cont.)

Sample No. and Source		H (°C.)	C (°C.)	Remarks
49-197	Brazil (Bates and Phelps, crystal C) ..	573.6	571.8	Cylinder.
		573.1	573.0	Equivalent granular sample.
49-198	Brazil	573.2	573.4	Core at base of crystal, double inversion on cooling.
		573.0	572.8	Center inside (core).
		573.3	573.3	Center outer zone; double inversion.
49-198 R	Brazil (same as above)	573.2	573.2	Termination of crystal, double inversion.
		572.0	....	
		573.3	572.5	Cylinder cut from termination of crystal.
			572.0	
49-199	Bahia, Brazil	572.8	573.4	Crystal with variable citrine color. Double inversion.
			572.6	
49-201	Pinkneyville, N. J.	573.0	573.3	Pegmatite cutting limestone. Standard Lime Company quarry.
49-202	Herkimer Co., N. Y.	574.4	573.0	Cylinder No. 1. Quartz from vug in dolomite.
		574.3	573.1	Cylinder No. 2.
		573.6	573.5	Crushed cylinder No. 2.
49-206	Teck Hughes Mine, Kirkland Lake, Ont.	571.7	574.3	Fine crushed sample from main vein, 2500-ft. level. Very sluggish inversion.

APPENDIX (cont.)

Sample No. and Source		H (°C.)	C (°C.)	Remarks
50-17	Westerly, R. I.	573.3	573.3	Granite.*
50-18	Milford, N. H.	573.3	573.2	Granite.*
50-19	Bradford, R. I.	573.5	573.3	Granite.*
50-20	Pownal, Maine	573.2	573.4	Granite.*
50-21	Hallowell, Maine	573.4	573.4	Granite.*
50-22	Westwood, Mass.	572.8	573.1	Granite.*
50-23	Clark Island, Mass.	573.3	573.5	Granite.*
50-24	Fitzwilliam, N. H.	573.4	573.3	Granite.*
50-25	Concord, N. H.	573.3	573.4	Granite.*
50-26	Woodbury, Vermont	573.4	573.3	Granite.*
50-27	Barre, Vermont	573.3	573.6	Granite.*
50-28	North Sullivan, Maine	572.7	572.8	Granite.*
50-29	Jonesport, Maine	572.6	572.9	Granite.*
50-30	Judith Peak, Mont.	573.6	573.3	Phenocrysts from porphyry.

* For description of New England granites, see F. Chayes, 1952, "Finer Grained Calcalkaline Granites of New England," Jour. Geology, vol. 60, pp. 207-254.

APPENDIX (cont.)

Sample No. and Source		H (°C.)	C (°C.)	Remarks
50-31	Six-Mile Creek, Llano, Texas	573.2	573.4	Granite.†
50-32	Cassady Group, Llano, Texas	573.3	573.3	Granite.†
50-33	Craig property, Kingsland, Texas ..	573.1	573.7	Granite.†
50-34	Curley Quarry, Llano, Texas	573.2	573.3	Granite.†
50-35	Sandstone Mt., Llano, Texas	573.2	573.2	Granite.†
50-36	Stribling Quarry, Llano, Texas	573.3	573.3	Granite.†
50-37	Old Nagel Quarry, Fredericksburg, Texas	573.3	573.5	Granite.†
50-38	Blodgett Quarry, Pontotoc, Texas ..	573.2	573.5	Granite.†
50-39	Fletcher Quarry, Chelmsford, Mass.	573.4	573.5	Medium-grained granite.*
50-40	Fletcher Quarry, Chelmsford, Mass.	573.5	574.0	Finer-grained granite.
50-43	Synthetic: Brush Development Company	573.0 573.9	573.3 572.9	Granular sample, 5500 psi, 376° C. Cylinder.
50-49	Cape Ann Granite Co., Rockport, Mass.	573.2	573.2	Vein of milky blue quartz in granite.

†For description of Texas specimens, see Virgil E. Barnes, Raymond F. Dawson and George A. Parkinson, 1942, "Building Stones of Central Texas," The University of Texas Bull., p. 246.

APPENDIX (cont.)

Sample No.	Source	H (°C.)	C (°C.)	Remarks
50-51	Helen Beryl pegmatite, Custer Co., S. D.	571.9	572.0	Zoned pegmatite: sample from zone of fine-grained albite, quartz, muscovite.
50-52	Helen Beryl pegmatite, Custer Co., S. D.	571.4	571.8	Zoned pegmatite: sample from perthite-quartz fracture filling.
50-55	1.5 miles west of Sedalia, Colorado	572.0	573.6	Disintegrated Pike's Peak granite.
50-56	20.5 miles southwest of Sedalia, Colorado	572.8	572.8	Relatively fresh Pike's Peak granite.
50-57	0.3 miles northwest of Deckers, Colorado	572.2	573.1	Relatively fresh Pike's Peak granite.
50-64	Sintered synthetic: on join Li_2O.Al_2O_3—SiO_2 at 80% SiO_2	—(see 50-217 below)		From R. H. Thomas, Rutgers University. No inversion found 440° to 635° C.
50-217	Synthetic: sintered mixture of Li_2CO_3, Al_2O_3 and potters flint, in molecular proportion Li_2O·Al_2O_3·12 SiO_2	463 ± 15		15 hours at 1300° C. Product quartz + β spodumene. Slow inversion located by X-ray goniometer furnace.
51-1	England, from R. A. Howie, Cambridge Univ.	573.4	573.8	Quartz concentrate from charnockite.

APPENDIX (cont.)

Sample No. and Source		H (°C.)	C (°C.)	Remarks
51-2	England, from R. A. Howie, Cambridge Univ.	573.4	573.7	Quartz concentrate from charnockite. Low thermal peak due to considerable amount of feldspar in sample.
51-3	England, from R. A. Howie, Cambridge Univ.	573.3	573.5	Quartz concentrate from charnockite.
51-6	Herkimer Co., N. Y.	573.5	573.5	Two doubly terminated crystals from cavities in dolomitic limestone. Both contain angular inclusions composed in part of two hydrocarbons, one of which melts at 70° to 80° C., the other at 200° to 220° C.

JAPANESE TWINS OF QUARTZ

S. KOZU*

ABSTRACT. The possible types of quartz twins which incorporate the "Japanese twin" law are enumerated. Etching was used to determine the twin law and composition plane. Differences in the crystals are related to their genetic conditions.

INTRODUCTION

TWINNED crystals of quartz in which the composition plane is $(11\bar{2}2)$, and the c-axes cross at an angle of 84° 33′, were noted in Japan many years ago, and this type is usually known as "Japanese twin." Although it is not clear who used the name for the first time, twinning of Japanese quartz according to this law was described by G. vom Rath as early as 1875; in 1905 Goldschmidt used the name "japaner Gesetz," and the term has since been used by many investigators (Klockmann, 1912; Zyndel, 1913; Brauns, 1919; Heide, 1927; Bragg and Bragg, 1933).

As a result of his study on many specimens of such twins from Japan by various approaches, especially morphologically and by etching, the writer has obtained some interesting information which is given in the following pages. The writer's thanks are due to S. Watanabe for his goniometric measurement, to I. Machiba for his etching experiments, and to K. Yagi for his help in preparing the paper.

MODES OF OCCURRENCE

Localities of Japanese-twinned quartz in Japan include the following:

1. Otomezaka, Yamanashi Pref.
2. Narushima, Gotō, Nagasaki Pref.
3. Kawahage, Nagano Pref.
4. Iwato, Miyazaki Pref.
5. Ade Mine, Ishikawa Pref.
6. Kiura, Miyazaki Pref.
7. Ofuku Mine, Yamaguchi Pref.

The first two localities are well known for their beautiful twinned crystals. At Otomezaka they occur in granitic pegmatites associated with topaz, tourmaline, feldspar, and apatite, or

*Member of Japanese Academy; Emeritus Professor, Tohoku University, Sendai.

rarely in quartz pegmatite without other minerals. In some parts of the pegmatites twinned quartz crystals are accompanied by such ore minerals as molybdenite, wolframite, chalcopyrite, galena, and sphalerite. At Narushima quartz twins are always confined to the central drusy cavities of many small quartz veins intrusive into sandstone. These crystals grow into free spaces together with prismatic crystals of quartz, and their size ranges from 1 to 3 cm. The Narushima veins are not pegmatitic, but probably are formed from low temperature solutions. It is possible that the solutions were produced by post-igneous activity associated with quartz porphyry, intruded along a tectonic line running parallel to the eastern coast of South Korea.

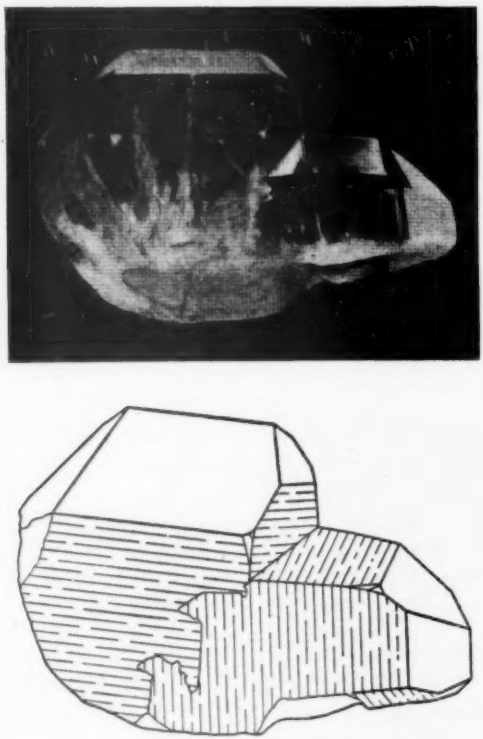

Fig. 1. Japanese twin of quartz from Otomezaka (natural size).

MORPHOLOGY

In Otomezaka crystals with well developed trapezohedron forms, it may be seen that the individuals of the twins are either right- or left-handed quartz, and that they may also be twinned after either the right- or left-Dauphine law (fig. 1). Many other habits may be detected by means of the etching technique described later.

Crystals from Narushima, however, have no trapezohedron faces, so that twin-types cannot be determined from the external form. From crystals of this sort (fig. 2) a plate about 1 mm. in thickness, cut perpendicular to the c-axis of each individual, was observed in sodium light to determine the distribution of left- and right-handed quartz within the crystal. There are at least three different types of combination; i.e., the individuals are both left-handed quartz, both right-handed quartz, or left- and right-handed quartz. The method, however, fails to determine the nature of the Dauphine twin in each individual.

Beautiful crystals from Narushima were measured by a

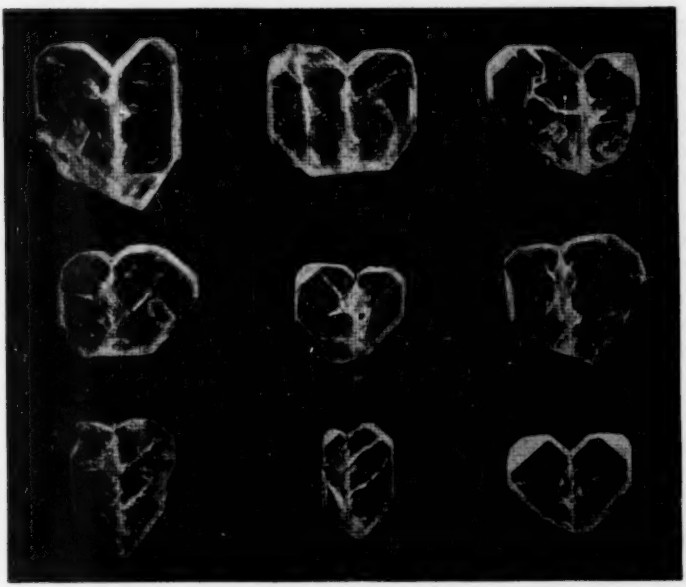

Fig. 2. Japanese twins of quartz from Narushima (natural size).

Goldschmidt two-circle goniometer to get an exact measurement of the angle of c-axes in the twinning. Vicinal planes belonging to two or three slightly different zones are developed on m($1\bar{1}00$), and similar faces of a gentle pyramid on r($10\bar{1}1$) were noted in all crystals. Determination of the angle is therefore difficult and probably not very accurate. The results are shown in table 1.

TABLE 1

Inclination of c-Axes in Narushima Quartz

84°	13.5′
84°	38′
85°	17′
84°	1′
83°	45′
84°	27′
Mean 84°	23.1′

The mean value is fairly close to the theoretically calculated value of 84° 33.4′.

THE JAPANESE TWIN

Composition plane of the Japanese twin is usually expressed as ($11\bar{2}2$), but this has also three other corresponding planes with similar indices, such as ($\bar{1}122$), ($11\bar{2}\bar{2}$) and ($\bar{1}12\bar{2}$); the relation between these is shown in figure 3. Suppose at first that the two halves are both left-handed. When the composition plane of the first half is ($11\bar{2}2$), the corresponding plane in the second can be either ($11\bar{2}2$), ($\bar{1}122$), ($11\bar{2}\bar{2}$) or ($\bar{1}12\bar{2}$). Because the first half can also assume ($\bar{1}122$), ($11\bar{2}\bar{2}$), and ($\bar{1}12\bar{2}$) as the composition plane, there should be sixteen possible types of twin by combination of these planes. From symmetry, however, thirteen of these sixteen coincide with others, and the actual types are reduced to the following three: L($11\bar{2}2$) and L($\bar{1}122$); L($11\bar{2}2$) and L($11\bar{2}\bar{2}$); and L($\bar{1}122$) and L($\bar{1}122$). Similarly, three types of twin are derived when the two halves are both right-handed quartz. If the one half is left-handed, and the second is right-handed quartz, there are four, instead of three, different types. In total, therefore, there should be ten types of Japanese twin as shown in table 2 and in figure 4.

OSBERVATION ON ETCHED TWINS

Etching was employed to determine the relation between composition plane and individuals in ten specimens from Otome-

zaka, and in twenty-five from Narushima. Concentration of the hydrofluoric acid used varied from 20 to 40 per cent, and the period of immersion varied from 2 to 6 hours. Individuals of Japanese twins from two localities are always twinned on the Dauphine law.

Observation on prisms.—In Narushima crystals the composition plane usually appears zigzag on natural prisms, but proves to be exactly $\{11\bar{2}2\}$ with sharp and straight trace on a polished surface, when the natural prisms are slightly ground (figs. 5 and 6). On the contrary, the composition plane of Otomezaka crystals is not only $\{11\bar{2}2\}$ but also assumes other planes which yield a zigzag trace even on the polished surface. This difference may be ascribed to the difference of thickness of the crystals, for Narushima twins are usually 2-4 mm. in thickness, while Otomezaka twins vary in size from 2 mm. to more than half a meter.

In the crystals from Narushima the two halves are sometimes in direct contact with each other at the composition plane (b and f in fig. 5), but usually there are intervening narrow strips along the composition plane (a and d in fig. 5). As noted later, this portion is composed of parallel growth of minute left- and right-handed quartz. In both cases, the Japanese twin belongs to I, IV, VII, or IX, as classified in table 2 (a and d . . . I, b and f . . . VII). Presence of such narrow strips is not governed by the type of twin. If there is another individual between the two halves, however, the type of twin will be different from those mentioned above, and will belong to II, III, V, VI, VIII, or X (a and e, III; c and d, VIII; a and f, X).

TABLE 2

Indices of Possible Composition Planes of Individuals in Japanese Twins

Type	Composition plane of individuals	
I	L(11$\bar{2}$2)	L($\bar{1}$122)
II	L(11$\bar{2}$2)	L(11$\bar{2}$2)
III	L($\bar{1}$122)	L($\bar{1}$122)
IV	R(11$\bar{2}$2)	R($\bar{1}$122)
V	R(11$\bar{2}$2)	R(11$\bar{2}$2)
VI	R($\bar{1}$122)	R($\bar{1}$122)
VII	L(11$\bar{2}$2)	R($\bar{1}$122)
VIII	L(11$\bar{2}$2)	R(11$\bar{2}$2)
IX	L($\bar{1}$122)	R(11$\bar{2}$2)
X	L($\bar{1}$122)	R($\bar{1}$122)

L.—Left-handed quartz, R—Right-handed quartz.

In other words, if the two halves, which are single crystals of either right- or left-handed quartz, are in direct contact at the composition plane of $\{11\bar{2}2\}$, the relation of the two is one of the types I, IV, VII, and IX. These four are therefore called fundamental types. If, on the other hand, the individuals are twinned after either the Dauphine or the Brazil law, the relation of those parts not in direct contact with each other, but separated by another individual, is either II, III, V, VI, VIII, or X. These latter types are the combination of two kinds of twinning, and are therefore called derivative types.

In the majority of the twinned crystals from Otomezaka, two halves are in direct contact with each other, and the narrow strip composed of parallel growth of left- and right-handed quartz is usually absent. Types of twinning in these crystals are quite similar to those observed at Narushima and need no further description.

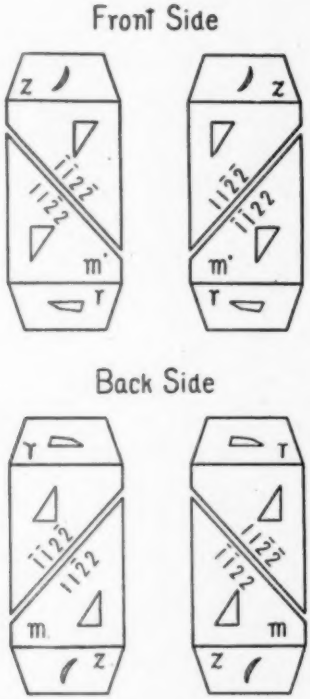

Fig. 3. Four planes of general indices of $\{11\bar{2}2\}$ in left-handed quartz, with etching figures on m, r and z.

Observations on composition planes.—Sections cut parallel to $(11\bar{2}2)$, $(\bar{1}\bar{1}22)$, $(11\bar{2}\bar{2})$ or $(\bar{1}\bar{1}2\bar{2})$ show two kinds of etching figures, namely shapes of the new moon, and of a flying bat, by which difference between left- or right-handed quartz can be determined. Etching on the sections cut perpendicular to $m(1\bar{1}00)$, or to the edge $[r(10\bar{1}1) : z(01\bar{1}1)]$, reveals traces of the composition plane on the section, and also etching figures, as shown in figures 6, 7, and 8. The trace of the actual composition plane is usually not a single straight line, but is composed of zigzag lines of various orientations. Of these, $\{11\bar{2}2\}$ is naturally the most important; it is developed in the central part of the crystals. Nevertheless there are many other planes, as determined by the angles between these traces and $\{11\bar{2}2\}$ or $m(1\bar{1}00)$; these less common planes are: $\epsilon(12\bar{3}1)$, $x(51\bar{6}1)$, $y(41\bar{5}1)$, $\tau_3(16\bar{7}6)$, $v(71\bar{8}1)$, $\beta(29\bar{7}9)$, $a(11\bar{2}0)$,

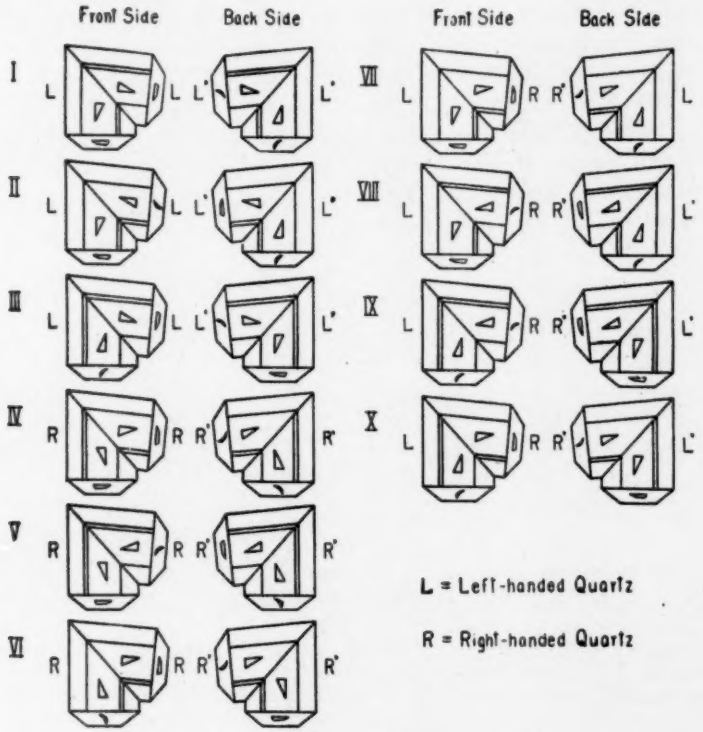

Fig. 4. Ten types of Japanese twins.

$k_6(32\bar{5}0)$, $(93\bar{1}\bar{2}1)$, $k_4(21\bar{3}0)$, $k_2(31\bar{4}0)$, $k(51\bar{6}0)$, $z(01\bar{1}1)$, and $r(10\bar{1}1)$.

In the sections of Narushima crystals there are hourglass-shaped parts, bounded by $r(10\bar{1}1)$, $z(01\bar{1}1)$ and $m(1\bar{1}00)$ (figs. 6 and 7), filled with fine-grained quartz crystals with structures entirely different from the main part of the crystals. By X-ray study it has been shown that this part consists of parallel growth of minute left- and right-handed quartz crystals which have the same crystallographic orientation with the main part of individuals of the twins. This hourglass-shaped part is a section of the same portion, which appears as a narrow strip on the prisms previously described (figs. 6 and 7). Probably after the crystallization of the main part of the individuals, the hourglass-shaped space between the two halves was filled by minute secondary crystals of quartz, crystallized under different conditions, where presumably colloidal silica was present.

Unlike the Narushima crystals, the Otomezaka twins have only poorly developed $\{11\bar{2}2\}$ as composition plane, although many other planes are well developed (fig. 8). They are $z(01\bar{1}1)$, $r(10\bar{1}1)$, $a(11\bar{2}0)$, $k_6(32\bar{5}0)$, $k(51\bar{6}0)$, $v(71\bar{8}1)$, $(93\bar{1}\bar{2}1)$, $\tau_3(16\bar{7}6)$, $\beta(29\bar{7}9)$, etc. The hourglass-shaped part is usually absent, and even when present it is composed of much coarser-grained quartz crystals. Probably in the Otomezaka crystals, there was no secondary growth of quartz at all, or, at any rate,

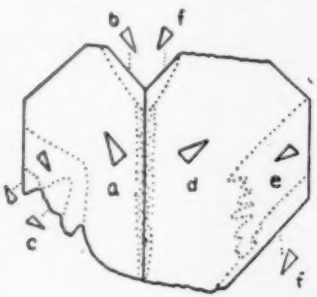

Fig. 5. Etching figures on the prisms of quartz twin from Narushima. Types of twins of various parts indicated in the figure are as follows:

a-d, b-e	I	b-f	VII
b-d	II	c-d	VIII
a-e	III	c-e	IX
c-f	IV	a-f	X

there were no drastic changes in the crystallization course in the pegmatites of this locality.

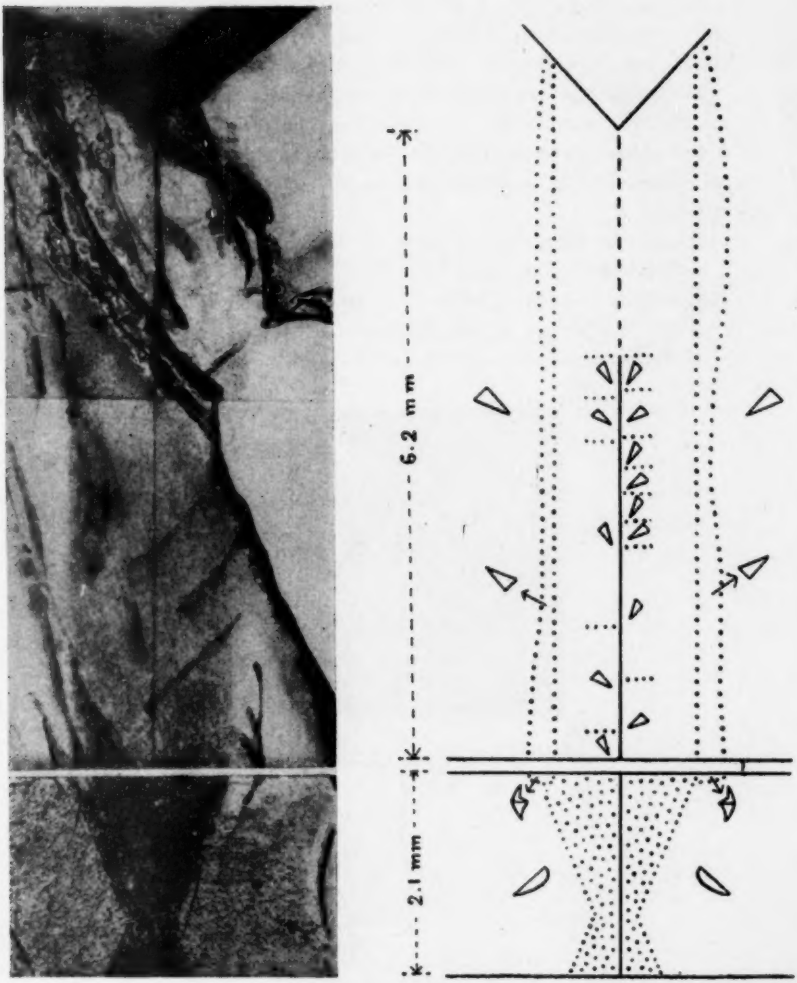

Fig. 6. Etching figures on m (upper), and on the section normal to the edge [r:z] (lower) of a twin from Narushima. Note that a narrow strip along the composition plane on m (upper) appears as hourglass-shaped part in the section (lower).

CONCLUSIONS

Ten types of Japanese twins of quartz are derived from the combination of composition plane $\{11\bar{2}2\}$.

Of these ten types, I, IV, VII, and IX are fundamental, and the others are derivative types, formed by the combination of the Japanese with either the Dauphine or the Brazil law.

Although the composition plane is usually taken theoretically as $\{11\bar{2}2\}$, in actual crystals it may be not only $\{11\bar{2}2\}$ but many other planes as well. In Narushima crystals the composition plane $\{11\bar{2}2\}$ is usually better developed than in Otomezaka crystals.

Along the composition plane of Narushima crystals, there is a sector bounded by $r(10\bar{1}1)$, $z(01\bar{1}1)$ and $m(1\bar{1}00)$ and filled with minute parallel growth of secondary quartz. In Otomezaka crystals this sector is usually absent.

Differences in the crystals from these two localities may be

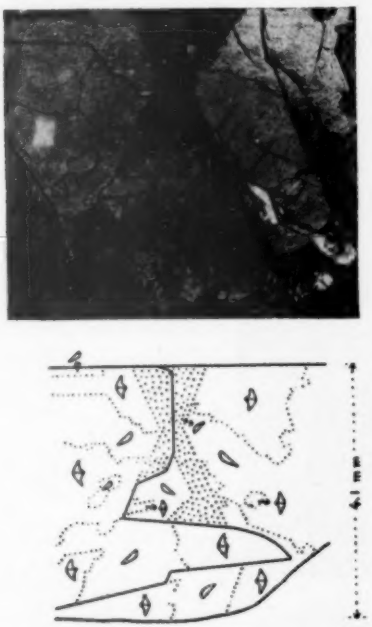

Fig. 7. Etching figures on the section normal to the edge [m:$\{11\bar{2}2\}$] of a twin from Narushima. Heavy line is a trace of composition planes.

ascribed to the differences in their genetic conditions. Otomezaka crystals formed in the pegmatites, while Narushima quartz probably crystallized out from colloidal silica solutions at much lower temperatures.

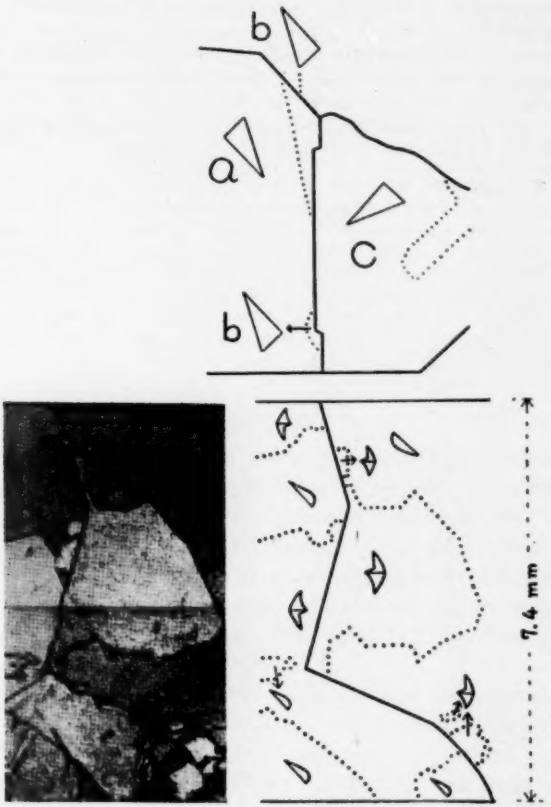

Fig. 8. Etching figures on m (upper), and on the section normal to the edge [r:z] (lower) of a twin from Otomezaka. Heavy lines in central part are traces of composition planes.

References

Bragg, W. H., and Bragg, W. L., 1933. The crystalline state. Volume I, A general survey, G. Bell and Sons, Ltd., London.

Brauns, R., 1919. Zwillinge nach ϵ aus Brasilien: Neues Jahrb., Band 1, pp. 29-49.

Goldschmidt, V., 1905*a*. Quarzzwilling nach r = 10: Min. pet. Mitt., Band 24, pp. 157-166.

———, 1905*b*. Über die Zwillingsgesetze des Quarz: Min. pet Mitt., Band 24, pp. 167-182.

Heide, F., 1927. Die Japaner Zwillinge des Quarzes und ihr Auftreten im Quarzporphyr vom Saubach i. V.: Zeitschr. Kristallographie, Band 66, pp. 239-281.

Klockmann F., 1912. Lehrbuch der Mineralogie, Ferdinand Enke, Stuttgart.

vom Rath, G., 1875. Mineralogische Mittheilungen: Annalen der Physik u. Chemie, Band 155, pp. 24-68.

Zyndel, F., 1913. Über Quarzzwillinge mit nichtparallelen Hauptaxen: Zeitschr. Kristallographie, Band 53, pp. 15-52.

Tohoku University
Sendai, Japan

THERMOCHEMISTRY OF PLAGIOCLASE AND ALKALI FELDSPARS

F. C. KRACEK and K. J. NEUVONEN*

ABSTRACT. Employing a hydrofluoric acid solution calorimeter, previously described, measurements of the heats of solution (decomposition) were performed in 20 per cent hydrofluoric acid at 74.7° for 21 feldspar materials in the plagioclase and alkali feldspar series. In combination with other pertinent measurements, these will lead to evaluation of the heats of formation of the feldspars. The results presented in this paper show that plagioclase feldspars in their natural state exist not as the simple, continuous, solid solution series that is found at the liquidus, but rather fall into three groups with dividing lines drawn at 30 and 65-70 mole per cent anorthite. The intermediate labradorite compositions appear to be mixtures of feldspars of the limiting compositions indicated. The alkali feldspars have thermal properties highly dependent on their origin and thermal history. Values of the latent heats of melting of albite and anorthite have been deduced from the thermochemical measurements. The average values are 49.2 cal/g for albite and 64.7 cal/g for anorthite. The heat of inversion of low, natural albite to high-temperature albite is 13 cal/g.

INTRODUCTION

THE only original data of basic significance on the thermal and thermochemical properties of feldspars that are recorded in the literature are given in two papers by White (1909, 1919) on the high-temperature specific heats of several individual feldspars including albite, anorthite, andesine, orthoclase, and microcline, crystalline and glassy, and in a paper by Mulert (1913) on the heats of solution in hydrofluoric acid of adularia and microcline.

Minor constituents aside, the feldspars may be regarded as solid solutions of three limiting compounds, $NaAlSi_3O_8$, $KAlSi_3O_8$, and $CaAl_2Si_2O_8$ which we may call, simply, soda feldspar, potash feldspar, and lime feldspar, respectively. However, we shall more usually designate them by their common names—albite, orthoclase, and anorthite—without necessarily implying the crystal structures denoted by these names. Natural feldspars represent two of the three possible series of solid solutions, namely, the soda-lime or plagioclase feldspars, and the soda-potash or alkali feldspars. In natural minerals of the two series the third constituent is usually present in relatively minor

* Visiting investigator of the Carnegie Institution of Washington associated with the staff of the Geophysical Laboratory, 1948-1950. Member of staff of the Geological Survey of Finland.

amounts. The phase equilibrium relations for the two series are now known in detail from the work of Bowen (1913), Morey and Bowen (1922), Schairer (1950), Bowen and Tuttle (1950) and Tuttle and Bowen (1950).

Thermochemical properties, such as the heats of formation of the feldspars, and of silicates in general, the determination of which require knowledge of the heats of reaction of chemical reactions, cannot be satisfactorily measured by allowing the formation reaction to take place directly in a calorimeter because of the indefinite products obtained in consequence of the sluggish manner in which silicates tend to react. As an alternative means there is available the much used method of measuring the heat of solution, i.e., the heat of decomposition, in a suitable solvent. For silicates, such a solvent is hydrofluoric acid. The heats of solution of the silicates, in combination with heats of solution of the constituent oxides or the elements, through proper combinations of the various reaction heats, and of heat capacity and entropy data lead to the evaluation of the different thermal quantities of interest in a thermodynamic treatment.

It is the purpose of the present paper to present results of measurements of the heats of solution of feldspars in hydrofluoric acid, and thereby to provide data which may ultimately lead to a thermodynamic treatment of these important minerals. The measurements presented at this time afford a direct means of determining (1) the heats of mixing of the feldspars in forming the naturally occurring solid solution series—in other words, the heats of formation of the solid solutions from their constituents, (2) latent heats of phase transformations, and (3) when combined with the heats of solution of the component oxides, the heats of formation of the feldspars, referred to the oxides.

APPARATUS AND METHODS OF STUDY

The heats of solution in hydrofluoric acid were measured in a calorimeter previously described by Kracek, Neuvonen, and Burley (1951). The calorimetric apparatus, except for minor details, is similar to that of Torgeson and Sahama (1948) and to that of Sahama and Neuvonen (1951). It is operated in an oil-bath thermostat kept at 74.7° C. The calorimeter is calibrated with electrical energy and its temperature change is measured with a copper resistance thermometer. Samples at room temperature are introduced into the calorimeter in gela-

tine capsules, and corrections are applied to bring the heat content changes to correspond to the process:

$$\text{Reactant (solid, 25°)} \rightarrow \text{Products (74.7°)}.$$

Although the reaction with the hydrofluoric acid occurs at 74.7°, this method of adjustment leads to values of the heats of formation at 25°.

Remarks on the calorimetric procedure.—The calorimetric apparatus is taken apart after each day's operation and reassembled the next day with a fresh filling of hydrofluoric acid. This is done in order that the solution reactions may be carried out under comparable conditions. Logically, the quantities of mineral samples dissolved in each filling of fresh acid would be fixed by stoichiometric relations so that the quantity of the products in the final solution be always the same. Such a procedure is described by Torgeson and Sahama (1948) who dissolved samples of silicates of such weight as would contain the stoichiometric equivalent of 0.6750 g. of quartz in 856 g. of 20.1 per cent (by weight) hydrofluoric acid. We found in early experiments that two samples could be dissolved in the same filling of acid with nearly identical results, so that the heat of dilution of the acid is not of great significance. Strict adherence to the stoichiometric relation is correct in principle, and would be demanded in all cases in which the heat of dilution is experimentally significant. However, it was found that the gain in weight of the samples, due to the absorption of moisture from the air in the relatively long time spent at the balance adjusting the sample to a specified weight, was more detrimental to accuracy—especially on humid days—than any error due to departure from stoichiometry. The procedure adopted, therefore, was to fill the containing gelatine capsule with a quantity of the sample and make as rapid a weighing as possible. All weighings were made with another similar empty capsule on the other balance pan as counterpoise. The sample weights were corrected for buoyancy and reduced to weight in a vacuum. The weights of the feldspar samples contained in the No. 000 capsules employed were near 0.8 g.

MINERALS STUDIED AND THEIR PURIFICATION

The feldspars employed in this work were all natural minerals with the exception of the pure anorthite, sample O, which was

synthesized from pure reagents (*vide infra*). Many of the minerals were supplied by the U. S. National Museum through the courtesy of W. F. Foshag; others were from the Harvard Mineralogical Museum, obtained through the courtesy of C. Frondel, and from the Princeton Mineralogical Collection through the courtesy of H. H. Hess. To all these donors we express our sincere thanks. Still other materials were obtained by purchase from Ward's Natural Science Establishment. Much of the material thus obtained could not be used because of inhomogeneity in its composition as revealed by microscopic examination; in some specimens the quantity of impurities which were present as small inclusions was so great that no effective purification could be made by any available method.

A brief description of the samples used is collected in tables 1 and 2. Most of the optical data given in these tables are by K. Hytönen of the Institute of Geology, University of Helsinki. A few of the materials were measured by O. F. Tuttle.

Purification of the materials.—In many of the specimens selected for purification the minerals were present as clear crystals large enough to permit separation from impurities by hand-picking. This was not true of the plagioclases rich in anorthite, of sanidine from Kokomo, Colorado, or of albite from Varuträsk, Sweden, all of which contained a great many small inclusions. These were put through a very laborious process of purification involving two major steps. First, the crushed rock was passed through a magnetic separator, following which it was given a gravity separation using heavy organic liquids. The second step involved centrifugation of the finely divided material suspended in Clerici solution of the proper density. For this the material was ground fine; a homogeneous fraction containing grain sizes from 5 to 10 microns was retained for use. The Clerici solution was used in preference to heavy organic liquids for the centrifugation because adsorbed moisture on the finely ground material prevented uniform wetting of the grains by the organic liquids. Good dispersions, however, were obtained when Clerici solution was used. The centrifugation was repeated several times whenever necessary in order to obtain the purification desired. The purity was checked under the microscope by grain counts using a mechanical tabulator. Any final preparation used was determined to contain less than 0.2 per cent

discrete impurities. Chemical analyses were made on the purified materials. The results of these are given in table 3.

The synthesis of artificial anorthite.—Inasmuch as the most anorthite-rich natural plagioclase available for this work, the Grass Valley, California, anorthite (sample 1), contains only 92.6 mole[1] per cent of the lime feldspar molecule, it was believed desirable to prepare a sample of pure anorthite. This was made up from quartz, alumina, and calcium carbonate, each of the highest purity available. The general procedure of synthesis used in this Laboratory was followed. The resulting glass of $CaAl_2Si_2O_8$ composition had a uniform refractive index of 1.576 after three meltings and quenchings. One half of this glass (10 g.) was crystallized by heating at 1350° for 3 days. X-ray powder diffraction records gave the pattern characteristic of anorthite-rich plagioclase; microscopic examination likewise gave agreement with the recorded properties of anorthite and showed the complete absence of any discrete impurities.

Final preparation of materials for dissolving in the calorimeter.—In preliminary experiments on the decomposition of feldspars in 20 per cent hydrofluoric acid in the calorimeter it was found that the materials should be in the form of very fine powder in order to dissolve rapidly. For this reason the samples after purification were further ground and the finest particles separated from the coarser ones by elutriation in distilled water. The grinding was done with a mechanical grinder in agate or mullite mortars. About 5 g. of the sample were placed in the mortar at one time and ground usually for 2 hours. It was discovered in later experiments that the heat of solution of tough materials such as jadeite depends on the kind of mortar and pestle used in the grinding. It is believed that the corresponding error in the case of the fragile feldspars cannot be larger than about 1 cal/g. The error is not systematic since both types of mortar and pestle were used without distinction before the effect was discovered, and in some instances both types of mortar and pestle were used for grinding the same single sample.

[1]A mole of a feldspar end member is defined here as that formula weight which contains 8 oxygen atoms—thus, $CaAl_2Si_2O_8$, $NaAlSi_3O_8$, $KAlSi_3O_8$. For intermediate feldspars the weight of a mole is proportional to the mole fractions of the component end members.

TABLE 1

Description of the Material in the Plagioclase Series

Optical properties for samples 1, 5, 6, 7, 8, 9, 10, 11, 12, and 13 determined by K. Hytönen; for samples 2, 3, and 4 by O. F. Tuttle. All 2V values are determined on the universal stage.

No.	Name and Locality	Received from	Mode of Occurrence	Character from analysis mol %		Nature of Purification	Refractive indices	2V
				an	92.6		1.574	
1	Anorthite, Grass Valley, California	Ward	olivine-norite	ab	7.1	centrif.	1.582	—78°
				or	0.3		1.586	
				an	86.0		1.5713	
2	Plagioclase, EB 18, Stillwater, Montana	Hess	anorthosite	ab	13.7	centrif.	1.5814	—84°
				or	0.3		1.5859	
				an	80.1			
3	Plagioclase, EB 38, Stillwater, Montana	Hess	anorthosite	ab	19.5	centrif.	zonal	
				or	0.4			
				an	76.0		1.5657	
4	Plagioclase 7510 Rustenburg Pt-mines, Transvaal	Hess	norite	ab	23.0	centrif.	1.5701	—89°
				or	1.0		1.5754	
				an	69.7		1.565	
5	Bytownite, Crystal Bay, Minnesota	Ward	anorthosite	ab	30.3	centrif.	1.568	+89°
				or	0.0		1.574	
				an	51.9		1.555	
6	Labradorite, Isle of Paul, Labrador	U. S. National Museum		ab	45.8	centrif.	1.558	+83°
				or	2.3		1.562	

TABLE 1 (*Cont.*)

No.	Name and Locality	Received from	Mode of Occurrence	Character from analysis mol %		Nature of Purification	Refractive indices	2V
7	Labradorite,	U. S.		an	63.8	hand picked	1.562	
	Clear Lake, Utah	National	phenocrysts	ab	35.0	magn. separ.	1.566	—83°
		Museum		or	1.2		1.571	
8	Oligoclase, 81822		pegmatite,	an	16.8		1.538	
	South Carolina	Frondel	as greenish,	ab	82.0	hand picked	1.543	—87°
			clear crystals	or	1.2		1.545	
9	Oligoclase, 103086	U. S.	crystals	an	21.1		1.539	
	Hawk Mine,	National	from	ab	75.5	hand picked	1.543	+85°
	North Carolina	Museum	pegmatite	or	3.4		1.546	
10	Oligoclase, 80165	U. S.	crystals	an	21.6		1.539	
	Hawk Mica Mine,	National	from	ab	74.5	hand picked	1.544	+84°
	Bakersville, N. C.	Museum	pegmatite	or	3.9		1.547	
11	Plagioclase labelled							
	'Orthoclase' 97490 Head	U. S.	coarse crystals	an	28.7	clear edges by	1.543	
	of Little Rock Creek,	National	from	ab	67.8	hand picking	1.548	+87°
	Mitchel Co., North	Museum	pegmatite	or	3.5		1.550	
	Carolina							
12	Albite, Amelia,	U. S.	crystals	an	0.0		1.529	
	Virginia	National	from	ab	98.3	hand picked	1.533	—79°
		Museum	pegmatite	or	1.7		1.539	
13	Albite, Varuträsk,		albite rock	an	0.6		1.530	
	Sweden			ab	98.6	centrif.	1.535	—80°
				or	0.7		1.540	

TABLE 2

Description of the Sample Material in the Alkaline Feldspar Series

Optical properties are determined by K. Hytönen, University of Helsinki.
All the 2V-values are determined on the universal stage. The column marked 001 gives the angle between the normal to the 001-plane and the stated vibration direction in the crystals.

No.	Name and Locality	Received from	Mode of Occurrence	Character from analysis mol %		Nature of Purification	Refractive indices	2V	001
14	Anorthoclase, 90422 Victoria, Australia	Frondel	two colorless crystals evidently from lava	or	22.3	hand picked	1.526		
				ab	76.5		1.532	+48°	
				an	1.2		1.533		
15	Anorthoclase (Moonstone) Island of Ceylon	Ward	weathered rock*	or	58.6	hand picked	1.522		
				ab	40.2		1.526	+74°	
				an	1.2		1.529		
16	Sanidine, Kokomo, Colorado	Ward	phenocrysts in lava	or	71.4	centrif.	1.522		
				ab	25.1		1.527	+27°	6°
				an	3.5		1.527		
17	Sanidine, Grant County, New Mexico	Ward	moonstone pegmatite†	or	57.6	one clear crystal no purif.	1.521		
				ab	42.1		1.525	+29°	5°
				an	0.3		1.526		

* L. Spencer, Mineralog. Mag. 22, 291-317. 1930.

† V. C. Kelley and O. T. Branson, Tertiary moonstone pegmatite (abstr.), Bull. Geol. Soc. Amer., 57, 1255. 1946.

TABLE 2 (*Cont.*)

No.	Name and Locality	Received from	Mode of Occurrence	Character from analysis mol %		Nature of Purification			
18	Sanidine, Wehr, Eifel, Germany	U. S. National Museum	phenocrysts	or	76.8	hand picked	1.520		
				ab	22.3		1.525	+ 4°	5°
				an	0.9		1.525		
19	Adularia‡ St. Gotthard, Switzerland	U. S. National Museum (R 2817)	one single crystal with many inclusions	or	88.8	clear pieces hand picked	1.519		
				ab	10.9		1.523	+61°	6°
				an	0.3‡		1.525		
20	Ferriferous orthoclase Fianarantsoa, Madagascar	Frondel	two clear crystals	or	91.8	none	1.521		
				ab	6.0		1.524	+23°	6°
				an	0.2		1.525		
				Fe-or	2.0				
21	Ferriferous orthoclase Itrongahy, Madagascar	U. S. National Museum (92977)	clear crystals	or	81.8	none	1.5	+28°	7°
				ab	13.8				
				Fe-or	4.3				
				an	0.0				

‡ Barium content included with anorthite.

TABLE 3

Results of the Chemical Analyses for the Feldspar Samples Used

No.	1	2	3	4	5	6	7	8	9	10	11
Analyst	v.K.	Ph.	Ph.	Ph.	v.K.	v.K.	v.K.	v.K.	G.	Ch.	Ch.
SiO_2	44.17	46.34	47.67	49.06	49.46	55.70	51.94	63.49	61.60	62.54	60.85
TiO_2	tr.	....	....	....	0.06	tr.	0.05	0.00	0.00	0.00	0.01
Al_2O_3	34.95	33.36	33.46	32.14	31.24	27.86	30.19	22.76	23.76	23.31	24.44
Fe_2O_3	0.56	0.54	tr.	0.27	0.88	0.20	0.35	0.14	0.52	0.03	0.06
FeO	0.08	....	....	....	0.07	0.03	0.04	0.04	0.00	0.04	0.04
MgO	0.00	0.38	0.35	0.20	0.10	0.00	tr.	0.00	0.05	0.03	0.03
CaO	18.63	17.31	16.23	15.38	14.00	10.20	12.80	3.51	4.32	4.38	5.81
Na_2O	0.79	1.55	2.19	2.57	3.36	4.97	3.88	9.46	8.55	8.33	7.59
K_2O	0.05	0.05	0.07	0.17	tr.	0.39	0.20	0.22	0.58	0.66	0.59
H_2O+	0.84	0.23	0.00	0.13	0.68	0.70	0.40	0.52	0.58	0.40	0.43
H_2O-	0.17	0.03	0.00	0.03	0.34	0.04	0.12	0.19	0.18	0.20	0.25
									0.03 BaO	0.01 MnO	
Total	100.24	99.79	99.97	99.95	100.19	100.09	99.97	100.33	100.17	99.93	100.10

TABLE 3 (*Cont.*)

No.	12	13	14	15	16	17	18	19	20	21
Analyst	Ch.	Zies	v.K.	v.K.	v.K.	v.K.	v.K.	G.	v.K.	G.
SiO_2	67.84	68.76	66.24	65.16	63.58	65.44	63.52	63.95	65.10	64.05
TiO_2	0.00	0.00	0.00	0.00	0.00	tr.	tr.	0.00	0.02	0.00
Al_2O_3	10.65	19.50	19.89	19.44	19.07	18.73	19.00	19.66	17.82	17.17
Fe_2O_3	0.03	0.13	0.08	0.10	0.18	0.04	0.11	0.05	0.57	1.31
FeO	0.02	....	0.07	0.00	0.07	0.07	0.00	0.00	0.06	0.00
MgO	0.04	0.00	0.00	0.00	0.65	0.00	0.00	0.04	tr.	0.07
		0.02 P_2O_5						0.08 BaO		0.03 BaO
CaO	0.00	0.13	0.25	0.16	0.69	0.06	0.18	0.04	0.04	0.00
Na_2O	11.07	11.51	8.93	4.56	2.77	4.82	2.60	1.17	0.67	1.62
K_2O	0.29	0.13	3.95	10.10	11.96	10.01	13.58	14.43	15.91	15.36
H_2O+	0.56	0.08	0.44	0.50	0.57	0.68	0.60	0.56	0.08	0.52
H_2O-	0.30	....	0.09	0.08	0.22	0.33	0.54	0.16	0.06	0.18
Total	99.80	100.26	99.94	100.20	99.76	100.18	100.13	100.14	100.33	100.31

Names of analysts identified by initials in the table:

v.K. Oleg von Knorring, University of Leeds, Leeds 2, England.
Ph. A.H. Phillips, Princeton University, Princeton, N. J.
G. F. A. Gonyer, Department of Mineralogy, Harvard University, Cambridge 38, Mass.
Ch. E. Chadbourn, University of Minnesota, Minneapolis, Minn.
Zies E. G. Zies, Geophysical Laboratory, 2801 Upton Street, Washington 8, D. C.

The elutriation was done in 3-liter Pyrex beakers. The powder from the fine grinding was completely dispersed in distilled water and allowed to settle, usually for 10 minutes. The water suspension of the finer particles was then siphoned off, allowed to settle again for 10 minutes, and siphoned off a second time. This was repeated three times for the feldspars, the finest fraction which remained in suspension after the third settling being then collected on a strong filter paper under suction. The final material was then dried and kept at 140°.

The elutriation was eliminated in some of the later work after it was discovered that fine-ground feldspars could be dissolved in the acid without the elutriation treatment. An effective advantage from avoiding the elutriation lies in eliminating the wetting and drying of the fine powder which tends to agglomerate it into fine lumps and balls which are then wetted poorly by the acid, and may not dissolve well in the calorimeter.

Stoichiometry of the materials. —Data of thermochemistry are expressed in terms of molar heats of reaction, and hence the compositions of the materials investigated must be stated in terms of moles, or in mole percentages of the minerals present. For our purified feldspar materials, estimated to contain no more than 0.2 per cent of discrete impurities, the requirement is to determine from the chemical analyses the mole percentages of the three feldspar end-member molecules anorthite (An), albite (Ab), and orthoclase (Or). It is customary in normative computations to evaluate the moles of An, Ab and Or from the analytical contents of the three oxides, CaO, Na_2O, and K_2O, respectively. This requires the assignment of the corresponding moles of SiO_2 and Al_2O_3, or $Al_2O_3 + Fe_2O_3$ as R_2O_3. For a pure feldspar, correct analysis should result in a perfect balance of the acid and base oxides. Since all analyses of rocks are subject to error, such an ideal balance is never realized in practice, and it is common to find an excess or deficiency of SiO_2 and R_2O_3. In all feldspar analyses that we have examined such discrepancies are found in greater or lesser measure.

In computing the results of feldspar analyses, we assign the required amount of SiO_2 to combine with the reported MgO + FeO as pyroxene, and disregard the usually minute quantity of TiO_2. In addition, we compute the weight percent-

age of the sample accounted for as feldspar and the total weight accounted for, taking into consideration the computed pyroxene and the reported water. The results of such accountings, reported for our materials in table 4, are often surprising by the magnitudes of the discrepancies they disclose. The "precision" analyses of feldspars given by Vogt (1926) incidentally exhibit discrepancies that are similar to those for analyses which he designates as of "inferior" quality, both in terms of the percentage weight accounted for, and of the excess or deficiency of SiO_2 and R_2O_3.

The evaluation of analyses of purified feldspars in terms of the analytical contents of the base oxides alone is equivalent to neglecting the determinations of SiO_2 and R_2O_3, unless an accounting such as indicated above is made. In searching for a more complete utilization of the analytical information we have developed the method described below for the plagioclase feldspars. In this the algebraic excess moles of SiO_2 and R_2O_3 are distributed between the moles of CaO and Na_2O, the usually small amount of K_2O in the plagioclase being first assigned its complement of SiO_2 and R_2O_3 as orthoclase. In effect, this procedure implies the neglect of the analytical determination of CaO and Na_2O, and assumes SiO_2 and R_2O_3 determinations to be without error. From this point of view, the proposed procedure is as unrealistic as the ordinary normative evaluation of the feldspars from the analyses for the base oxides alone. For full utilization of analytical information it would be required to have statistical data on the probable errors of determination of the various oxides in feldspars by the group of analysts participating in this problem: such information as, for example, was obtained in a recent study of analyses of two standard rocks (Fairbairn, *et al.*, 1951).

Although the proposed method of recomputing the results of plagioclase analyses does not give the complete information desired, it is of interest, nevertheless, to learn what composition values it assigns to the different samples, and how well it accounts for the weight of the sample.

The algebra of the proposed computation is as follows:

Consider the analyses as first evaluated by computing An, Ab, and Or from the determinations of CaO, Na_2O, and K_2O. This yields the mole per cent compositions listed in columns 2, 3 and 4 of table 4, and the weights of feldspar per 100 g. sample

TABLE 4
Stoichiometry of the Materials

Sample No.	Feldspar Compositions Computed From the Analytical Content of CaO, Na_2O and K_2O: Moles Per Cent An	Ab	Or	Analytical Excess 10^5 moles/g SiO_2	R_2O_3	g Feldspar 100 g	g H_2O 100 g	g Pyroxene 100 g	Total g 100 g	Revised Plagioclase Compositions Adjusted to Eliminate Excess SiO_2 and R_2O_3: Moles Per Cent An	Ab	Or	Revised g Feldspar 100 g	Total g 100 g
(1)	(2)	(3)	(4)	(5)	(6)	(7)	(8)	(9)	(10)	(11)	(12)	(13)	(14)	(15)
						a) Plagioclase Series								
0	100.0	...	...	...	...	....	...	...	....	100.0	...	..	....	....
1	92.6	7.1	0.3	−8.7	0.9	99.38	0.97	0.15	100.50	94.0	5.7	0.3	98.91	100.07
2	85.8	13.9	0.3	−8.4	−3.6	99.26	0.23	0.94	100.43	85.8	13.9	0.3	98.19	99.39
3	80.1	19.5	0.4	−9.8	2.8	99.31	0.0	0.87	100.18	82.1	17.5	0.4	99.22	100.09
4	76.0	23.0	1.0	3.4	−2.3	99.02	0.26	0.50	99.78	76.3	22.7	1.0	99.62	100.58
5	69.7	30.3	0.0	−4.4	8.2	97.85	1.02	0.46	99.33	72.8	27.2	0.0	98.84	100.30
6	51.9	45.7	2.4	57.4	7.1	94.93	0.74	0.06	95.73	48.4	49.4	2.2	99.50	100.30
7	63.8	35.0	1.2	19.6	5.5	97.48	0.52	0.08	98.08	63.4	35.5	1.1	99.51	100.11
8	16.8	82.0	1.2	1.9	6.7	98.72	0.70	0.08	99.50	19.2	79.6	1.2	99.85	100.63
9	21.1	75.5	3.4	15.4	15.1	97.17	0.76	0.12	98.05	25.4	71.3	3.3	100.46	101.34
10	21.6	74.5	3.9	35.4	9.4	96.08	0.60	0.15	96.83	22.2	74.0	3.7	99.71	100.46
11	28.7	67.8	3.5	32.5	7.8	96.50	0.68	0.15	97.33	28.7	67.9	3.4	99.70	100.53
12	0.0	98.3	1.7	38.0	11.3	95.33	0.86	0.14	96.33	2.0	96.4	1.6	99.46	100.46
13	0.6	98.7	0.7	18.0	2.7	98.76	0.0	0.0	98.76	0.5	98.8	0.7	100.29	100.29
						b) Alkali Series								
14	1.2	76.5	22.3	−22.4	5.2	100.11	0.52	0.13	100.76	....	...	..	....	....
15	0.8	40.4	58.8	−5.5	7.7	99.04	0.68	0.0	99.72	....	...	..	....	....
16	3.5	25.1	71.4	3.0	4.3	97.51	0.78	0.13	98.42	....	...	..	....	....
17	0.3	42.1	57.6	−17.6	−1.2	100.20	1.01	0.13	101.34	....	...	..	....	....
18	0.9	22.3	76.8	−65.4	−2.2	103.10	1.14	0.0	104.24	....	...	..	....	....
19	0.2	10.9	88.9	30.0	20.4	95.35	0.72	0.10	96.17	....	...	..	....	....
20	0.2	6.0	93.8	3.4	2.0	97.52	0.14	0.11	97.77	....	...	..	....	....
21	0.0	13.8	86.2	−70.5	−12.6	104.45	0.70	0.18	105.33	....	...	..	....	....

listed in column 7. The algebraic excess of SiO_2 and R_2O_3 listed in columns 5 and 6, when positive, denotes moles/g of SiO_2 and R_2O_3 from the analysis in excess of the quantities which combine with CaO, Na_2O and K_2O to form feldspars and with FeO + MgO to form pyroxene.

Now,

let A = the algebraic excess of SiO_2 in moles/g
B = the algebraic excess of R_2O_3 in moles/g
x = the algebraic deficiency of Na_2O in moles/g
y = the algebraic deficiency of CaO in moles/g

Then $A = 6x + 2y$
$B = x + y$

The simultaneous solution of these equations,

$$4x = A - 2B \text{ and } 4y = 6B - A$$

yields the algebraic correction to the analytically determined moles/g of Na_2O and CaO, respectively, in order to reduce the algebraic excess of SiO_2 and R_2O_3 to zero. Upon determination of x and y the revised compositions of the feldspars listed in columns 11, 12, and 13, and the revised weights of feldspar per 100 g. sample, listed in column 14, are obtained. Columns 8 and 9 furnish the weights of water and pyroxene per 100 g. sample to be added to the values in columns 7 and 14 in order to arrive at the percentage of the weight of sample accounted for. Such values are listed in columns 10 and 15 for the two methods of computation. It is to be noted that an algebraic method cannot distinguish between Na_2O and K_2O since each of these combines with 6 SiO_2 and 1 R_2O_3.

Considering now the values listed in columns 10 and 15, as well as those in 7 and 14, it will be noted that in most cases the revised compositions accounted for close to 100 per cent of the sample weight in column 15, whereas the results of the ordinary normative computations in column 10 in certain cases depart from 100 per cent more than would be expected. Further, it will be noted that the revised compositions tend to correct the obviously low normative accounting for the feldspars in samples 5 to 12 inclusive.

Sample 12, albite from Amelia, Virginia, presented a special problem. As may be seen in table 3, the analysis reported the absence of CaO. Absence of CaO is very improbable, as in-

dicated by analyses of two other samples of Amelia albite, one by E. T. Allen in Day and Allen (1905), the other by R. E. Stevens of the U. S. Geological Survey, furnished by C. S. Ross (1950). Both of these accounted for slightly more than 100 per cent of the sample, and agree on CaO being present in this feldspar. Analysis of sample 12 accounted for 95.33 per cent of the sample as feldspar, and only for 96.33 per cent of the total weight. After computation by the outlined procedure, the revised composition is found to be near that given by Day and Allen (1905) and accounts for 99.46 per cent of the sample as feldspar and for 100.46 per cent of the total weight.

It will be realized that the compositions given by the outlined procedure are as arbitrary as those computed directly from the analytical values for CaO, Na_2O and K_2O. The fact that, in general, the accounting for the sample weight is improved by the method, however, indicates that the analysts apparently determined SiO_2 and R_2O_3 with greater accuracy than CaO, Na_2O, and K_2O. We may mention at this point that in figure 1 we plot the molar heats of solution of the plagioclases against the composition as calcuated by both of the methods under discussion, in order to remove any bias we may have unwittingly introduced in the presentation.

In comparison with the lengthy discussion of plagioclase stoichiometry, there is very little that can be said concerning that of the alkali feldspars, other than to point out what appear to be very obvious defects in some of the analyses. The mole per cent compositions in columns 2, 3 and 4 and the accounting for the feldspar and the total weight in columns 7 and 10 are computed from the analytical contents of CaO, Na_2O, and K_2O giving the algebraic excess of SiO_2 and R_2O_3 in columns 5 and 6. The accounting indicates that the reported alkalis were high for samples 17, 18 and 21 and low for 16, 19 and 20. There is no criterion to decide which of the alkalis was high and which was low. The data for samples 14 and 15 are indecisive.

HEAT OF SOLUTION MEASUREMENTS AND RESULTS

The materials were dissolved in 20.0 per cent (by weight) hydrofluoric acid at 74.7° in the acid solution calorimeter.

The heats of solution were measured in terms of the defined calorie equal to 4.1833 int. joules.

The heat of reaction measured when a sample composed of more than one discrete phase reacts with the acid solution in the calorimeter is the sum of the heats of solution of the separate phases, provided that a subsequent reaction, such as precipitation of the products, does not take place. Thus the heat of solution of mechanical mixtures of two or more phases is normally a linear function of the composition of the mixture. When on the other hand the sample is a member of a series of solid solutions the heats of solution of the various compositions along the series will be linear functions of the composition only when the series is formed from the component end members without any heat of formation of the solid solution. Sahama and Torgeson (1949) have concluded from their data on the solution in hydrofluoric acid of natural olivines and orthopyroxenes that the heat of solution in these two series is linear in terms of mole fractions, and hence, that the Fe-Mg replacement is thermally an ideal one. On the other hand, studies by Eastman and Milner (1933), Fineman and Wallace (1948), Wallace (1949), Fineman (1950), and Fontell (1939), of solid solutions of AgCl—AgBr, NaCl—NaBr, KCl—KBr and certain other simple pairs show with certainty that a heat of formation of solid solutions exists even for relatively perfect series of solid solutions, such as AgCl—AgBr. The term "heat of formation of solid solutions from end members" M and N is defined here as the change in the heat content ΔH of the process:

$$mM\ (c., t) + nN\ (c., t) = (M_m—N_n)\ \text{solid solution}\ (c., t)$$
$$\Delta H = \Delta H_f$$

The quantity ΔH_f varies with the concentration of M and N in the solid solution, being zero for the end members, and having a maximum at some concentration in the interior of the system. It is often numerically small, and usually the course of the curve cannot be measured accurately except with the use of special calorimetric techniques (Fineman and Wallace, 1948).

Precipitates formed upon dissolving plagioclases rich in anorthite.—Precipitates were found in the calorimeter after solution of lime-rich plagioclases in hydrofluoric acid. These have not been competely identified. X-ray diffraction patterns indicate the presence of calcium fluoride and several more complex fluorides such as prosopite, $CaF_2 \cdot 2Al(OH,F)_3$, and $Al_2(SiF_6)_3$, and in some cases also chiolite, $5NaF \cdot 3AlF_3$. The

latter compound was first found upon dissolving nephelite, $NaAlSiO_4$. Sometimes the formation of these precipitates is a slow process which makes itself evident in the calorimeter as a continued small heat evolution after the main solution process is completed, so that the calorimeter does not arrive at a steady state after the solution experiment. This slow after-effect is not always observed. Calcium fluoride may form first as a gelatinous precipitate which later reacts with the products of solution to give more complex phases. The formation of the complex precipitates, and the accompanying heats of precipitation are matters of some concern for the ultimate evaluation of the heats of formation of the minerals from the oxides, for there is no assurance that the same heats of precipitation will always be released and accounted for in the heat of solution of a given mineral, or of its component oxides.

The heats of solution in hydrofluoric acid of plagioclase and alkali feldspars.—Table 5 lists the results of the heat of solution measurements on the two feldspar series. The compositions of the plagioclase feldspars are given in terms of the albite-anorthite content after removal of the relatively small content of potash feldspar indicated by the analyses; similarly, the anorthite content has been removed from the alkali feldspar series. The measured heats of solution were in all cases corrected for the plus-water content, for the pyroxene computed from the analysis, and for the removed potash feldspar or lime feldspar, respectively, in the two series. For evaluating the water correction we have dissolved water in the acid solution in the calorimeter obtaining

H_2O (liq. 25°) = H_2O (soln. 74.7°) $\Delta H = 788 \pm 1$ cal/mole.

To this was added the heat of melting of ice, 1436 cal/mole on the assumption that the plus-water is present in the mineral as solid water. The total correction per mole of plus-water was 2224 cal. The correction for pyroxene was made using the Sahama and Torgeson (1949) values of the heats of solution of orthopyroxenes, $\Delta H = -57{,}010 - 58.7\ X_{Mg}$ cal/mole, where X_{Mg} is the molecular percentage of the enstatite component. Corrections for anorthite in the alkali series and for potash feldspar in the plagioclase series were made using our own heat of solution values, the value chosen for the potash feldspar being the extrapolated value at 100 per cent Or in figure 2, used because a pure potash feldspar was not available.

TABLE 5

Molar Heats of Solution, $\Delta H_{soln.}$ of Feldspars in 20.0 Per Cent Hydrofluoric Acid at 74.7°

Material No.	Normative Compositions in mole per cent from columns 2, 3 & 4 of table 4 corrected for removal of Or or An			Corrected* $\Delta H_{soln.}$	Uncertainty of measurement	Revised Compositions in mole per cent from columns 11, 12 & 13 of table 4 corrected for removal of Or			Corrected* $\Delta H_{soln.}$	Uncertainty of measurement	Condition of albite in the material
	An	Ab	Or	kcal/mole		An	Ab	Or	kcal/mole		
					a) Plagioclase Series						
0	100.	...	...	−185.11	0.77	100.	...	...	−185.11	0.77	...
1	92.9	7.1	...	−180.50	0.07	94.3	5.7	...	−180.62	0.07	?
2	86.1	13.9	...	−174.29	0.16	86.1	13.9	...	−174.25	0.16	?
3	80.4	19.6	...	−173.41	0.13	82.4	17.6	...	−173.61	0.13	?
4	76.8	23.2	...	−173.45	0.03	77.1	22.9	...	−173.48	0.03	?
5	69.7	30.3	...	−171.32	0.26	72.8	27.2	...	−171.63	0.26	?
6	53.1	46.9	...	−166.71	0.21	49.5	50.5	...	−166.35	0.21	low
7	64.6	35.4	...	−172.05	0.77	64.1	35.9	...	−172.02	0.77	?
8	17.0	83.0	...	−156.10	0.22	19.4	80.6	...	−156.33	0.22	low
9	21.9	78.1	...	−157.33	0.09	26.3	73.7	...	−158.72	0.09	low
10	22.5	77.5	...	−155.97	0.20	23.1	76.9	...	−156.02	0.20	low
11	29.7	70.3	...	−158.85	0.04	29.7	70.3	...	−158.85	0.04	low
12 natural	0.0	100.0	...	−149.96	0.11	2.0	98.0	...	−149.79	0.11	low
13	0.6	99.4	...	−148.12	0.21	0.5	99.5	...	−148.12	0.21	low
					b) Alkali Series						
12 heated	...	98.3	1.7	−151.99	0.11	...	...	...	.....	...	high
13 heated	...	99.3	0.7	−150.55	0.21	...	...	...	.....	...	high
14	...	77.5	22.5	−151.20	0.18	...	...	...	.....	...	high
15	...	40.7	59.3	−147.97	0.27	...	...	...	.....	...	high
16	...	26.0	74.0	−145.99	0.58	...	...	...	.....	...	high
17	...	42.2	57.8	−149.32	0.03	...	...	...	.....	...	high
18	...	22.5	77.5	−147.41	0.13	...	...	...	.....	...	high
19	...	11.0	89.0	−146.48	0.06	...	...	...	.....	...	low
20	...	6.0	94.0	−145.55	0.08	...	...	...	.....	..	low
21	...	13.8	86.2	−145.57	0.23	...	...	...	.....	...	low
			(100.0)	(−144.7)	(1.0) (Extrapolated)						

* Corrected for H_2O^+, the pyroxene computed from analysis, and for removal of Or or An. The somewhat different values of $\Delta H_{soln.}$ in columns 5 and 10 arise from the differences of molecular weights of the feldspars for the two sets of compositions.

Uncertainties of the heat of reaction values were computed by the methods recommended by Rossini and Deming (1939). In view of the large number of measurements involved, we present the average values with their uncertainties rather than the individual values, in order to conserve space.

The results presented in table 5 are represented graphically in figure 1 for the plagioclase and in figure 2 for the alkali feldspars. Compositions given for the plagioclase system in table 5 and figure 1 are computed by both the methods discussed in the section on stoichiometry.

Remarks on the results of the thermochemical measurements of the feldspars.—(a) Plagioclase feldspars. Evidence accumulating in the literature has led increasingly to the conviction that natural plagioclase feldspars depart from the perfect albite-anorthite solid solutions found at the liquidus temperatures by Bowen (1913). Chao and Taylor (1940) showed that at ordinary temperatures the relationship is much more complicated. They found that the unit cell of anorthite is twice as high as that of albite, and that labradorite is not a solid solution of the two end members, but rather a composite mixture of them. Köhler (1942*a*, 1942*b*) compared the optical orientations of high-temperature plagioclases with those of ordinary low-temperature plagioclases and found them different. From thermodynamic considerations Buerger (1948) concludes that because of the increasing tendencies toward order at lowered temperatures, solid solutions which are stable at high temperatures tend to become unstable at low temperatures, and he presents a tentative composition diagram of the plagioclase system. Finally, Cole, Sörum, and Taylor, (1951) find that plagioclases containing up to about 30 per cent anorthite are isomorphous with albite, while those with more than 72 per cent anorthite are isomorphous with anorthite. At intermediate compositions the relationship is complex; Cole, Sörum, and Taylor suggest that the structure of the intermediate feldspars may consist of alternating slabs of albite- and anorthite-type structures.

It will be noted that according to the data as represented in figure 1 the natural plagioclase feldspars at the albite end up to about 30 mole per cent anorthite are characterized by a positive ΔH of formation and those at the anorthite end, beginning at some point above 64 mole per cent anorthite by a negative

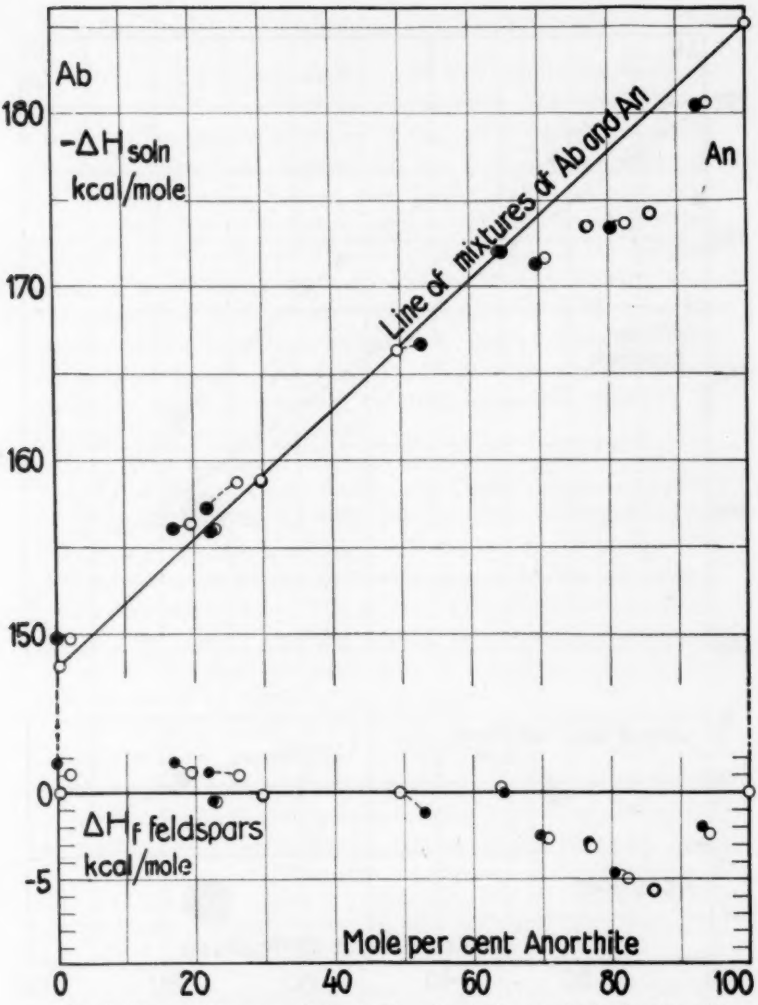

Fig. 1. Upper diagram: Molar heats of solution in hydrofluoric acid, $-\Delta H_{soln.}$ of plagioclase feldspars in kilocalories, represented by circles, and the corresponding values for mechanical mixtures of the two end members, albite and anorthite, represented by the line of mixtures. Black circles: compositions computed from CaO, Na_2O and K_2O as given by analysis; open circles: compositions computed by the procedure discussed in the section on stoichiometry, both after removal of the Or content. The sizes of the circles bear no relation to the uncertainty of measurement.

Lower diagram: Molar heats of formation of solid solution for plagioclase feldspars in kilocalories, given by the difference of the observed points from the line of mixtures in the upper diagram. Note the departures of the experimental points for the feldspars from the line of mixtures in the two regions, 0 to 30 and 65 to 100 mole per cent anorthite, as discussed in the text.

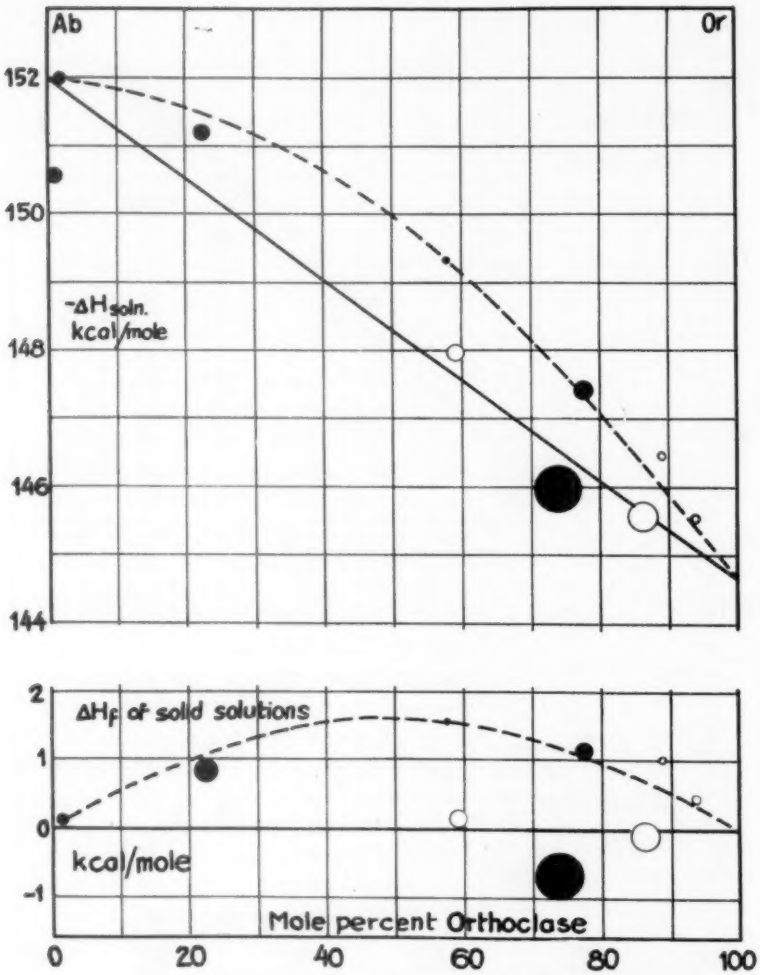

Fig. 2. Upper diagram: Molar heat of solution in hydrofluoric acid, $-\Delta H_{soln.}$, of high temperature albite and intermediate alkali feldspars in kilocalories, and the corresponding values for mechanical mixtures of the two end members high albite and orthoclase, represented by the solid line. Black circles: experimental points for feldspars in which albite is in the high temperature modification; open circles: albite in feldspar is in low temperature modification, as determined by O. F. Tuttle. Sizes of the circles are roughly proportional to the uncertainty of measurement.

Lower diagram: Molar heats of formation of solid solution for alkali feldspars from high albite and orthoclase in kilocalories, given by the difference of the observed points from the line of mixtures in the upper diagram. Note the scatter of the experimental points, and the discussion in the text.

ΔH of formation from natural (Varuträsk) albite and synthetic anorthite while the intermediate labradorites yield values characteristic of mechanical mixtures of the two solid solution limits. It would appear that these results are in close agreement with the findings of Cole, Sörum, and Taylor (1951), and confirm the various lines of evidence suggesting that the plagioclases are not a simple solid solution series when aged at low temperatures. This obviously does not vitiate Bowen's (1913) early phase diagram work on the crystallization of albite-anorthite solid solutions from high-temperature melts; thermochemical work on at least a few synthetic plagioclase compositions is needed in order to establish the thermochemical relations for the high-temperature feldspars.

(b) Alkali feldspars. Through the recent work of Bowen and Tuttle (1950), Schairer (1950), and Tuttle and Bowen (1950) the phase equilibrium relations for the alkali feldspars are now known in great detail, not only with respect to the liquidus and solidus, but more particularly with respect to the unmixing at subsolidus temperatures. The solvus region discovered by Bowen and Tuttle (1950) explains among other things the scarcity in nature of alkali feldspars from 30 to 40 per cent Or and the occurrence of perthitic intergrowths.

The results of our thermochemical measurements for the alkali feldspars, represented in figure 2, are not wholly conclusive, partly because the compositions studied are insufficient in number to define clearly the course of the curve, particularly in the soda-rich region of the system. It will be noted, moreover, that the heats of solution of the two albites (samples 12 and 13) differ by nearly 2 kcal/mole which is a large fraction of the difference between the values for albite and orthoclase, that from Amelia, Virginia (sample 12), giving numerically the larger value. Furthermore, the extrapolation to 100 per cent Or is somewhat uncertain because of the scatter of the various observed points. This scatter far exceeds the estimated uncertainties of measurement, which are roughly proportional to the sizes of the circles. It is likely that the scatter arises partly from the errors of analysis, and partly from the different physical conditions of the individual feldspars, as indicated by the work of Bowen and Tuttle who have found four different series of alkali feldspars (Adams, 1951, pp. 34-36).

The lower part of the diagram of figure 2 represents tenta-

tively the heats of formation of high-temperature alkali feldspars from the two end members, albite and orthoclase. It is clearly evident that this heat of formation is positive, but the actual course of the curve is uncertain.

Further work is needed on compositions intermediate between those investigated in this study, and on synthetic preparations, all of well defined composition and physical condition. Differences in the heats of solution such as were observed for the two nearly pure albites, samples 12 and 13, are especially difficult to explain; since the differences persist in varying degrees upon inversion to the high form, and even on melting, it must be concluded that they arise from some unknown factor in the composition of the samples. However, it appears logical to assume that the thermochemical properties of alkali feldspars are highly dependent on their origin and thermal history.

Latent heats of phase transformations in albite and anorthite.—Heats of solution of the two albites and anorthites in their different states were measured under comparable conditions and corrected for the water present in the unheated natural materials, and for the other impurities present according to the demands of analysis. Difference of the corrected heats of solution of each material in two different states yields the latent heat for the particular phase change at 25°. This must be corrected for the difference of the heat necessary to heat the two phases from 25° to the transition temperature in order to obtain the latent heat at this temperature. The heat content data for this correction are available from the work of White (1909, 1919) as summarized in a convenient form by Kelley (1949). Unfortunately White's data extend only to 700° for anorthite glass and to 900° for albite glass. This fact makes the heat content correction somewhat uncertain in the case of albite, and only very approximate in the case of anorthite. The data for the latent heats are collected in table 6.

Discussion of latent heat data.—Bowen (1913) computed the latent heats of melting for albite and anorthite from the plagioclase phase equilibrium diagram and obtained 12,740 cal/mole or 48.5 cal/g for albite, and 29,000 cal/mole or 104.2 cal/g for anorthite. Vogt and Akerman, as reported by Vogt (1904) computed 95 and 105 and quote 100 cal/g from their measurements for anorthite. H. S. Roberts (unpublished) measured 70 cal/g

TABLE 6

Heats of Phase Transformations in Albite and Anorthite

Substance and its condition	$-\Delta H_{soln.}$ kcal/mole	L_{298} kcal/mole	Correction for heat content 298° to T_{tr} kcal/mole	$^{L}T_{tr}$ kcal/mole	$^{L}T_{tr}$ cal/g	T_{tr} deg K	ΔS_{tr} cal/mole deg
(12) Albite, Amelia, Virginia							
Glass	161.44	9.45	*ca.* 3.15	12.6	48.1	1393	9.0
Heated crystals	151.99	2.20	*ca.* 1.1	3.3	12.6	1350	2.4
Natural crystals	149.79						
(13) Albite, Varuträsk, Sweden							
Glass	160.65	10.10	*ca.* 3.15	13.2	50.4	1393	9.5
Heated crystals	150.55	2.43	*ca.* 1.1	3.5	13.4	1350	2.6
Natural crystals	148.12						
(1) Anorthite, Grass Valley, California							
Glass	198.27	17.65	*ca.* 0.6	18.2	65.8	1803	10.1
Natural crystals	180.62						
(0) $CaAl_2Si_2O_8$, Synthetic							
Glass	202.27	17.16	*ca.* 0.6	17.7	63.7	1803	9.8
Crystals	185.11						

for albite in his furnace calorimeter (Roberts, 1938). Our values from the heat of solution data and White's heat content measurements for the heat of melting of high albite, 48.1 cal/g for Amelia albite, and 50.4 cal/g for Varuträsk albite, agree with Bowen's computed values as well as can be expected. In the case of anorthite the small, doubtful heat content correction makes the thermochemical values at the melting point 65.8 and 63.7 cal/g for the Grass Valley and the synthetic anorthite, respectively, very uncertain. It is of interest to note that the computed entropy of melting is of the order of 10 entropy units per mole for the anorthites, and 9.2 on the average for the two albites, while Bowen's value for the heat of melting of anorthite leads to 16 e. u/mole for the entropy of melting. The average value for the heat of transition of low to high albite is 13 cal/g.

HEATS OF FORMATION OF FELDSPARS

Measurements have been made of the heats of solution of CaO, of γ Al_2O_3, SiO_2 and of NaCl and KCl as well as of hydrochloric acid in the acid solution calorimeter for the purpose of evaluating the heats of formation of the feldspars. These will be reported in a later communication.

ACKNOWLEDGMENTS

The authors take pleasure in thanking W. F. Foshag and the U. S. National Museum, C. Frondel and the Harvard Mineralogical Museum, and H. H. Hess and the Princeton Mineralogical Collection for supplying many valuable materials for study. They are indebted to Th. G. Sahama for taking part in the extensive and laborious task of purification of the materials, and to L. H. Adams, Director of the Geophysical Laboratory, for his interest and continuing encouragement and support of the work.

REFERENCES

Adams, L. H., 1951. Report of the Director, Geophysical Laboratory: Carnegie Inst. of Washington Year Book 50, pp. 33-63.

Bowen, N. L., 1913. The melting phenomena of the plagioclase feldspars: Am. Jour. Sci., 4th ser., vol. 35, pp. 577-599.

———, and Tuttle, O. F., 1950. The system $NaAlSi_3O_8$—$KAlSi_3O_8$—H_2O: Jour. Geology, vol. 58, pp. 489-511.

Buerger, M., 1948. The role of temperature in mineralogy: Am. Mineralogist, vol. 33, pp. 101-121.

Chao, S. H., and Taylor, W. H., 1940. Isomorphous replacement and superlattice structures in the plagioclase feldspars: Royal Soc. London Proc., ser. A, vol. 176, pp. 76-87.

Cole, W. F., Sörum, H., and Taylor, W. H., 1951. The structures of the plagioclase feldspars. I: Acta Christallographica, vol. 4, pp. 20-29.

Day, A. L., and Allen, E. T., 1905. The isomorphism and thermal properties of the feldspars: Carnegie Inst. Washington Pub. 31.

Eastman, E. D., and Milner, R. T., 1933. The entropy of a crystalline solution of silver bromide and chloride in relation to the third law of thermodynamics: Jour. Chem. Phys., vol. 1, pp. 444-456.

Fairbairn, H. W., *et al.*, 1951. A cooperative investigation of precision and accuracy in chemical, spectrochemical and modal analysis of silicate rocks: U. S. Geol. Survey Bull. 980.

Fineman, M., 1950. Calculation of the heats of formation of alkali halide solid solutions from Hildebrand's equation: Jour. Chem. Phys., vol. 18, pp. 771-772.

———, and Wallace, W. E., 1948. Heats of formation and some derived thermodynamic properties of NaCl—NaBr solid solutions: Am. Chemical Soc. Jour., vol. 70, pp. 4165-4169.

Fontell, N., 1939. The phase diagram of potassium chloride—potassium bromide solid solutions: Soc. sci. Fennica, Commentationes Phys.-math., vol. 10, no. 12, pp. 1-10.

Kelley, K. K., 1949. Contributions to the data on theoretical metallurgy, X. High temperature heat content, heat capacity and entropy for inorganic compounds: U. S. Bur. Mines Bull. 476.

Köhler, A., 1942*a*. Die abhängigkeit der plagioklas optik von vorangegangenen wärmeverhalten: Min. pet. Mitt., vol. 53, pp. 24-48.

———, 1942*b*. Drehtischmessungen an Plagioklas-Zwillingen von Tief- und Hoch-temperaturoptic: Min. pet. Mitt., vol. 53, pp. 157-179.

Kracek, F. C., Neuvonen, K. J., and Burley, G., 1951. Thermochemistry of mineral substances. I. A thermodynamic study of the stability of jadeite: Washington Acad. Sci. Jour., vol. 41, pp. 373-383.

Morey, G. W., and Bowen, N. L., 1922. The melting of potash feldspar: Am. Jour. Sci., 5th ser., vol. 4, pp. 1-21.

Mulert, O., 1913. Über die Thermochemie der Kieselsäure und der Silikate: Zeitschr. anorg. Chemie, vol. 75, pp. 198-240.

Roberts, H. S., 1938. Direct measurement of silicate heats of melting: Am. Jour. Sci., 5th ser., vol. 35-A, pp. 273-287.

Ross, C. S., 1950. Private communication to the authors, giving the results of an analysis of albite, Amelia, Va., performed by R. E. Stevens, reported in a letter dated March 8, 1938.

Rossini, F. D., and Deming, W. E., 1939. The assignment of uncertainties to the data of chemistry and physics, with specific recommendations for thermochemistry: Washington Acad. Sci. Jour., vol. 29, pp. 416-441.

———, and Neuvonen, K. J., 1951. A solution calorimeter for silicates: Soc. géol. Finlande Comptes rendus, vol. 24, pp. 177-180.

Sahama, Th. G., and Torgeson, D. R., 1949. Thermochemical study of the olivines and orthopyroxenes: U. S. Bur. Mines Rept. Inv. 4408.

Schairer, J. F., 1950. The alkali-feldspar join in the system $NaAlSiO_4$—$KAlSiO_4$—SiO_2: Jour. Geology, vol. 58, pp. 514-517.

Torgeson, D. R., and Sahama, Th. G., 1948. A hydrofluoric acid solution calorimeter and the determination of the heats of formation of Mg_2SiO_4, $MgSiO_3$ and $CaSiO_3$: Am. Chemical Soc. Jour., vol. 70, pp. 2156-2160.

Tuttle, O. F., and Bowen, N. L., 1950. High-temperature albite and contiguous feldspars: Jour. Geology, vol. 58, pp. 572-583.

Vogt, J. H. L., 1904. Die silikatschmelzlösungen. II. Ueber die schmelzpunkt Erniedrigung bei Silikatschmelzloesungen: Skriften Norske vidensk.-akad. Oslo, I, Math.-naturvid. Kl., no. 1, pp. 1-236.

———, 1926. The physical chemistry of the magmatic differentiation of igneous rocks. II. On the feldspar diagram Or:Ab:An: Skriften Norske vidensk.-akad. Oslo, I, Math.-naturvid. Kl. no. 4, pp. 1-101.

Wallace, W. E., 1949. The Born-Mayer model for ionic solids and the heats of formation and the lattice spacings of alkali halide solid solutions: Jour. Chem. Phys., vol. 17, pp. 1095-1099.

White, W. P., 1909. Specific heats of silicates and platinum: Am. Jour. Sci., 4th ser., vol. 28, pp. 334-346.

———, 1919. Silicate specific heats. Second series: Am. Jour. Sci., 4th ser., vol. 47, pp. 1-43.

Geophysical Laboratory
Carnegie Institution of Washington
Washington, D.C.